

ENZYMATIC MECHANISMS AND REGULATORY PATHWAYS
UNDERLYING THE FORMATION OF THE TOMATO (*SOLANUM
LYCOPERSICUM*) FRUIT CUTICLE

A Dissertation

Presented to the Faculty of the Graduate School

of Cornell University

In Partial Fulfillment of the Requirements for the Degree of

Doctor of Philosophy

by

Laetitia Brigitte Blanche Martin

January 2015

© 2015 Laetitia Brigitte Blanche Martin

ENYMATIC MECHANISMS AND REGULATORY PATHWAYS UNDERLYING
THE FORMATION OF THE TOMATO (*SOLANUM LYCOPERSICUM*) FRUIT
CUTICLE

Laetitia Brigitte Blanche Martin, Ph. D.

Cornell University 2015

The plant cuticle, a complex hydrophobic membrane covering the aerial surfaces of land plants, has many critical functions, including limiting desiccation and preventing microbial infection. The cuticle consists of a polyester matrix of fatty acids, termed cutin, which is covered by and impregnated with a range of organic solvent soluble waxes. Genetic and biochemical strategies have uncovered many of the genes involved in wax and cutin precursor biosynthesis, but far less is known about the mechanisms that mediate the regulation, trafficking and subsequent assembly of cuticle components. This dissertation describes the results of three studies that focused on cuticle regulation and assembly, using tomato (*Solanum lycopersicum*) as an experimental system. In the first study, characterization of the *cutin deficient 1* (*cd1*) tomato mutant revealed that *CDI* encodes for an extracellular GDSL-motif lipase/hydrolase family protein that is preferentially expressed in developing organs with a high rate of cuticle production. Biochemical analysis demonstrated that CD1

polymerizes the cutin monomer 2-mono(10,16-dihydroxyhexadecanoylglycerol) (2-MHG) *in vitro*. Collectively these results suggest that CD1 catalyzes cutin polymerization and is a cutin synthase. The second study focused on tomato *Cutin Deficient 2 (CD2)*, a putative HD-ZIP IV transcription factor. *CD2* is widely expressed in various organs and tissues; however, the preferential accumulation of *CD2* in the fruit epidermis is consistent with a role in regulating the expression of cuticle biosynthesis related genes. Indeed, an analysis of genes that are differentially expressed in the epidermis of *cd2* mutant and wild type fruit revealed numerous genes implicated in cuticle biosynthesis, transport and assembly. *CD2* is also potentially important for other aspects of plant development as genes involved in lipid metabolism, anthocyanin biosynthesis, fruit ripening and stress responses were also differentially expressed in *cd2* fruit. The third study focused on another potential regulator of cuticle biosynthesis, the hormone abscisic acid (ABA). The leaf cuticle of ABA-deficient tomato mutants was observed to be thinner and to have structural abnormalities. Additionally, the cuticular wax composition was altered in the mutant genotypes compared to the corresponding wild types, with a relative increase in levels of alkanes shorter than C₃₁ and isoalkanes, relative decreases in the abundance of alkanes \geq C₃₁, the anteisoalkane C₃₂, amyrins and taraxasterol. Taken together, these results show that ABA is necessary for cuticle formation during leaf ontogeny.

BIOGRAPHICAL SKETCH

Laetitia Martin was born in Paris, France and moved to Viarmes (Val d'Oise), which provided for a much greener environment. She studied agricultural sciences at VetAgro Sup (Clermont-Ferrand), and during these studies she had the chance and opportunity to take a sabbatical year to cross the Atlantic and immerse herself in science and languages, by first studying nuclear-chloroplastic interactions in Dr. David Stern's lab (Cornell University) and then by studying phytopathogenic nematodes in Costa Rica, under the supervision of Dr. Tomás Guzmán (Instituto Tecnológico de Costa Rica). After completing her master's degree, she decided to continue studying molecular biology by entering into the doctoral program in Plant Biology at Cornell University in 2008, where an excellent presentation given by Dr. Jocelyn Rose led to her joining his lab.

ACKNOWLEDGMENTS

There are many people who contributed to this work, either by being directly involved in the research projects or by providing me with invaluable emotional support during these intense years.

First of all, I would like to thank my advisor, Joss Rose, for giving me the chance to join his lab and for providing me with a challenging and rewarding experience in graduate school. I learned a lot from Joss both as a scientist and as a person. I also want to thank my committee members, Karl Niklas and Jim Giovannoni, for feedback, discussion and help with all of these projects.

My experience in the lab would not have been as successful without the help and support of my labmates. I have seen many people joining and leaving the lab during these years and I want to thank all of them for contributing one way or another to my thesis. More particularly, I want to acknowledge the people who helped me in the initial steps of my Ph.D., including Tal Isaacson, Trevor Yeats and Antonio Matas and those who became close friends such as Eliel Ruiz-May, Eric Fich and Gloria Lopez-Casado.

Last but not least, I would like to thank my friends and family. First, I want to thank my mother who has always supported the choices I made and gave her ear to my concerns and my father and grand-parents who shaped who I am. I am so grateful to

my siblings and nieces for grounding me and providing me with such caring environment. I want to thank Jonathan and his daughter Sienna for accepting me as I am and for being there for me all these years. I also want to thank Dezi and Margaret without whom my experience in grad school would not have been nearly as enjoyable and Antoine, my best friend for so many years, with whom I have shared all the ups and downs of my life.

TABLE OF CONTENTS

BIOGRAPHICAL SKETCH	vi
ACKNOWLEDGMENTS	vii
TABLE OF CONTENTS	ix
CHAPTER 1. Introduction: The Structure, Formation and Functions of Fruit Cuticles	1
CHAPTER 2. Enzymatic Synthesis of the Plant Biopolyester Cutin by Cutin Deficient 1 (CD1), an extracellular GDSL Lipase Hydrolase	58
CHAPTER 3. Tomato Cuticle Biosynthesis is Regulated by Cutin Deficient 2 (CD2), an HD-ZIP IV Transcription Factor	96
CHAPTER 4. Abscisic Acid is Required for Cuticle Formation	204
CHAPTER 5. Conclusions and Future Directions	266
APPENDIX 1. Catalyzing Plant Science Research with RNA-seq	276

CHAPTER 1

Introduction:

The Structure, Formation and Functions of Fruit Cuticles

* A version of this chapter has been published in:

The Journal of Experimental Biology. (2014). 65(16), 4639-465.
doi: 10.1093/jxb/eru301

Introduction

The plant cuticle, a protective hydrophobic layer that coats the epidermal surfaces of all above-ground organs, plays many roles, including controlling gas and water exchange with the environment, filtering potentially damaging UV light and limiting invasion by pathogens (Yeats and Rose, 2013). Studies of cuticle structure and function using the experimental model plant *Arabidopsis thaliana* have provided insights into some of these functions, such as preventing organ fusion (Tanaka and Machida 2006; Hua *et al.*, 2010; Shi *et al.*, 2011), and have revealed many of the details of the underlying biosynthetic pathways (Pollard *et al.*, 2008; Samuels *et al.*, 2008; Schreiber, 2010). In addition, surveys of the cuticle compositions of a wide range of plant species have uncovered considerable compositional diversity (Holloway 1982; Jeffree 2006; Jetter *et al.*, 2006; Kallio *et al.*, 2006). Most such analyses have focused on vegetative organs, and on leaves in particular, but fleshy fruits, and more specifically those of tomato (*Solanum lycopersicum*), have recently emerged as an extremely valuable model for cuticle research. In part this reflects several experimentally attractive characteristics of tomato fruit cuticles: they are far thicker than those of *Arabidopsis* or other standard models, they are more readily extractable for *in vitro* characterization, and they are astomatous. As such, they provide substantial amounts of uniform material for structural and biochemical analysis that is free of ‘holes’ for biomechanical and permeability studies. However, in addition to their value for basic research, studies of fleshy fruits cuticles are also motivated by their critical influence on fruit quality and postharvest shelf life, given that they are

key factors in limiting desiccation and microbial infection (Domínguez *et al.*, 2011; Ruiz-May and Rose, 2013; Seymour *et al.*, 2013; Lara *et al.*, 2014).

This introduction summarizes recent discoveries and unresolved questions in the field of fleshy fruit cuticle structure, formation and function. For broader overviews that relate to cuticles in general, rather than specifically those of fruits, the reader is referred to other topical reviews that describe cuticle biosynthetic pathways (Pollard *et al.*, 2008; Samuels *et al.*, 2008; Schreiber 2010; Yeats and Rose 2013), cuticle biomechanics and structure-function relationships (Bargel *et al.*, 2006; Domínguez *et al.*, 2011; Rosaldo and Holder, 2013) and the associations with postharvest fruit quality (Lara *et al.*, 2014).

Overview of fruit cuticle composition and compositional diversity

A major component of plant cuticles is the structurally complex polymer cutin, a polyester derived from long-chain C16 and C18 ω -hydroxy fatty acids that can also contain dicarboxylic acids, alkanolic acids, phenylpropanoids and glycerol (Kolattukudy, 2001; Figure 1.1). The cutin matrix is impregnated with, and covered by, a diverse collection of organic solvent soluble compounds that are collectively referred to as waxes; termed intracuticular and epicuticular waxes, respectively (Figure 1.2). Cuticular waxes comprise a mixture of very-long-chain fatty acids and their derivatives: alkanes, aldehydes, ketones, alcohols and esters, together with cyclic compounds, such as triterpenoids and sterols (Jetter *et al.*, 2006; Figure 1.3). Although cutin and waxes typically predominate, another constituent of some cuticles is a less well defined, non-saponifiable polymer referred to as cutan, the subunits of which may

be linked via ether bonds (Villena *et al.*, 1999). Lastly, isolated cuticles can contain a structurally significant cell wall polysaccharide fraction that includes both cellulose and pectins (López-Casado *et al.*, 2007; Tsubaki *et al.*, 2012; Tsubaki *et al.*, 2013).

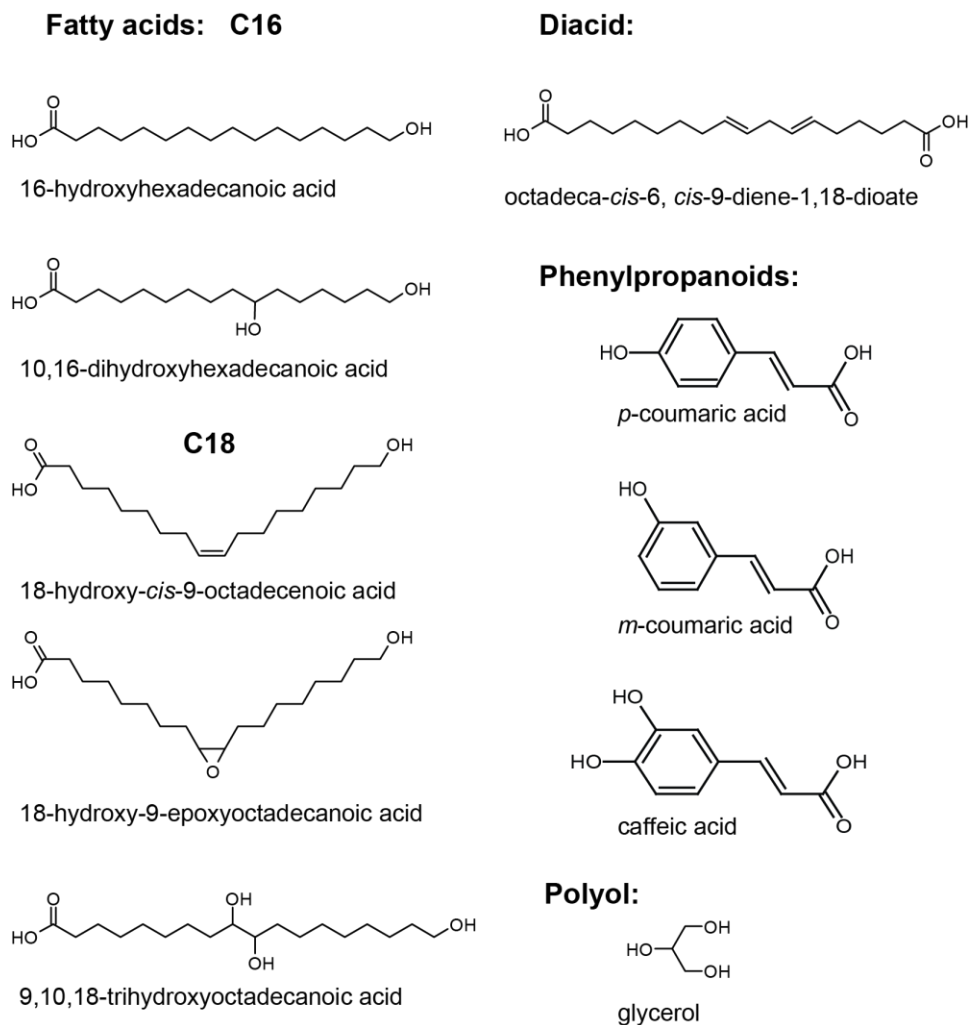


Figure 1.1. Structure of some cutin monomers.

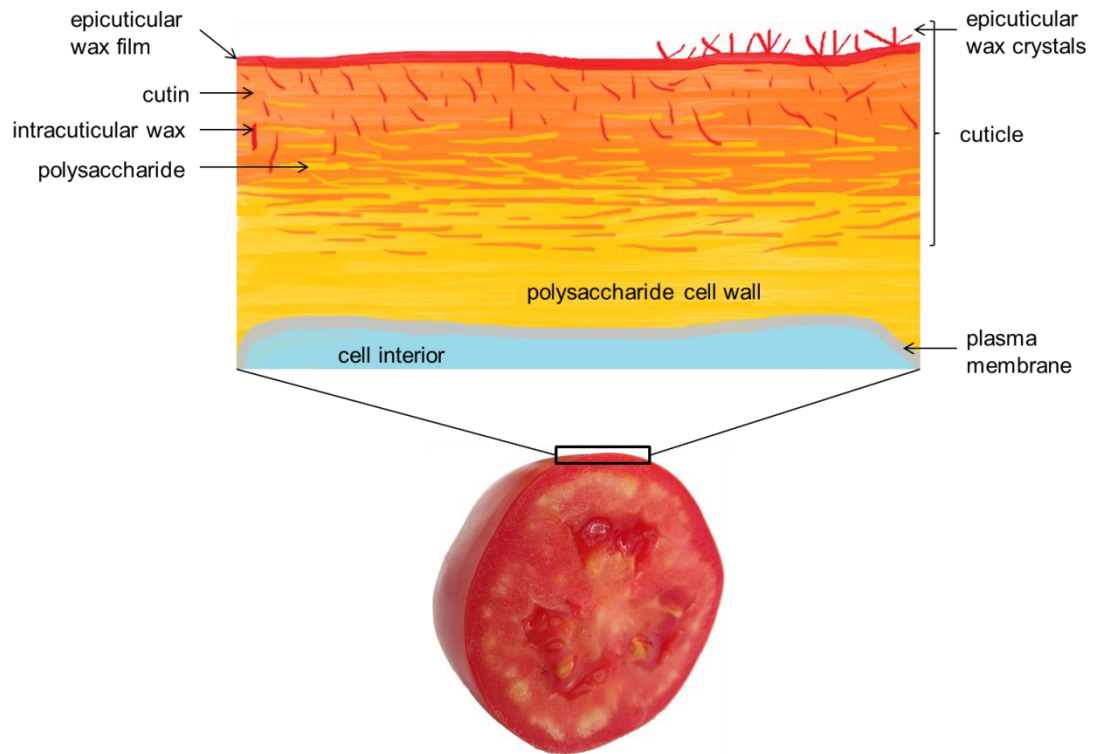
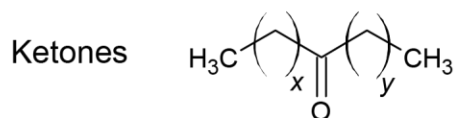
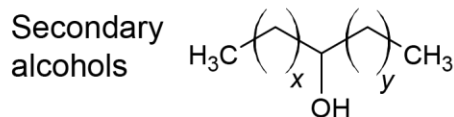
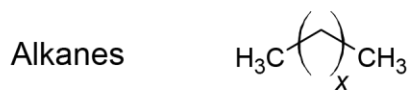
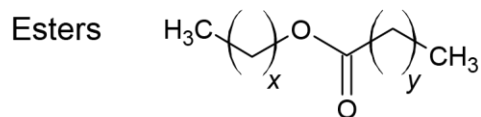
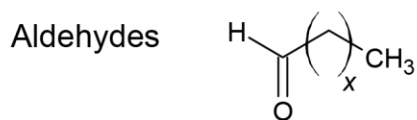
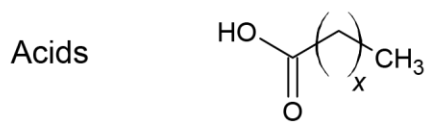
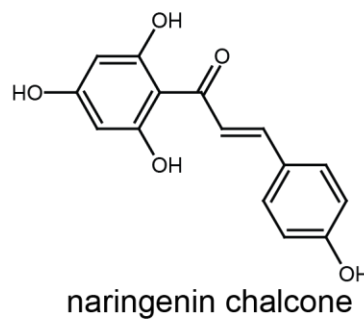
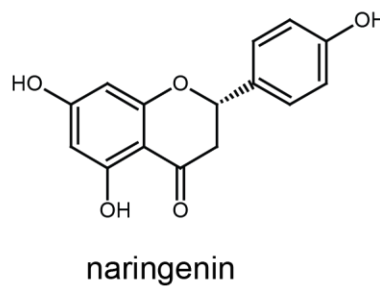


Figure 1.2. Generic model of a fruit cuticle. Cross section of an expanding tomato fruit showing the localization of the cuticle, represented below.

Acyl lipids:



Flavonoids:



Triterpenoids:

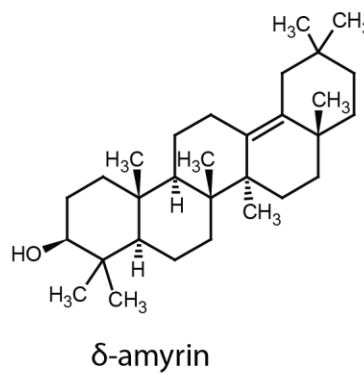


Figure 1.3. Structures of some common cuticular waxes.

In general terms, the cuticles of fruits have the same classes of compounds as those of vegetative organs and they show just as much compositional diversity as has been reported following biochemical surveys of leaf cuticles from different species (Holloway, 1973; Gérard *et al.*, 1992; Belding *et al.*, 1998; Graça *et al.*, 2002; Bauer *et al.*, 2004; Jeffree, 2006; Jetter *et al.*, 2006; Kallio *et al.*, 2006). This variation in fruit cuticle composition is evident at different levels:

1) Organ specific qualitative or quantitative differences in cutin or wax are often observed, such that the composition of the fruit cuticle can differ from that of a cuticle from a vegetative organ of the same species. For example, the cutin of apple (*Malus domestica*) leaves has been reported to have greater amounts of C16 compounds and lower levels of unsaturated monomers than that of apple fruit (Holloway, 1973). Another well characterized example is that of tomato, whose fruit cuticles accumulate extremely large amounts of flavonoids, and particularly naringenin (Hunt and Baker, 1980; Baker *et al.*, 1982; Muir *et al.*, 2001). Indeed, during maturation, flavonoids can constitute >75% of the cuticular waxes (Bauer *et al.*, 2004), but are not major components of tomato leaf cuticles. Such inter-organ variation may be the norm, and indeed has been observed in *Arabidopsis*, where the cutin of the stems and leaves is composed mostly of dicarboxylic acids, unlike that of flowers (Bonaventure *et al.*, 2004; Franke *et al.*, 2005).

2) The cuticles of fruits from different species can vary substantially in the proportion of waxes and cutin: to give just one comparison, persimmon (*Diospyros kaki*) fruit cuticles were reported to be composed of ~22-38% wax and ~50% cutin

(Tsubaki *et al.*, 2013), whereas equivalent values for tomato are 2-10% and 60-70%, respectively (Domínguez *et al.*, 2009). The proportion of cutan in fruit cuticles is also extremely variable, ranging from no detectable levels in tomato to ~94% in bilberry (*Vaccinium myrtillus*; Kallio *et al.*, 2006). Similarly, the relative amounts of polysaccharides can also vary considerably, constituting ~3% and 30% of isolated cuticles from persimmon and tomato fruits, respectively (Domínguez *et al.*, 2009; Tsubaki *et al.*, 2013). Other examples of this compositional variability among species are shown in Tables 1.1 and 1.2.

Table 1.1. The abundance of major cutin constituents in mature fruit from a range of species ($\mu\text{g}/\text{cm}^2$ or % in parentheses).

Species	Total cutin	Alkan-1- oic acids	ω -Hydroxyacids		ω -Hydroxyacids, “mid-chain” oxygenated		a, ω - Dicarboxyli c acids	Coumaric acid	Reference
			C16	C18	C16	C18			
<i>Malus pumila</i> (apple) 2 cultivars*	N/A	(0.7-2.5)	(1.5-2.9)	(12.8-23.8)	(0.0-0.0)	(71.0-82.8)	N/A	N/A	Gérard <i>et al.</i> (1992)
<i>Capsicum</i> <i>annuum</i> (pepper) 31 cultivars*	357.6- 4104.3	N/A	9.4-80.1 (1.7-4.0)	9.4-446.1 (0.9-30.2)	180.2-3319.3 (50.4-80.9)	54.9-454.8 (7.4-24.7)	2.5-49.8 (0.4-1.9)	2.0-167.7 (0.2-6.5)	Parson <i>et al.</i> (2013)
<i>Solanum</i> <i>lycopersicum</i> (tomato)	717.0	0.0 (0.0)	30.1 (4.2)	3.6 (0.5)	603.7 (84.2)	20.8 (2.9)	N/A	1.4 (0.2)	Graça <i>et al.</i> (2002)
<i>Diospyros kaki</i> (persimmon)	803.0	N/A	N/A	N/A	139.7 (17.4)	657.7 (81.9)	N/A	N/A	Tsubaki <i>et al.</i> (2013)
<i>Prunus avium</i> (sweet cherry)	35.1	0.3 (1.0)	0.6 (1.8)	0.6 (1.8)	23.0 (65.3)	6.0 (17.3)	0.7 (2.0)	0.1 (0.3)	Peschel <i>et al.</i> (2007)
<i>Citrus paradisi</i> (grapefruit)	N/A	(2.4)	(1.3)	(2.5)	(77.4)	(15.9)	N/A	N/A	Gérard <i>et al.</i> (1992)
<i>Cucurbita pepo</i> (pumpkin)	N/A	(12.0)	(1.7)	(0.0)	(0.0)	(96.0)	N/A	N/A	Gérard <i>et al.</i> (1992)
<i>Vaccinium</i> <i>oxycoccos</i> (cranberry)	N/A	N/A	(1.0)	(6.0)	(9.0)	(81.0)	N/A	N/A	Kallio <i>et al.</i> (2006)

Table 1.2. The abundance of some major wax constituents in mature fruits from of a range of species ($\mu\text{g}/\text{cm}^2$ or % in parentheses).

	Total wax	Fatty acids	Aldehydes	Alkanes	Alcohols	Triterpenoids	Other compounds	Reference
<i>Malus pumila</i> (apple) 12 cultivars*	366.0- 793.5	N/A	5.2-22.3 (0.7-3.3)	58.2-360.5 (15.9-49.2)	79.0-201.6 (15.1-31.7)	178.9-296.3 (32.0-53.8)	8.4-18.7 (1.5-3.2) Ketones	Belding <i>et al.</i> (1998)
<i>Capsicum annuum</i> (pepper) 31 cultivars*	1.0-13.8	0.2-4.6 (4.6-33.6)	0.0-0.4 (0.1-4.7)	0.3-3.7 (13.0-60.1)	0.0-1.6 (2.1-11.9)	0.3-4.7 (20.3-74.5)	N/A	Parsons <i>et al.</i> (2013)
<i>Capsicum chinense</i> (chili pepper)	2.2	0.3 (14.5)	0.1 (5.4)	1.2 (55.2)	0.2 (8.1)	0.3 (14.6)	0.0 (2.1) Alkenes	Parsons <i>et al.</i> (2012)
<i>Solanum lycopersicum</i> (tomato)	8.4	0.5 (6.1)	0.3 (3.5)	3.3 (38.6)	0.8 (8.9)	1.6 (19.3)	1.2 (14.5) Alkenes	Isaacson <i>et al.</i> (2009)
<i>Diospyros kaki</i> (persimmon)	576.0	38.6 (6.7)	N/A	2.3 (0.4)	39.2 (6.8)	442.9 (76.9)	N/A	Tsubaki <i>et al.</i> (2013)
<i>Prunus avium</i> (sweet cherry)	20.1	N/A	N/A	3.8 (19.1)	0.2 (1.1)	15.2 (75.6)	N/A	Peschel <i>et al.</i> (2007)
<i>Citrus limon</i> (lemon)	N/A	(18.7)	(43.4)	(22.9)	(15.0)	N/A	N/A	Baker <i>et al.</i> (1975)
<i>Citrus reticulata</i> (Clementine)	N/A	(7.9)	(43.6)	(42.4)	(6.0)	N/A	N/A	Baker <i>et al.</i> (1975)

*The abundance in $\mu\text{g}/\text{cm}^2$ and percentages are not necessarily from the same cultivar. Note that not all compounds are shown.

3) In addition to species specific compositional characteristics, considerable qualitative and quantitative variation has also been reported between cultivars of a single species. This is particularly the case for cuticular waxes, as illustrated by analyses of a range of apple (Belding *et al.*, 1998), persimmon (Tsubaki *et al.*, 2012) and tomato (Bauer *et al.*, 2004) cultivars. Additionally, a recent evaluation of pepper (*Capsicum annuum*) varieties revealed a >10 fold range for both cutin and wax amounts, and the predominant wax constituent was not consistent among the genotypes (Parsons *et al.*, 2013; Tables 1.1 and 1.2).

4) Dynamic changes are often observed in cuticular composition and coverage during fruit development (Baker *et al.*, 1982; Comménil *et al.*, 1997; Peschel *et al.*, 2007; Kosma *et al.*, 2010; Dong *et al.*, 2012). For example, it has been shown that the deposition of cuticular waxes on apple fruits increases significantly during ripening, coincident with a burst in ethylene production, with the fatty acid and alcohol fractions of the cuticular wax increasing by more than 120% (Ju and Bramlage, 2001). Dynamic changes in cutin and wax composition also occur throughout fruit growth, since substantial biosynthesis and remodeling of structurally significant cuticle polymers and incorporation of new material must be coordinated with expansion of the fruit surface in order to maintain structural integrity. Such cuticle restructuring has recently been proposed to occur in tomato fruit through a decrease of the number of ester bonds in the cutin matrix, together with an increase in the abundance of hydroxyl and carboxylic acid groups (España *et al.*, 2014).

5) While there is clearly considerable compositional diversity between organs, species and cultivars, there may also be variation among fruits of a single plant, or even spatially across the surface of a single fruit, as suggested by cuticular permeability studies of mango and apple (Maguire *et al.*, 1999; Léchaudel *et al.*, 2013). It is likely that these differences reflect both intrinsic genetic variation and the influence of growth and micro-environmental conditions, but the relative contributions of these factors have not been explored in any detail.

Another potentially important issue is that most studies of fruit cuticles have targeted species that have been subjected to extensive breeding, with selection and cultivation frequently extending back many hundreds of years, as is the case with tomato. As described later, cuticles make critical contributions to several horticulturally important traits, such as resistance to water loss, microbial infection and fruit cracking. Domestication, and in some cases breeding for the purposes of intensive cultivation, has therefore likely involved selection that favors particular structural and compositional features that are less prevalent in the fruits of wild species, which experience different selective pressures. Whether there are indeed specific cuticle compositional attributes that are typically more common among cultivated fruits is not clear, but this may be resolved by comparing the fruit cuticles of cultivated species with those of their wild relatives. An example of this was provided in a study of the cuticles of several wild *Solanum* species that are endemic to the northern Andes and Galapagos Islands, and that share a common ancestry with domesticated tomato (Yeats *et al.*, 2012). Numerous qualitative and quantitative

differences were observed in both the cutin and wax components when comparing the wild species with each other and with domesticated tomato. For example, the cuticular wax coverage of the domesticated species *S. lycopersicum* was lower than that of any of the wild relatives, and an inverse correlation was noted between the phylogenetic distance from *S. lycopersicum* and the abundance of cuticular triterpenoids. The implications of such differences have yet to be resolved and it will also be interesting to determine whether such correlations hold true for other domesticated fruit species versus their wild relatives. It may be that the lower wax levels in domesticated tomato reflect a reduced selective pressure to retain water as a consequence of the more consistent water supply associated with cultivation, particularly compared with native ecological niches that are prone to drought conditions. However, this remains speculation and represents an important area for future investigation.

Fruit cuticle architectural diversity

The cuticles of fleshy fruits are often far thicker than those of vegetative organs, a characteristic that facilitates their architectural analysis. For example, the cuticle of an expanded *Arabidopsis* leaf, which has long provided the primary experimental model, is approximately ~130 nm thick, while that of mature tomato fruit is about 2,000-9,000 nm (Jeffree, 2006). It is important to note, however, that a thick cuticle is not unique to fruits: the leaf cuticle of *Hakea suaveolens*, a drought tolerant shrub that thrives in a Mediterranean climate, has a reported thickness of 11,500 nm (Jeffree, 2006). Thus, it is possible that in some instances conclusions

derived from studies of fleshy fruit cuticle architecture may be applied more broadly to other organs.

A range of microscopy techniques has been applied to characterize the two dimensional (2D) and three dimensional (3D) architectures of fruit cuticles (Holloway 1982; Fernández *et al.*, 1999; Domínguez *et al.*, 2008; Buda *et al.*, 2009). One goal of such a characterization is to identify any structural heterogeneity in the cuticular membrane. It is known that intra-cuticular and epicuticular waxes generally differ in composition (Buschhaus and Jetter, 2011), but assessing spatial variation of cutin composition is more challenging. The use of lipophilic dyes can provide some insights into spatial differences in structure and composition. This was exemplified by a report that the dye Nile blue A stains the external cuticular layer of a ripe tomato fruit pink, suggesting a higher proportion of neutral fats and waxes, while the internal cuticular layer shows a blue coloration, indicative of acidic precursors (Buda *et al.*, 2009). Similarly, developmental structural variations have been highlighted by staining the cuticles of grape (*Vitis vinifera*) berries with the fluorescent stain auramine O (Considine and Knox, 1979). Specifically, the cuticle exhibits a uniform brilliant yellow/orange fluorescence early in development, while the cuticle of the mature fruit shows evidence of differentiation, with the inner and outer zones fluorescing brightly, separated by a middle zone with less staining. However, it should be noted that while such staining techniques indicate variation in architecture, they cannot typically be associated with particular compounds or structural features.

Cuticle images taken using transmission electron microscopy (TEM) have been used to define classes of cuticle organization, such as reticulate, lamellate, amorphous or a mixture of several classes, depending on the species or the organ (Holloway 1982; Jeffree 2006). The cuticles of only a few fleshy fruit species have been described in this context, and in general their cuticles have been described as fully reticulate (e.g. *Citrus sinensis*, *Malus domestica* and *S. lycopersicum*). It has been hypothesized that these structures reflect the predominant type of ester linkage in the constituent polymeric cutin. When the C18-epoxy ω -hydroxyacids are dominant, as is the case with ivy (*Hedera helix*) leaf cuticles, the cutin matrix is thought to be mostly composed of linear chains, resulting in the lamellae structure, while when C16-dihydroxy ω -hydroxyacids predominate, as is the case in tomato fruit, the branched cutin network may result in a reticulate type cuticle (Graça and Lamosa, 2010). Future studies of a broader range of fruits will likely help determine whether this holds true for all or most fleshy fruits, or whether greater structural diversity exists.

While visualizing fruit cuticles in 2D provides an overview of macro-architecture (Figure 1.4A), this approach does not allow insights into the 3D architecture on and around the epidermal cells, or an accurate quantitative assessment of cuticular thickness. However, such information can be obtained using a 3D imaging technique, involving confocal microscopy imaging and tomographic reconstruction of fluorescently stained cuticles (Buda *et al.*, 2009). The first application of this approach to study tomato fruit cuticle architecture revealed several new features that had not previously been reported. For example, 3D visualization established that the tomato

fruit subepidermal apoplast contains patches of cuticular material that are apparently not physically connected to the epidermal cuticle (Figure 1.4B). This raises the question of whether these arise by detachment from the ‘parent’ cuticle and subsequent movement down the anticlinal cell walls, or whether they are formed by sporadic sub-epidermal synthesis. Another remarkable structural feature of the tomato fruit cuticle that was revealed by 3D imaging was the presence of large anticlinal cuticular channels, which are far too wide (1-3 μm) to be considered as plasmodesmata, which are typically ~ 30 nm in diameter (Burch-Smith and Zambryski, 2012). Buda *et al.* (2009) hypothesized that these channels may play a role in water transport and maintaining cytoplasmic continuity between adjacent epidermal cells. Similar features have been described in apple fruits, as numerous pores are distributed over the outer and inner cuticular surfaces and appear to be the external apertures of transcuticular canals (Miller, 1982). These structures, which are visible early in fruit development, are perpendicular to the cuticle surface and are not connected to each other. The cuticular pores in apple fruits are reported to have a diameter (0.8-1.6 μm) that is similar to the anticlinal cuticular channels of tomato and there are distinct similarities between the two, such as their presence in the anticlinal cuticular deposits (flanges, or pegs) of both species. It has been suggested that these trans-cuticular canals in apple fruit may represent a pathway for lipid secretion (Miller, 1982); however, their function, and even their existence, has been questioned (Jeffree, 2006). Key questions still remain regarding the fine structure of these architectural features, the mechanisms of their formation and their ubiquity in fleshy fruits or other organs across plant species.

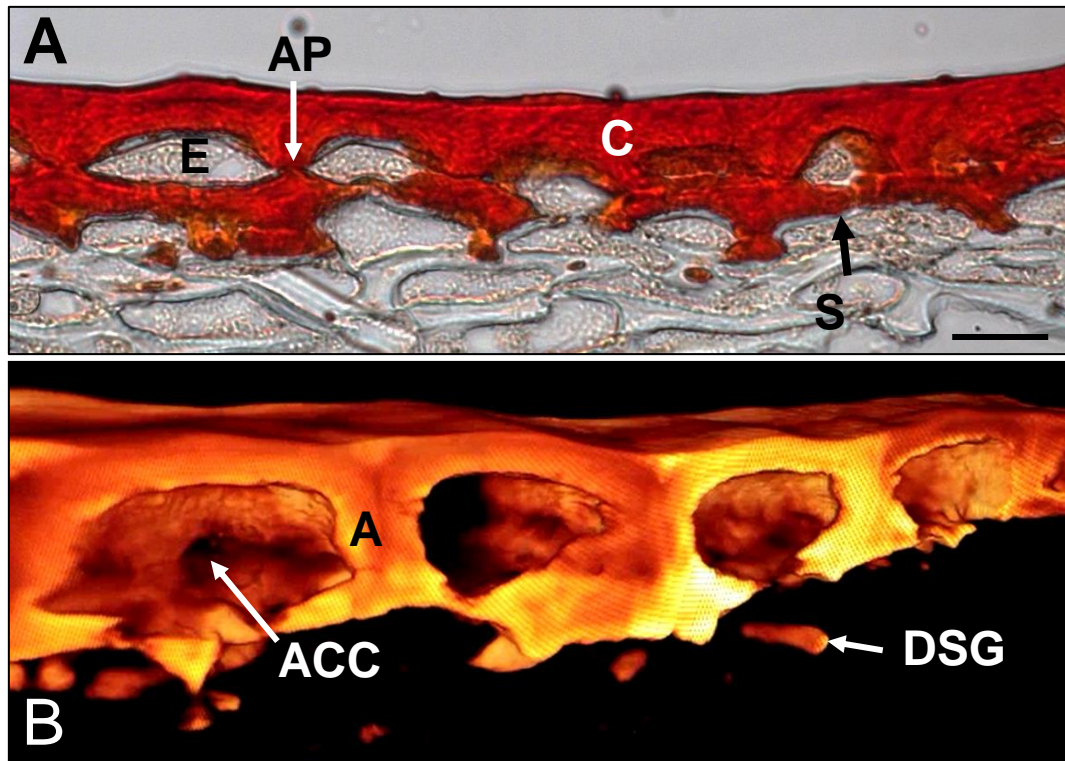


Figure 1.4. The cuticle of a mature green stage tomato (cv. M82) fruit. (A) Cuticle stained red with Oil Red O. AP, anticlinal peg; C, cuticle; E, epidermal cell; SD, sub-epidermal deposit. Scale bar = 20 μm . (B) 3D tomographic reconstruction of the tomato fruit cuticle (see Buda *et al.*, 2009 for details). ACC, anticlinal cuticular channel; AP, anticlinal peg; DSG, detached sub-epidermal globule. Scale bar = 20 μm .

In order to gain a more extensive overview of variability in fleshy fruit cuticle architecture, light microscopy was performed on commercially purchased ripe fruits to visualize the Oil Red O stained pericarp sections, some examples of which are shown in Figure 1.5. Considerable structural variation in cuticle thickness and shape is evident. In some cases, such as grape, cherry (*Prunus avium*), blueberry (*Vaccinium corymbosum*), star fruit (*Averrhoa carambola*), dragon fruit (*Hylocereus undatus*) and chayote (*Sechium edule*), the cuticle is relatively thin ($\sim 1.5\text{-}4.7 \mu\text{m}$) and is only

present on the outer epidermal cell wall. In contrast, the cuticle of some fruits, including mango, pear (*Pyrus communis*) and apple, is far thicker (~14-21 μm) or can extend through the apoplast of multiple cell layers, as is the case for jalapeño pepper (*Capsicum annuum*). Interestingly, the presence of anticlinal cuticular deposits, also called ‘pegs’, does not correlate with thickness of the outer epidermal cuticle, which suggests that their formation is not solely a consequence of excess cuticular material. Peg morphology also varies considerably, mirroring the thickness and shape of the intercellular regions where they are deposited. No discernable relationships between fruit size, growth habit, or preferred climate and cuticle architecture were detected and the significance of this considerable variation is unclear. In addition to cultivated fruits, cuticular morphology has been investigated in the fleshy fruits of wild tomato relatives (Yeats *et al.*, 2012). Here too, even within fruits of *Solanum* Sect. *Lycopersicon*, considerable diversity was observed in both overall thickness and structure, with variation in surface topology and substantial differences in the architecture, thickness and depth of the anticlinal and subepidermal cuticular deposits.

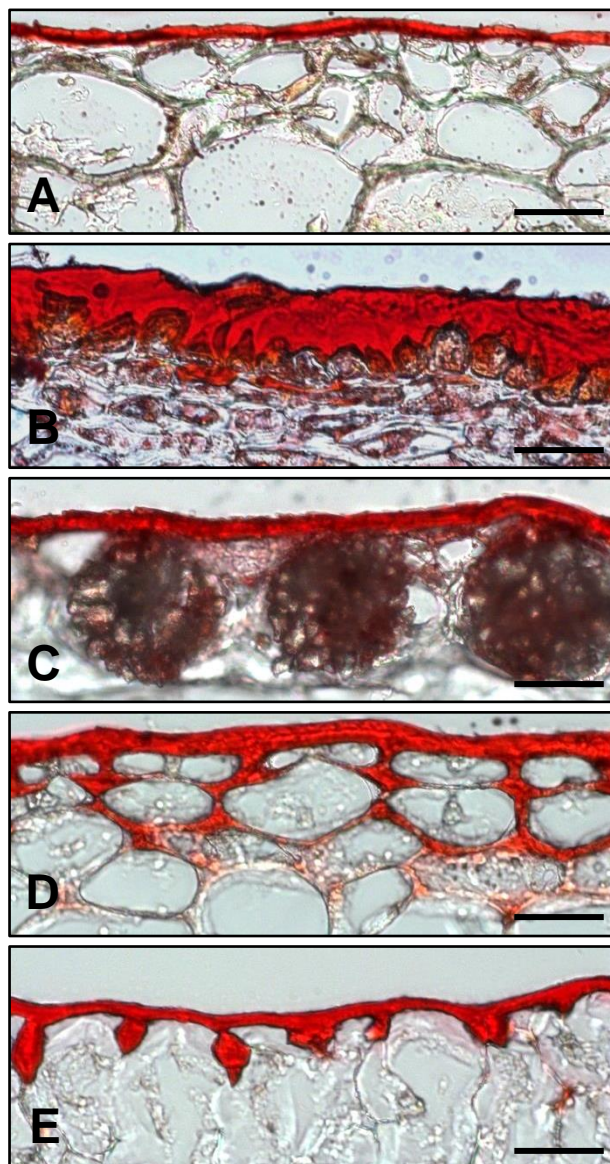


Figure 1.5. Fruit cuticle structural diversity among different fruit crop species. Cuticles were stained with Oil Red O for 30 min. (A) grape, (B) mango, (C) cactus fruit (*Opuntia*), (D) jalapeño pepper, (E) nectarine (*Prunus persica* variety *nectarina*). Scale bar = 20 μm .

Furthermore, the structural diversity of the fruit cuticle can also reflect major anatomical and developmental differences. For example, fruits of *Mespilus germanica* and *Sorbus torminalis*, from the Rosaceae family, have a multi-cell layered cuticle due

to the duplication of the epidermis during fruit development: at maturity, the fruit has 4-5 layers of epidermal cells, each layer covered with its own cuticle (Miller 1984; Bednorz and Wojciechowicz, 2009).

The diversity of fruit cuticle architectures is remarkable, but to date nothing is known about its functional significance, or the factors that determine the various patterns of cuticular deposition. For example, it may be that they are actively regulated at the molecular level, or that they result from biomechanical constraints imposed by cellular morphology, cell wall structure and cell-cell adhesion, or by the amount, rate and pattern of cuticular material that is generated. Furthermore, cuticle structure at various scales almost certainly influences properties such as water permeability or pathogen adhesion, for example through increased surface area due to undulating topography (Yeats *et al.*, 2012). The resolution of such structure-function relationships represents one of the most challenging issues in the field.

Genes implicated in fruit cuticle biosynthesis

Numerous genes involved in the biosynthesis of cuticle components have been characterized, mostly from studies of *Arabidopsis* mutants with visually apparent abnormal phenotypes (Pollard *et al.*, 2008; Samuels *et al.*, 2008; Schreiber, 2010). Using this resource as a platform, homologous genes with similar predicted functions have been identified in a range of fruit species using transcriptomic approaches (Mintz-Oron *et al.*, 2008; Matas *et al.*, 2010; Alkio *et al.*, 2012; Albert *et al.*, 2013). However, the small size of *Arabidopsis* and its relatively thin cuticle have likely limited the range of genes that can be identified through mutant characterization.

Moreover, while a homology-based approach is useful, in that it can suggest mechanistic conservation, it does not lend itself to the discovery of molecular pathways and processes that are fruit specific. Given that fruit cuticles are often far more substantial than those of *Arabidopsis*, they provide potentially excellent opportunities for identifying new genes involved in cuticle formation and restructuring. Indeed, several studies have contrasted transcript expression in the fruit peel/epidermis and the underlying cell layers ('flesh') with this specific aim in mind. For example, hundreds of genes were found to be preferentially expressed in the tomato fruit peel, a subset of which are known to be involved in cuticle biosynthesis (Mintz-Oron *et al.*, 2008). Laser capture microdissection (LCM) of different fruit cell types has also been used as an approach to identify genes that are specifically expressed in the epidermis and thus generate a candidate list of those that may be cuticle related. For example, Matas *et al.* (2010) used LCM to isolate epidermal and subepidermal cells of *Citrus clementina* fruit, from which transcripts were isolated and then used in a microarray analysis. This gene-enrichment strategy resulted in the identification of a high percentage of known cuticle related genes/gene homologs in the epidermal sample, along with a number of highly expressed genes of unknown function which represent targets for further analysis. Taking this approach a step further, Matas *et al.* (2011) coupled LCM with RNA-seq and characterized the transcriptomes of five classes of tomato pericarp cell/tissue types, including the outer and inner epidermis. The accuracy and sensitivity of this approach not only expanded the list of putative cuticle associated genes, but also uncovered a subset of genes with predicted functions in cuticle biosynthesis in the inner epidermis. Subsequent

histochemical, biochemical and spectroscopic analyses confirmed the presence of a thin internal epidermal cuticle that lines the locular cavity, the function of which has yet to be established.

In addition to a transcriptomic approach, proteomic analysis has also proved to be a useful and complementary method to identify genes involved in cuticle biosynthesis. The isolation of a protein fraction that is enriched in cuticle-associated proteins can be achieved by dipping entire fruits, or isolated cutin, into an organic solvent (Yeats *et al.*, 2010; Girard *et al.*, 2012). While this technique targets secreted cuticle localized proteins, a degree of contamination with intracellular proteins is difficult to avoid. Nonetheless, the overlap of a number of identified proteins with an epidermal-specific expression of their transcript has demonstrated its value (Yeats *et al.*, 2010).

Cuticle research can also benefit greatly from the identification of fruit cuticle mutants, which can in some cases be more readily identified than those of smaller model plants, such as *Arabidopsis*, since the thick fruit cuticle can provide obvious phenotypes. For example, a tomato fruit cutin deficiency phenotype was easily discernable in the *cd2/sticky peel* mutant, leading to the identification of the corresponding gene (Isaacson *et al.*, 2009; Nadakuduti *et al.*, 2012), while this was not the case for an *Arabidopsis* mutant with a mutation in the homologous gene (Kubo *et al.*, 1999). Importantly, genetic tools and techniques are now well established for tomato, thus facilitating the characterization of cuticle related genes or mutants. For example, transgenic tomato lines have been generated to explore and confirm cuticle

related gene function (e.g. Vogg *et al.*, 2004; Hovav *et al.*, 2007; Girard *et al.*, 2012; Shi *et al.*, 2013, as just some examples). The application of new genomic techniques and genetic resources to study existing lists of cuticle associated candidate genes will doubtless be valuable in addressing many aspects of cuticle biology that are currently poorly understood.

Regulatory mechanisms of cuticle biosynthesis

Various classes of transcription factors (TFs) have been implicated in regulating cuticle biosynthesis through studies of *Arabidopsis* or the vegetative organs of other plant species (Borisjuk *et al.*, 2014; Hen-Avivi *et al.*, 2014). The first such cuticle-related TF to be characterized, WIN1/SHN1, belongs to the APETALA2/ethylene response factor family (Aharoni *et al.*, 2004; Broun *et al.*, 2004), and has been shown to directly regulate cutin biosynthesis and indirectly affect wax formation in *Arabidopsis* (Kannangara *et al.*, 2007). Other members of this family have been associated with wax regulation in rice (*Oryza sativa*; Wang *et al.*, 2012) and alfalfa (*Medicago truncatula*; Zhang *et al.*, 2005; Zhang *et al.*, 2007) and SISHN3 has recently been shown to directly regulate some cutin-related genes in tomato fruit (Shi *et al.*, 2013). Other classes of TFs that play a role in cuticle biosynthesis regulation are the R2R3-type MYB and the MYB-related (MIXTA) families (Cominelli *et al.*, 2008; Seo *et al.*, 2009; Gilding and Marks, 2010; Seo *et al.*, 2011; Oshima *et al.*, 2013). The only cuticle-related MYB TF that has been characterized in fleshy fruit to date regulates many genes of the phenylpropanoid/flavonoid pathway, which is important for the accumulation of naringenin chalcone into the cuticle of the ripening

tomato fruit (Adato *et al.*, 2009). Members of the HD-Zip IV family have also been linked to cuticle regulation in Arabidopsis (Wu *et al.*, 2011; ANL2; Nadakuduti *et al.*, 2012), maize (*Zea mays*; Javelle *et al.*, 2010) and tomato (Isaacson *et al.*, 2009; Nadakuduti *et al.*, 2012). Many members of this family have previously been associated with epidermal cell identity, and a model involving the coordinated regulation of epidermis development and cuticle formation is emerging (Javelle *et al.*, 2011) as some genotypes with mutations in members of this family have both an abnormal cuticle and a defective epidermis phenotype. For example, the *cd2* tomato mutant has a reduction in cutin but also a reduced number of glandular trichomes and stomata (Nadakuduti *et al.*, 2012). Other cuticle-related TF have also been associated with epidermal cell differentiation, such as the SHN TFs, which appear to regulate epidermal cell elongation in Arabidopsis floral organs (Shi *et al.*, 2011) and influence trichome numbers and the stomatal index of Arabidopsis leaves (Aharoni *et al.*, 2004). Furthermore, MYB106 and MYB16 not only regulate cuticle formation, but are also involved in epidermal cell shape formation. Indeed, the *myb106* mutant has over-branched trichomes (Jokobi *et al.*, 2008) and MYB16 modulates the shape of petal epidermal cells (Baumann *et al.*, 2007). Recently, other processes have been identified as being regulated by cuticle-related TFs, as exemplified by SHN2 and AtMYB41, which have been shown to play a role in cell wall biosynthesis (Ambavaram *et al.*, 2011; Cominelli *et al.*, 2008). Such a function is not surprising as epidermal cell elongation or differentiation into stomata or trichomes must involve cell wall modifications and/or restructuring. Furthermore, various cuticle-related TF appear to be positive regulators of anthocyanin production, suggesting that these TF modulate

the synthesis of various compounds important for stress adaptation (Nadakuduti *et al.*, 2012; Seo and Park, 2010; Navarro *et al.*, 2011). In addition, it has recently been shown that two TFs that regulate fruit ripening, FRUITFULL1 and FRUITFULL2, are also involved into the production of cuticle components (Bemer *et al.*, 2012), suggesting a complex relationship between cuticle development and plant growth and physiology.

Since the cuticle is typically a central component of a plant's strategy to resist water loss and tolerate drought conditions, Kosma *et al.* (2009) tested the hypothesis that drought, salinity and an hormone central to water stress response, abscisic acid (ABA), influence cuticle biosynthesis. They observed that each of these three conditions lead to an increase in cuticular wax levels and that water deficit and sodium chloride treatments trigger an increase in total amounts of cutin monomers for the former and an altered cutin composition for the former and the latter. Several transcription factors that have been associated with cuticle biosynthesis are known to respond to some, or all, of the aforementioned conditions (Zhang *et al.*, 2005; Cominelli *et al.*, 2008; Seo and Park, 2010; Seo *et al.*, 2011; Navarro *et al.*, 2011; Wang *et al.*, 2012). For example, the ABA-responsive R2R3-type MYB transcription factor, MYB96, activates the transcription of cuticular wax biosynthetic genes under drought conditions (Seo *et al.*, 2011). Similarly, the expression of OsWR1, a rice homolog of SHN1, is induced by drought, ABA and salt and positively regulates cuticular wax synthesis (Wang *et al.*, 2012). Likewise, the overexpression of the *M. truncatula* AP2 domain-containing TF, WXP, which is inducible by cold, ABA and

drought treatment, increases cuticular wax accumulation and enhances drought tolerance in transgenic *M. sativa* (Zhang *et al.*, 2005).

Such studies strongly suggest that ABA, which is well-known for its role in stomatal closure under drought condition (Chater *et al.*, 2014), also triggers cuticular changes: surprisingly, the opposite also appears to hold true, since several cutin-deficient mutants are more susceptible to osmotic stress likely as a consequence of a reduced expression of ABA biosynthetic and signaling genes (Wang *et al.*, 2011). The regulation of cuticle formation as a response to the environmental conditions appears to be complex and the cuticle-related TFs may also have a role in the regulation other water deficit-related responses. Indeed, MYB96 not only affects cuticular wax biosynthesis but also controls stomatal aperture and root development (Seo *et al.*, 2011). Furthermore, the association of members of the HD-ZIP IV family with stomata formation, as well as the demonstrated role of the HD-ZIP IV protein HDG11 in drought tolerance (Yu *et al.*, 2008), suggest the integrated regulation of drought and cuticle formation.

Fruit cuticle functions

The fruit cuticle fulfills many functions, as summarized in Figure 1.6, a subset of which is described in the following section.

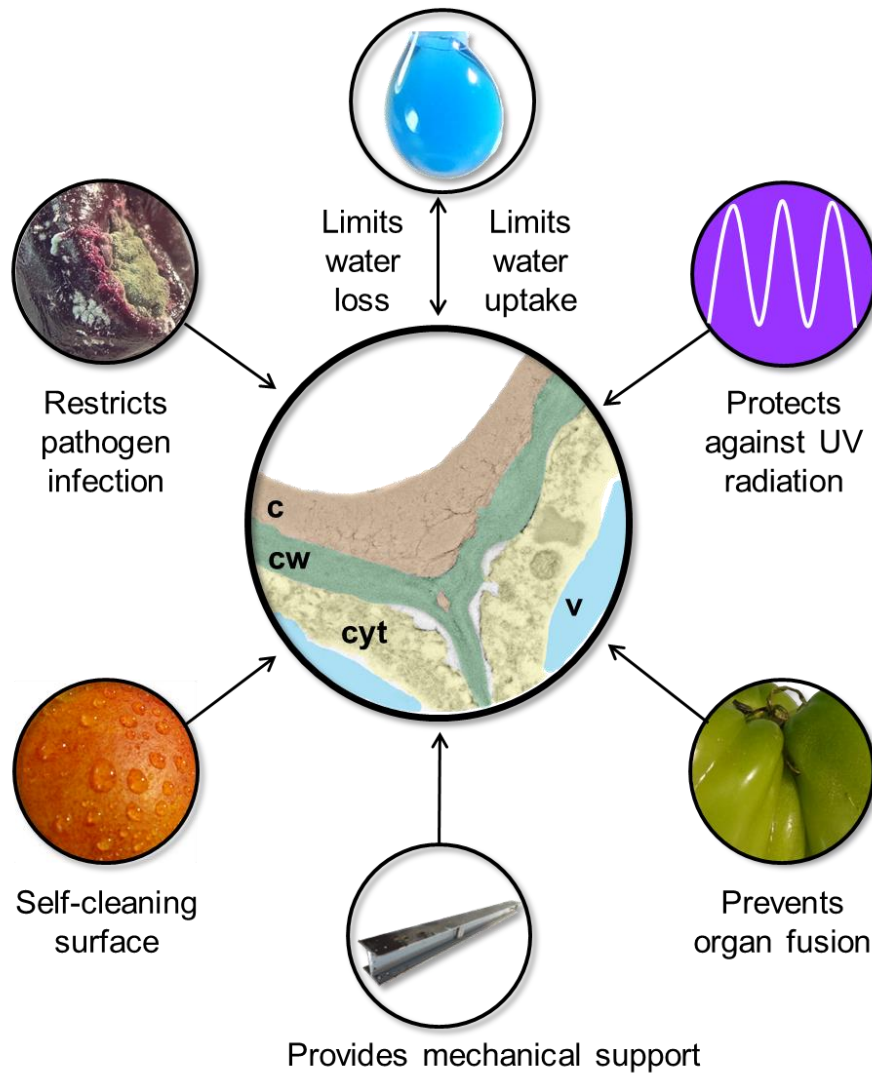


Figure 1.6. A summary of fruit cuticle functions. The central image shows a manually colorized transmission electron microscopy image of the cuticle and underlying structures of a small green tomato fruit; c, cuticle; cw, polysaccharide cell wall; cyt, cytoplasm; v, vacuole.

A permeability barrier

The hydrophobic nature of the cuticle makes it an effective barrier against water loss and so transpiration in leaves occurs predominantly through stomata. However, while stomatal transpiration can be significant at early stages of fruit development in some species, such as sweet cherry (Knoche *et al.*, 2001), most mature fleshy fruits have no or few stomata, or stomata that have become non-functional. In such cases, transpiration through the cuticle is the primary mode of water loss (Johnson and Brun, 1966; Schreiber and Riederer, 1996; Bukovac *et al.*, 1999; Knoche *et al.*, 2001; Peschel *et al.*, 2003; Veraverbeke *et al.*, 2003b). Some species, such as apple, have porous surface structures called lenticels and it has been suggested that these can contribute to a high transpiration rate (Veraverbeke *et al.*, 2003a). However, it has also been reported that five to ten times more water is lost through the cuticle than through lenticels (Pieniazek, 1944). Additionally, in another study the size and number of lenticels did not correlate with the rate of fruit transpiration, which may be explained by suberization or wax coverage of some of the lenticels (Veraverbeke *et al.*, 2003b).

Despite their typically greater thickness, rates of water loss through fruit cuticles appear to be higher than through leaf cuticles (Becker *et al.*, 1986; Araus *et al.*, 1991; Schreiber and Riederer, 1996). This may be significant for fruit development and physiology as evapotranspiration could help drive water import through the phloem, thereby increasing nutrient uptake (Lee, 1989; Schreiber and Riederer, 1996). Indeed, the rate of evapotranspiration in fruits is highest very early in

development (Maguire *et al.*, 2001; Montanaro *et al.*, 2012), which coincides with the highest growth rate of this sink organ, a developmental stage that presumably requires greater nutrient import. Increased permeance of the cuticle may also be a side effect of growth, as suggested by studies of sweet cherry, where cuticle thickness decreases during fruit expansion, a phenomenon that correlates with increased cuticular permeability (Knoche *et al.*, 2001). In contrast, some varieties of apples exhibit a post-maturity increase in cuticle permeance, which may be explained by the cessation of wax production, as well as mechanical degradation of surface wax crystals (Maguire *et al.*, 2001). As far as I am aware, physiological or other biological benefits to increasing water loss in mature fruits have yet to be determined.

In addition to cuticle permeability being developmentally determined, environmental conditions, such as temperature or relative humidity, can also have an effect. For example, differences of cuticle permeance have been detected in grapefruit (*Citrus paradise*) and mango (McDonald *et al.*, 1993; Nordby and McDonald, 1995; Léchaudel *et al.*, 2013) between the side of the fruit receiving sunshine and the shaded side. The observed lower water conductance of the sun exposed side has been attributed to differences in epicuticular wax morphology and composition (McDonald *et al.*, 1993; Nordby and McDonald, 1995). However, such a response is apparently not ubiquitous as no such differences in permeability have been detected for apple (Maguire *et al.*, 1999).

Water can diffuse through the cuticle from the inside of the fruit to the surface, but conversely, external water can also penetrate into the cuticle, resulting in water

uptake. The phenomenon of water uptake has received considerable attention due to its negative consequences for horticultural production, in the form of fruit cracking. Environmental conditions can affect the amount of water a cuticle will absorb and it has been shown that more is taken up at higher temperatures (Beyer and Knoche, 2002; Becker and Knoche, 2011) and relative humidities (Chamel *et al.*, 1991). One explanation that has been proposed for this phenomenon is that hydrated pathways are created through the cuticle, facilitating the passage of more water molecules (Lendzian and Kerstiens, 1991). Importantly, cuticle hydration also changes cuticle properties and a hydrated cuticle becomes more plastic and susceptible to fracture (Petracek and Bukovac, 1995; Matas *et al.*, 2004a).

The relative contribution of different cuticular components and thickness to cuticle permeability has been a long standing question. It would seem reasonable to hypothesize that thicker cuticles are less permeable to water, and indeed water deficit has been reported to trigger an increase in both cuticular thickness and wax content in sunflower pericarp (Franchini *et al.*, 2010). However, it is now accepted that cuticle thickness and permeability coefficients do not correlate (Schreiber and Riederer, 1996), suggesting that the regulation of cuticle permeability is complex and depends on qualitative characteristics. It has been reported that mutations that result in a massive reduction in cutin levels can lead to increased water loss (Isaacson *et al.*, 2009; Bessire *et al.*, 2011); however, the significance of such gross mutations is difficult to determine and it may be that the phenotypes reflect a general perturbation of cuticle architecture, rather than indicating that cutin alone is an effective

transpirational barrier. Interestingly, a recent study of pepper fruits suggested a positive correlation between water loss with total cutin amounts, as well as with specific cutin monomeric constituents (Parsons *et al.*, 2012), suggesting that influence of the abundance of cutin on evapotranspiration remains to be resolved.

Studies of leaf cuticles have led to the conclusion that waxes, rather than cutin, provide the main barrier to transcuticular water loss (Schöherr, 1976; Jenks *et al.*, 2002), although the amount of wax does not correlate with permeance (Schreiber and Riederer, 1996). This also appears to be the case for at least some fruit cuticles. For example, in a survey of a population of pepper lines, water loss rate was not found to strongly correlate with total wax levels, although an association was seen with specific waxes, suggesting that composition, rather than the quantity of cuticular waxes is a critical determinant of cuticle permeability. Studies of both tomato (Leide *et al.*, 2007) and pepper (Parsons *et al.*, 2012) fruit cuticles revealed that high levels of cyclic triterpenoids and a low concentration of alkanes correlate with a high water permeance. Furthermore, intracuticular, rather than epicuticular, waxes have been proposed to play a key role in determining permeability (Knoche *et al.*, 2000). In support of this idea, epicuticular waxes of tomato fruits were shown to have only a moderate effect on transpiration, while a reduction of 50% of the intracuticular aliphatic compounds correlated with a 4-fold increase in permeability (Vogg *et al.*, 2004).

In addition to preventing transpiration, intracuticular waxes limit movement of surface water into the fruit. This was illustrated by a study of sweet cherry where

water uptake across the cuticle increased when total cuticular waxes were removed, but removing epicuticular waxes had no effect (Beyer and Knoche, 2002). However, the role of the hydrophilic polysaccharides present in the cutin layer should not be ignored as nearly 70% of water sorption is attributed to them (Chamel *et al.*, 1991). The relative contribution of fruit cuticle constituents to compound sorption has also been studied to predict the fate of foliar pesticides following application. Removal of cuticular waxes generally results in a significant increase of cuticular sorption (Shafer and Bukovac, 1987; Chen and Li, 2007), but the polyester fraction (cutin and cutan) is believed to be the major sorption medium, while the polysaccharide fraction plays only a minor role for both polar and non-polar compounds (Chen *et al.*, 2005; Chen *et al.*, 2008; Li and Chen, 2009). Moreover, charged molecules have been shown to diffuse through the cuticle (Schönherr, 2000; Schönherr and Schreiber, 2004) but are not soluble in the lipophilic cutin and wax domains of the cuticle. This observation, as well as other experimental evidence suggests that charged molecules cross the cuticle via aqueous polar pores (Schreiber, 2005; Kerstiens, 2006) of an estimated diameter of 0.45 to 1.18 nm (Schreiber, 2005; Schönherr, 2006). However, these studies have been performed with leaf cuticles and the existence and functionality of such potential pores remain to be demonstrated in thicker cuticles such as those of fleshy fruits.

Given their relative ease of isolation, thickness and astomatous nature, fruit cuticles will likely continue to provide a valuable experimental system to resolve such questions. Moreover, given that cuticular components are shared among organs, it is likely that the results obtained from studies of fruit cuticles will apply more broadly to

those of other organs, and it will be interesting to learn whether mechanisms of diffusion are conserved despite the variation in cuticle composition and architecture that is evident across species.

A protective barrier

The cuticle provides an important physical barrier to pathogens and fruit susceptibility to fungal colonization has been linked to cuticle thickness in several species, including pepper (Manandhar *et al.*, 1995) and olive (*Olea europaea*; Gomes *et al.*, 2012). In addition, tomato fruit mutants with a severely reduced cutin layer were reported to show increased susceptibility to *Botrytis cinerea* and microbial opportunists (Isaacson *et al.*, 2009). The fact that the wax coverage of these mutants was similar to those of wild type fruit suggests that in this case cutin, rather than waxes, provides the key barrier. Another tomato mutant, *delayed fruit deterioration* (*dfd*), whose fruit are highly resistant to both water loss and microbial infection, was shown to have unusually high levels of fruit cutin (Saladié *et al.*, 2007), although the authors noted that the cuticle was not proportionally thicker. It may be that as well as quantity, polymeric organization and cutin density are significant attributes for both water loss and defense against pathogens. In addition to providing a pre-formed barrier, fruit cuticles can exhibit a dynamic and localized change in response to pathogen challenge, as was suggested by an observed increase in cuticle thickness in areas of sweet oranges (*Citrus sinensis*) affected by the fungus *Guignardia citricarpa* (Marques *et al.*, 2012). The importance of cutin as an obstacle to infection is further emphasized by the fact that many fungal pathogens secrete cutinases in order to

penetrate the surface of plant host organs (Vidhyasekaran, 2010), and indeed in some cases they have been shown to be essential. For example, a cutinase is required for penetration of *Colletotrichum gloeosporioides* into papaya (*Carica papaya*) fruits (Dickman *et al.*, 1982).

While considerable evidence points to cutin as playing a major part in plant defenses, cuticular waxes may also have a role, although this is less documented. It was reported that pepper fruits dipped in chloroform, to remove epicuticular waxes, were more susceptible to anthracnose, a fungal disease; a result that might be interpreted as suggesting that waxes also limit pathogen invasion (Manandhar *et al.*, 1995). However, it is important to note that the chloroform treatment may have resulted in major structural changes in cuticle architecture, and so more precise approaches to modifying wax levels, such as genetic strategies, may be required to resolve this question.

It is increasingly clear that the contribution of cuticular lipids to plant-pathogen interactions is more involved than merely providing a passive, physical obstruction, (Reina-Pinto and Yephremov, 2009). For example, the basal secretion of cutinases by fungi results in the release of cutin monomers, which in turn trigger the secretion of large amounts of cutinase by the pathogen, thereby facilitating pathogen infection of the host (Agrio, 2005; Vidhyasekaran, 2010). Moreover, wax compositions may serve as a complex mediator of host-pathogen interactions, as suggested by a study of avocado (*Persea Americana*) fruits, where isolated cuticular waxes triggered appressorium formation from the spores of *C. gloeosporioides*, whereas those of other

species did not (Podila *et al.*, 1993). Conversely, other species of *Colletotrichum* failed to form appressoria when in contact with avocado waxes, demonstrating the host specificity of the reaction. These intriguing observations suggest a complex and poorly understood layer of regulation, and studies are necessary to identify the specific cuticle components that modulate plant/pathogen interactions, which may include secreted plant proteins or peptides that reside in the cuticle.

In addition to deterring microbes, the cuticle also provides protection against excessive solar radiation, a phenomenon that has been studied in the context of fruit crop physiological disorders, such as sunscald (Barber and Sharpe, 1971; Solovchenko and Merzlyak, 2003). UV radiation can be particularly damaging and the leaf or fruit cuticles of a range of species has been shown to strongly attenuate its effects by filtering light of certain wavelengths at the surface while still allowing photosynthetically useful radiation to reach the chloroplasts (Krauss *et al.*, 1997). These filtering abilities are adaptable as UV light has been shown to trigger changes in wax amount and ultrastructural arrangement in tomato fruit (Charles *et al.*, 2008). The primary mechanism by which this protection is provided is thought to involve scattering of UV radiation by the specific orientation of surface waxes, as has been shown in a study of apple fruit (Solovchenko and Merzlyak, 2003). The same study showed that cuticular phenolic compounds absorb a significant amount of UV radiation, although the sun exposed face of the apple fruit accumulates high levels of flavonoids in the epidermal and subepidermal cell vacuoles (Solovchenko and

Merzlyak, 2003), so the relative contribution of the cuticular compounds remains unclear.

Mechanical support

Biomechanical stresses are highest at the surface of a plant organ (Niklas, 1992) and so it is not surprising that epidermal cells are particularly tightly connected, and often have a polysaccharide cell wall that is thicker on the outer periclinal face (Kutschera and Niklas, 2007; Javelle *et al.*, 2011). A comparison of tomato fruit peels, which retain several layers of cells and associated cell walls, and isolated cuticles from which the polysaccharides had largely been removed, revealed that they have similar mechanical properties, suggesting that the cuticle provides a significant mechanical support (Matas *et al.*, 2004b; Bargel and Neinhuis, 2005). Differences in fruit cuticle mechanical properties have been observed among different tomato cultivars and developmental stages, which can partly be explained by anatomical differences such as the extent of cuticular growth into subepidermal cell layers and by compositional variation, such as the accumulation of flavonoids during ripening (Matas *et al.*, 2004b; Bargel and Neinhuis, 2005; España *et al.*, 2014). The cuticles of sweet cherry fruits have also been shown to vary in their biomechanical properties during development (Knoche *et al.*, 2004). It remains to be determined whether the changes in the cuticle mechanical properties are necessary for coordinated and controlled growth or are merely a consequence of expansion.

Failure of the cuticle results in fruit cracking, a major horticultural problem (previously reviewed in Opara *et al.*, 1997; Simon, 2006; Balbontín *et al.*, 2013) as the

fruit becomes more susceptible to fungal infections (Børve and Sekse, 2000), which in turn makes it more susceptible to further cracking (Becker and Knoche, 2011). The severity of the cracking can vary, ranging from microcracks, which cannot be detected without a microscope, to large cracks that penetrate more deeply into the fruit (Opara *et al.*, 1997; Simon, 2006; Balbontín *et al.*, 2013). Microcracks are believed to develop into visually apparent macrocracks under certain conditions (Peschel and Knoche, 2005). The occurrence of cracking depends on various environmental, developmental and genetic variables: i) Rainwater and high humidity have been linked to fruit cracking in many species, with water adsorption from the fruit surface triggering cuticle cracking (Emmons and Scott, 1997; Measham *et al.*, 2009; Becker and Knoche, 2012b). Horticultural practices such as irrigation and fruit thinning can also promote the occurrence of cracking by altering fruit size, water potential or cuticle strain (Emmons and Scott, 1997; Gibert *et al.*, 2007); ii) Microcracking mostly occurs at the later stages of development and can result from a thinning/strained cuticle, changes in biomechanical properties and/or composition, depending on the species (Christensen, 1973; Emmons and Scott, 1997; Bargel and Neinhuis, 2005; Peschel and Knoche, 2005; Knoche and Peschel, 2007; Gibert *et al.*, 2007; Reig *et al.*, 2010; Becker and Knoche, 2012a); iii) The cuticle of cracking-resistant tomato fruits is thicker, stronger, stiffer and often penetrates more extensively into the apoplast of subepidermal layers (Matas *et al.*, 2004b). However, despite extensive study and its great economic impact, to date, little is known about the genetic basis of cuticle cracking (Balbontín *et al.*, 2013).

Research objectives

Decades of research have revealed much about the composition of the cuticles of a range of species, as well as many of the key enzymes and biochemical intermediates leading to the formation of wax and cutin monomers. Nevertheless, key aspects of cuticle formation still remain to be characterized. For example, one important and longstanding unresolved question is the identity of the enzyme, or process that is responsible for cutin polymerization and deposition at the cell surface. In addition, the complex regulatory mechanisms that control cuticle formation are only now being elucidated and it is clear that current models are highly simplified and rudimentary.

The research described in this thesis relates to both these important aspects of cuticle biology. A valuable resource in this regard was a tomato mutant collection that contains several fruit cuticular mutants (<http://zamir.sgn.cornell.edu/mutants/>), the characterization of which has resulted in the discovery of new genes associated with cuticle formation (Isaacson *et al.*, 2009). My studies involved the characterization of two of the mutants and in so doing I have contributed to the elucidation of two distinct aspects of the cuticle pathway: the polymerization of cutin and the transcriptional regulation of cuticle biosynthesis. Chapter 2 describes the characterization of the *cutin deficient 1 (cd1)* mutant, which has a mutation in a GDSL motif lipase/hydrolase family gene. The *cd1* fruit cuticle is extremely thin and biochemistry, microscopy and molecular techniques were used to demonstrate that CD1 is the long sought cutin synthase. Chapter 3 focuses on the *cutin deficient 2 (cd2)* mutant, which has a

mutation in a gene encoding an HD-ZIP IV transcription factor, resulting in a ~95% reduction of the fruit cutin levels. I hypothesized that CD2 is a major regulator of cuticle biosynthesis and present evidence that CD2 regulates additional pathways. Chapter 4 describes an investigation into the role of abscisic acid in the regulation of cuticle biosynthesis using the *cd* mutants and ABA deficient tomato lines. A relationship between ABA and cuticle formation is suggested by the altered structure and function of the ABA deficient plants. The appendix of this dissertation is a review of the applications of RNA-seq analysis, a technique that has been valuable in the research reported here and its broad applications in plant science research.

REFERENCES

- Adato A, Mandel T, Mintz-Oron S, Venger I, Levy D, Yativ M, Domínguez E, Wang Z, De Vos RCH, Jetter R, Schreiber L, Heredia A, Rogachev I, Aharoni A. (2009). Fruit-surface flavonoid accumulation in tomato is controlled by a SIMYB12-regulated transcriptional network. *PLoS Genetics* 5:e1000777.
- Adato A, Mandel T, Mintz-Oron S, Venger I, Levy D, Yativ M, Domínguez E, Wang Z, De Vos RCH, Jetter R, Schreiber L, Heredia A, Rogachev I, Aharoni A. (2009). Fruit-surface flavonoid accumulation in tomato is controlled by a SIMYB12-regulated transcriptional network. *PLoS Genetics* 5:e1000777.
- Agrio GN. (2005). *Plant Pathology*. 5th ed. Academic Press.
- Aharoni A, Dixit S, Jetter R, Thoenes E, van Arkel G, Pereira A. (2004). The SHINE clade of AP2 domain transcription factors activates wax biosynthesis, alters cuticle properties, and confers drought tolerance when overexpressed in *Arabidopsis*. *The Plant Cell* 16, 2463–80.
- Albert Z, Ivanics B, Molnár A, Miskó A, Tóth M, Papp I. (2013). Candidate genes of cuticle formation show characteristic expression in the fruit skin of apple. *Plant Growth Regulation* 70, 71–78.
- Alkio M, Jonas U, Sprink T, van Nocker S, Knoche M. (2012). Identification of putative candidate genes involved in cuticle formation in *Prunus avium* (sweet cherry) fruit. *Annals of Botany* 110, 101–112.
- Ambavaram MM, Krishnan A, Trijatmiko KR, Pereira A. (2011). Coordinated activation of cellulose and repression of lignin biosynthesis pathways in rice. *Plant Physiology* 155, 916–31.
- Araus JL, Febrero A, Vendrell P. (1991). Epidermal conductance in different parts of durum wheat grown under Mediterranean conditions: the role of epicuticular waxes and stomata. *Plant, Cell and Environment* 14, 545-558.
- Assimakopoulou A, Tsougrianis C, Elena K, Fasseas C, Karabourniotis G. (2009). Pre-harvest rind-spotting in ‘Clementine’ mandarin. *Journal of Plant Nutrition* 32, 1486–1497.
- Bai Y, Lindhout P. (2007). Domestication and breeding of tomatoes: What have we gained and what can we gain in the future? *Annals of Botany* 100, 1085-1094.

- Baker EA, Procopiou J, Hunt GM. (1975). The cuticles of *Citrus* species. Composition of leaf and fruit waxes. *Journal of the Science of Food and Agriculture* 26, 1093-1101.
- Baker EA, Bukovac MJ, Hunt GM. (1982). Composition of tomato fruit cuticle as related to fruit growth and development. In: D. Cutler, K. Alvin and C. Price, eds. The plant cuticle. Academic Press, 33-44.
- Balbontín C, Ayala H, Bastías RM, Tapia G, Ellena M, Torres C, Yuri JA, Quero-García J, Ríos JC, Silva H. (2013). Cracking in sweet cherries: A comprehensive review from a physiological, molecular, and genomic perspective. *Chilean Journal of Agricultural Research* 73, 66-72.
- Barber HN, Sharpe PJH. (1971). Genetics and physiology of sunscald of fruits. *Agricultural Meteorology* 8, 175-191.
- Bargel H, Neinhuis C. (2004). Altered tomato (*Lycopersicon esculentum* Mill.) fruit cuticle biomechanics of a pleiotropic non ripening mutant. *Journal of Plant Growth Regulation* 23, 61-75.
- Bargel H, Koch K, Cerman Z, Neinhuis C. (2006). Structure–function relationships of the plant cuticle and cuticular waxes—a smart material? *Functional Plant Biology* 33, 893-910.
- Bargel H, Neinhuis C. (2005). Tomato (*Lycopersicon esculentum* Mill.) fruit growth and ripening as related to the biomechanical properties of fruit skin and isolated cuticle. *Journal of Experimental Botany* 56, 1049–1060.
- Bauer S, Schulte E, Thier H-P. (2004). Composition of the surface wax from tomatoes II. Quantification of the components at the ripe red stage and during ripening. *European Food Research and Technology* 219, 487-491.
- Baumann K, Perez-Rodriguez M, Bradley D, Venail J, Bailey P, Jin H, Koes R, Roberts K, Martin C. (2007). Control of cell and petal morphogenesis by R2R3 MYB transcription factors. *Development* 134, 1691–701.
- Becker M, Kerstiens G, Schönherr J. (1986). Water permeability of plant cuticles: permeance, diffusion and partition coefficients. *Trees* 1, 54-60.
- Becker T, Knoche M. (2011). Water movement through the surfaces of the grape berry and its stem. *American Journal of Enology and Viticulture* 62, 340-350.
- Becker T, Knoche M. (2012a). Deposition, strain, and microcracking of the cuticle in developing 'Riesling' grape berries. *Vitis* 51, 1-6.
- Becker T, Knoche M. (2012b). Water induces microcracks in the grape berry cuticle. *Vitis* 51, 141-142.

- Bednorz L, Wojciechowicz MK. (2009). Development of the multilayered epidermis covering fruit of *Sorbus torminalis* (Rosaceae). *Dendrobiology* 62, 11-16.
- Belding RD, Blankenship SM, Young E, Leidy RB. (1998). Composition and variability of epicuticular waxes in apple cultivars. *Journal of the American Society of Horticultural Science* 123, 348-356.
- Bemer M, Karlova R, Ballester AR, Tikunov YM, Bovy AG, Wolters-Arts M, Rossetto PeB, Angenent GC, de Maagd RA. (2012). The tomato FRUITFULL homologs TDR4/FUL1 and MBP7/FUL2 regulate ethylene-independent aspects of fruit ripening. *The Plant Cell* 24, 4437-4451.
- Bemis SM, Torii KV. (2007). Autonomy of cell proliferation and developmental programs during *Arabidopsis* aboveground organ morphogenesis. *Developmental Biology* 304, 367-381.
- Bessire M, Borel S, Fabre G, Carraça L, Efremova N, Yephremov A, Cao Y, Jetter R, Jacquat A-C, Métraux J-P, Nawrath C. (2011). A member of the PLEIOTROPIC DRUG RESISTANCE family of ATP binding cassette transporters is required for the formation of a functional cuticle in *Arabidopsis*. *The Plant Cell* 23, 1958-1970.
- Beyer M, Knoche M. (2002). Studies on water transport through the sweet cherry fruit surface: V. Conductance for water uptake. *Journal of the American Society of Horticultural Science* 127, 325-332.
- Bonaventure G, Beisson F, Ohlrogge J, Pollard M. (2004). Analysis of the aliphatic monomer composition of polyesters associated with *Arabidopsis* epidermis: occurrence of octadeca-cis-6, cis-9-diene-1,18-dioate as the major component. *The Plant Journal* 40, 920-930.
- Borisjuk N, Hrmova M, Lopato S. (2014). Transcriptional regulation of cuticle biosynthesis. *Biotechnology Advances* 23, 526-540.
- Børve J, Sekse L. (2000). Cuticular fractures promote postharvest fruit rot in sweet cherries. *Plant Disease* 84, 1180-1184.
- Broun P, Poindexter P, Osborne E, Jiang CZ, Riechmann JL. (2004). WIN1, a transcriptional activator of epidermal wax accumulation in *Arabidopsis*. *Proceedings of the National Academy of Sciences of the USA* 101, 4706-11.
- Buda G, Isaacson T, Matas AJ, Paolillo DJ, Rose JKC. (2009). Three-dimensional imaging of plant cuticle architecture using confocal scanning laser microscopy. *The Plant Journal* 60, 378-385.
- Bukovac MJ, Petracek PD. (1993). Characterizing pesticide and surfactant penetration with isolated plant cuticles. *Pesticide Science* 37, 179-194.

- Bukovac MJ, Knoche M, Pastor A, Fader RG. (1999). The cuticular membrane: A critical factor in rain-induced cracking of sweet cherry fruit. *HortScience* 34(549).
- Burch-Smith TM, Zambryski PC. (2012). Plasmodesmata paradigm shift: regulation from without versus within. *Annual Review of Plant Biology* 63, 239-260.
- Buschhaus C, Jetter R. (2011). Composition differences between epicuticular and intracuticular wax substructures: How do plants seal their epidermal surfaces? *Journal of Experimental Botany* 62, 841-853.
- Çelikkol I, Türkben C. (2012). Effects of postharvest applications on berry quality, microbial population and morphological (epicuticular wax) deterioration of ready-to-eat table grapes. *Journal of Food, Agriculture and Environment* 10, 213-220.
- Chamel A, Pineri M, Escoubes M. (1991). Quantitative determination of water sorption by plant cuticles. *Plant, Cell and Environment* 14, 87-95.
- Charles MT, Makhlouf J, Arul J. (2008). Physiological basis of UV-C induced resistance to *Botrytis cinerea* in tomato fruit II. Modification of fruit surface and changes in fungal colonization. *Postharvest Biology and Technology* 47, 21-26.
- Chater CCC, Oliver J, Casson S, Gray JE. (2014). Putting the brakes on: abscisic acid as a central environmental regulator of stomatal development. *New Phytologist* 202, 376-391.
- Chen B, Johnson EJ, Chefetz B, Zhu L, Xing B. (2005). Sorption of polar and nonpolar aromatic organic contaminants by plant cuticular materials: Role of polarity and accessibility. *Environmental Science and Technology* 39, 6138-6146.
- Chen B-L, Li Y-G. (2007). Sorption of 1-naphthol by plant cuticular fractions. *Journal of Environmental Sciences* 19, 1214-1220.
- Chen B, Li Y, Guo Y, Zhu L, Schnoor JL. (2008). Role of the extractable lipids and polymeric lipids in sorption of organic contaminants onto plant cuticles. *Environmental Science and Technology* 42, 1517-1523.
- Christensen JV. (1973). Cracking in cherries: VI. Cracking susceptibility in relation to the growth rhythm of the fruit. *Acta Agriculturae Scandinavica* 23, 52-54..
- Cline J, Sekse L, Meland M, Webster AD. (1995). Rain-induced fruit cracking of sweet cherries: I. Influence of cultivar and rootstock on fruit water absorption, cracking and quality. *Acta Agriculturae Scandinavica Section B, Soil and Plant Science*. 45, 213-223.

- Cline JA, Trought M. (2007). Effect of gibberellic acid on fruit cracking and quality of Bing and Sam sweet cherries. *Canadian Journal of Plant Science*, 87, 545-550.
- Comménil P, Brunet L, Audran J-C. (1997). The development of the grape berry cuticle in relation to susceptibility to bunch rot disease. *Journal of Experimental Botany* 48, 1599-1607.
- Cominelli E, Sala T, Calvi D, Gusmaroli G, Tonelli C. (2008). Over-expression of the *Arabidopsis* AtMYB41 gene alters cell expansion and leaf surface permeability. *The Plant Journal* 53: 53–64.
- Considine JA, Knox RB. (1979). Development and histochemistry of the cells, cell walls, and cuticle of the dermal system of fruit of the grape, *Vitis vinifera* L. *Protoplasma* 99, 347-365.
- Curry EA. (2005). Ultrastructure of epicuticular wax aggregates during fruit development in apple (*Malus domestica* Borkh.). *Journal of Horticultural Science and Biotechnology* 80, 668-676.
- Dickman MB, Patil SS, Kolattukudy PE. (1982). Purification, characterization and rôle in infection of an extracellular cutinolytic enzyme from *Colletotrichum gloeosporioides* Penz. on *Carica papaya* L. *Physiological Plant Pathology* 20, 333-347.
- Domínguez E, López-Casado G, Cuartero J, Heredia A. (2008). Development of fruit cuticle in cherry tomato (*Solanum lycopersicum*). *Functional Plant Biology* 35, 403-411.
- Domínguez E, España L, López-Casado Gloria, Cuartero J, Heredia A. (2009). Biomechanics of isolated tomato (*Solanum lycopersicum*) fruit cuticles during ripening: the role of flavonoids. *Functional Plant Biology* 36, 613–620.
- Domínguez E, Cuartero J, Heredia A. (2011). An overview on plant cuticle biomechanics. *Plant Science* 181, 77-84.
- Domínguez E, Fernández MD, López Hernández JC, Pérez Parra J, España L, Heredia A, Cuartero J. (2012). Tomato fruit continues growing while ripening, affecting cuticle properties and cracking. *Physiologia Plantarum* 146, 473–486.
- Dong X, Rao J, Huber DJ, Chang X, Xin F. (2012). Wax composition of ‘red fuji’ apple fruit during development and during storage after 1-methylcyclopropene treatment. *Horticultural and Environmental Biotechnology* 53, 288-297.
- Emmons C, Scott J. 1997. Environmental and physiological effects on cuticle cracking in tomato. *Journal of the American Society for Horticultural Science* 122, 797-801.

- España L, Heredia-Guerrero JA, Segado P, Benítez JJ, Heredia A, Domínguez E. (2014). Biomechanical properties of the tomato (*Solanum lycopersicum*) fruit cuticle during development are modulated by changes in the relative amounts of its components. *New Phytologist* 202, 790-802.
- Fava J, Hodara K, Nieto A, Guerrero S, Maris Alzamora S, Agueda Castro M. (2011). Structure (micro, ultra, nano), color and mechanical properties of *Vitis labrusca* L. (grape berry) fruits treated by hydrogen peroxide, UV-C irradiation and ultrasound. *Food Research International* 44, 2938–2948.
- Fernández S, Osorio S, Heredia A. (1999). Monitoring and visualising plant cuticles by confocal laser scanning microscopy. *Plant Physiology and Biochemistry* 10, 789-794.
- Flaishman MA, Kolattukudy PE. (1994). Timing of fungal invasion using host's ripening hormone as a signal. *Proceedings of the National Academy of Sciences, USA* 91, 6579-6583.
- Franchini MC, Hernández LF, Lindström LI. (2010). Cuticle and cuticular wax development in the sunflower (*Helianthus annuus* L.) pericarp grown at the field under a moderate water deficit. *Revista Internacional de Botánica Experimental* 79, 153-161.
- Franke R, Briesen I, Wojciechowski T, Faust A, Yephremov A, Nawrath C, Schreiber L. (2005). Apoplastic polyesters in *Arabidopsis* surface tissues—a typical suberin and a particular cutin. *Phytochemistry* 66, 2643-2658.
- Gérard HC, Osman SF, Fett WF, Moreau RA. (1992). Separation, identification and quantification of monomers from cutin polymers by high performance liquid chromatography and evaporative light scattering detection. *Phytochemical Analysis* 3, 139-144.
- Gibert C, Chadoeuf J, Vercambre G, Génard M, Lescourret F. (2007). Cuticular cracking on nectarine fruit surface: spatial distribution and development in relation to irrigation and thinning. *Journal of the American Society for Horticultural Science* 132, 583–591.
- Gilding EK, Marks MD. (2010). Analysis of purified glabra3-shape shifter trichomes reveals a role for NOECK in regulating early trichomemorphogenic events. *The Plant Journal* 64, 304–17.
- Girard A-L, Mounet F, Lemaire-Chamley M, Gaillard C, Elmorjani K, Vivancos J, Runavot J-L, Quemener B, Petit J, Germain V, Rothan C, Marion D, Bakan B. (2012). Tomato GDSL1 is required for cutin deposition in the fruit cuticle. *The Plant Cell* 24, 3119–3134.

- Glenn GM, Poovaiah BW. (1989). Cuticular properties and postharvest calcium applications influence cracking of sweet cherries. *Journal of the American Society for Horticultural Science*, 114.
- Gomes S, Bacelar E, Martins-Lopes P, Carvalho T, Guedes-Pinto H. (2012). Infection process of olive fruits by *Colletotrichum acutatum* and the protective role of the cuticle and epidermis. *Journal of Agricultural Science* 4, 101-110.
- Graça J, Schreiber L, Rodrigues J, Pereira H. (2002). Glycerol and glyceryl esters of ω -hydroxyacids in cutins. *Phytochemistry* 61, 205-215.
- Graça J, Lamosa P. (2010). Linear and branched poly(ω -hydroxyacid) esters in plant cutins. *Journal of Agricultural Food Chemistry* 58, 9666–9674.
- Grimm E, Khanal BP, Winkler A, Knoche M, Köpcke D. (2012). Structural and physiological changes associated with the skin spot disorder in apple. *Postharvest Biology and Technology* 64, 111-118.
- Guetsky R, Kobiler I, Wang X, Perlman N, Gollop N, Avila-Quezada G, Hadar I, Prusky D. (2005). Metabolism of the flavonoid epicatechin by laccase of *Colletotrichum gloeosporioides* and its effect on pathogenicity on avocado fruits. *Biochemistry and Cell Biology* 95, 1345-1348.
- Hen-Avivi S, Lashbrooke J, Costa F, Aharoni A. (2014). Scratching the surface: genetic regulation of cuticle assembly in fleshy fruit. *Journal of Experimental Botany* 65(16), 4653-4664.
- Heredia-Guerrero JA, de Lara R, Domínguez E, Heredia A, Benavente J, Benítez JJ. (2012). Chemical–physical characterization of isolated plant cuticles subjected to low-dose γ -irradiation. *Chemistry and Physics of Lipids* 165, 803-808.
- Holloway PJ. (1973). Cutins of *Malus pumila* fruits and leaves. *Phytochemistry* 12, 2913-2920.
- Holloway PJ. (1982). Structure and histochemistry of plant cuticular membranes: an overview. In: K. Cutler, K. Alvin and C. Price, eds. *The Plant Cuticle*. London: Academic Press, 1-32.
- Hovav R, Chehanovsky N, Moy M, Jetter R, Schaffer AA. (2007). The identification of a gene (*Cwp1*), silenced during *Solanum* evolution, which causes cuticle microfissuring and dehydration when expressed in tomato fruit. *The Plant Journal* 52, 627-639.
- Hua W, Molina I, Shockey J, Browse J. (2010). Organ fusion and defective cuticle function in a *lacs1 lacs2* double mutant of Arabidopsis. *Planta* 231, 1089-1100.

- Hunt G, Baker E. (1980). Phenolic constituents of tomato fruit cuticles. *Phytochemistry* 19, 1415-1419.
- Isaacson T, Kosma DK, Matas AJ, Buda GJ, He Y, Yu B, Pravitasari A, Batteas JD, Stark RE, Jenks MA, Rose JKC. (2009). Cutin deficiency in the tomato fruit cuticle consistently affects resistance to microbial infection and biomechanical properties, but not transpirational water loss. *The Plant Journal* 60, 363–377.
- Jakoby MJ, Falkenhan D, Mader MT, Brininstool G, Wischnitzki E, Platz N, Hudson A, Hülskamp M, Larkin J, Schnittger A. (2008). Transcriptional profiling of mature *Arabidopsis* trichomes reveals that NOECK encodes the MIXTA-like transcriptional regulator MYB106. *Plant Physiology* 148, 1583–602.
- Javelle M, Vernoud V, Depège-Fargeix N, Arnould C, Oursel D, Domergue F, Sarda X, Rogowsky PM. (2010). Overexpression of the epidermis-specific homeodomain-leucine zipper IV transcription factor outer cell layer1 in maize identifies target genes involved in lipid metabolism and cuticle biosynthesis. *Plant Physiology* 154, 273–86.
- Javelle M, Vernoud V, Rogowsky PM, Ingram GC. (2011). Epidermis: the formation and functions of a fundamental plant tissue. *New Phytologist* 189, 17-39.
- Jeffree E. (2006). The fine structure of the plant cuticle. In: M. Riederer and C. Müller, eds. *Biology of the plant cuticle*. Blackwell, New York: Annual Plant Reviews, 11-125.
- Jenks MA, Eigenbrode SD, Lemieux B. (2002). Cuticular waxes of *Arabidopsis*. American Society of Plant Biologists. *The Arabidopsis Book* 1:e0016
- Jetter R, Kunst L, Samuels AL. (2006). Composition of plant cuticular waxes. In: M. Riederer and C. Müller, eds. *Biology of the Plant Cuticle*. Oxford: Blackwell, 145-181.
- Johnson B, Brun, WA. (1966). Stomatal density and responsiveness of banana fruit stomates. *Plant Physiology* 41, 99-101.
- Ju Z, Bramlage WJ. (2001). Developmental changes of cuticular constituents and their association with ethylene during fruit ripening in ‘Delicious’ apples. *Postharvest Biology and Technology* 21, 257-263.
- Kallio H, Nieminen R, Tuomasjukka S, Hakala M. (2006). Cutin composition of five Finnish berries. *Journal of Agricultural Food Chemistry* 54, 457-462.
- Kannangara R, Branigan C, Liu Y, Penfield T, Rao V, Mouille G, Hofte H, Pauly M, Riechmann JL, Broun P (2007) The Transcription Factor WIN1/SHN1 Regulates Cutin Biosynthesis in *Arabidopsis thaliana*. *Plant Cell* 19, 1278–1294
- Kasai S, Hayama H, Kashimura Y, Kudo S, Osanai Y. (2008).

- Relationship between fruit cracking and expression of the expansin gene MdEXPA3 in 'Fuji' apples (*Malus domestica* Borkh.). *Scientia Horticulturae* 116, 194-198.
- Kerstiens G. (2006). Water transport in plant cuticles: an update. *Journal of Experimental Botany* 57, 2493–2499.
- Khanal B, Grimm E, Knoche M. (2011). Fruit growth, cuticle deposition, water uptake, and fruit cracking in jostaberry, gooseberry, and black currant. *Scientia Horticulturae* 128, 289-296.
- Khanal BP, Grimm E, Knoche M. (2013). Russetting in apple and pear: a plastic periderm replaces a stiff cuticle. *AoB PLANTS* 5, pls048.
- Knoche M, Peschel S, Hinz M, Bukovac MJ. (2000). Studies on water transport through the sweet cherry fruit surface: characterizing conductance of the cuticular membrane using pericarp segments. *Planta* 212, 127-135.
- Knoche M, Peschel S, Hinz M, Bukovac MJ. (2001). Studies on water transport through the sweet cherry fruit surface: II. Conductance of the cuticle in relation to fruit development. *Planta* 213, 927-936.
- Knoche M, Beyer M, Peschel S, Oparlakov B, Bukovac MJ. (2004). Changes in strain and deposition of cuticle in developing sweet cherry fruit. *Physiologia Plantarum* 120, 667-677.
- Knoche M, Peschel S. (2006). Water on the surface aggravates microscopic cracking of the sweet cherry fruit cuticle. *Journal of the American Society for Horticultural Science* 131, 192-200.
- Knoche M, Grimm E. (2008). Surface moisture induces microcracks in the cuticle of 'Golden Delicious' apple. *Hortscience* 43, 1929–1931.
- Knoche M, Khanal BP, Stopar M. (2011). Russetting and microcracking of 'golden delicious' apple fruit concomitantly decline due to gibberellin A4+7 application. *Journal of the American Society for Horticultural Science* 136, 159-164.
- Knoche M, Peschel S. (2007). Deposition and strain of the cuticle of developing european plum fruit. *Journal of the American Society for Horticultural Science* 132, 597-602.
- Kolattukudy PE, Rogers LM, Li D, Hwang C-S, Flaishman MA. (1995). Surface signaling in pathogenesis. *Proceedings of the National Academy of Sciences, USA* 92, 4080-4087.

- Kolattukudy PE, Rogers LM, Li D, Hwang C-S, Flaishman MA. (2001). Polyesters in higher plants. *Advances in Biochemical Engineering/Biotechnology* 71, 1-49.
- Konarska A. (2013). The structure of the fruit peel in two varieties of *Malus domestica* Borkh. (Rosaceae) before and after storage. *Protoplasma* 250, 701-714.
- Kosma DK, Bourdenx B, Bernard A, Parsons EP, Lü S, Joubès J, Jenks MA. 2009. The impact of water deficiency on leaf cuticle lipids of *Arabidopsis*. *Plant Physiology* 151, 1918-1929.
- Kosma DK, Parsons EP, Isaacson T, Lü S, Rose JKC, Jenks MA. (2010). Fruit cuticle lipid composition during development in tomato ripening mutants. *Physiologia Plantarum* 139, 107-117.
- Krauss P, Markstädter C, Riederer M. (1997). Attenuation of UV radiation by plant cuticles from woody species. *Plant, Cell and Environment* 20, 1079-1085.
- Kubo H, Kishi M, Goto K. (1999). ANTHOCYANINLESS2, a homeobox gene affecting anthocyanin distribution and root development in *Arabidopsis*. *The Plant Cell* 11, 1217-1226.
- Kutschera U, Niklas KJ. (2007). The epidermal-growth-control theory of stem elongation: An old and a new perspective. *Journal of Plant Physiology* 164, 1395-1409.
- Lara I, Belge B, Goulao LF. (2014). The fruit cuticle as a modulator of postharvest quality. *Postharvest Biology and Technology* 87, 103-112.
- Léchaudel M, Lopez-Lauri F, Vidal V, Sallanon H, Joas J. (2013). Response of the physiological parameters of mango fruit (transpiration, water relations and antioxidant system) to its light and temperature environment. *Journal of Plant Physiology* 170, 567-576.
- Lee DR. (1989). Vasculature of the abscission zone of tomato fruit: implications for transport. *Canadian Journal of Botany* 67(6), 1898-1902.
- Leide J, Hildebrandt U, Reussing K, Riederer M, Vogg G. (2007). The developmental pattern of tomato fruit wax accumulation and its impact on cuticular transpiration barrier properties: effects of a deficiency in a β -ketoacyl-Coenzyme A synthase (LeCER6). *Plant Physiology* 144, 1667-1679.
- Leide J, Hildebrandt U, Vogg G, Riederer M. (2011). The *positional sterile* (*ps*) mutation affects cuticular transpiration and wax biosynthesis of tomato fruits. *Journal of Plant Physiology* 168, 871-877.

- Lendzian KJ, Kerstiens G. (1991). Sorption and transport of gases and vapors in plant cuticles. *Reviews of Environmental Contamination and Toxicology* 121, 65-128.
- Liu D-C, Zeng Q, Ji Q-X, Liu C-F, Liu S-B, Liu Y. (2012). A comparison of the ultrastructure and composition of fruits' cuticular wax from the wild-type 'Newhall' navel orange (*Citrus sinensis* [L.] Osbeck cv. Newhall) and its glossy mutant. *Plant Cell Reports* 31, 2239-2246.
- Li Y, Chen B. (2009). Phenanthrene sorption by fruit cuticles and potato periderm with different compositional characteristics. *Journal of Agricultural Food Chemistry* 57, 637-644.
- López-Casado G, Matas AJ, Domínguez E, Cuartero J, Heredia A. (2007). Biomechanics of isolated tomato (*Solanum lycopersicum* L.) fruit cuticles: the role of the cutin matrix and polysaccharides. *Journal of Experimental Botany* 58, 3875-3883.
- Lundqvist J. (2007). From field to fork. Wasteage in the food chain.: Stockholm International Water Institute. *Water Front Magazine* 3 <http://www.siwi.org>.
- Maguire KM, Banks NH, Lang A. (1999). Sources of variation in water vapour permeance of apple fruit. *Postharvest Biology and Technology* 17, 11-17.
- Maguire KM, Banks NH, Opara LU. (2001). Factors affecting weight loss of apples. *Horticultural Reviews* 25, 197-234.
- Manandhar JB, Hartman GL, Wang TL. (1995). Anthracnose development on pepper fruits inoculated with *Colletotrichum gloeosporioides*. *The American Phytopathological Society* 79, 380-383.
- Marques JPR, Spósito MB, Mello AFS, Amorim L, Mondin M, Appezzato-da-Glória B. (2012). Histopathology of black spot symptoms in sweet oranges. *European Journal of Plant Pathology* 33, 439-448.
- Matas AJ, Cuartero J, Heredia A. (2004a). Phase transitions in the biopolyester cutin isolated from tomato fruit cuticles. *Thermochimica Acta* 409, 165-168.
- Matas AJ, Cobb ED, Bartsch JA, Paolillo DJ, Niklas KJ. (2004b). Biomechanics and anatomy of *Lycopersicon esculentum* fruit peels and enzyme-treated samples. *American Journal of Botany* 91, 352-360.
- Matas AJ, Agustí J, Tadeo FR, Talón M, Rose JKC. (2010). Tissue-specific transcriptome profiling of the citrus fruit epidermis and subepidermis using laser capture microdissection. *Journal of Experimental Botany* 61, 3321-3330.

- Matas AJ, Yeats TH, Buda GJ, Zheng Y, Chatterjee S, Tohge T, Ponnala L, Adato A, Aharoni A, Stark R, Fernie AR, Fei Z, Giovannoni JJ, Rose JKC. (2011). Tissue- and cell-type specific transcriptome profiling of expanding tomato fruit provides insights into metabolic and regulatory specialization and cuticle formation. *The Plant Cell* 23, 3893–3910.
- McDonald RE, Nordby HE, McCollum TG. (1993). Epicuticular wax morphology and composition are related to grapefruit chilling injury. *HortScience* 28, 311-312.
- Measham PF, Bound SA, Gracie AJ, Wilson SJ. (2009). Incidence and type of cracking in sweet cherry (*Prunus avium* L.) are affected by genotype and season. *Crop and Pasture Science* 60, 1002–1008.
- Miller RH. (1982). Apple fruit cuticles and the occurrence of pores and transcuticular canals. *Annals of Botany* 50, 355-371.
- Miller RH. (1984). The multiple epidermis-cuticle complex of medlar fruit *Mespilus germanica* L. (Rosaceae). *Annals of Botany* 53, 779-792.
- Mintz-Oron S, Mandel T, Rogachev I, Feldberg L, Lotan O, Yativ M, Wang Z, Jetter R, Venger I, Adato A, Aharoni A. (2008). Gene expression and metabolism in tomato fruit surface tissues. *Plant Physiology* 147, 823-851.
- Moco S, Capanoglu E, Tikunov Y, Bino RJ, Boyacioglu D, Hall RD, Vervoort J, De Vos RCH. (2007). Tissue specialization at the metabolite level is perceived during the development of tomato fruit. *Journal of Experimental Botany* 58, 4131–4146.
- Montanaro G, Dichio B, Xiloyannis C. (2012). Fruit transpiration: mechanisms and significance for fruit nutrition and growth. In: G. Montanaro and B. Dichio eds. *Advances in Selected Plant Physiology Aspects*. InTech. ISBN 978-953-51-0557-2.
- Moral J, Bouhmidi K, Trapero A. (2008). Influence of fruit maturity, cultivar susceptibility, and inoculation method on infection of olive fruit by *Colletotrichum acutatum*. *Plant Disease* 92, 1421-1426.
- Morice IM, Shorland FB. (1973). Composition of the surface waxes of apple fruits and changes during storage. *Journal of the Science of Food and Agriculture* 24, 1331-1339.
- Muir SR, Collins GJ, Robinson S, Hughes S, Bovy S, Ric De Vos CH, van Tunen AJ, Verhoeyen ME. (2001). Overexpression of petunia chalcone isomerase in tomato results in fruit containing increased levels of flavonols. *Nature Biotechnology* 19, 470-474.

- Müller IK, Fellman J. (2007). Pre-harvest application of soybean oil alters epicuticular wax crystallisation patterns and resistance to weight loss in ‘Golden Delicious’ apples during storage. *Journal of Horticultural Science and Biotechnology* 82, 207-216.
- Nadakuduti SS, Pollard M, Kosma DK, Allen C Jr, Ohlrogge JB, Barry CS. (2012). Pleiotropic phenotypes of the sticky peel mutant provide new insight into the role of CUTIN DEFICIENT2 in epidermal cell function in tomato. *Plant Physiology* 159, 945–960.
- Navarro M, Ayax C, Martinez Y, Laur J, El Kayal W, Marque C, Teulieres C. (2011). Two EguCBF1 genes overexpressed in *Eucalyptus* display a different impact on stress tolerance and plant development. *Plant Biotechnology J* 9, 50–63.
- Niklas KJ. (1992). Plant biomechanics: an engineering approach to plant form and function. Chicago: University of Chicago Press.
- Nordby HE, McDonald RE. (1995). Variations in chilling injury and epicuticular wax composition of white grapefruit with canopy position and fruit development during the season. *Journal of Agricultural and Food Chemistry* 43, 1828-1833.
- Opara LU, Studman CJ, Banks NH. (1997). Fruit skin splitting and cracking. In: J. Janick, ed. *Horticultural Reviews* 19. Oxford, U.K.: John Wiley and Sons, Inc. 217–262.
- Oshima Y, Mitsuda N. (2013). The MIXTA-like Transcription factor MYB16 is a major regulator of cuticle formation in vegetative organs. *Plant Signaling & Behavior* 9 [pii:e26826].
- Parsons EP, Popopvsky S, Lohrey GT, Lü S, Alkalai-Tuvia S, Perzelan Y, Paran I, Fallik E, Jenks MA. (2012). Fruit cuticle lipid composition and fruit post-harvest water loss in an advanced backcross generation of pepper (*Capsicum* sp.). *Physiologia Plantarum* 146, 15-25.
- Parsons EP, Popopvsky S, Lohrey GT, Alkalai-Tuvia S, Perzelan Y, Bosland P, Bebeli PJ, Paran I, Fallik E, Jenks MA. (2013). Fruit cuticle lipid composition and water loss in a diverse collection of pepper (*Capsicum*). *Physiologia Plantarum* 49, 160–174.
- Peschel S, Beyer M, Knoche M. (2003). Surface characteristics of sweet cherry fruit: stomata-number, distribution, functionality and surface wetting. *Scientia Horticulturae* 97, 265-278.
- Peschel S, Knoche M. (2005). Characterization of microcracks in the cuticle of developing sweet cherry fruit. *Journal of the American Society for Horticultural Science* 130, 487-495.

- Peschel S, Franke R, Schreiber L, Knoche M. (2007). Composition of the cuticle of developing sweet cherry fruit. *Phytochemistry* 68, 1017-1025.
- Peschel S, Knoche M. (2012). Studies on water transport through the sweet cherry fruit surface: XII. Variation in cuticle properties among cultivars. *Journal of the American Society for Horticultural Science* 137, 367–375.
- Petracek PD, Bukovac MJ. (1995). Rheological properties of enzymatically isolated tomato fruit cuticle. *Plant Physiology* 109, 675-679.
- Pham TTM, Singh Z, Behboudian M. (2012). Different surfactants improve calcium uptake into leaf and fruit of 'washington navel' sweet orange and reduce albedo breakdown. *Journal of Plant Nutrition* 35, 889-904.
- Pieniasek SA. (1944). Physical characters of the skin in relation to apple fruit transpiration. *Plant Physiology* 19, 529-536.
- Podila GK, Rogers LM, Kolattukudy PE. (1993). Chemical signals from avocado surface wax trigger germination and appressorium formation in *Colletotrichum gloeosporioides*. *Plant Physiology* 103, 267-272.
- Pollard M, Beisson F, Li Y, Ohlrogge JB. (2008). Building lipid barriers: biosynthesis of cutin and suberin. *Trends in Plant Science* 13, 236-246.
- Prasanna V, Prabha, TN, Tharanathan RN. (2007). Fruit ripening phenomena—an overview. *Critical Reviews in Food Science and Nutrition* 47, 1-19.
- Ranathunge NP, Mongkolporn O, Ford R, and Taylor PWI. (2012). *Colletotrichum truncatum* pathosystem on *Capsicum* spp: infection, colonization and defence mechanisms. *Australasian Plant Pathology* 41, 463-473.
- Reig C, Mesejo C, Martínez-Fuentes A, Agustí M. (2010). Climatic factors affecting the occurrence of cloudy stain on the fruit skin of 'Triumph' Japanese persimmon. *Annals of Applied Biology* 156, 421-429.
- Reina-Pinto JJ, Yephremov A. (2009). Surface lipids and plant defenses. *Plant Physiology and Biochemistry* 47, 540–549.
- Richmond DV, Martin JT. (1959). Studies on plant cuticle III. The composition of the cuticle of apple leaves and fruits. *Annals of Applied Biology* 47, 583-596.
- Rosado BHP, Holder CD. (2013). The significance of leaf water repellency in ecohydrological research: a review. *Ecohydrology* 6, 150-161.
- Roy S, Conway WS, Watada AE, Sams CE, Erbe EF, Wergin WP. (1999). Changes in the ultrastructure of the epicuticular wax and postharvest calcium uptake in apples. *HortScience* 341, 121-124.

- Ruiz-May E, Rose JKC. (2013). Cell wall architecture and metabolism in ripening fruit and the complex relationship with softening. In: Wiley, ed. *The Molecular Biology and Biochemistry of Fruit Ripening*. Giovannoni JJ, Poole M, Seymour GB, Tucker GA, 163-187.
- Saladié M, Matas AJ, Isaacson T, Jenks MA, Goodwin SM, Niklas KJ, Xiaolin R, Labavitch JM, Shackel KA, Fernie AR, Lytovchenko A, O'Neill MA, Watkins CB, Rose JKC. (2007). A reevaluation of the key factors that influence tomato fruit softening and integrity. *Plant Physiology* 144, 1012-1028.
- Samuels L, Kunst L, Jetter R. (2008). Sealing plant surfaces: Cuticular wax formation by epidermal cells. *Annual Review of Plant Biology* 59, 683–707.
- Schönherr J. (1976). Water permeability of isolated cuticular membranes: the effect of cuticular waxes on diffusion of water. *Planta* 131, 159-164.
- Schönherr J. (2000). Calcium chloride penetrates plant cuticles via aqueous pores. *Planta* 212, 112-118.
- Schönherr J, Schreiber L. (2004). Size selectivity of aqueous pores in astomatous cuticular membranes isolated from *Populus canescens* (Aiton) Sm. leaves. *Planta* 219, 405-411.
- Schönherr J. (2006). Characterization of aqueous pores in plant cuticles and permeation of ionic solutes. *Journal of Experimental Botany* 57, 2471-2491.
- Schreiber L, Riederer M. (1996). Ecophysiology of cuticular transpiration: comparative investigation of cuticular water permeability of plant species from different habitats. *Oecologia* 107, 426-432.
- Schreiber L. (2005). Polar paths of diffusion across plant cuticles: New evidence for an old hypothesis. *Annals of Botany* 95, 1069-1073.
- Schreiber L. (2010). Transport barriers made of cutin, suberin and associated waxes. *Trends in Plant Science* 15, 546-553.
- Seo PJ, Xiang F, Qiao M, Park J-Y, Lee YN, Kim S-G, Lee Y-H, Park WJ, Park C-M. (2009). The MYB96 transcription factor mediates abscisic acid signaling during drought stress response in *Arabidopsis*. *Plant Physiology* 151, 275-289.
- Seo PJ, Park CM. (2010). MYB96-mediated abscisic acid signals induce pathogen resistance response by promoting salicylic acid biosynthesis in *Arabidopsis*. *New Phytologist* 186, 471–83.
- Seo PJ, Park CM. (2011). Cuticular wax biosynthesis as a way of inducing drought resistance. *Plant Signal & Behavior* 6,1043–5.

- Seymour GB, Chapman NH, Chew BL, Rose JKC. (2013). Regulation of ripening and opportunities for control in tomato and other fruits. *Plant Biotechnology Journal* 11, 269-278.
- Shafer WE, Bukovac MJ. (1987). Studies on octylphenoxy surfactants III. sorption of triton X-100 by isolated tomato fruit cuticles. *Plant Physiology* 85, 965-970.
- Shechter M, Xing B, Kopinke F-D, Chefetz B. (2006). Competitive sorption-desorption behavior of triazine herbicides with plant cuticular fractions. *Journal of Agricultural Food Chemistry* 54, 7761-7768.
- Shi JX, Malitsky S, De Oliveira S, Branigan C, Franke RB, Schreiber L, Aharoni A. (2011). SHINE transcription factors act redundantly to pattern the archetypal surface of *Arabidopsis* flower organs. *PLoS Genetics* 7, e1001388.
- Shi JX, Adato A, Alkan N, He Y, Lashbrooke J, Matas AJ, Meir S, Malitsky S, Isaacson T, Prusky D, Leshkowitz D, Schreiber L, granell AR, Widemann E, Grausem B, Pinot F, Rose JKC, Rogachev I, Rothan C, Aharoni A. (2013) The tomato SISHINE3 transcription factor regulates fruit cuticle formation and epidermal patterning. *New Phytologist* 197, 468-480.
- Simon G. (2006). Review on rain induced fruit cracking of sweet cherries (*Prunus avium* L.), its causes and the possibilities of prevention. *International Journal of Horticultural Science* 12, 27-35.
- Solovchenko A, Merzlyak M. (2003). Optical properties and contribution of cuticle to UV protection in plants: experiments with apple fruit. *Photochemistry and Photobiology Science* 2, 861-866.
- Tanaka H, Machida Y. (2006). The cuticle and cellular interactions. In: M. R. and C. Mülle, ed. Biology of the plant cuticle. Blackwell, New York: *Annual Plant Reviews* 313-333.
- Tessmer MA, Antonioli, LR, Appezzato-da-Glória B. (2012). Cuticle of 'Gala' and 'Galaxy' apples cultivars under different environmental conditions. *Brazilian Archives of Biology and Technology* 55, 709-714.
- Tsubaki S, Ozaki Y, Yonemori K, Azuma J-I. (2012). Mechanical properties of fruit-cuticular membranes isolated from 27 cultivars of *Diospyros kaki* Thunb. *Food Chemistry* 132, 2135-2139.
- Tsubaki S, Sugimura K, Teramoto Y, Yonemori K, Azuma J-I. (2013). Cuticular membrane of Fuyu persimmon fruit is strengthened by triterpenoid nano-fillers. *PLOS One* 8, e75275. doi:10.1371/journal.pone.0075275.

- Veraverbeke EA, Lammertyn J, Saevels S, Nicolai BM. (2001a). Changes in chemical wax composition of three different apple (*Malus domestica* Borkh.) cultivars during storage. *Postharvest Biology and Technology* 23, 197-208.
- Veraverbeke EA, Van Bruaene N, Van Oostveldt P, Nicolai, BM. (2001b). Non destructive analysis of the wax layer of apple (*Malus domestica* Borkh.) by means of confocal laser scanning microscopy. *Planta* 213, 525-533.
- Veraverbeke EA, Verboven P, Scheerlinck N, Lan Hoang M, Nicolai BM. (2003a). Determination of the diffusion coefficient of tissue, cuticle, cutin and wax of apple. *Journal of Food Engineering* 58, 285-294.
- Veraverbeke EA, Verboven P, Van Oostveldt P, Nicolai BM. (2003b). Prediction of moisture loss across the cuticle of apple (*Malus sylvestris* subsp. *mitis* (Wallr.)) during storage Part 1. Model development and determination of diffusion coefficients. *Postharvest Biology and Technology* 30, 75-88.
- Vidhyasekaran P. (2010). Fungal pathogenesis in plants and crops: molecular biology and host defense mechanisms. second ed.:Taylor and Francis Group.
- Villena JF, Domínguez E, Stewart D, Heredia A. (1999). Characterization and biosynthesis of non-degradable polymers in plant cuticles. *Planta* 208, 181-187.
- Vogg G, Fischer S, Leide J, Emmanuel E, Jetter R, Levy AA, Riederer M. (2004). Tomato fruit cuticular waxes and their effects on transpiration barrier properties: functional characterization of a mutant deficient in a very-long-chain fatty acid β -ketoacyl-CoA synthase. *Journal of Experimental Botany* 55, 1401-1410.
- Wang Y, Lu W, Li J, Jiang Y. (2006). Differential expression of two expansin genes in developing fruit of cracking-susceptible and -resistant litchi cultivars. *Journal of the American Society for Horticultural Science* 131, 118-121.
- Wang Z-Y, Xiong L, Li W, Zhu J-K, Zhu J. (2011). The plant cuticle is required for osmotic stress regulation of abscisic acid biosynthesis and osmotic stress tolerance in *Arabidopsis*. *The Plant Cell* 23,1971-1984.
- Wang Y, Wan L, Zhang L, Zhang Z, Zhang H, Quan R, Zhou S, Huang R. (2012). An ethylene response factor OsWR1 responsive to drought stress transcriptionally activates wax synthesis related genes and increases wax production in rice. *Plant Molecular Biology* 78:275–88.
- Watkins CB. (2006). The use of 1-methylcyclopropene (1-MCP) on fruits and vegetables. *Biotechnology Advances* 24, 389-409.

- Wu R, Li S, He S, Waßmann F, Yu C, Qin G, Schreiber L, Qu L-J, Gu H. (2011). CFL1, a WW domain protein, regulates cuticle development by modulating the function of HDG1, a class IV homeodomain transcription factor, in rice and *Arabidopsis*. *The Plant Cell* 23, 3392–411.
- Yeats TH, Howe, KJ, Matas AJ, Buda GJ, Thannhauser TW, Rose JKC. (2010). Mining the surface proteome of tomato (*Solanum lycopersicum*) fruit for proteins associated with cuticle biogenesis. *Journal of Experimental Botany* 13, 3759–3771.
- Yeats TH, Buda GJ, Wang Z, Chehanovsky N, Moyle LC, Jetter R, Schaffer AA, Rose JKC. (2012). The fruit cuticles of wild tomato species exhibit architectural and chemical diversity, providing a new model for studying the evolution of cuticle function. *The Plant Journal* 69, 655-666.
- Yeats TH, Rose JKC. (2013). The formation and function of plant cuticles. *Plant Physiology* 163, 5-20.
- Yu H, Chen X, Hong Y-Y, Wang Y, Xu P, Ke S-D, Liu H-Y, Zhu J-K, Oliver DJ, Xiang C-B. (2008). Activated expression of an Arabidopsis HD-START protein confers drought tolerance with improved root system and reduced stomatal density. (2008). *The Plant Cell* 20, 1134-1151.
- Zhang JY, Broeckling CD, Blancaflor EB, Sledge MK, Sumner LW, Wang ZY. (2005). Overexpression of WXP1, a putative *Medicago truncatula* AP2 domain-containing transcription factor gene, increases cuticular wax accumulation and enhances drought tolerance in transgenic alfalfa (*Medicago sativa*). *The Plant Journal* 42, 689-707.
- Zhang JY, Broeckling CD, Sumner LW, Wang ZY. (2007). Heterologous expression of two *Medicago truncatula* putative ERF transcription factor genes, WXP1 and WXP2, in *Arabidopsis* led to increased leaf wax accumulation and improved drought tolerance, but differential response in freezing tolerance. *Plant Molecular Biology* 64, 265-278.
- Zoffoli JP, Latorre BA, Naranjo P. (2008). Hairline, a postharvest cracking disorder in table grapes induced by sulfur dioxide. *Postharvest Biology and Technology* 47, 90-97.
- Zoffoli JP, Latorre BA, Rodriguez J, Aguilera JM. (2009). Biological indicators to estimate the prevalence of gray mold and hairline cracks on table grapes cv. Thompson Seedless after cold storage. *Postharvest Biology and Technology* 52, 126–133.

CHAPTER 2

Enzymatic Synthesis of the Plant Biopolyester Cutin by Cutin Deficient 1 (CD1), an Extracellular GDSL Lipase Hydrolase

* A version of this chapter has been published in:

Nature Chemical Biology. (2012). 8, 609–611. doi:10.1038/nchembio.960

Abstract

A hydrophobic cuticle consisting of waxes and the polyester cutin covers the aerial epidermis of all land plants, providing essential protection from desiccation and other stresses. In this study, the enzymatic basis of cutin polymerization through characterization of a tomato extracellular acyltransferase, CD1, and its substrate, 2-mono(10,16-dihydroxyhexadecanoyl)glycerol was determined. CD1 has in vitro polyester synthesis activity and is required for cutin accumulation in vivo, indicating that it is a cutin synthase.

Introduction

Fossil evidence suggests that evolution of a hydrophobic cuticle was essential for terrestrial colonization by plants ~400 million years ago (Edwards, 1993). As the primary interface between the plants and their above-ground environment, the cuticle is critical in limiting water loss and has additional key roles in defense against pests and pathogens, as well as in establishing organ boundaries during development (Nawrath, 2006). The cuticle consists of an insoluble polyester of hydroxy fatty acids, known as cutin, which is covered with and infiltrated by a variety of waxes. Although the generic composition of the cutin polymer has been established, the mechanism and site of cutin polymerization have remained unknown (Heredia *et al.*, 2009; Pollard *et al.*, 2008).

Cutin is typically exceptionally abundant in the fruit cuticles of tomato (*Solanum lycopersicum*); however, several tomato mutants with substantial deficiencies in cutin were previously identified (Isaacson *et al.*, 2009). One of these

mutants, which carries the *cutin deficient 1* (*cd1*) mutation, has approximately 5–10% the amount of fruit cutin of the wild-type (M82) fruit, an extremely thin cuticle and increased sensitivity to water loss and pathogen susceptibility (Fig. 2.1a,b; Isaacson *et al.*, 2009). Fine mapping of the *cd1* mutation revealed it to lie within a five-exon gene (*CD1*; Materials and Methods, Fig. 2.2) that is predicted to encode a member of the glycine–aspartic acid–serine-leucine motif lipase/hydrolase (GDSL) family of proteins (Fig. 2.3). GDSLs collectively have diverse functions and substrate specificities (Akoh *et al.*, 2004) and are broadly distributed among multiple taxa, including prokaryotes and eukaryotes. In plants they are present as large gene families (Volkita *et al.*, 2011) and, on the basis of their expression patterns, it has been speculated that GDSLs may have a role in cuticle biosynthesis (Reina *et al.*, 2007; Irshad *et al.*, 2008; Mintz-Oron *et al.*, 2008; Yeats *et al.*, 2010; Matas *et al.*, 2011).

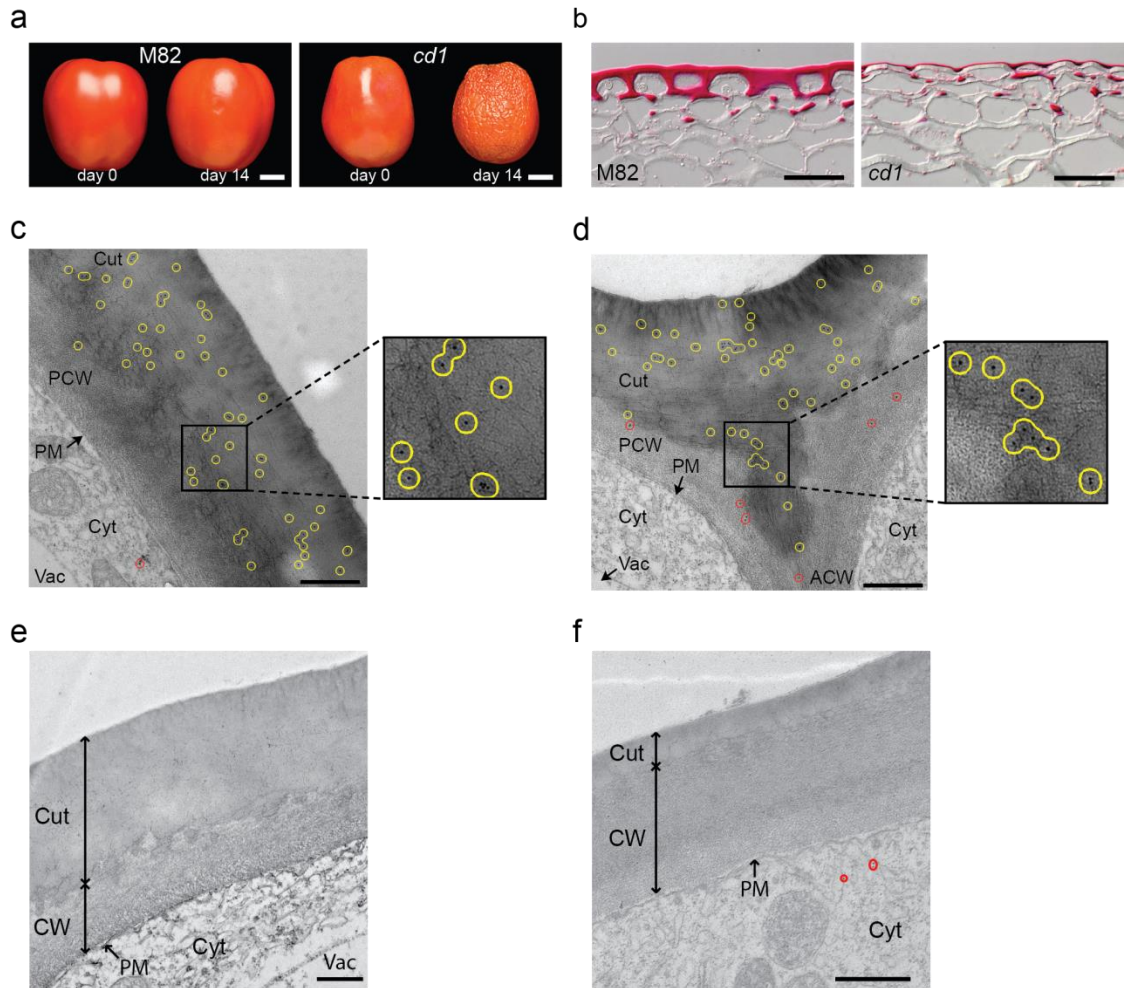


Figure 2.1. CD1 is a GDSL family protein that localizes to the nascent cuticle. (a) Fruits of the M82 wild-type tomato cultivar and the *cd1* mutant on the day of harvest at the fully ripe stage and after 14 d of storage at 20 °C. Scale bars, 1 cm. (b) Light microscopy showing the cuticle of M82 and *cd1* ripe fruit stained with Sudan Red 7b. Scale bars, 50 μ m. (c,d) TEM immunolocalization of CD1 in the cuticle of M82 fruits 15 d post anthesis, over the periclinal cell wall of an epidermal cell (c) and in the anticlinal peg of cuticle between two adjacent epidermal cells (d). (e,f) Immunolocalization negative controls: pre-immune serum tested on M82 15 days post anthesis (DPA) fruits (e) and immunogold labeling of *cd1* 15 DPA fruits (f). Scale bars, 500 nm. Gold particles are highlighted with yellow circles in the cuticle or red circles elsewhere, and areas of images c and d magnified 2.5 \times are shown to the right. Cut, cuticle; Cyt, cytoplasm; ACW, anticlinal cell wall; PCW, periclinal cell wall; PM, plasma membrane; Vac, vacuole.

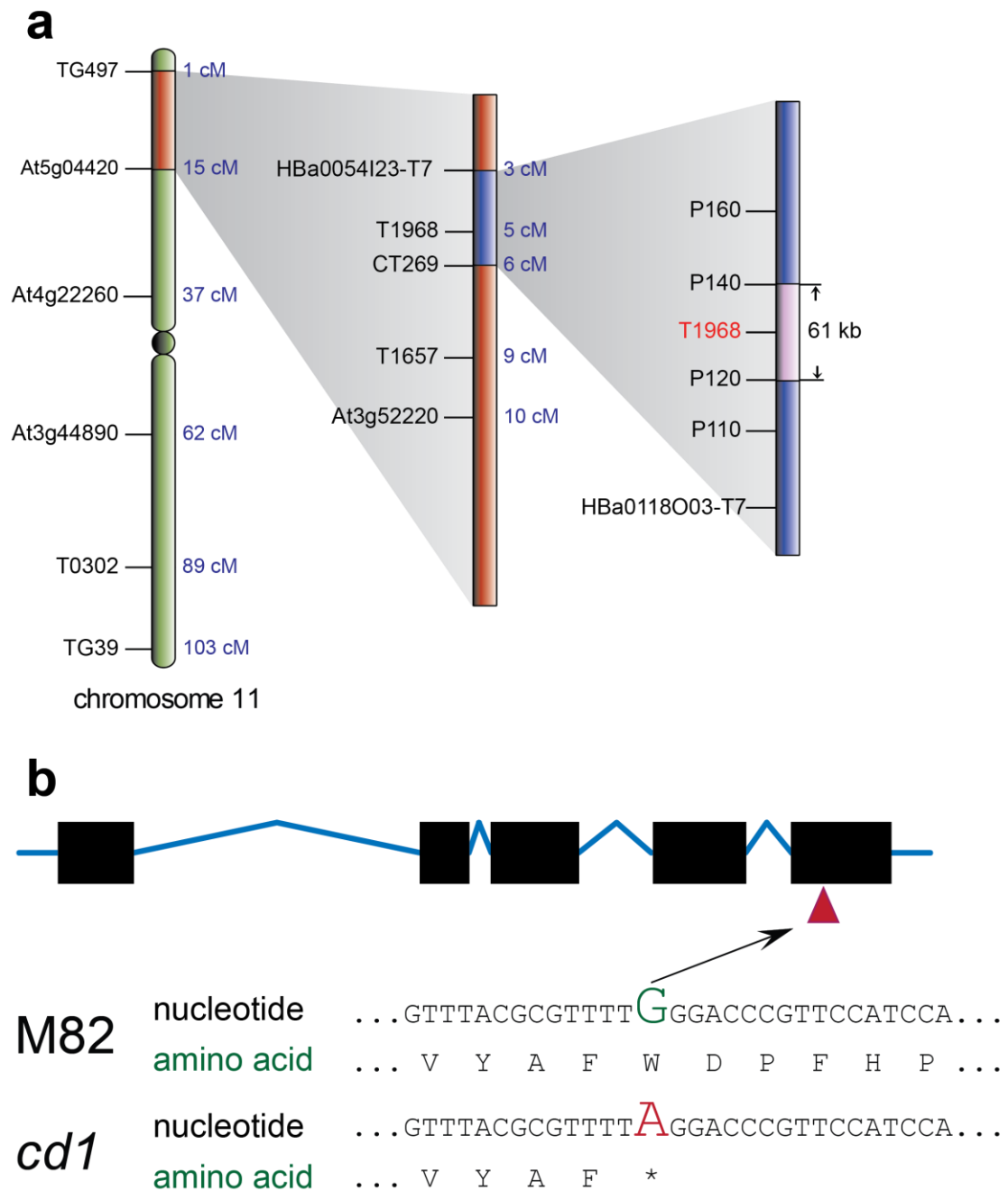


Figure 2.2. Map-based cloning of *CDI*. (a) Schematic diagram showing the mapping of *CDI* to chromosome 11 between the markers P120 and P140. Marker T1968 cosegregates with *CDI*. (b) *CDI* gene splicing model with exons represented by black boxes and introns by blue lines. In *cd1*, the substitution G to A introduces a stop codon (TAG) in the last exon leading to the truncation of the last 41 amino acids including 2 residues of the catalytic triad.

1 acaaaccaatttataatatttttgaacaacacttttttttttttttttggccaaaatggcc 61
 62 acacctaactattttttgagcttcttggtgatttttggagtggtctatttgtcaaagtgaa 121
 3 T P T I I L S F L L I F G V A I C Q S E 22
 122 gctagggcattttttgtggttgggtgattacttggatagtggaataataattatttg 181
 23 A R A F F V F G D S L V D S G N N N Y L 42
 182 gctactactgcaagggctgattcaccaccttatgggtattgattatccaacacgtagagca 241
 43 A T T A R A D S P P Y G I D Y P T R R A 62
 242 actggctgctttctctaattggctacaacattcctgacattatcagtcaacaaattggttca 301
 63 T G R F S N G Y N I P D I I S Q Q I G S 82
 302 tcagagtcaccactaccttacttagatccagctcttactggacaaagacttcttggttggt 361
 83 S E S P L P Y L D P A L T G Q R L L V G 102
 362 gctaactttgcatctgctggaattggaataactaaatgacactggaatccaatttattaat 421
 103 A N F A S A G I G I L N D T G I Q F I N 122
 422 attattcgaatgccacaacaattggcttatttttagacaatatcaaagtagagtaagtggc 481
 123 I I R M P Q Q L A Y F R Q Y Q S R V S G 142
 482 cttattggtgaagcaataactcaaagacttgtaaatcaagctcttggttcttatgactctt 541
 143 L I G E A N T Q R L V N Q A L V L M T L 162
 542 ggaggcaatgattttgtcaacaactattatcttggcccaattctgcgcgatcacgcca 601
 163 G G N D F V N N Y Y L V P N S A R S R Q 182
 602 ttttctatcaagattatgccccttatttgataagagaatatcgtaaatcttggatgaat 661
 183 F S I Q D Y V P Y L I R E Y R K I L M N 202
 662 gtgtataatcttgagctcgctgtaattgtaactggaactggaccggttaggtgtgtt 721
 203 V Y N L G A R R V I V T G T G P L G C V 222
 722 ccagcagaactagctcaactgtagcaggaacggggaatggtcaccgagttgcaacgagct 781
 223 P A E L A Q R S R N G E C S P E L Q R A 242
 782 gcaggcctgtttaacccccagcttacgcaaatggtgaggggttaaatagtgaactaggc 841
 243 A G L F N P Q L T Q M L Q G L N S E L G 262
 842 agcgatgtttttattgctgcaatacacacaacaaatgcatacgaatttcattactaatcca 901
 263 S D V F I A A N T Q Q M H T N F I T N P 282
 902 caagcatatggatttataacatcaaaggtagcatgttgggacaaggaccatataacggt 961
 283 Q A Y G F I T S K V A C C G Q G P Y N G 302
 962 cttggctatgtacaccgctctctaattttgtgcccgaatagagatgtttacgcggtttgg 1021
 303 L G L C T P L S N L C P N R D V Y A F W 322
 1022 gacccttccatccatctgagagggcaataagatcattgtgcagcaaatcatgtctggt 1081
 323 D P F H P S E R A N K I I V Q I M S G 342
 1082 acaacggagcttatgaatccaatgaaatcagtagcattctggctatggattccatgca 1141
 342 T T E L M N P M N L S T I L A M D S H A 362
 1142 taagacatatctaagatatctggaatctgattcacttgtaccttttttgggttaat 1201
 1202 tggctataaataagatgtatgcaacacttcatgttggctacttttaatttacaaaaa 1261
 1262 gtttgggtgtgctatgtttttattcacataattcagtaattctaattttaggggtggag 1321
 1322 tgtgatattggtgaagatgtaaaccaagtgtttttattaatttatatagtaatatatt 1381
 1382 tcagtgtaa 1391

Figure 2.3. CD1 nucleotide and deduced amino acid sequences. The four conserved sequence blocks of GDSL lipases are circled in green. The catalytic triad residues are indicated by a magenta star and the oxyanion hole residues by a blue hexagon. The conserved residues giving its name to GDSLs are in red while the four residues strictly conserved are in bold font. The predicted secretory signal peptide (first 19 residues) is underlined. The mutated nucleotide in *cd1* and its corresponding amino acid residue are shown in light blue and bold font.

Results and discussion

The *cdl* mutant has a point mutation introducing a stop codon upstream of two of the three predicted catalytic amino acid residues (Figs. 2.2b and 2.3). In the mutant, CD1 transcript levels were reduced (Fig. 2.4a), but the CD1 protein was not detected (Fig. 2.4c,d), indicating that it is a null mutant. Complementation of the *cdl* mutant with the wild-type gene driven by the constitutive cauliflower mosaic virus 35S promoter rescued the phenotype (Fig. 2.5a,b), confirming that the mutation in *CDI* is responsible for the cutin deficiency.

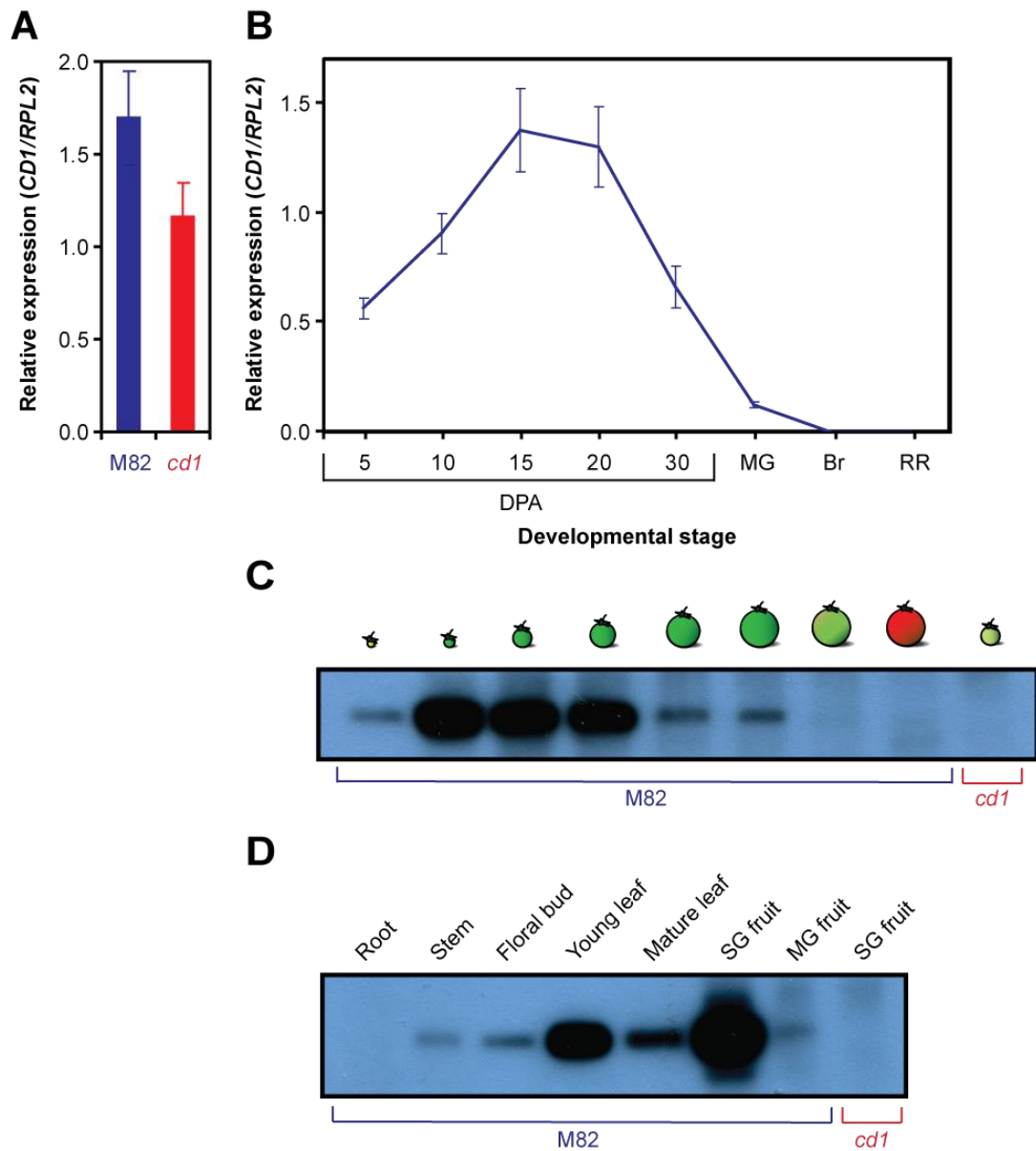


Figure 2.4. CD1 expression through fruit ontogeny and in different organs. (a) CD1 transcript levels (relative to *RPL2*) in *cd1* and M82 15 days post anthesis (DPA) fruit pericarp obtained by qRT-PCR. **(b)** CD1 transcript levels (relative to *RPL2*) in M82 fruit pericarp during fruit ontogeny, determined by qRT-PCR. **(c)** Immunoblot analysis of CD1 protein abundance levels in M82 fruit pericarp during fruit ontogeny. **(d)** Immunoblot analysis of CD1 protein expression in various tomato plant organs. SG, small green (15 DPA); MG, mature green; Br, breaker; RR, red ripe stages. RPL2: Ribosomal protein L2 (constitutive control). Error bars are SE for $n = 3$ with 3 technical replicates for (a) and $n = 2$ technical replicates for (b).

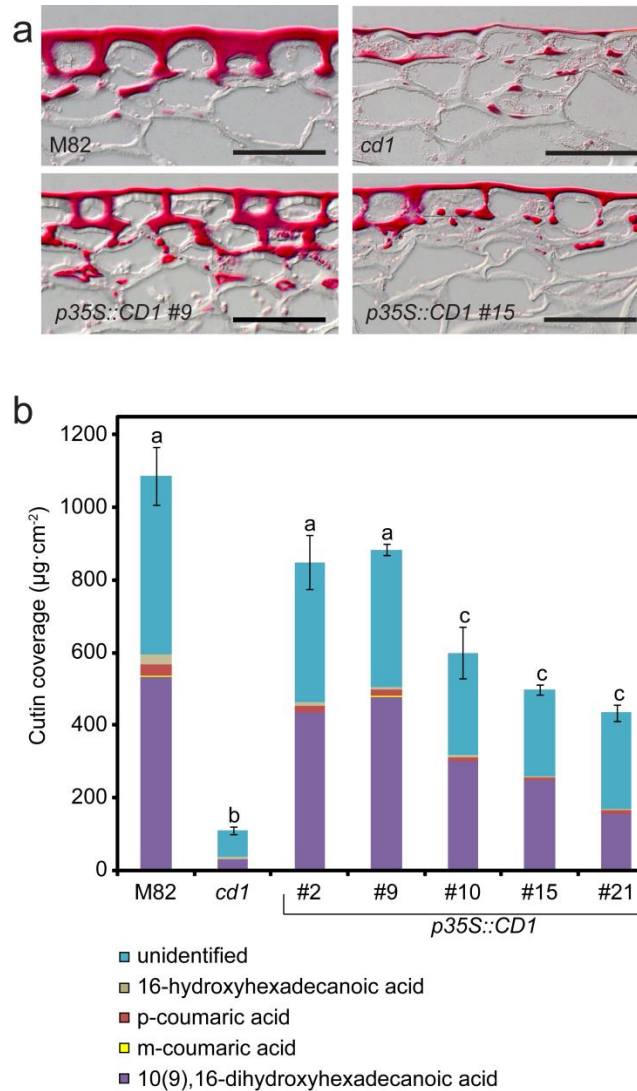


Figure 2.5. Complementation of the *cd1* mutant. (a) Light micrographs of mature green (MG) fruit pericarp sections showing fruit cuticles of M82, *cd1* and 2 independent transgenic complementation lines expressing the wild type *CDI* sequence driven by the 35S constitutive promoter, stained with Sudan Red 7b. Scale bars = 50 µm. (b) Cutin analysis of enzymatically isolated MG fruit cuticles from M82, *cd1* and 5 independent transgenic complementation lines driven by the 35S constitutive promoter. 9,16-dihydroxyhexadecanoic acid and 10,16-dihydroxyhexadecanoic acid were not separated chromatographically, so they are reported together. Typically, the 10-isomer predominates by a ratio of ~ 10:1 (Baker *et al.*, 1982). Data represent the mean of three replicates. Error bars = SE of the total cutin load. Two-tailed *t*-tests were performed on the complementation lines versus M82 and versus *cd1* at $\alpha = 0.05$. All complementation lines are statistically different from *cd1* ($P = 0.0094, 0.0001, 0.0189, 0.0001, \text{ and } 0.0011$, respectively) and lines #2 and #9 are not statistically different from M82 ($P = 0.0974 \text{ and } 0.1208$, respectively).

An analysis of the spatial distribution of CD1 proteins or the transcripts encoding them showed that expression is highest in expanding organs, which require rapid cuticle synthesis to accommodate growth (Baker *et al.*, 1982), but is undetectable in roots, which have no cuticle (Fig. 2.4b–d). Additionally, laser-capture microdissection of various pericarp tissues from young fruit was used to show that *CD1* transcript levels are highest in the outer and inner epidermal cell layers (Fig. 2.6), both of which are responsible for cuticle synthesis (Matas *et al.*, 2011). Thus, *CD1* expression parallels spatial and temporal patterns of cuticle deposition at several levels.

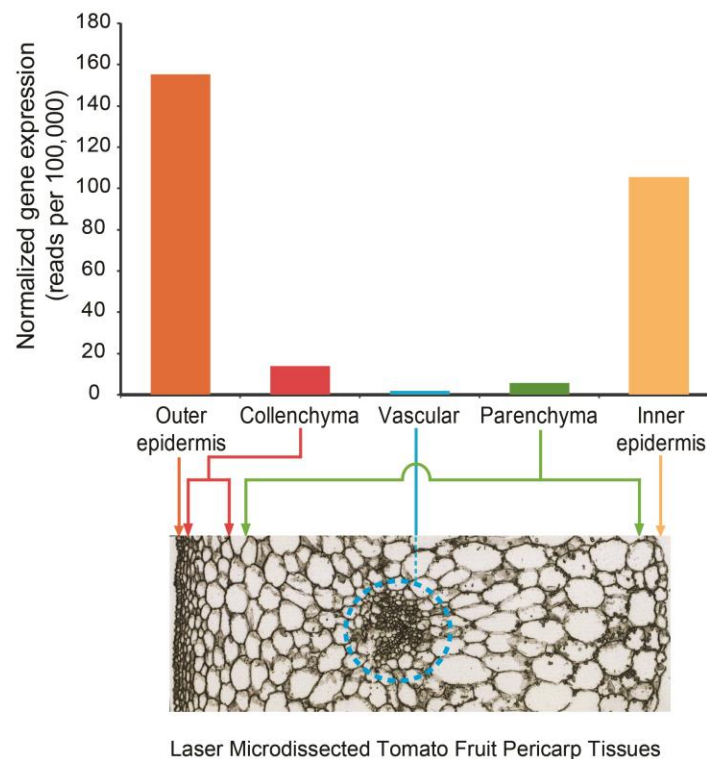


Figure 2.6. Expression of CD1 transcripts in the tomato fruit pericarp tissues. Tissues are represented in a light micrograph of a 10 DPA fruit pericarp section, based on data derived from 454 sequencing of laser capture derived cDNA libraries. Scale bar = 100 μ m.

Immunolocalization of CD1 in M82 fruits indicates that the protein is almost exclusively localized in the cuticle (Fig. 2.1c, e and f). More specifically, labeling density follows the contour of the cuticle over both the periclinal and anticlinal cell walls (Fig. 2.1d). This localization pattern suggests a role for CD1 late in the cutin biosynthetic pathway, so a direct role of CD1 in cutin polymerization was therefore investigated. Several enzymes have been shown through analysis of *Arabidopsis thaliana* mutants to be required for formation of the cutin polymer, including glycerol phosphate acyltransferase enzymes (GPATs; Pollard *et al.*, 2008). Recently, biochemical characterization of GPAT4 and GPAT6 showed them to have both glycerol 3-phosphate acyltransferase activity specific to the *sn*-2 position and phosphatase activity (Yang *et al.*, 2010). This may indicate a structural role for 2-monoacylglyceryl esters (2-MAGs) in the cutin polymer, as these were identified in small quantities in the products of partially depolymerized cutin (Graça *et al.*, 2002). Alternatively, the 2-MAG products of GPAT4 and GPAT6 may act primarily as acyl donors for the polymerization reaction. If this is true, and if CD1 is indeed a cutin polymerase, it would be expected that 2-MAGs would accumulate as free lipids in the surface tissues of the *cd1* mutant fruit, but not in the M82 wild type.

Soluble surface lipids, collectively termed cuticular waxes, can readily be extracted from plants by brief immersion of intact organs in organic solvents (Jetter *et al.*, 2006). In tomato fruits, these waxes consist primarily of a mixture of high-melting-point alkanes and triterpenoids, whereas the cutin, a polyester of principally 10,16-dihydroxyhexadecanoic acid, is not extracted and remains insoluble. Although soluble 2-MAGs can be found in the waxes associated with suberin, they are not

observed in cuticular waxes (Li *et al.*, 2007). Gas chromatography (GC)-MS analysis identified the 2-MAG species 2-mono(10,16-dihydroxyhexadecanoyl)glycerol (2-MHG, **1**) in soluble surface lipids from *cd1* fruit at the rapidly expanding stage, when CD1 is normally most highly expressed (Fig. 2.4c), but not in equivalent extracts from M82 fruit (Fig. 2.7). Although chromatographic resolution was incomplete, the coincident single-ion chromatograms of diagnostic fragments clearly show the specific accumulation of 2-MHG in the mutant (Fig. 2.7). An additional, later-eluting trace peak of these ions most likely corresponds to the thermodynamically favored 1-mono(10,16-dihydroxyhexadecanoyl)glycerol (1-MHG) isomer. The identity of the larger of the two peaks as representing the 2-isomer is confirmed by its earlier elution and the absence of the M-103 ion ($547m/z$) ion produced by α -cleavage between the 2- and 3-carbons in 1-MHG (Fig. 2.8; Graça *et al.*, 2002). Despite the clear accumulation of 2-MHG in the *cd1* mutant and not in M82 fruit, the amount detected was relatively low (on the order of $0.1 \mu\text{g cm}^{-2}$, based on comparison to wax compound abundance), possibly because of feedback regulation of the upstream biosynthetic pathway or the relatively polar nature of 2-MHG compared with other soluble surface lipids.

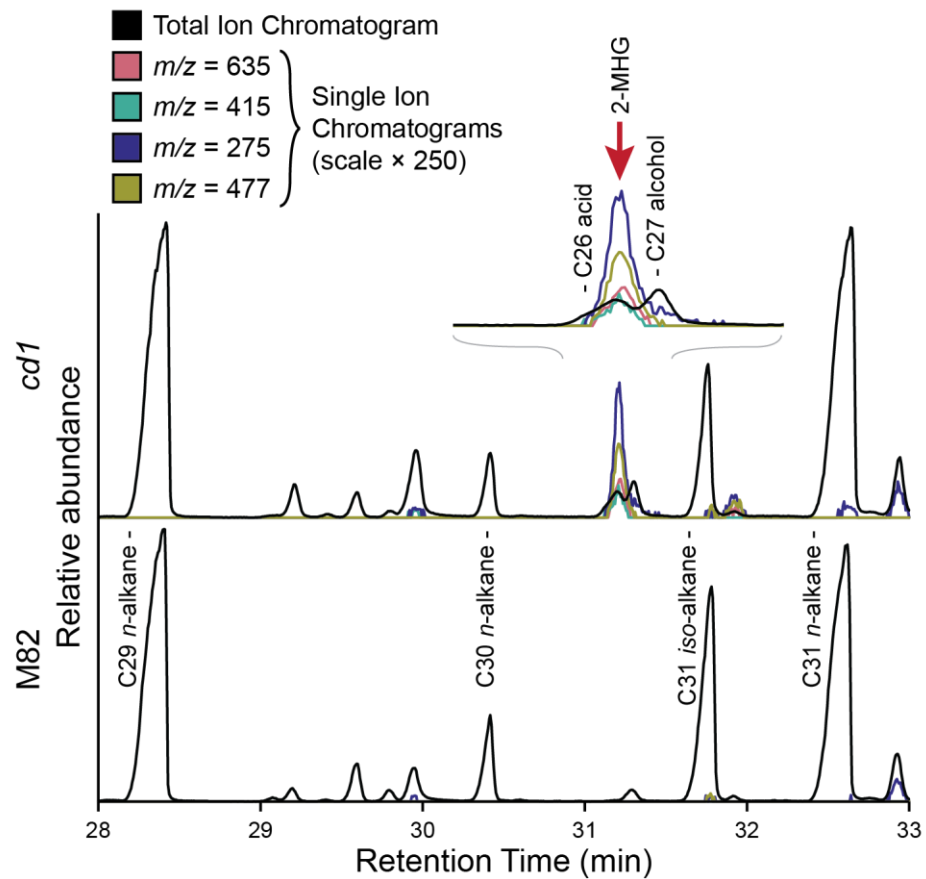


Figure 2.7. The detection of 2-MHG in the soluble surface lipids of *cd1* fruit. GC-MS chromatograms of the *cd1* mutant and M82 wild-type trimethylsilyl (TMS)-derivatized extracts. The total ion chromatograms and several single-ion chromatograms corresponding to characteristic fragments of 2-MHG are shown. Inset is an enlargement of the region surrounding the 2-MHG peak. For reference, several of the wax compounds common to both mutant and wild type are labeled.

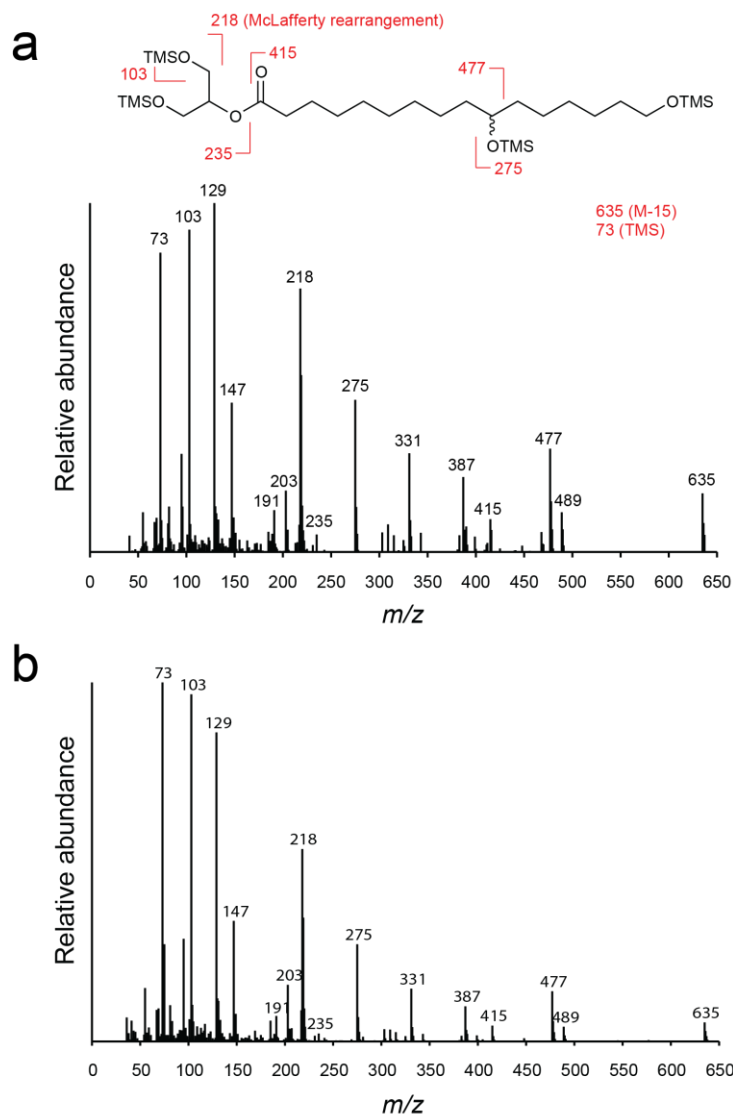


Figure 2.8. The identification of 2-MHG in the soluble surface lipids of *cd1* fruit (a) Mass spectrum from the 2-MHG peak found in the *cd1* mutant extract, with interpretation of the spectrum inset. Though the molecular ion (M) is not observed, loss of a methyl group yields the M-15 ion ($m/z = 635$). (b) EI-MS spectrum of synthetic 2-MHG. More detailed discussion of the spectrum of 2-MHG is in Graça *et al.*, 2002.

A model for cutin polymerization wherein CD1 transfers the hydroxyacyl group of 2-MHG to either another molecule of 2-MHG or the growing cutin polymer

itself is proposed in Fig. 2.9a. Experiments involving partial depolymerization of tomato cutin have identified oligomers primarily consisting of directly coupled 10,16-dihydroxyhexadecanoic acid monomers (Osman *et al.*, 1999; Graça and Lamosa, 2010). These findings, combined with the observation that glycerol is quantitatively a minor component of tomato cutin (Graça *et al.*, 2002), suggests that the principal linkage in tomato cutin is between the carboxylic acid and hydroxyl groups of 10,16-dihydroxyhexadecanoic acid. The detection of small amounts of 2-MHG in the cutin polymer (Graça *et al.*, 2002) may therefore reflect the presence of 2-MHG 'primers' remaining in the polymer. The presence of polymerized 1-MHG could be a consequence of spontaneous acyl migration accelerated by the alkaline conditions used for *in vitro* depolymerization. To test the hypothesis that CD1 acts as an acyltransferase, heterologously expressed recombinant tomato CD1 protein was purified from *Nicotiana benthamiana* (Fig. 2.10). Racemic 2-MHG was synthesized in six steps from monobenzyl-protected decane-1,10-diol (Materials and Methods and Scheme 2.1) and was used as a substrate for *in vitro* polymerization assays. Lipid products of the assay were extracted with ethyl acetate and analyzed by MALDI-TOF MS. A major series of ions separated by $m/z = 270.2$ was observed, consistent with the expected masses of sodium and potassium adducts of polyester oligomers with a glycerol end group and up to seven 10,16-dihydroxyhexadecanoyl monomers (Fig. 2.9b). A control assay was performed using the CD1^{S32A} mutant, which was prepared by site-directed mutagenesis. As expected, mutation of the conserved catalytic serine of CD1 to an alanine eliminated acyltransferase activity (Fig. 2.9c).

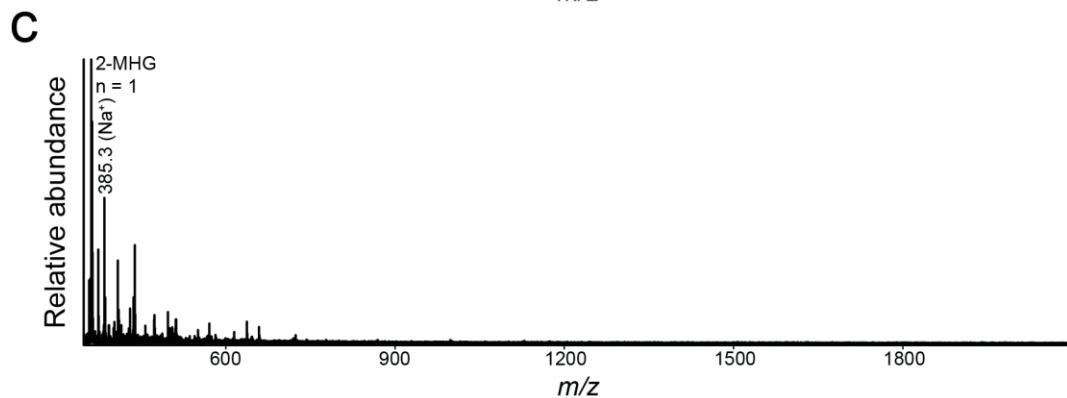
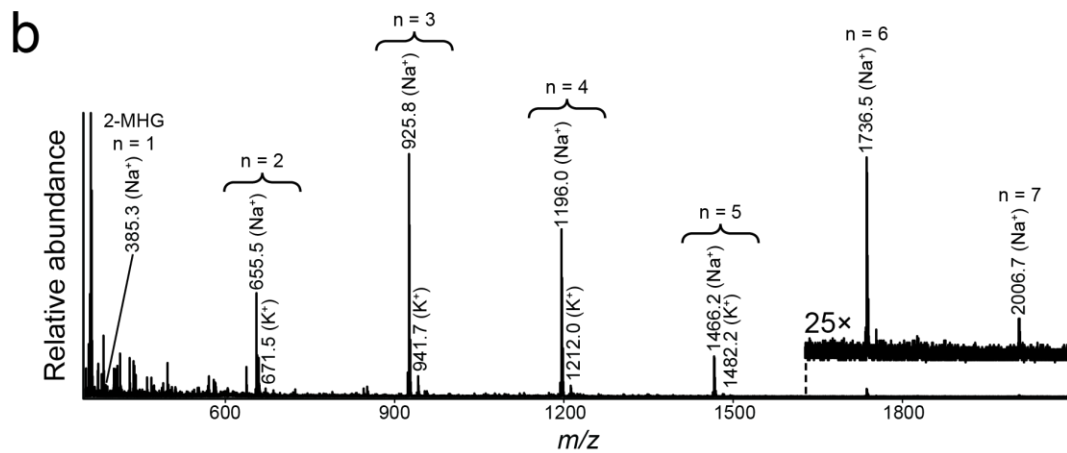
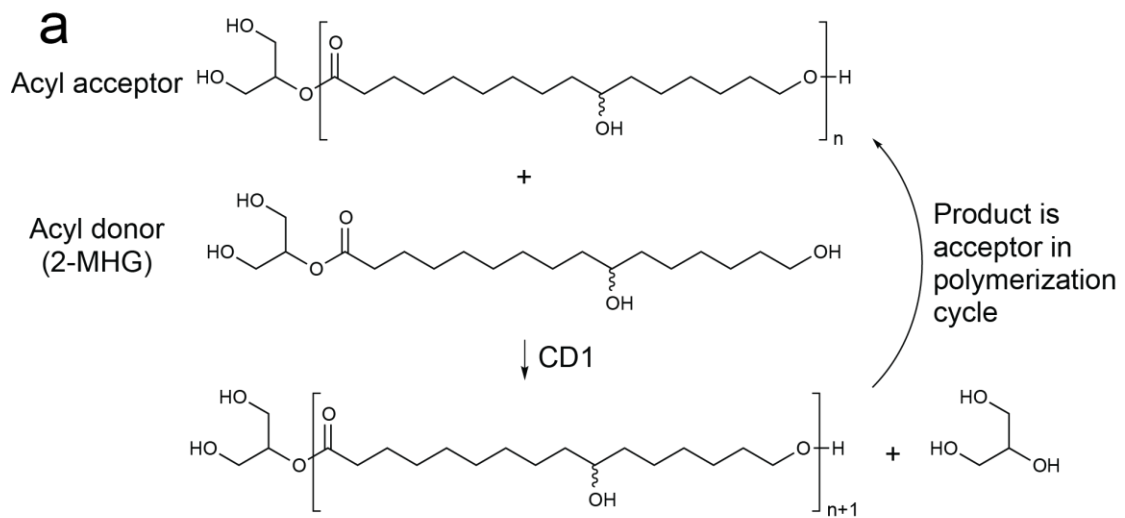


Figure 2.9. Acyltransferase activity of CD1. (a) Proposed model for CD1-catalyzed cutin biosynthesis by transfer of the hydroxyacyl group from 2-MHG to the growing polymer. For simplicity, ester linkage via the primary hydroxyl is shown, although linkage via the secondary hydroxyl can also occur in cutin (Graça and Lamosa, 2010). (b) MALDI-TOF positive-ion spectra of lipid products from *in vitro* assays with 2-

MHG substrate and purified recombinant CD1 enzyme. (c) MALDI-TOF positive ion spectra of lipid products from *in vitro* assays with the S32A variant of the CD1 enzyme.

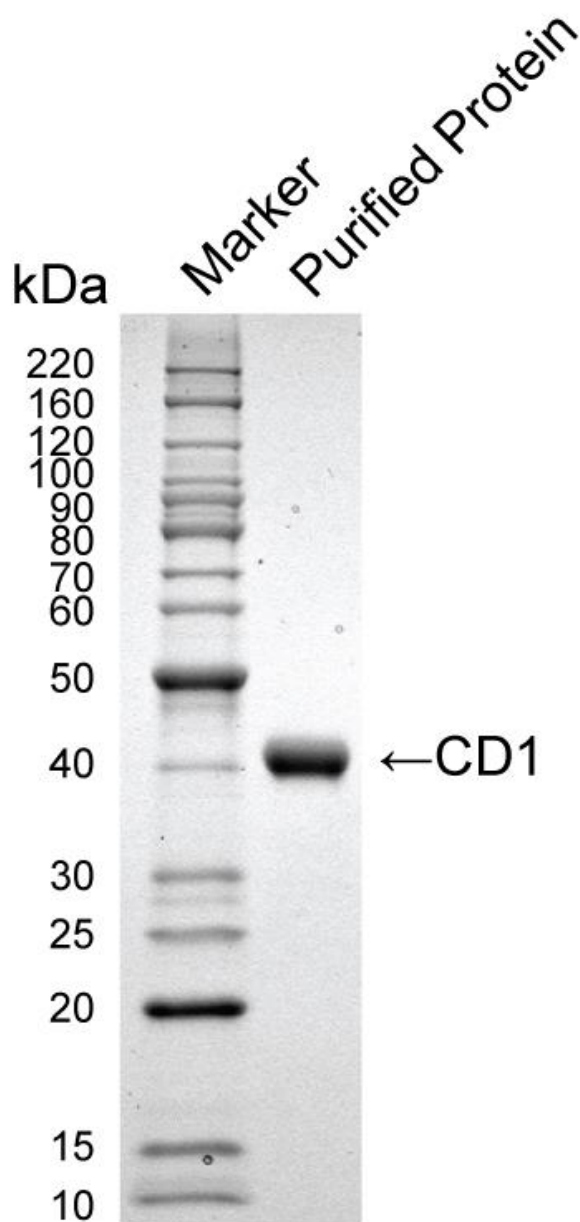
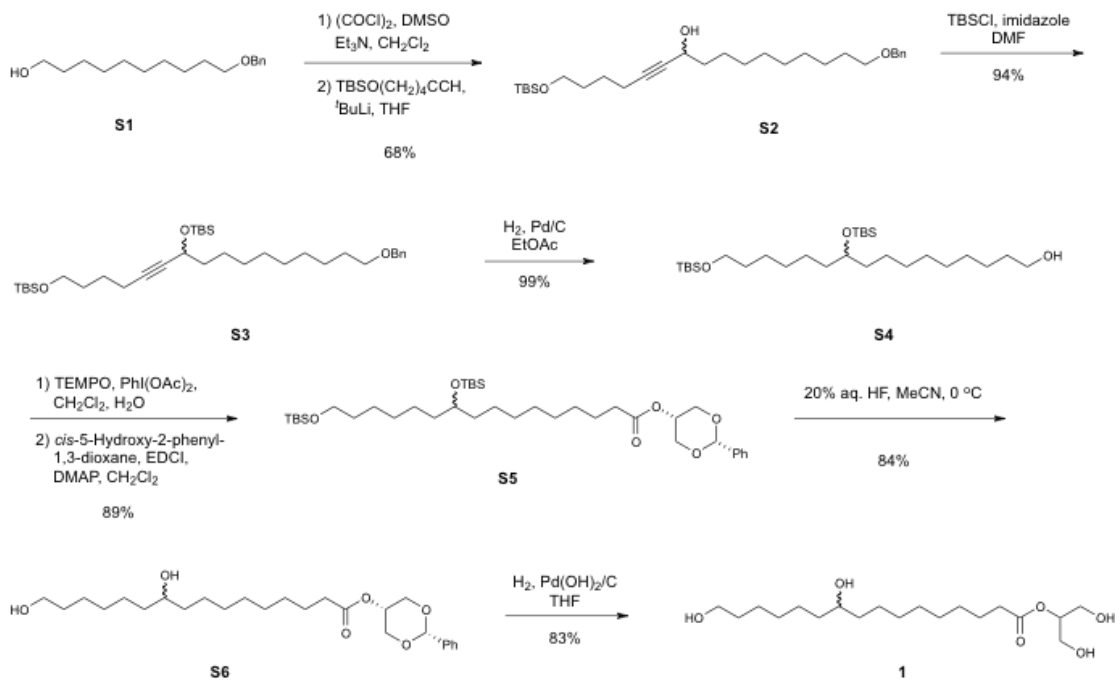


Figure 2.7. The purification of CD1 from agroinfiltrated *Nicotiana benthamiana*. Coomassie stained SDS-PAGE of recombinant his-tagged CD1 purified by nickel-affinity and size exclusion chromatography.



Scheme 2.1. Synthesis of the cutin monomeric precursor 1 (2-MHG).

In vivo ester synthesis via transesterification of acyl glycerol by a lipase-like enzyme is not without precedent. For example, in animals, the extracellular acylation of cholesterol by the transesterification of lecithin is catalyzed by lecithin cholesterol acyltransferase. In the absence of cholesterol as an acyl acceptor, lecithin cholesterol acyltransferase has acyl esterase activity (Jonas, 2000). The unique feature necessary for this transesterification reaction is the action of the enzyme at the lipid-aqueous interface of high-density lipoproteins. Here cholesterol concentrations are high enough to favor the resolution of the acyl-enzyme intermediate by transesterification rather than by hydrolysis. CD1 is likely to act through a similar mechanism at the interface between the aqueous environment of the plant cell wall and the lipid phase of the

nascent cuticle. Thermodynamically, the aqueous solubility of 2-MHG and insolubility of the polyester product would further drive the reaction toward polyester synthesis.

Conclusion

In vitro incorporation of fatty acids into the cutin polymer by crude plant enzyme preparations was first reported in 1974 (Croteau, Kolattukudy, 1974). Moreover, recent molecular-genetic characterization of cutin polymer synthesis has identified several intracellular acyltransferases that are involved in biosynthesis of presumed cutin precursors (Pollard *et al.*, 2008; Panikashvili *et al.*, 2009). However, the molecular basis of cutin polymerization following secretion of the precursors into the cell wall has remained a mystery. Here the data show that CD1 is an extracellular enzyme that localizes in the developing cuticle and is required for cutin biosynthesis. Furthermore, accumulation of 2-MHG, the corresponding 2-MAG of the major cutin monomer of tomato, was detected in the cutin-deficient *cd1* mutant and recombinant CD1 was shown to catalyze the successive transesterification of 2-MHG to yield polyester oligomers *in vitro*. Taken together, these results indicate that CD1 is the principal catalyst of cutin polymerization and that the polymerization process is extracellular and occurs at the site of cuticle deposition. Furthermore, a survey of protein sequences revealed *CD1* homologs in taxonomically diverse plant species (Fig. 2.11), and it has been reported that silencing the expression of two *A. thaliana* homologs of CD1 resulted in phenotypes similar to other cutin-deficient mutants (Shi *et al.*, 2011), suggesting an evolutionarily conserved and ubiquitous mechanism of cutin biosynthesis in land plants.

Accession codes. GenBank: The sequence for CD1 has been deposited under accession code JF968592.

Materials and Methods

Fine mapping of the CD1 gene

For fine genetic mapping of *cd1*, 880 F2 plants of *cd1* (in *S. lycopersicum* cv. M82 background) × *S. pimpinellifolium* were screened for recombinants using the markers TG497 and At5g04420 (position 11.001 and 11.015 respectively, according to EXPEN2000 map, <http://solgenomics.net>). A total of 105 recombinant plants were generated and their fruit cuticles were phenotyped (Isaacson *et al.*, 2009) and the fruits genotyped using newly designed CAPS (or dCAPS) markers. The location of *CDI* was narrowed down first to the 3.22 Mbp tomato WGS scaffold SL1.03sc01386, (corresponding to SL2.40sc03748 in version 2.3 of the ITAG tomato genome annotation, <http://solgenomics.net>) and subsequently to a 61 kb region between markers P120 and P140 (Fig. 2.2a and Table 2.1). Six putative genes were found in this 61 kb region and sequencing of one of these (subsequently termed *CDI*) revealed a polymorphism (G→A) between M82 and *cd1* in the last exon that showed perfect cosegregation with marker T1968 (position 11.005), a previously developed marker corresponding to an EST encoded by SL2.40sc03748. The chromosomal position of *CDI* is: SL2.40ch11:1004362...1007293. Genbank accession number for CD1: JF968592.

Table 2.1. Primer sequences, PCR product length and phenotyping methods used for mapping markers P110, P120, P140 and P160.

Primers	Primer sequence	PCR product length (bp)	Polymorphism (position on scaffold SL1.03sc01386, <i>S. lycopersicum</i> / <i>S. pimpinellifolium</i>) or enzyme
P110F	CGCCCATCATATGCCAACCTCCT	1009	2154299 GA/AT
P110R	CCCTTTTGGTCTGCGGAAG		
P120F	CACTATGCAGTGGGCGTTTG	1025	2183872 C/T
P120R	ACGTTTTTCAGCCACCTAAACC		
P140F	GGAGAGCGAGATTCGCTAGG	980	2244420 T/A
P140R	GCAATTTAAGAGTGCAGGCGTAC		
P160F	TCTGTTTCGGCAGGCAACTG	1014	<i>FokI</i>
P160R	TCAAACCCGCGACCGGTGTGA		

General molecular biology techniques

RNA extraction, cDNA synthesis and qRT-PCR (using previously designed primers for the corresponding unigene of CD1, SGN-U585129, <http://solgenomics.net>) analysis were performed as described in Yeats *et al.* (2010). For transgenic complementation, the coding sequence of *CDI* was introduced into pCAMBIA1305.1. using standard PCR-based cloning protocols. The resulting *CaMV35S::CDI* plasmid was introduced via *Agrobacterium tumefaciens*-mediated transformation into calli generated from *cd1* mutant seeds, at the Boyce Thompson Institute for Plant Research, Ithaca, NY.

Light microscopy

Fixation and embedding were performed as in Buda *et al.* (2009). Four micron cryosections of each sample were obtained using a Microm HM550 cryostat (ThermoFisher Scientific). Sections were melted onto room temperature VistaVision Histobond (VWR) slides and air dried. The slides were then heated on a hot plate at 200°C for 2 min immediately prior to staining. Preparation of Sudan Red 7b followed the protocol outlined in Brundrett *et al.* (1991). The staining solution was applied directly to the slides in a humidity chamber and left for 1 h. The slides were washed and mounted with 75% glycerol. The stained slides were viewed on an AxioImager A1 microscope (Zeiss) using Zeiss EC-Plan NeoFluar 40x/0.75 dry and 100x/1.3 oil immersion objectives, a Zeiss AxioCam MRc color video camera and Zeiss Axio Vs40 4.6.3.0 software. The images were taken using differential interference contrast optics (DIC) and were processed using Photoshop CS4 software (Adobe) to adjust levels and color balance.

Recombinant protein production in E. coli

The *CDI* coding region lacking the 57 nucleotides encoding the predicted native signal peptide and the stop codon was amplified by PCR and cloned into the pET-26b(+) vector (Novagen/Merck). The resulting pet26b(+):*CDI* plasmid, encoding the *pelB* leader sequence followed by the *CDI* mature sequence and a C-terminal hexahistidine tag was transformed into BL21(DE3) *E. coli*. Protein expression was induced and inclusion bodies were harvested according to the pET system manual (Novagen/Merck). Protein was solubilized and purified using a 1 mL

HisTrap FF column with denaturing conditions according to the product manual (GE Healthcare Life Sciences).

Antibody-based techniques

A polyclonal antibody to recombinant CD1 was produced in rabbits (Pacific Immunology Corporation). To generate a high titer antiserum, CD1 specific antibodies were purified by absorption to purified CD1 immobilized on a PVDF membrane (Ritter, 1991). For Western blot analysis, protein was extracted by boiling frozen ground tissue in 3X Laemmli buffer (6% SDS, 30% glycerol, 300 mM DTT, 187 mM Tris, pH 6.8) for 5 min. Protein concentration was determined by Bradford assay (Bio-Rad) and 25 µg were analyzed by Western blot using an HRP conjugated secondary antibody and Pierce ECL Western Blotting Substrate (Thermo Scientific). For immunolocalization experiments, fruit tissue sections on Formvar-coated nickel grids were prepared as previously described (Domozych *et al.*, 2009) with minor modifications: Cacodylate buffers were 0.1 M, initial fixation was with 1% glutaraldehyde at room temperature. The grids were incubated in 5% H₂O₂ for 5 min, washed with deionized water (dH₂O), incubated in 0.1 M NH₄Cl for 20 min, washed with dH₂O and then blocked for 30 min with 1% fat free milk in phosphate buffered saline containing 0.1% Tween-20 (PBS-T). The grids were washed with dH₂O and incubated in primary antibody diluted 1/25 in PBS-T at 4°C overnight. The grids were washed, blocked again and incubated in the anti-rabbit antibody conjugated to 15 nm gold particles (diluted 1/100 in PBS-T) for 2 h at 37°C. The grids were washed extensively with dH₂O, stained in conventional uranyl acetate/lead citrate, washed

again with dH₂O and dried. The sections were viewed with a Zeiss Libra 120 transmission electron microscope (TEM).

Chemical analysis

All cuticle isolations were performed as described in Isaacson *et al.* (2009). For cutin monomer analysis, 0.32 cm² disks of dewaxed cuticles were depolymerized using a base-catalyzed transmethylation protocol (Li-Beisson *et al.*, 2010). The subsequent dry extracts were derivatized by heating with 10 μL N,O-bis(trimethylsilyl)trifluoroacetamide (BSTFA) and 10 μL pyridine for 10 min at 90°C. They were then evaporated to dryness by heating under a gentle stream of nitrogen, resuspended in 100 μL of chloroform and analyzed by GC-FID using a model 6850 GC equipped with cool-on-column inlet (Agilent). Compounds were identified based on retention behavior compared to authentic standards and by parallel GC-MS analysis using a model 6890 GC (Agilent) coupled to a GC Mate II mass spectrometer (JEOL) operating in electron impact mode. For chemical analysis of soluble surface lipids, M82 and *cdl* fruits were harvested at the immature green developmental stage (Gonzalez-Bosch *et al.*, 1996). Soluble surface lipids were extracted by immersing 6 fruits from each genotype twice for 30 s in two beakers containing 2:1 mixture of chloroform and methanol. The extracts were combined and dried over anhydrous sodium sulfate. The solutions were then filtered and the solvent was evaporated by rotary evaporation. Trimethylsilyl (TMS) derivatization and GC-MS analysis was performed as described above. For the spectrum shown, the signal was averaged and background from neighboring peaks was subtracted.

Chemical synthesis

Summary

The cutin monomeric precursor **1** (2-MHG) was prepared in 6 steps from the known (Shioiri *et al.*, 1998) monobenzyl protected decane-1,10-diol **S1** as shown in Scheme 2.1. The starting material **S1** was prepared from commercially available decane-1,10-diol and benzyl bromide analogous to Shioiri *et al.* (1998). Swern oxidation to the aldehyde followed by addition of the lithium acetylide of 6-((*tert*-butyldimethylsilyl)oxy)hex-1-yne (Arbour *et al.*, 2009) afforded alcohol **S2**, which was TBS protected to give the triether **S3**. Combined catalytic hydrogenation of the triple bond and hydrogenolysis of the benzyl ether provided alcohol **S4**. TEMPO mediated oxidation to the acid followed by coupling with *cis*-5-hydroxy-2-phenyl-1,3-dioxane procured ester **S5**. Surprisingly, TBAF failed to remove both TBS groups, affording cleanly the primary alcohol, even after prolonged treatment with a large excess. Instead, **S6** was prepared by treatment of **S5** with 20% aqueous HF in acetonitrile at 0°C. Care had to be taken in this reaction, since treatment with stronger HF solutions at ambient temperature led to concomitant removal of the benzylidene acetal and partial acyl migration to afford a mixture of 1- and 2-glyceryl esters. Finally, hydrogenolysis of **S6** using Pearlman's catalyst gave the desired cutin monomeric precursor **1**, which could be crystallized from a mixture of ethyl acetate and heptane (83% yield). Fortunately, no acyl migration was observed during the deprotection and the choice of THF as solvent is likely important, since a sample of **1** in deuterated methanol showed significant (approximately 20%) migration to the 1-glyceryl ester after 8 hours at ambient temperature.

Synthesis details

General: Starting materials, reagents, and solvents were purchased from Sigma-Aldrich and used without further purification. THF was dried over sodium/benzophenone and distilled before use. Evaporation of solvents was done under reduced pressure (*in vacuo*). TLC was performed on Merck aluminum sheets precoated with silica gel 60 F₂₅₄. Compounds were visualized by charring after dipping in a solution of Ce(IV) (6.25 g of (NH₄)₆Mo₇O₂₄ and 1.5 g of Ce(SO₄)₂ in 250 mL of 10% aqueous H₂SO₄), a solution of *p*-anisaldehyde (10 mL of H₂SO₄ and 10 mL of *p*-anisaldehyde in 200 mL of 95% EtOH) or an ethanolic solution of phosphomolybdic acid (48 g/L). Flash column chromatography was performed using Matrex 60 Å silica gel. NMR spectra were recorded using a Varian Mercury 300 MHz spectrometer. Chemical shifts were measured in ppm and coupling constants in Hz. Melting points are uncorrected. HRMS was recorded on an Ionspec Ultima Fourier transform mass spectrometer.

Synthesis of 16-Benzyloxy-1-((*tert*-butyldimethylsilyl)oxy)hexadec-5-yn-7-ol (**S2**):

To a solution of DMSO (1.95 g, 1.8 mL, 24.96 mmol) in CH₂Cl₂ (45 mL) at -78 °C under an atmosphere of N₂ was added a solution of oxalyl chloride (1.58 g, 1.1 mL, 12.49 mmol) in CH₂Cl₂ (2.3 mL) slowly, maintaining the temperature below -60°C while stirring. A solution of **S1** (3.00 g, 11.35 mmol) in CH₂Cl₂ (11 mL) was added dropwise to the resulting mixture while still keeping the temperature below -60°C. After stirring for 1.5 h, Et₃N (5.74 g, 8.2 mL, 56.8 mmol) was added and the reaction was allowed to warm slowly to 20°C over 3 h. The reaction mixture was

poured into water (60 mL), the phases were separated and the aqueous phase was extracted with CH₂Cl₂ (3 × 60 mL). The combined organic phases were washed with 1% aq. HCl (90 mL), water (90 mL), sat. aq. NaHCO₃ (90 mL) and sat. aq. NaCl (90 mL) and then dried with MgSO₄, concentrated and used without further purification. To a solution of 6-((*tert*-butyldimethylsilyl)oxy)hex-1-yne (1.00 g, 4.70 mmol) in THF (4.7 mL) at -78°C was added *t*-BuLi (2.50 mL, 1.7 M in pentane, 4.24 mmol) dropwise. The resulting mixture was allowed to warm to 20°C and then a solution of the crude aldehyde (1.11 g, 4.24 mmol) in THF (4.2 mL) was added dropwise. The reaction mixture was stirred at 20°C for 1 h, poured into sat. aq. NH₄Cl (20 mL) and extracted with CH₂Cl₂ (3 × 30 mL). The combined organic phases were dried with MgSO₄, filtered, concentrated and purified by column chromatography (EtOAc:heptane 1:9) affording **S2** as a colorless oil (1.37 g, 68%).

NMR specifications of **S2**:

¹H NMR (CDCl₃) δ 7.37-7.24 (m, 5H), 4.50 (s, 2H), 4.38-4.29 (m, 1H), 3.62 (t, *J* = 5.9 Hz, 2H), 3.46 (t, *J* = 6.6 Hz, 2H), 2.24 (td, *J* = 6.4, 3.3 Hz, 2H), 1.72-1.54 (m, 6H), 1.46-1.24 (m, 14H), 0.89 (s, 9H), 0.05 (s, 6H). ¹³C NMR (CDCl₃) δ 138.83, 128.48 (2C), 127.77 (2C), 127.61, 85.43, 81.66, 73.00, 70.65, 62.91, 62.79, 38.35, 32.06, 32.03, 29.92, 29.64, 29.61, 29.42, 26.33, 26.11 (3C), 25.36, 25.27, 18.64, 18.49, -5.12, -5.14. HRMS (ESI+) C₂₉H₅₀O₃Si, *m/z* [M+Na⁺] 497.3427, found 497.3413.

Synthesis of 16-Benzyloxy-1,7-bis((*tert*-butyldimethylsilyl)oxy)hexadec-5-yne (**S3**):

To a solution of **S2** (1.09 g, 2.30 mmol) in DMF (4.6 mL) was added imidazole (234 mg, 3.44 mmol) and TBSCl (415 mg, 2.76 mmol). The resulting mixture was stirred for 3 h, poured into sat. aq. NH₄Cl (20 mL) and extracted with CH₂Cl₂ (3 × 25 mL). The combined organic phases were dried with MgSO₄, filtered, concentrated and purified by column chromatography (EtOAc:heptane 1:19) affording **S3** as a colorless oil (1.27 g, 94%).

NMR specifications of **S3**:

¹H NMR (CDCl₃) δ 7.37-7.24 (m, 5H), 4.50 (s, 2H), 4.36-4.24 (m, 1H), 3.62 (t, *J* = 5.9 Hz, 2H), 3.46 (t, *J* = 6.6 Hz, 2H), 2.21 (td, *J* = 6.7, 1.8 Hz, 2H), 1.75-1.50 (m, 6H), 1.45-1.23 (m, 14H), 0.90 (s, 9H), 0.89 (s, 9H), 0.12 (s, 3H), 0.10 (s, 3H), 0.05 (s, 6H).
¹³C NMR (CDCl₃) δ 138.85, 128.48 (2C), 127.76 (2C), 127.60, 84.27, 82.35, 72.99, 70.66, 63.35, 62.80, 39.17, 32.09, 32.03, 29.92, 29.69, 29.63, 29.42, 29.18, 26.10 (6C), 26.01, 25.50, 25.31, 18.66, 18.48, -4.29, -4.81, -5.16 (2C).

Synthesis of 10,16-Bis((*tert*-butyldimethylsilyl)oxy)hexadecan-1-ol (**S4**):

To a solution of **S3** (1.21 g, 2.05 mmol) in EtOAc (20.5 mL) under a N₂ atmosphere was added 10% Pd/C (218 mg) and an atmosphere of H₂ was installed by bubbling H₂ through the solution for 5 min. The reaction was stirred under H₂ for 20 h, filtered through Celite and concentrated, affording **S4** as a colorless oil (1.02 g, 99%).

NMR specifications of **S4**:

^1H NMR (CDCl_3) δ 3.66-3.55 (m, 5H), 1.62-1.21 (m, 26H), 0.89 (s, 9H), 0.88 (s, 9H), 0.04 (s, 6H), 0.03 (s, 6H). ^{13}C NMR (CDCl_3) δ 72.49, 63.46, 63.19, 37.25, 32.98, 32.93, 29.98, 29.81, 29.72, 29.56, 26.13 (4C), 26.08 (4C), 25.96, 25.88, 25.47 (2C), 18.52, 18.30, -4.27 (2C), -5.11 (2C).

Synthesis of *cis*-2-Phenyl-1,3-dioxan-5-yl 10,16-bis(*tert*-butyldimethylsilyl)oxy)hexadecanoate (**S5**):

To a solution of **S4** (991 mg, 1.97 mmol) in CH_2Cl_2 (8 mL) and water (4 mL) was added $\text{PhI}(\text{OAc})_2$ (1.65 g, 5.12 mmol) and TEMPO (62 mg, 0.39 mmol). The resulting mixture is stirred vigorously for 3 h, poured into 10% aq. $\text{Na}_2\text{S}_2\text{O}_3$ (20 mL) and extracted with EtOAc (3×25 mL). The combined organic phases were dried with MgSO_4 , filtered, concentrated and taken up in CH_2Cl_2 (20 mL). To this solution was added *cis*-5-hydroxy-2-phenyl-1,3-dioxane (461 mg, 2.56 mmol), DMAP (409 mg, 3.35 mmol) and EDC-HCl (567 mg, 2.96 mmol). The reaction was stirred for 18 h, SiO_2 was added, the mixture was concentrated and purified by column chromatography (EtOAc:heptane 1: 9) affording **S5** as a colorless oil (1.19 g, 89%).

NMR specifications of S5:

^1H NMR (CDCl_3) δ 7.56-4.47 (m, 2H), 7.43-7.34 (m, 3H), 5.57 (s, 1H), 4.75-4.71 (m, 1H), 4.29 (d, $J = 12.9$ Hz, 2H), 4.18 (d, $J = 12.9$ Hz, 2H), 3.65-3.56 (m, 3H), 2.44 (t, $J = 7.6$ Hz, 2H), 1.76-1.59 (m, 2H), 1.56-1.45 (m, 2H), 1.45-1.18 (m, 20H), 0.89 (s, 9H), 0.88 (s, 9H), 0.05 (s, 6H), 0.03 (s, 6H). ^{13}C NMR (CDCl_3) δ 174.03, 138.11, 129.22, 128.43 (2C), 126.15 (2C), 101.37, 72.49, 69.28 (2C), 65.81, 63.46, 37.28,

37.22, 34.54, 33.00, 29.81, 29.63, 29.42, 29.26, 26.13 (3C), 26.09 (4C), 26.03, 25.97, 25.48, 25.08, 18.38, 18.30, -4.27 (2C), -5.11 (2C).

Synthesis of *cis*-2-Phenyl-1,3-dioxan-5-yl 10,16-dihydroxyhexadecanoate (**S6**):

To a solution of **S5** (150 mg, 0.22 mmol) in MeCN (23 mL) at 0°C was added 20% aq. HF (1.0 mL, 10 mmol) and the resulting mixture was stirred at 0°C for 4 h. TMSOMe (3.9 mL, 28 mmol) was added, stirring was continued at 0°C for 20 min, the mixture was poured into sat. aq. NH₄Cl (30 mL) and extracted with CH₂Cl₂ (2 × 30 mL). The combined organic phases were dried over MgSO₄, filtered, concentrated and purified by column chromatography (CH₂Cl₂:EtOAc 1:0 → 1:1) affording **S6** (84 mg, 84%) as a white solid, m.p.: 70.5-72.1 °C.

NMR specifications of **S6**:

¹H NMR (CDCl₃) δ 7.56-7.48 (m, 2H), 7.42-7.34 (m, 3H), 5.56 (s, 1H), 4.72 (s, 1H), 4.29 (d, *J* = 12.9 Hz, 2H), 4.18 (d, *J* = 12.9 Hz, 2H), 3.64 (t, *J* = 6.6 Hz, 2H), 3.62-3.52 (m, 1H), (t, *J* = 7.5 Hz, 2H), 1.73-1.51 (m, 4H), 1.50-1.21 (m, 20H). ¹³C NMR (CDCl₃) δ 174.03, 137.94, 129.23, 128.45 (2C), 126.16 (2C), 101.38, 72.07, 69.29 (2C), 65.84, 63.16, 37.61, 37.48, 34.52, 32.85, 29.73, 29.59, 29.53, 29.33, 29.20, 25.85, 25.74 (2C), 25.05. HRMS (ESI+) C₂₆H₄₂O₆, *m/z* [M+Na⁺] 473.2879, found 473.2872.

Synthesis of 1,3-Dihydroxypropan-2-yl 10,16-dihydroxyhexadecanoate (**1** [2-MHG]):

To a solution of **S6** (118 mg, 0.26 mmol) in THF (13 mL) under a N₂ atmosphere was added 10% Pd(OH)₂/C (60 mg) and an atmosphere of H₂ was installed by bubbling H₂ through the solution for 5 min. The reaction was stirred under H₂ for 10 h, filtered through Celite, concentrated and crystallized from EtOAc and heptane, affording **1** (79 mg, 83%) as a white solid, m.p.: 66.7-68.1°C

NMR specifications of 2-MHG:

¹H NMR (CD₃OD) δ 4.68-4.59 (m, 1H), 3.68 (dd, *J* = 12.1, 3.7 Hz, 2H), 3.64 (dd, *J* = 12.1, 3.7 Hz, 2H), 3.54 (t, *J* = 6.6 Hz, 2H), 3.53-3.50 (m, 1H), 2.37 (t, *J* = 7.4 Hz, 2H), 1.71-1.25 (m, 24H). ¹³C NMR (CD₃OD) δ 175.33, 76.51, 72.40, 62.98, 61.68 (2C), 38.42, 38.38, 35.13, 33.62, 30.79, 30.68, 30.59, 30.38, 30.17, 30.12, 26.95, 26.79, 25.97. HRMS (ESI+) C₁₉H₃₈O₆, m/z [M+Na⁺] 385.2566, found 385.2553.

The EI-MS spectrum of the tetra-TMS ether derivative of **1** obtained by GC-MS as previously described is shown in Fig. 2.8b.

Expression of functional CD1 in *Nicotiana benthamiana*

Despite trying a variety of bacterial expression conditions and vectors, no soluble recombinant CD1 protein was produced. A transient expression system with agroinfiltrated *Nicotiana benthamiana* leaves was therefore used. The coding sequence of CD1 lacking the stop codon was inserted into pEAQ-*HT* (Sainsbury *et al.*, 2009) using PCR to incorporate *Age*I and *Sma*I restriction sites. The resulting construct, pEAQ-*HT*::CD1, encoded CD1 followed by the sequence PGHHHHHH.

Infiltration of *N. benthamiana* with *A. tumefaciens* was as described by Arbour *et al.* (2009) except that strain GV2260 was used and plants were harvested 5 days after infiltration. Tissue was flash frozen, ground in liquid nitrogen and stored at -80°C until use.

For protein purification, 25 g of frozen tissue was added to 75 mL of chilled buffer A (5 mM sodium acetate, 500 mM NaCl, 0.1% (v/v) Triton X-100, pH 4.5) and 2.5 g of polyvinylpolypyrrolidone. Tissue was homogenized using a PowerGen 125 homogenizer (Fisher Scientific), filtered through three layers of Miracloth (EMD) and centrifuged (40,000 x g, 30 min, 4°C). The supernatant was adjusted to pH 7 by addition of 1 M sodium phosphate to a final concentration of 50 mM and 2 M imidazole was added to a final concentration of 10 mM. The extract was centrifuged as before and the supernatant was passed through a 0.45 µm filter. The clarified extract was then rocked on ice with 200 µL (settled volume) of equilibrated HisPur Ni-NTA agarose (Pierce). After 1 h, the resin was collected by centrifugation and transferred to a 5 mL column. The beads were then washed with 5 mL of buffer B (50 mM sodium phosphate, 500 mM NaCl, 50 mM imidazole, pH 7.0). Protein was then eluted with 1 mL of the same buffer with 300 mM imidazole. The eluate was applied to an equilibrated Superdex 75 HR 10/30 column (GE Healthcare Life Sciences), eluting with buffer C (50 mM sodium phosphate, 150 mM NaCl, 0.02% sodium azide, pH 7.0). Fractions containing the 40 kD CD1 protein were pooled and concentrated by ultrafiltration. Protein concentration was determined by absorbance at 280 nm using the theoretical extinction coefficient based on the sequence of the protein (Gill and von Hippel, 1989).

For expression of the CD1 S32A variant, site-directed mutagenesis was performed on the pEAQ-*HT::CD1* plasmid using the QuikChange protocol (Agilent). The sequence of the entire coding region was verified and protein expression and purification was performed as described for the wild type enzyme.

Acyltransferase assay

The 30 μ L assay mixture contained 5 mM 2-MHG (from a 100 mM stock in DMSO), 50 mM sodium phosphate, 150 mM NaCl, pH 6.0. The assay was initiated by addition of CD1 (6 μ g), and left to shake at 300 rpm, 37°C for 3 h. In these conditions, 2-MHG was soluble, while an insoluble white film on the surface of the tubes was formed by wild type CD1. To extract the products, 30 μ L of ethyl acetate was added to the tubes and the samples were vortexed for 30 s before centrifugation (1 min, 20,000 x g, 24°C). Lipid products were recovered in the upper organic phase and dried down under a gentle stream of nitrogen. These were resuspended in 10 μ L methanol and then diluted 100 fold in 75% methanol/25% water (v/v). 0.5 μ L of the diluted extract was applied to a MALDI target plate and allowed to evaporate. To the same spot, 0.6 μ L of matrix was applied (10 mg.mL⁻¹ 2,5-dihydroxybenzoic acid in 75% methanol/25% water [v/v]) and allowed to dry. The spot was then recrystallized by addition of 0.2 μ L 85% methanol/15% water (v/v). MALDI-TOF spectra were collected in positive ion mode using the reflecting detector of a 4700 Proteomics Analyzer mass spectrometer (Applied Biosystems).

Relative contribution:

T.H.Y. purified recombinant proteins and performed chemical analysis of soluble surface lipids and acyltransferase assays. L.B.B.M. performed gene and protein expression experiments, generated the antibody and performed cutin analysis. H.M.-F.V. and M.H.C. synthesized 2-MHG. Y.H. and L.Z. performed fine genetic mapping experiments and constructed the transgenic complementation vector. L.B.B.M. and G.J.B. conducted light microscopy experiments. L.B.B.M. and D.S.D. performed immunolocalization experiments. T.H.Y., L.B.B.M. and J.K.C.R. designed the study, analyzed the data and wrote the paper on which this chapter is based.

REFERENCES

- Akoh CC, Lee GC, Liaw YC, Huang TH, Shaw JF. (2004). GDSL family of serine esterases/lipases. *Progress in Lipid Research* 43, 534-552.
- Arbour M, Roy S, Godbout C, Spino C. (2009). Stereoselective Synthesis of (+)-Euphococcinine and (-)-Adaline. *The Journal of Organic Chemistry* 74, 3806-3814.
- Baker EA, Bukovac MJ, Hunt GM. in *The Plant Cuticle*. (1982) eds Cutler DF, Alvin KL, Price CE. Academic Press, London. 33-44
- Brundrett MC, Kendrick B, Peterson CA. (1991) Efficient lipid staining in plant material with sudan red 7B or fluorol yellow 088 in polyethylene glycol-glycerol. *Biotechnic & Histochemistry* 66, 111-116.
- Buda GJ, Isaacson T, Matas AJ, Paolillo DJ, Rose JKC. (2009). Three-dimensional imaging of plant cuticle architecture using confocal scanning laser microscopy. *The Plant Journal* 60, 378-385.
- Croteau R, Kolattukudy PE. Biosynthesis of hydroxyfatty acid polymers. Enzymatic synthesis of cutin from monomer acids by cell-free preparations from the epidermis of *Vicia faba* leaves. (1974). *Biochemistry* 13, 3193-3202.
- Domozych DS, Sorensen I, Willats WGT. (2009). The distribution of cell wall polymers during antheridium development and spermatogenesis in the Charophycean green alga, *Chara corallina*. *Annals of Botany* 104, 1045-1056.
- Edwards D. (1993). Cells and tissues in the vegetative sporophytes of early land plants *New Phytologist* 125, 225-247.
- Gill SC, von Hippel PH. (1989). Calculation of protein extinction coefficients from amino acid sequence data *Analytical Biochemistry* 182, 319-326.
- Gonzalez-Bosch C, Brummell DA, Bennett AB. (1996). Differential expression of two endo-1,4- β -glucanase genes in pericarp and locules of wild-type and mutant tomato fruit. *Plant Physiology* 111, 1313-1319.
- Graca J, Lamosa P. (2010). Linear and branched poly(omega-hydroxyacid) esters in plant cutins. *Journal of Agricultural and Food Chemistry* 58, 9666-9674.
- Graca J, Schreiber L, Rodrigues J, Pereira H. (2002). Glycerol and glyceryl esters of omega-hydroxyacids in cutins. *Phytochemistry* 61, 205-215.

- Heredia A, Heredia-Guerrero JA, Dominguez E, Benitez JJ. (2009). Cutin synthesis: A slippery paradigm. *Biointerphases* 4, P1-3.
- Irshad M, Canut H, Borderies G, Pont-Lezica R, Jamet E. (2008). A new picture of cell wall protein dynamics in elongating cells of *Arabidopsis thaliana*: confirmed actors and newcomers. *BMC Plant Biology* 8, 94.
- Isaacson T, Kosma DK, Matas AJ, Buda GJ, He Y, Yu B, Pravitasari A, Batteas JD, Stark RE, Jenks MA, Rose JKC. (2009). Cutin deficiency in the tomato fruit cuticle consistently affects resistance to microbial infection and biomechanical properties, but not transpirational water loss. *The Plant Journal* 60, 363-377.
- Jetter R, Kunst L, Samuels AL. in *Biology of the Plant Cuticle*. (2006). eds Riederer, M., Müller, C. Blackwell, Oxford, UK. 145-181.
- Jonas A. (2000). Lecithin cholesterol acyltransferase. *Biochimica et Biophysica Acta* 1529, 245-256.
- Li Y, Beisson F, Ohlrogge J, Pollard M. (2007). Monoacylglycerols are components of root waxes and can be produced in the aerial cuticle by ectopic expression of a suberin-associated acyltransferase. *Plant Physiology* 144, 1267-1277.
- Li-Beisson Y. *et al.* (2010). Acyl-Lipid Metabolism. *The Arabidopsis Book* 8, e0133.
- Matas AJ, Yeats TH, Buda GJ, Zheng Y, Chatterjee S, Tohge T, Ponnala L, Adato A, Aharoni A, Stark R, Fernie AR, Fei Z, Giovannoni JJ, Rose JKC. (2011). Tissue- and cell-type specific transcriptome profiling of expanding tomato fruit provides insights into metabolic and regulatory specialization and cuticle formation. *The Plant Cell* 23, 3893-3910.
- Mintz-Oron S, Mandel T, Rogachev I, Feldberg L, Lotan O, Yativ M, Wang Z, Jetter R, Venger I, Adato A, Aharoni A. (2008). Gene expression and metabolism in tomato fruit surface tissues. *Plant Physiology* 147, 823-851.
- Nawrath, C. (2006). Unraveling the complex network of cuticular structure and function. *Current Opinion in Plant Biology* 9, 281-287.
- Osman SF, Irwin P, Fett WF, O'Connor JV, Parris N. (1999). Preparation, isolation, and characterization of cutin monomers and oligomers from tomato peels. *Journal of Agricultural and Food Chemistry* 47, 799-802.
- Panikashvili D, Shi JX, Schreiber L, Aharoni A. (2009). The *Arabidopsis* DCR encoding a soluble BAHD acyltransferase is required for cutin polyester formation and seed hydration properties. *Plant Physiology* 151, 1773-1789
- Pollard M, Beisson F, Li Y, Ohlrogge JB. (2008). Building lipid barriers: biosynthesis of cutin and suberin. *Trends in Plant Science* 13, 236-246

- Reina JJ, Guerrero C, Heredia A. (2007). Isolation, characterization, and localization of AgaSGNH cDNA: a new SGNH-motif plant hydrolase specific to *Agave americana* L. leaf epidermis. *Journal of Experimental Botany* 58, 2717-2731
- Ritter K. (1991). Affinity purification of antibodies from sera using polyvinylidenedifluoride (PVDF) membranes as coupling matrices for antigens presented by autoantibodies to triosephosphate isomerase. *Journal of Immunological Methods* 137, 209-215
- Sainsbury F, Thuenemann EC, Lomonosoff GP. (2009). pEAQ: versatile expression vectors for easy and quick transient expression of heterologous proteins in plants. *Plant Biotechnology Journal* 7, 682-693.
- Shi JX, Malitsky S, De Oliveira S, Branigan C, Franke RB, Schreiber L, Aharoni A. (2011). SHINE transcription factors act redundantly to pattern the archetypal surface of *Arabidopsis* flower organs. *PLoS Genetics* 7, e1001388
- Shioiri T, Terao Y, Irako N, Aoyama T. (1998). Synthesis of topostins B567 and D654 (WB-3559D, flavolipin), DNA topoisomerase I inhibitors of bacterial origin. *Tetrahedron* 54, 15701-15710
- Volokita M, Rosilio-Brami T, Rivkin N, Zik M. (2011). Combining comparative sequence and genomic data to ascertain phylogenetic relationships and explore the evolution of the large GDSL-lipase family in land plants. *Molecular Biology and Evolution* 28, 551-565.
- Yang W, Pollard M, Li-Beisson Y, Beisson F, Feig M, Ohlrogge J. (2010). A distinct type of glycerol-3-phosphate acyltransferase with *sn*-2 preference and phosphatase activity producing 2-monoacylglycerol. *Proceedings of the National Academy of Sciences of the USA* 107, 12040-12045.
- Yeats TH, Howe, KJ, Matas AJ, Buda GJ, Thannhauser TW, Rose JKC. (2010). Mining the surface proteome of tomato (*Solanum lycopersicum*) fruit for proteins associated with cuticle biogenesis. *Journal of Experimental Botany* 61, 3759-3771

CHAPTER 3

Tomato Cuticle Biosynthesis is Regulated by Cutin Deficient 2 (CD2), an HD-ZIP IV Transcription Factor

Abstract

In order to survive in terrestrial habitats, plants require a hydrophobic cuticle composed of cutin and of a structurally diverse collection of waxes, to limit water loss and reduce microbial infection. While many steps in the underlying biosynthetic pathways have been elucidated, the molecular mechanisms that regulate cuticle formation are still poorly understood. A key regulatory factor has been identified through mapping and characterization of the *cutin deficient 2 (cd2)* tomato mutant, the fruit cuticles of which show a ~95% reduction in polymeric cutin. The *CD2* gene is predicted to encode a member of the HD-ZIP IV family of transcription factors; proteins that have been shown to control epidermal cell identity. Accordingly, in this study, it was determined that CD2 is highly expressed in the epidermis; however, expression in other tissues suggests that CD2 may also regulate non-epidermis related pathways. To identify downstream targets of *CD2* action, RNA-seq based transcriptome profiling of the epidermis of the *cd2* mutant and wild type expanding and ripening fruits was performed, using cells isolated by laser-capture microdissection (LCM). Comparative analysis revealed approximately 60 and 100 differentially expressed genes at the expanding and ripening stages of development, respectively. Almost all the genes (~90%) that were differentially expressed in the early stage of development showed lower expression in the mutant, with the notable exception of a homolog of CD2. The expression levels of many cutin biosynthesis and transport related genes were lower in the mutant, as well as many additional genes encoding enzymes involved in lipid biosynthesis and signaling in both stages of development. Additionally, genes involved in anthocyanin biosynthesis, stress

responses and fruit ripening were identified. The potential role of CD2 in these pathways is discussed in this chapter.

Introduction

The epidermis of all aerial plant organs has a specialized protective waxy layer termed the cuticle, the main component of which is cutin, a polymer of esterified C₁₆ and/or C₁₈ hydroxy fatty acids and derivatives (Stark and Tian, 2006). In addition, glycerol represents a structurally important constituent of the cutin matrix through the formation of ester bonds with the cutin monomers (Graça *et al.*, 2002). The cutin matrix is infiltrated with, and covered by, a structurally diverse range of unpolymerized waxes (Jetter *et al.*, 2006; Stark and Tian, 2006). These are mostly derived from Very-Long-Chain Fatty Acids, but triterpenoids, sterols and phenolic compounds, including cinnamic acids and flavonoids, are also common cuticle constituents (Hunt and Baker, 1980; Muir *et al.*, 2001; Jetter *et al.*, 2006).

The characterization of mutants with defective cuticles, which often have pleiotropic phenotypes, has led to the identification of many enzymes that catalyze the biosynthesis of cuticular components (Yeats and Rose, 2013). In addition, several transcription factor encoding genes have been revealed that influence cuticle formation, including those that are more broadly involved in regulating epidermal cell identity. For example the R2R3-MYB transcription factor GLABRA1 (GL1), known to be responsible for trichome formation and stomata patterning, has a mutant with reduced loads of cutin and wax (Xia *et al.*, 2010; Tsuji and Coe, 2013). Similarly, the AP2-domain super family member SISHINE3 not only regulates cuticular gene

expression, but also affects genes associated with epidermal cell patterning (Shi *et al.*, 2013). Another transcription factor family that has been closely associated with the regulation of epidermal cell related processes is the HD-ZIP IV family, members of which are characterized by a homeodomain (HD) coupled with a zipper-loop-zipper (ZLZ) motif and a StAR-related lipid-transfer (START) domain paired with a HD-START-associated domain (HD-SAD) (Rerie *et al.*, 1994; Masucci *et al.*, 1996; Schrick *et al.*, 2004; Ariel *et al.*, 2007; Chew *et al.*, 2013). This family is relatively small and is specific to land plants, with ~10-20 members in angiosperm species and 4 members in moss (*Physcomitrella patens*) and *Selaginella moellendorffii* (Mukherjee *et al.*, 2009; Zhao *et al.*, 2011; Fu *et al.*, 2013). Consistent with an epidermal function, HD-ZIP IV genes have been shown to be preferentially expressed in the outer cell layer of plant organs (Nakamura *et al.*, 2006), such as *ATML1* and *PDF2* from *Arabidopsis thaliana*, which are expressed in the outermost cell layer (L1) of the shoot apex and are essential for epidermal cell differentiation. Moreover, the *Arabidopsis* HD-ZIP IV gene *GL2* regulates trichome and root hair formation, while *HDG2* promotes stomatal differentiation (Rerie *et al.*, 1994; Di Cristina *et al.*, 1996; Masucci *et al.*, 1996; Abe *et al.*, 2003; Peterson *et al.*, 2013). Functional redundancy appears to be common among members of this family as double or triple mutants are often necessary to detect a phenotype, and they may act together through heterodimerization (Sessa *et al.*, 1993; Abe *et al.*, 2003; Nakamura *et al.*, 2006; Kamata *et al.*, 2013).

HD-ZIP IV genes also play various roles in non-epidermal cell layers. For example, the *Arabidopsis* gene *ANTHOCYANINLESS2* (*ANL2*) affects both anthocyanin accumulation in the shoot sub-epidermal cell layer, and cellular

organization in primary root (Kubo *et al.*, 1999; Kubo and Hayashi, 2011). Accordingly, *ANL2* is expressed more strongly in sub-epidermal cells than in epidermal cells of rosette leaves, which is congruent with a reduction in anthocyanin levels in the *anl2* mutant (Kubo *et al.*, 2008). However, *anl2* also has a reduced leaf cutin content (Nadakuduti *et al.*, 2012), suggesting a role in cuticle formation.

A functional association between HD-Zip IV proteins and the regulation of cuticle formation was further suggested through the characterization of the tomato (*Solanum lycopersicum*) mutant *cutin deficient 2 (cd2)* that, along with its allelic mutant *sticky peel (pe)*, has severely reduced levels of cutin in both fruits and leaves, as well as an altered cuticular wax composition (Isaacson *et al.*, 2009; Nadakuduti *et al.*, 2012). *CD2* is the closest tomato homolog of *ANL2* and similarly to *anl2*, the *pe* mutant was reported to have a reduced anthocyanin accumulation in stem (Nadakuduti *et al.*, 2012). Additional phenotypes include a lower density of glandular trichomes and stomata (Nadakuduti *et al.*, 2012).

To gain an increased understanding of *CD2* role in epidermal processes, and particularly in cuticle regulation, the set of genes regulated by *CD2* at two stages of fruit development was investigated.

Results

CD2 belongs to the HD-ZIP IV family and regulates cuticle formation

The *cd2* mutation was mapped to the Solyc01g091630 locus located on chromosome 1 (Isaacson *et al.*, 2009). This gene encodes for a protein composed of 821 amino acids and has a predicted molecular weight of 89.9 kDa (Fig. 3.1A). To date, two allelic mutations that affect *CD2* expression have been reported, both of which are located in the HD-START associated domain (HD-SAD). The *pe* mutation, which has been introgressed into the Ailsa Craig (AC) cultivar background (Nadakuduti *et al.*, 2012), consists of a truncation of the last 160 amino acids. In contrast, the *cd2* mutation, which is in the M82 cultivar background, corresponds to a G to A substitution, resulting in an arginine instead of a conserved glycine of position 736 (Isaacson *et al.*, 2009; Fig 3.1A). Both mutations result in a severe reduction of the fruit cuticle (~95% decrease; Isaacson *et al.*, 2009; Nadakuduti *et al.*, 2012; Fig. 3.1B).

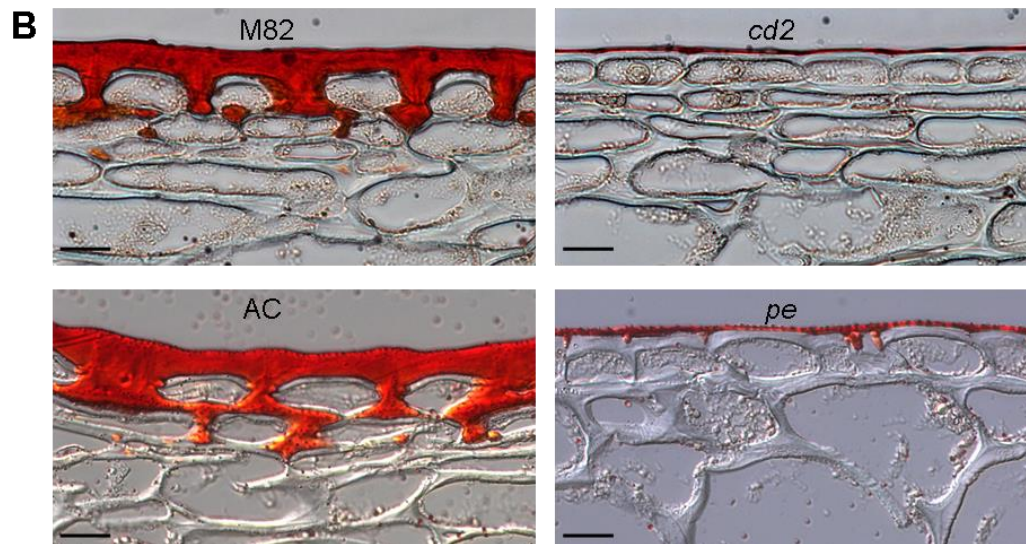
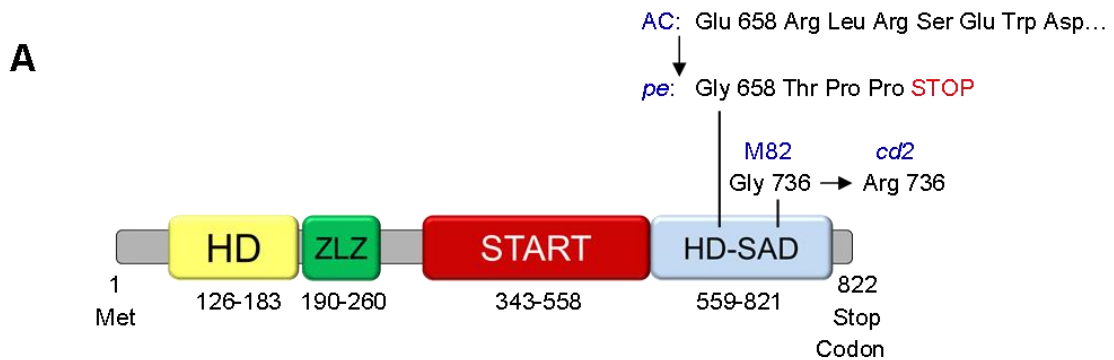


Figure 3.1. The HD-ZIP IV transcription factor CD2 (Solyc01g091630) is necessary for cuticle formation. (A) Diagram of the CD2 protein, showing the relative positions of the domains and mutations in the *cutin deficient 2* (*cd2*) and *sticky peel* (*pe*) mutants. HD, homeodomain; ZLZ, leucine zipper-loop-zipper; START, steroidogenic acute regulatory related lipid transfer; HD-SAD, HD-START associated domain. Numbers correspond to the first and last amino acid of the domain, or position of the mutations. M82 and AC (Ailsa Craig) refer to the cultivar genotypes of *cd2* and *pe*, respectively. (B) Light micrographs of mature green fruit cuticle stained with Oil red O. Scale bars, 20 μ m.

Although systematic characterization of the HD-ZIP IV family has been carried out in Arabidopsis, little is known about HD-ZIP IV genes in tomato. To identify the tomato members of this family, the SGN database (<http://solgenomics.net/>; ITAG2.3) was searched using the CD2 amino acid sequence, or the START domain sequences of CD2 and HDG11 (At1g73360). *HDG11* belongs to the Arabidopsis HD-ZIP IV family and is one of the members with the lowest degree of homology to *CD2* (there is 50% identity between the protein sequences of CD2 and HDG11, while this percentage rises to 64% for CD2 and ANL2). HDG11 start domain was included in the search to ensure that all members of the family were identified. This database search led to the selection of seventeen sequences, based on the criteria of having both a HD and a START domain, and of not possessing a MEKHLA domain, which is specific for the HD-ZIP III family (Ariel *et al.*, 2007). Phylogenetic analysis of the 17 tomato sequences with the 16 members of the Arabidopsis HD-ZIP IV family confirmed that *ANL2* is a close homolog of *CD2* and revealed that *HDG1* is also closely related (65% of HDG1 amino acids are identical to the ones of *CD2* ; Fig. 3.2). The *hdg1* mutant has no detected phenotype but suppression of HDG1 function by chimeric repression technology resulted in a permeable cuticle and organ fusion (Nakamura *et al.*, 2006; Wu *et al.*, 2011). Of the 17 tomato sequences, only 3 clustered with an Arabidopsis protein rather than with a paralogous tomato sequence, and this subset included *CD2*.

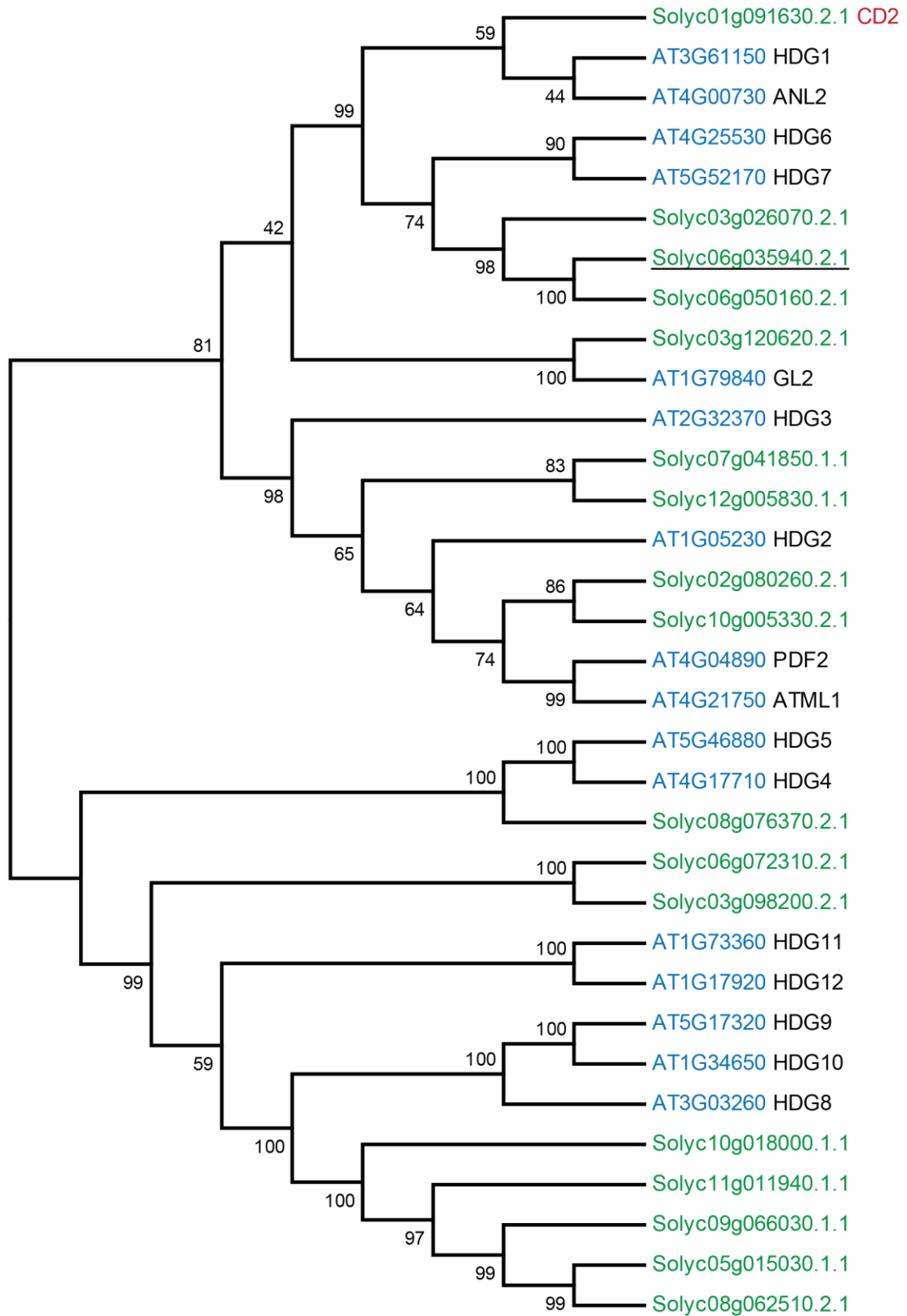


Figure 3.2. Phylogenetic tree of the Arabidopsis (16) and tomato (17) HD-ZIP IV family. The tree was constructed from amino acid sequences. The underlined gene was found to be expressed in higher levels in the *cd2* mutant than in the wild type, based on the differential expression analysis of RNA-seq data of 15 days post anthesis (dpa) fruit (see later in the chapter). Arabidopsis gene accession numbers are represented in blue and tomato accession numbers in green.

Expression of CD2

- qPCR analysis

To gain further insight into CD2 function, its expression pattern was assessed in a variety of organs and fruit developmental stages. qPCR analysis showed that CD2 is expressed in leaves, fruits, flowers, stems and roots (Fig. 3.3A,B). Despite the reported association between CD2 function and cuticle formation (Isaacson *et al.*, 2009), CD2 was not preferentially expressed in early stages of organ development and transcripts accumulated in comparable amounts in immature and mature leaves, flowers and fruits (Fig. 3.3A,B). More specifically, CD2 transcripts were present throughout fruit development with no clear change in expression levels (Fig. 3.3B). Additionally, the *cd2* mutant point mutation did not lead to a consistent decrease of transcript levels, suggesting that *CD2* transcript stability is not impaired in the mutant (Fig. 3.3A,B).

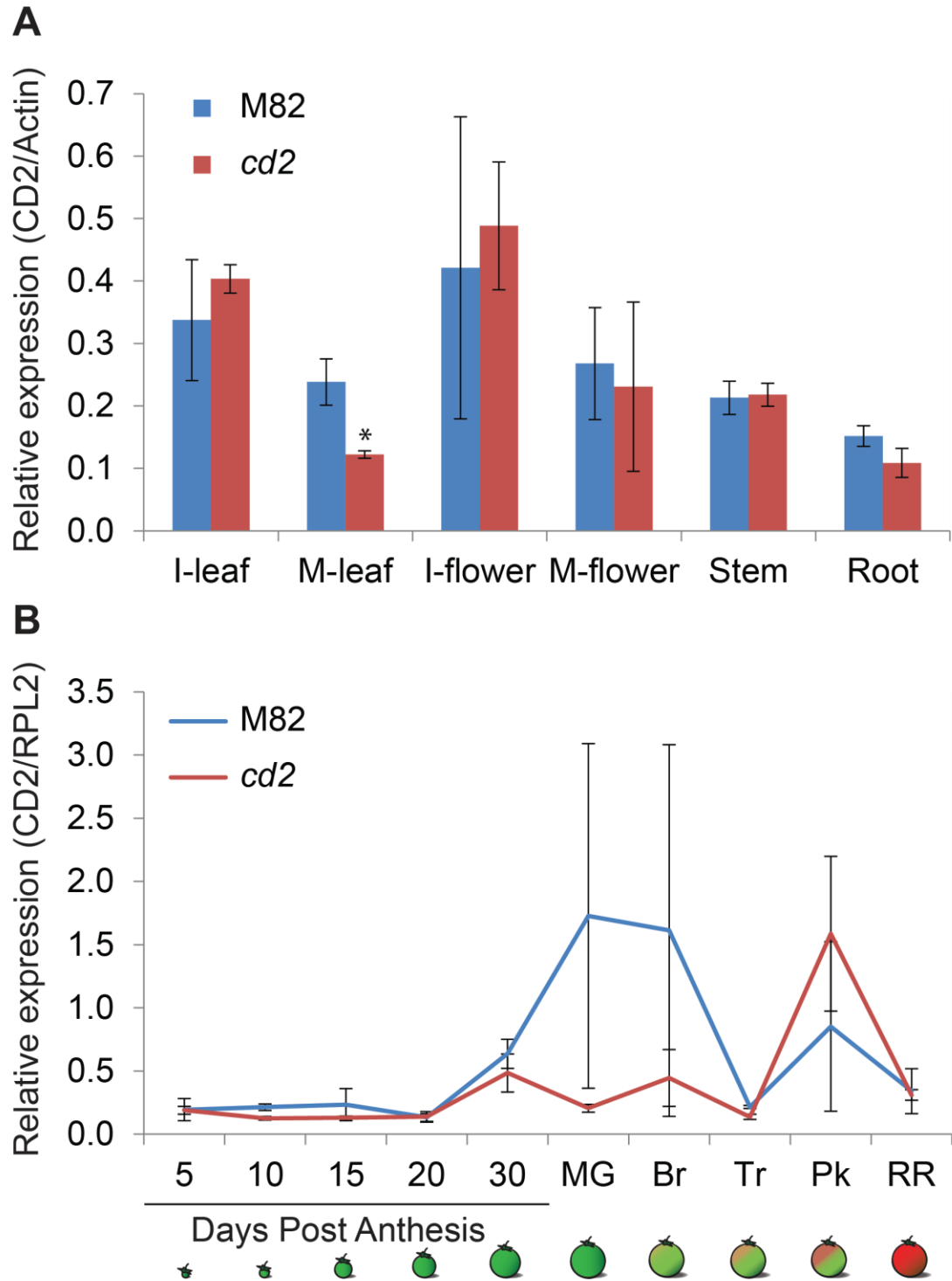


Figure 3.3. *CD2* expression in wild type M82 and the *cd2* mutant. (A) qPCR analysis of *CD2* transcript levels in various plant organs of *cd2* and its WT, M82. (B) qPCR analysis of *CD2* transcript levels at different growth stages of *cd2* and M82 fruit. I-leaf, immature leaf; M-leaf, mature leaf; I-flower, immature flower; M-flower,

mature flower; MG, Mature Green; Br, Breaker; Tr, Turning; Pk, Pink; RR, Red Ripe.
*, statistically significant at $\alpha = 0.05$.

- *Western blot analysis*

The expression patterns of transcript and protein may be distinct from each other, so a polyclonal antibody was raised in rabbit against the CD2 recombinant protein to test protein accumulation pattern. This recombinant protein was obtained by inducing the *E. coli* strain BL21(DE3), containing the construct *pET-26b(+):CD2*, with isopropyl β -D-1-thiogalactopyranoside (IPTG; Fig. 3.4). The recombinant protein was expressed as early as 1 h after induction and the accumulation was the highest 5 to 7 hours after induction. The recombinant protein is expected to be slightly bigger than the native protein (91.14 kDa versus 89.86 kDa) because of the addition of a Histidine tag. The western blot revealed a double band with an upper band of ~100 kDa and a lower band of ~90 kDa. Sequencing of these two bands indicated that they are both CD2. The reason for the recombinant protein to segregate in two bands is unclear but could result from some post-translational modification in *E. coli*.

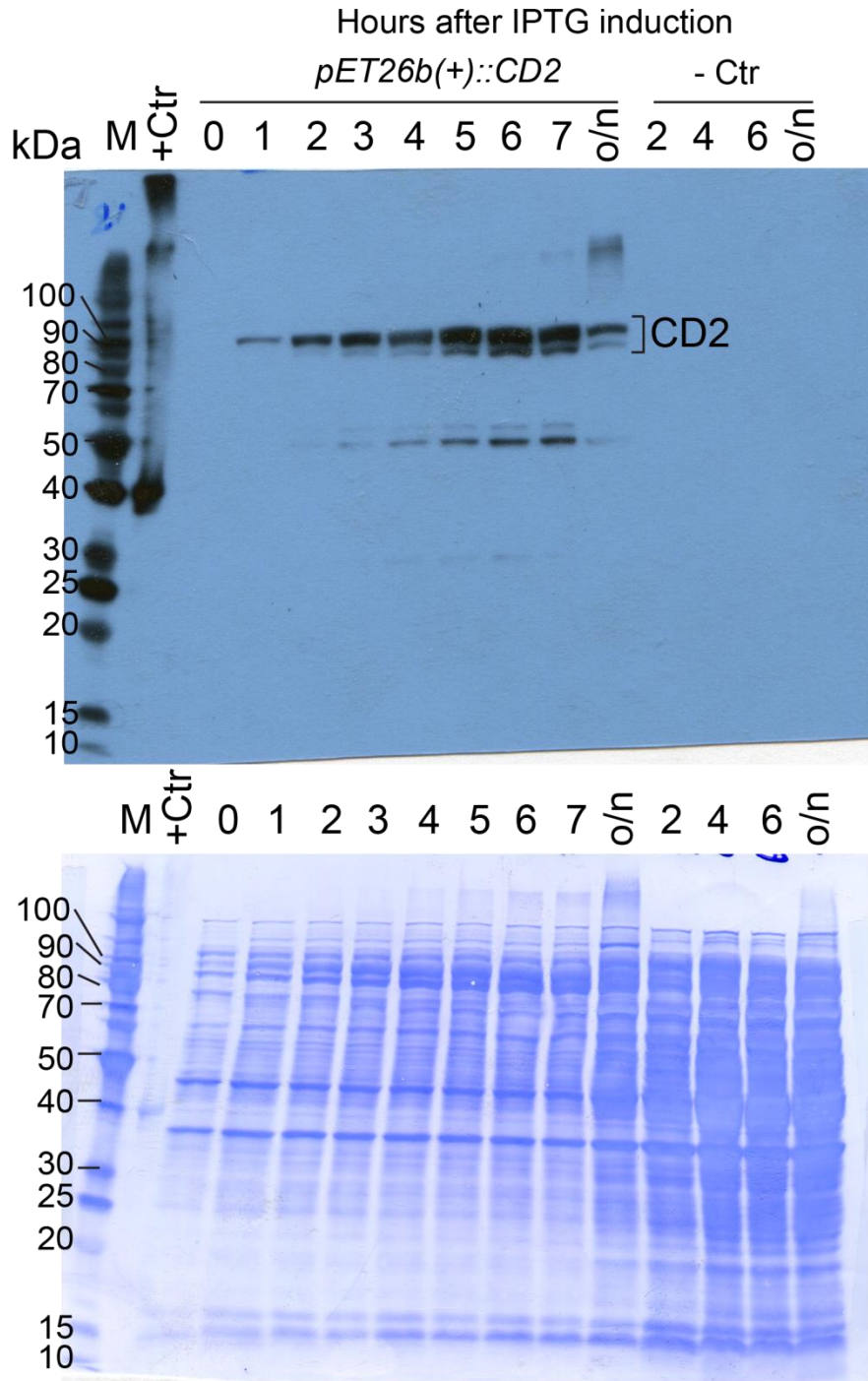


Figure 3.4. CD2 recombinant protein expression in *E. coli*. The upper panel is the western blot obtained from blotting the membrane of the lower panel with Histidine tag antibody to recognize CD2 recombinant protein. CD2 expression was induced with IPTG, and total cell proteins were denatured and ran on a SDS-polyacrylamide gel. +Ctr, positive control: CD1 recombinant protein (39.7 kDa); o/n, over night

incubation; - Ctr, negative control: *E.coli* strain devoid of the *pET26b(+)::CD2* construct; IPTG, isopropyl β -D-1-thiogalactopyranoside.

The antibody generated from CD2 recombinant protein was used to assess CD2 expression pattern in tomato. Western blot analysis showed that the protein and the transcript expression patterns are similar. The CD2 protein was detected in the pericarp throughout fruit development although it tended to accumulate less at and after Pink (Pk) stage (Fig. 3.5A). A single band of ~90 kDa was observed up to 30 days post anthesis (dpa) while an additional band of ~100 kDa was present after 30 dpa (Fig. 3.5A). Both bands likely correspond to *CD2* gene products since sequencing the polypeptides that resulted from the expression of CD2 in *E.coli* confirmed that both bands were CD2. The CD2 protein was also highly expressed in immature leaves, roots and stems, but not in seeds (Fig. 3.5B). It was observed that the CD2 protein was also present in the fruit of the *pe* and the *cd2* mutants (Fig. 3.5C), and while the mutated CD2 protein is predicted to be 17 kDa smaller in the *pe* mutant, this was not apparent in the immunoblot analysis. However, the band of ~90kDa was much fainter in protein extracts from *pe* than in those from the WT, consequently, the truncated CD2 protein may be degraded and the faint band may result from non-specific binding.

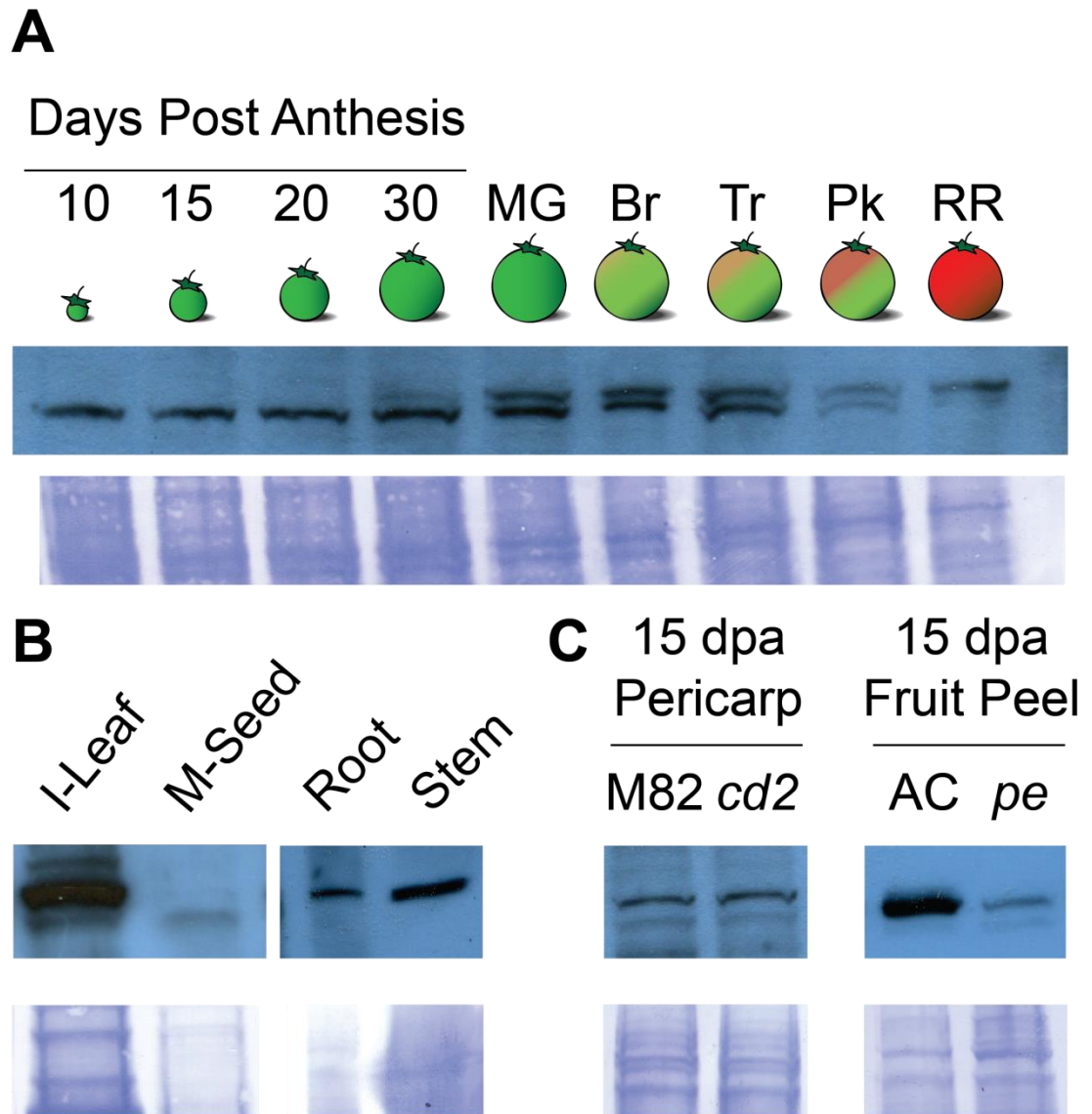


Figure 3.5. CD2 protein expression. (A) CD2 protein accumulation through fruit development in M82 pericarp. (B) CD2 protein levels in I-Leaf, immature leaf (< 2 cm); M-Seed, mature seed. (C) CD2 expression in the fruit of the *cd2* and *pe* mutants, using a purified antibody.

- *GUS-promoter analysis*

Spatial and temporal expression patterns of *CD2* were further examined by studying M82 plants transformed with a *CD2 promoter:: β -glucuronidase* (*GUS*) fusion construct. *GUS* expression happened early in plant development in the vascular tissue of the leaves, stem and roots of seedlings (Fig. 3.6). Strong staining of the vascular tissue, and more specifically of the phloem, is retained later in development for leaves (Fig. 3.7B), petals (Fig. 3.8A,B), flower and fruit pedicels (Fig. 3.9A-C), roots (Fig. 3.9F), stems (Fig. 3.9D) and petioles (Fig. 3.9E). The area between the veins of the petals also showed blue staining, indicating *CD2* expression in additional tissues. In flower longitudinal-sections, staining of the pedicel stopped at the base of the ovary, the rest of which was stain-free (Fig. 3.8A). However, the anther expressed the reporter gene (Fig. 3.8A) and anther cross-sections showed expression in the tissues located between epidermis and microsporocyte (Fig. 3.8C,D). *GUS* expression was very weak, or non-existent, in stem and petiole epidermal cells (Fig. 3.9d,e); however, weak expression was apparent in pedicels 7 dpa and older (Fig. 3.9B,C). Leaf trichomes and the upper and lower epidermis of leaves also expressed the reporter gene (Fig. 3.7A-C). Weak staining was sometimes observed in the pith and cortex of the stem and pedicel, and in the parenchyma cells of petiole (Fig. 3.9D,E). The cell layers underlying the outer epidermis of the fruit pedicel and stem were devoid of staining (Fig. 3.9C-D); however, this may reflect reduced penetration of the substrate into these layers, the cells of which had walls that could be lignified and suberized as suggested by a yellowish color.



Figure 3.6. *pCD2::GUS* expression pattern in seedling. Scale bar, 1 mm.

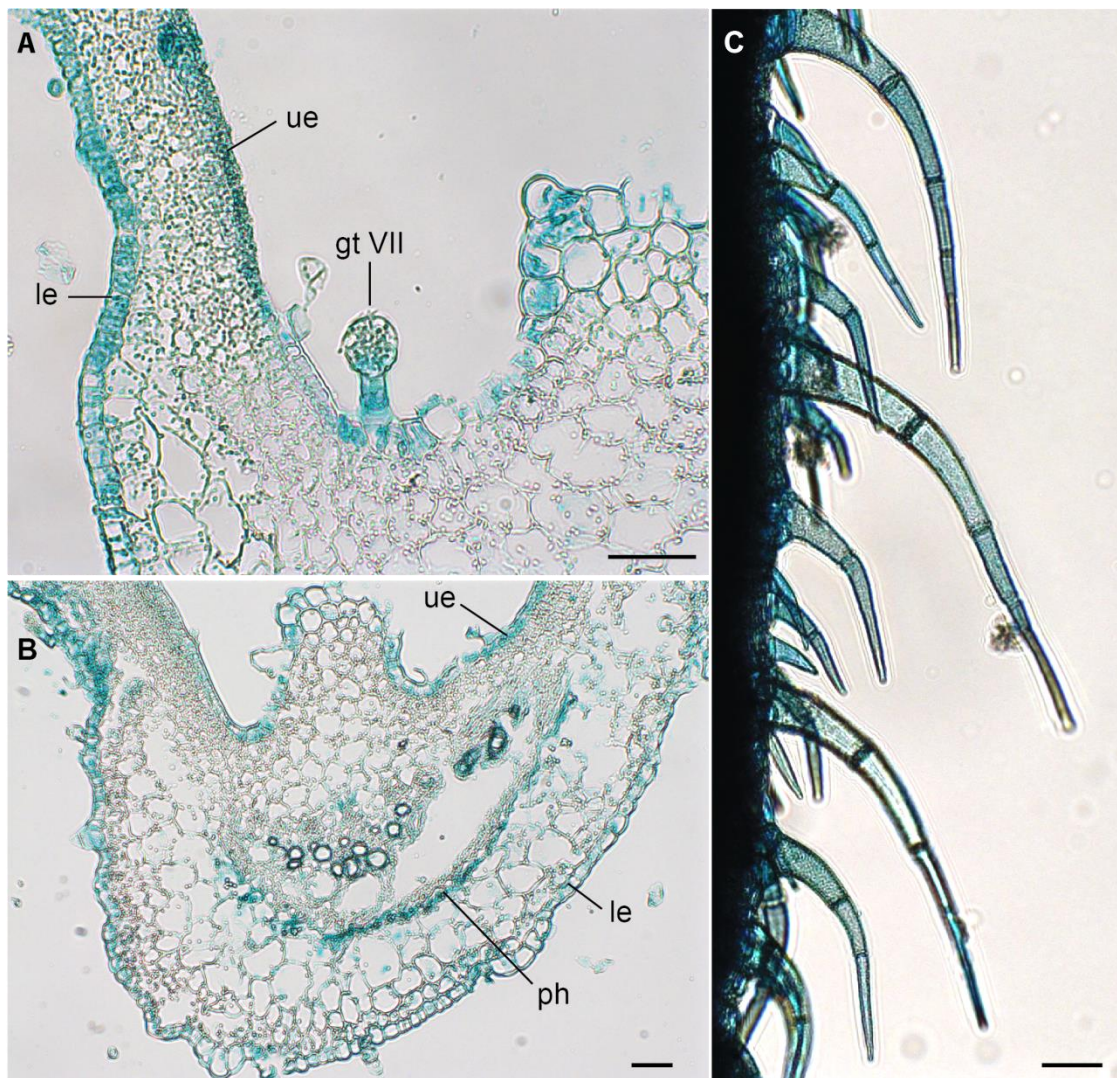


Figure 3.7. *pCD2::GUS* expression analysis in leaf. (A) Cross section of a developing leaf. (B) Cross-section of the midrib vein of a developing leaf. (C) Trichomes covering a developing leaf. gt VII, glandular trichome type VII; le, lower epidermis; ph, phloem; ue, upper epidermis. Scale bars, 50 μ m.

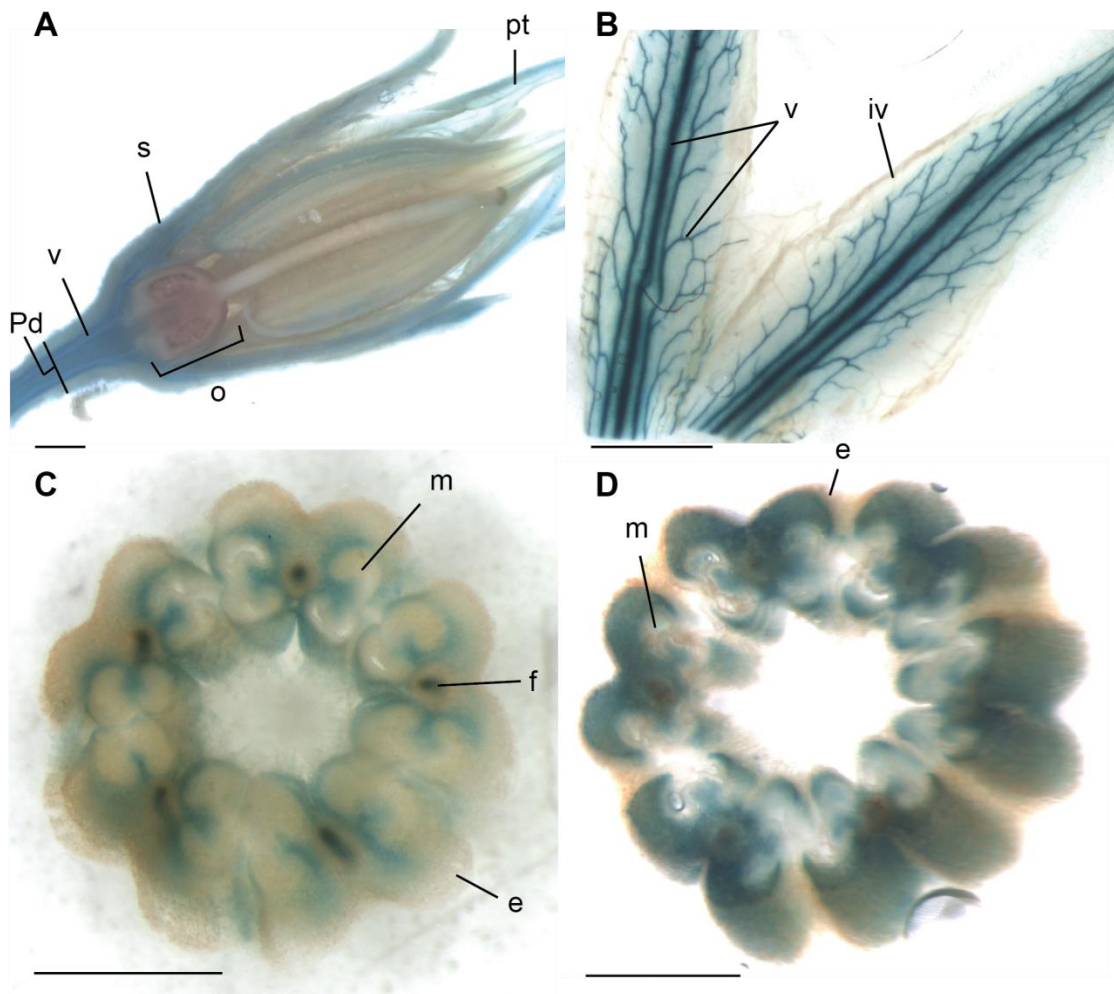


Figure 3.8. *pCD2::GUS* expression analysis in flowers. (A) Longitudinal section of a flower. (B) Petals. (C and D) Anther. e, epidermis; f, filament; iv, inter-vein area; m, microsporocyte; o, ovary; pd, pedicel; pt, petal; s, sepal; v, vascular tissue. Scale bars, 1 mm.

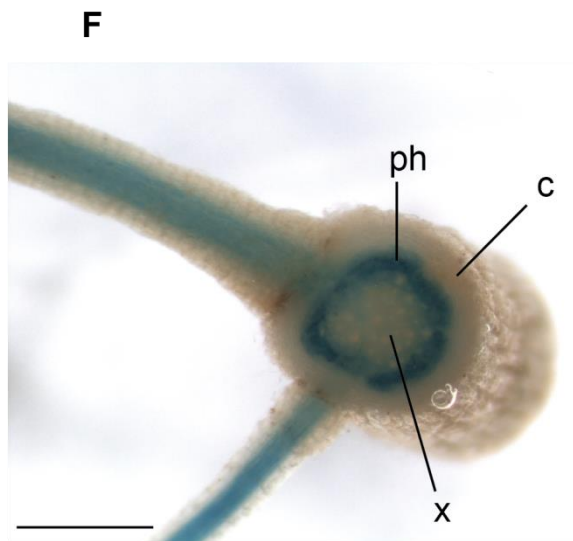
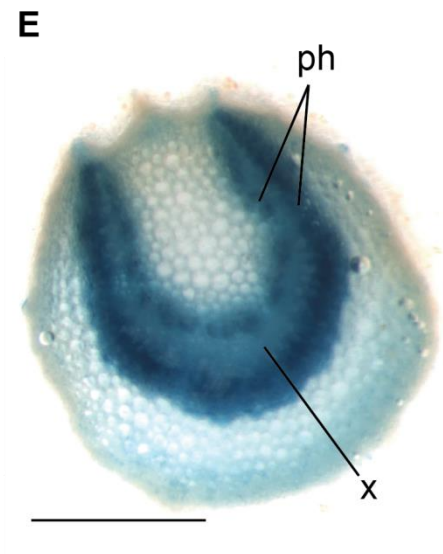
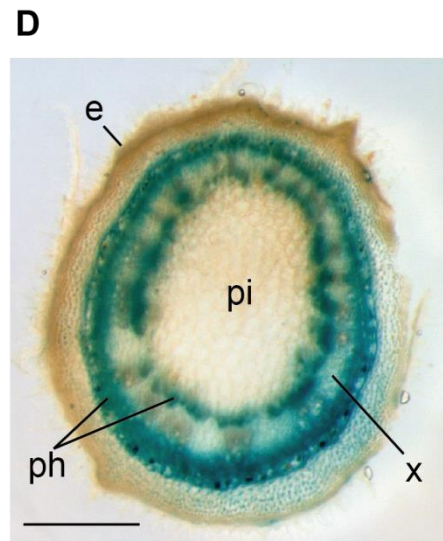
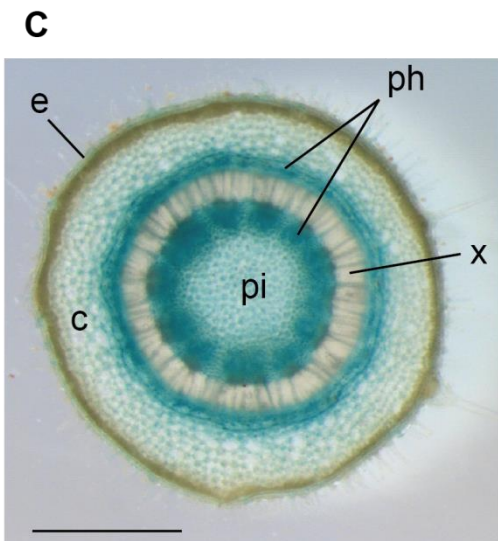
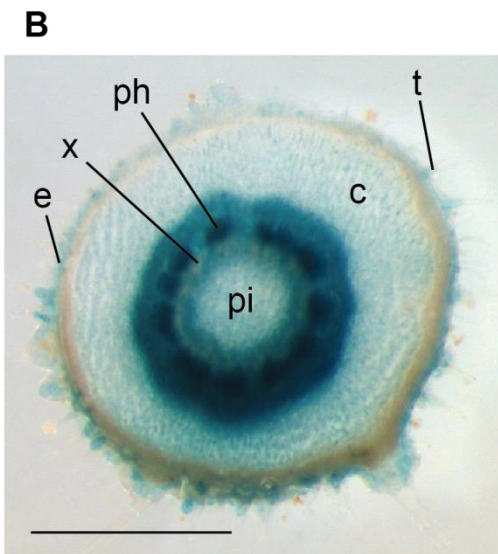
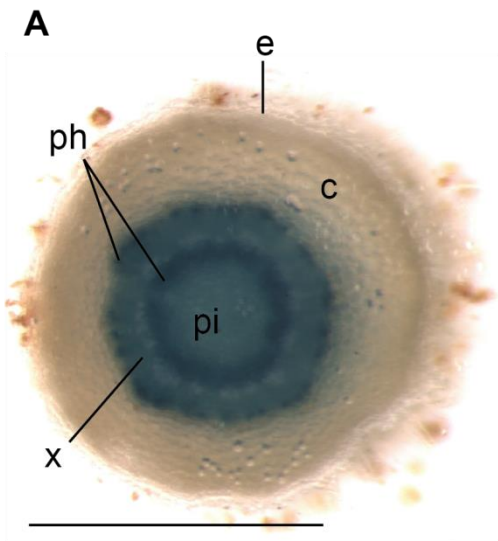


Figure 3.9. *pCD2::GUS* expression analysis. (A) Pedicel of flower. (B) Pedicel of 7 dpa fruit. (C) Pedicel of 20 dpa fruit. (D) Stem (E) Petiole (F) Root. c, cortex; e, epidermis; pi, pith; ph, phloem; x, xylem. Scale bars, 1 mm.

With respect to expression during fruit ontogeny, at 5 dpa, the inner epidermis of the fruit pericarp showed GUS expression while the corresponding tissue of the ovary did not (Figs. 3.10A and 3.8A). At 10 dpa, staining of the inner epidermis was maintained and the outer epidermis started to show blue staining in some fruits (Fig. 3.10 Ba,c,d), and by 15 dpa, the outer epidermis was consistently stained (Fig. 3.10C). The cell layers beneath the outer epidermis also strongly expressed the reporter gene (Figs. 3.10C, 3.11A, 3.12A, 3.13A). Subsequently, the outer and inner epidermis showed GUS expression up until the Mature Green (MG) stage (Figs. 3.11A, 3.12A, 3.13A). The vasculature connected to the columella was stained throughout fruit development, while expression in the vascular bundles of the pericarp and funiculus was first evident at 10 dpa, although these tissues did not consistently express GUS in maturing fruits (Fig. 3.10-3.14). The vascular tissue of fruit is likely mostly composed of phloem rather than xylem which would explain why free of stain xylem was not observed (Ho *et al.*, 1987; Lee, 1988). GUS expression was not observed in unfertilized ovules, while the seed coat of fertilized seeds stopped expressing it at MG stage, which is consistent with low levels of protein expression seen in the Western blot analysis of mature seed proteins (Fig. 3.5B). GUS staining was observed in the adaxial side of the cotyledons, possibly in the protophloem, and the vascular tissue of the radicle also showed GUS expression (Figs. 3.13B-E and 3.14D,E). Staining was also observed in the placenta but not in the locular tissue (Figs. 3.12B and 3.13C).

Additionally, the inner epidermis of the pericarp, septa and placenta is stained but there is no staining of the outer cell layer of the locular tissue (Fig. 3.11D).

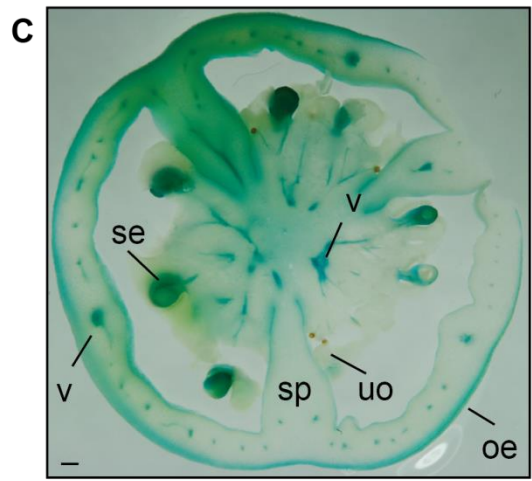
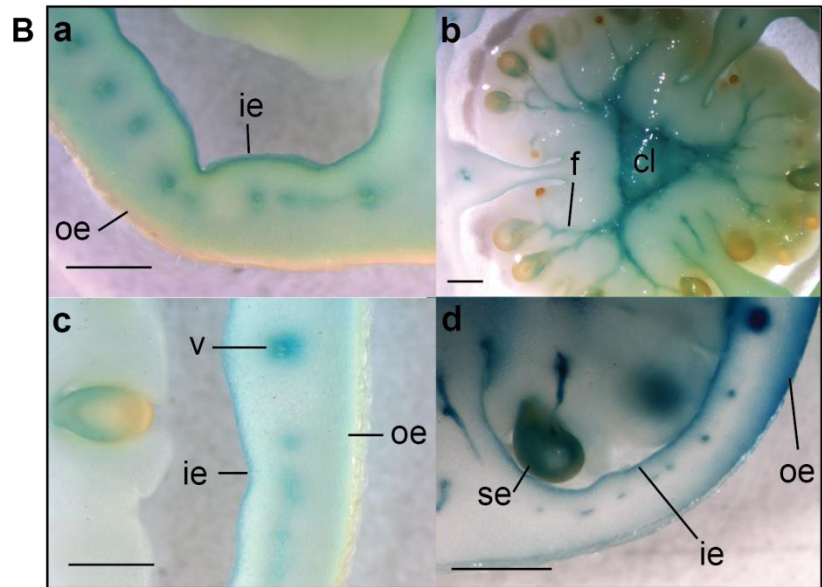
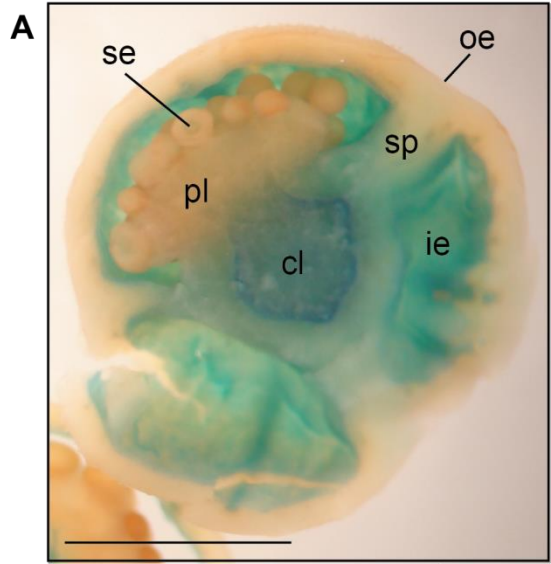


Figure 3.10. *pCD2::GUS* expression analysis of immature fruits. (A) The proximal half of a 5 dpa fruit. (B) Sections of 10 dpa fruits. (C) Section of a 15 dpa fruit. cl, columella; ie, inner epidermis; oe, outer epidermis; f, funiculus; pl, placenta; se, seed; sp, septa; uo, unfertilized ovule; v, vascular tissue. Scale bars, 1 mm.

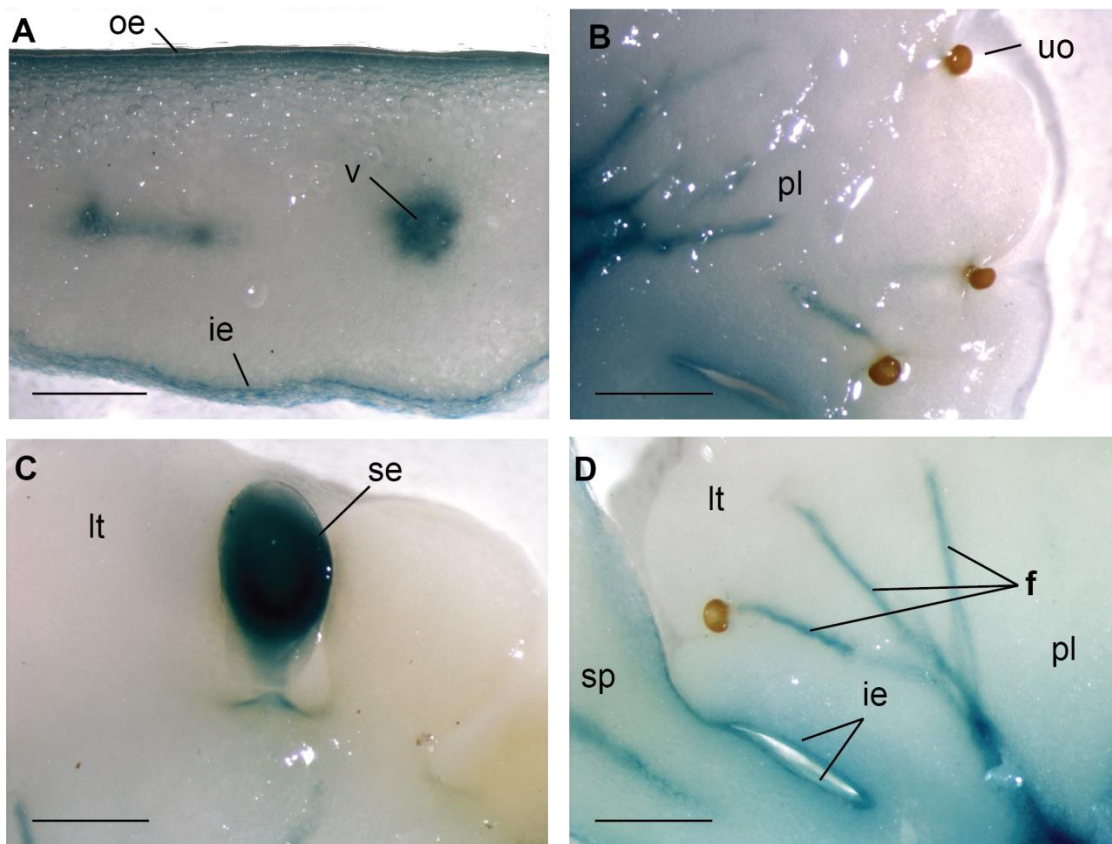


Figure 3.11. *pCD2::GUS* expression analysis of 20 dpa fruits. (A) Pericarp. (B) Placenta. (C) Seed. (D) Placenta and septa. ie, inner epidermis; oe, outer epidermis; f, funiculus; lt, locular tissue; pl, placenta; se, seed; sp, septa; uo, unfertilized ovule; v, vascular tissue. Scale bars, 1 mm.

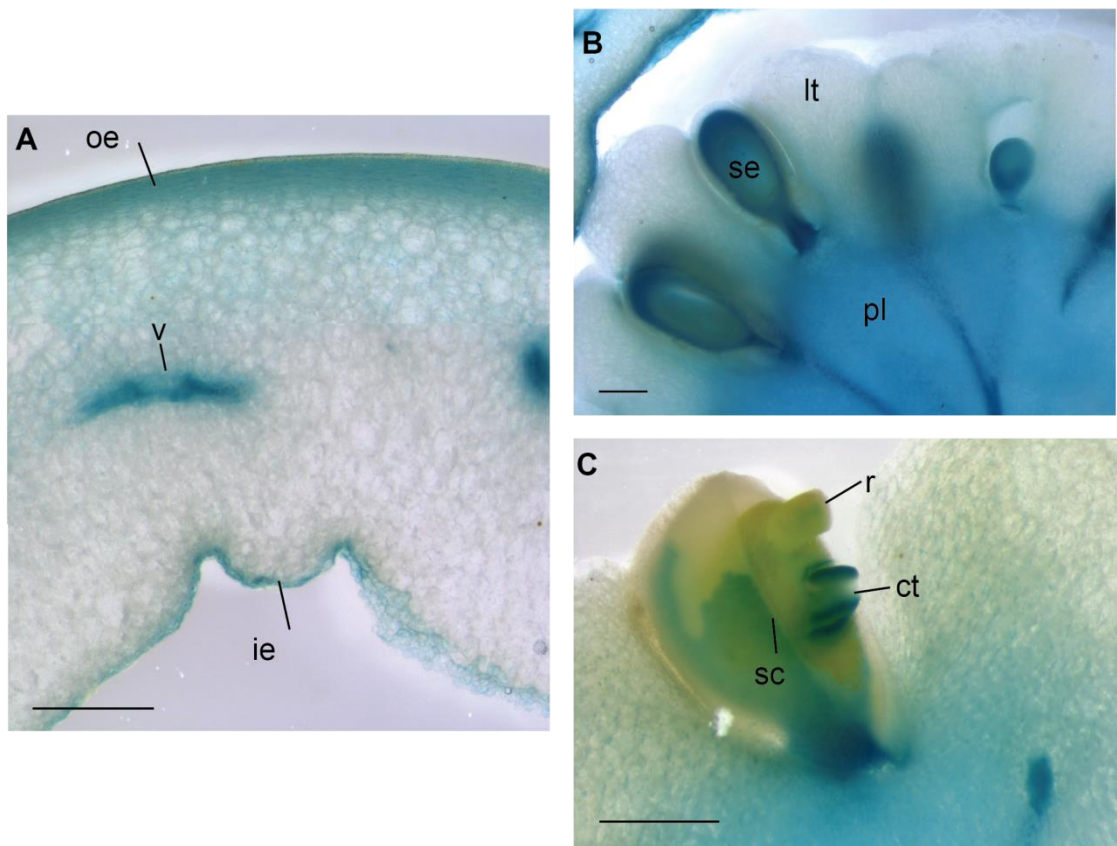


Figure 3.12. *pCD2::GUS* expression analysis of 30 dpa fruits. (A) Pericarp. (B) Locular tissue and placenta. (C) Seed. ct, cotyledon; ie, inner epidermis; oe, outer epidermis; lt, locular tissue; pl, placenta; r, radicle; sc, seed coat; se, seed; v, vascular tissue. Scale bars, 1 mm.

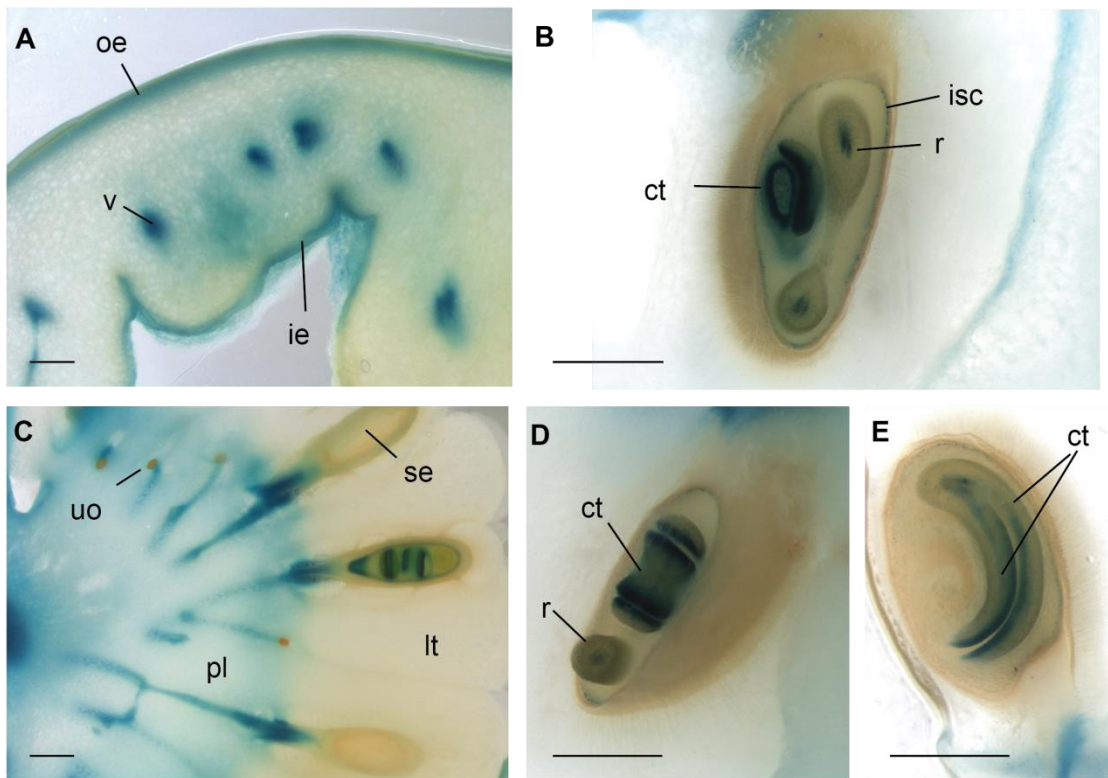


Figure 3.13. *pCD2::GUS* expression analysis of Mature Green (MG) fruits. (A) Pericarp. (B, D and E) Seeds. (C) Placental area. ct, cotyledon; ie, inner epidermis; isc, inner seed coat; oe, outer epidermis; lt, locular tissue; pl, placenta; r, radicle; se, seed; uo, unfertilized ovule; v, vascular tissue. Scale bars, 1 mm.

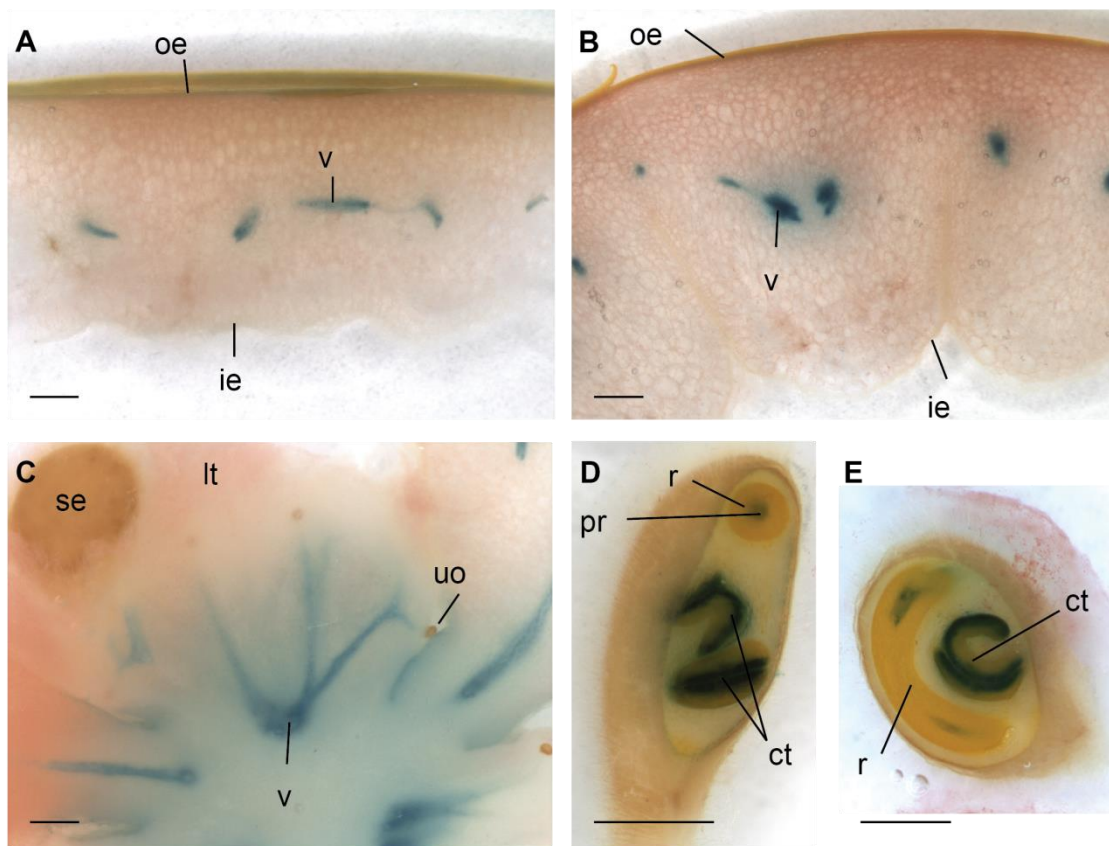


Figure 3.14. *pCD2::GUS* expression analysis of ripening fruits. (A) Pericarp from a Pink stage fruit. (B) Pericarp from a Red Ripe stage fruit. (C) Placental area from a Light Red stage fruit. (D and E) Seeds from Pink stage fruits. ct, cotyledon; ie, inner epidermis; oe, outer epidermis; lt, locular tissue; pr: procambium; r, radicle; se, seed; uo, unfertilized ovule; v, vascular tissue. Scale bars, 1 mm.

- Meta-analysis of CD2 transcript expression based on public data sets

The low expression of the GUS reporter gene in maturing fruits was unexpected, since *CD2* transcript was expressed during fruit ripening (Figs. 3.3B and 3.7G). A meta-analysis of *CD2* transcript expression based on public data sets was therefore undertaken to determine *CD2* expression in ripening fruits. Two independent RNA-seq analyses, experiments D004 and D006 (<http://ted.bti.cornell.edu/cgi-bin/TFGD/digital/home.cgi>), showed that *CD2* is present in the fruits of *Solanum pimpinellifolium*, a wild species of tomato, and of the *Solanum lycopersicum* domesticated cultivar Heinz (Fig. 3.15A,B). Furthermore, the transcript levels were equivalent between immature green fruits and ripening fruits. RNA-seq analyses confirmed that *CD2* is widely expressed in plant organs, including flowers, fruits, leaves and roots at many developmental stages (Fig. 3.15A,B).

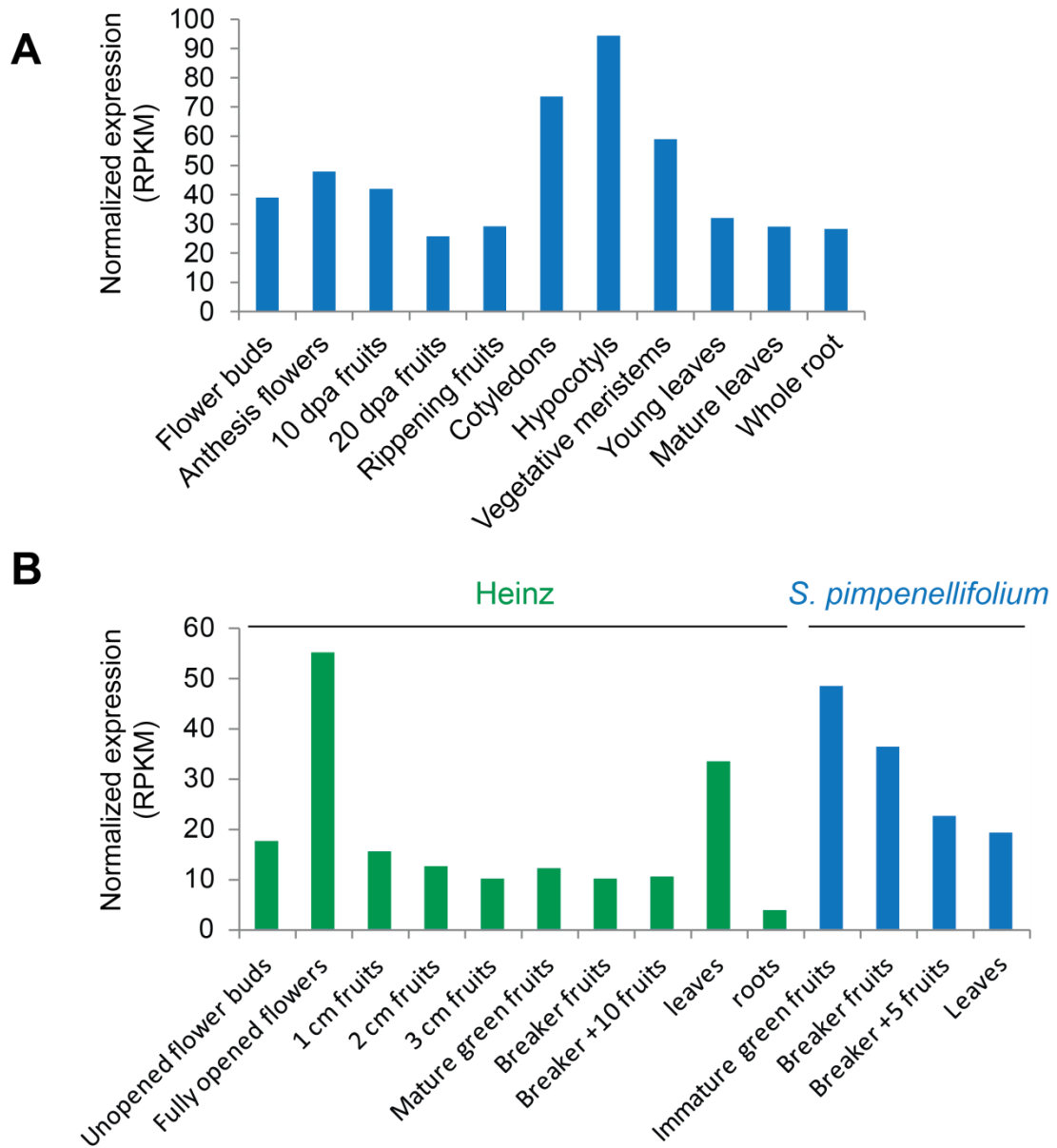


Figure 3.15. Expression of CD2 in the organs of two *Solanum* genotypes from publicly available RNA-seq datasets. (A) CD2 expression in various organs of *S. pimpinellifolium* (accession LA1589) based on RNA-seq data from the Tomato Functional Genomics Database, experiment D006 (<http://ted.bti.cornell.edu/cgi-bin/TFGD/digital/home.cgi>). (B) CD2 expression in various organs of *S. lycopersicum* (cv. Heinz) and *S. pimpinellifolium* based on data from the Tomato Functional Genomics Database, experiment D004 (<http://ted.bti.cornell.edu/cgi-bin/TFGD/digital/home.cgi>).

pCD2::GUS expression analysis provided information on *CD2* transcript distribution at the tissue level. To corroborate these results, publically available RNA-seq datasets targeting cell-type specific transcriptome were used (experiments D009 (<http://ted.bti.cornell.edu/cgi-bin/TFGD/digital/home.cgi>; Matas *et al.*, 2011; Fig.3.16A,B). *CD2* expression was detected in the ovary, contradicting the GUS expression data (Fig.3.16A). However, it should be noted that the fruit tissues were harvested using laser capture microdissection (LCM) so it was necessary to perform RNA-amplification before sequencing, which allows the detection of extremely low levels of transcripts, while the same amount of expression may not be visible in GUS-expressing lines. At 4 dpa, the expression of *CD2* was higher in the seed coat, funiculus, septum and pericarp than in the placenta (Fig. 3.16A), which was also the case during early fruit development in the GUS-expressing lines (Fig. 3.10B). In the pericarp of 10 dpa *S. lycopersicum* Ailsa Craig fruits, *CD2* accumulated to the highest levels in the outer epidermis, the tissue responsible for the synthesis of the cuticle (Fig. 3.16B). *CD2* was also expressed in the inner epidermis, which is covered by a thin cuticle (Matas *et al.*, 2011), as well as in the collenchyma and the parenchyma (Fig. 3.16B), while *CD2* transcript levels were the lowest in the vascular tissue (Fig. 3.16B), which again is contrary to the intense GUS expression in the phloem (Figs. 3.10 - 3.14). However, the presence of *CD2* transcript in the funiculus (Fig.3.16A), which is mainly constituted of vascular tissue, indicates that *CD2* is indeed expressed in the vascular tissue.

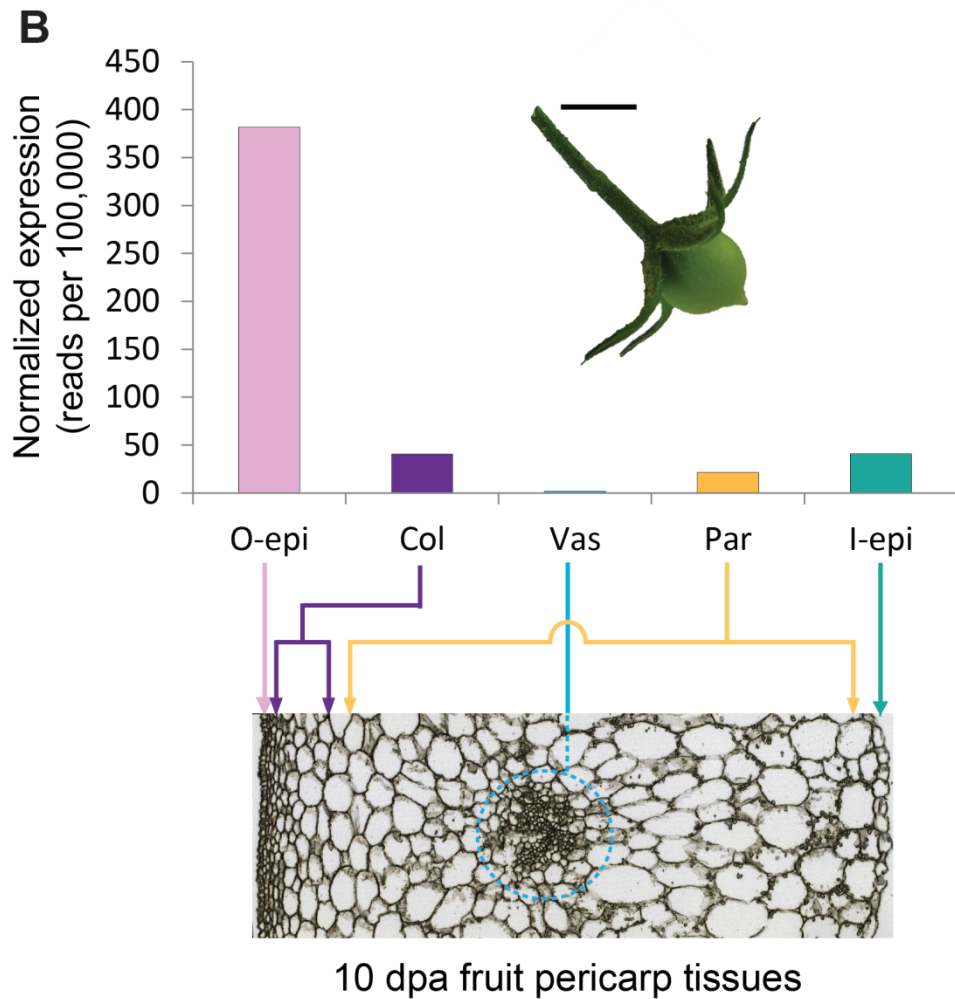
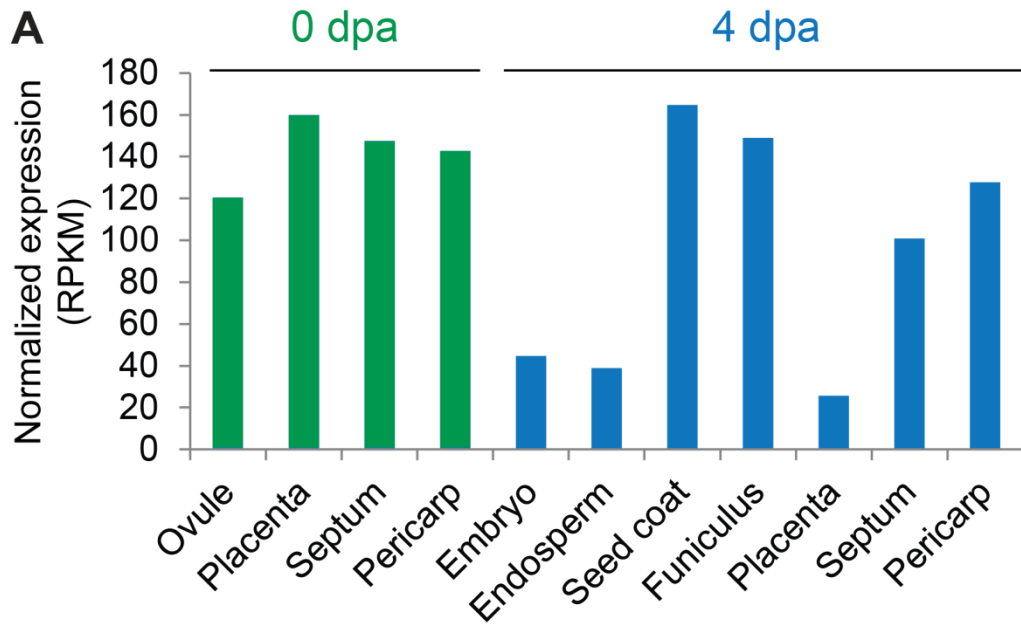


Figure 3.16. Expression of *CD2* transcript in ovary and fruit tissues from publically available RNA-seq datasets. (A) Tissue-specific *CD2* expression in *S. pimpinellifolium* (accession LA1589) ovaries and 4 dpa fruits based on LCM-coupled to Illumina RNA-seq analysis. Data were obtained from the Tomato Functional Genomics Database, experiment D009 (<http://ted.bti.cornell.edu/cgi-bin/TFGD/digital/home.cgi>). (B) *CD2* expression in the pericarp of 10 dpa AC fruits. O-epi, outer epidermis; Col, collenchyma; Vas, vascular tissue; Par, parenchyma; I-epi, inner epidermis. Data from Illumina re-sequencing of the amplified RNAs published in Matas *et al.* (2011). Scale bar, 1 mm.

- Subcellular localization of *CD2*

As a transcription factor, *CD2* is expected to localize in the nucleus. A Red Fluorescent Protein (RFP) was therefore fused to the C-terminal end of the whole protein and expressed in onion epidermal cells to assess the intra-cellular localization of *CD2*. Transient expression of the fused RFP protein was detected by confocal microscopy (Fig. 3.17). The nuclei were stained with 4',6-diamidino-2-phenylindole (DAPI), a stain that fluoresces when bound to A-T rich regions of DNA (Kapuscinski, 1995). The red fluorescence signal perfectly overlapped with the DAPI stained nuclei and with the nuclei seen under bright field condition (Fig. 3.17). This result indicates that *CD2* localizes in the nucleus, which is consistent with *CD2* acting as a transcription factor.

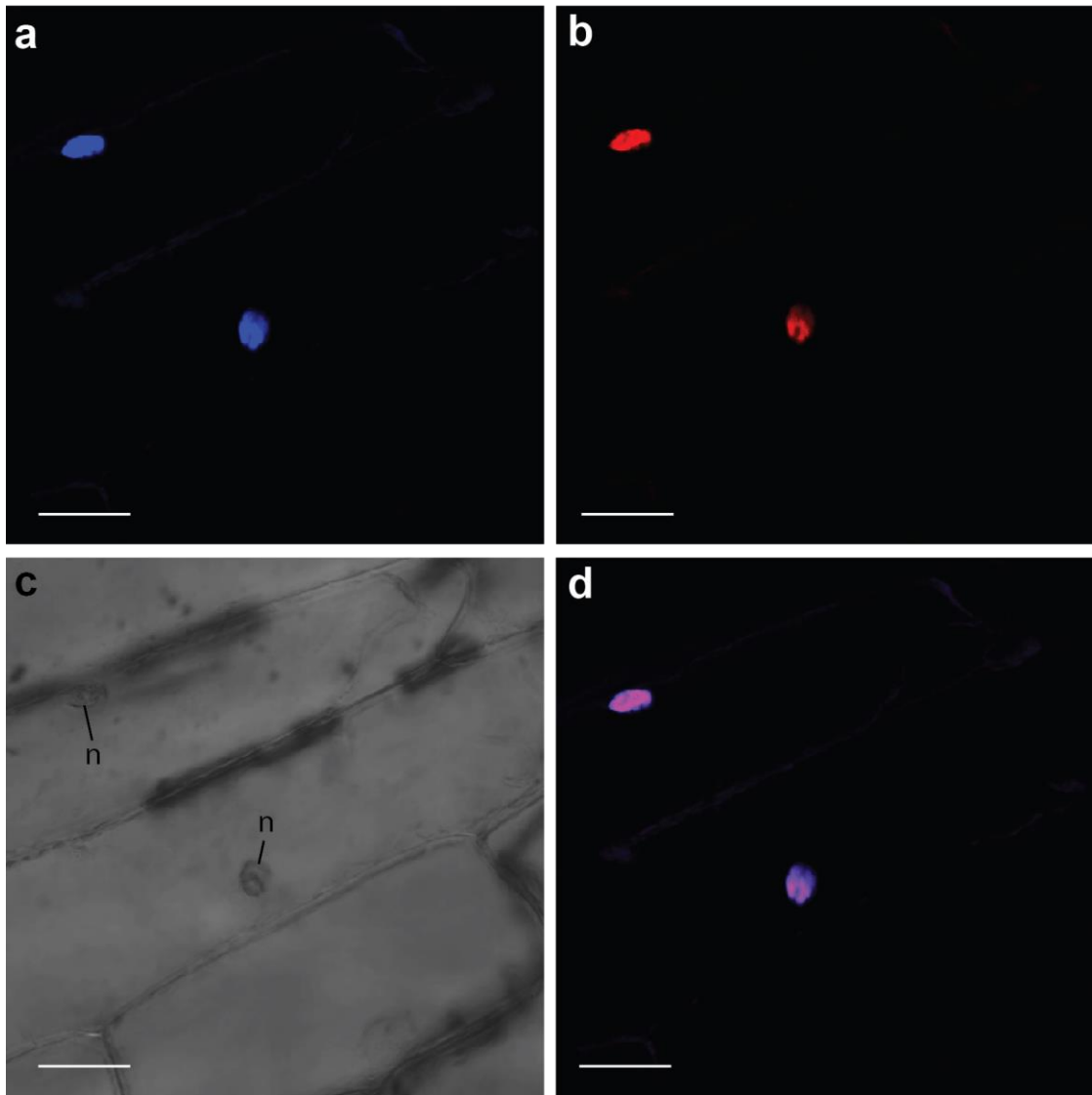


Figure 3.17. *pCaMV35S::CD2/RFP* expression in epidermal onion cells. (a) DAPI staining of the nuclei. (b) RFP reporter signal. (c) Bright field image. (d) Merged DAPI and RFP. Scale bar, 50 μ m.

Genes directly or indirectly regulated by CD2

The nuclear localization of CD2 and the cutin deficient phenotype of the *cd2* mutant suggest that CD2 is a transcription factor that regulates cuticle biosynthesis. Consequently, the identification of genes targeted by CD2 was undertaken to answer several questions: do the cutin deficiency and abnormal cuticular wax load of *cd2* result from a general disruption of the cuticle pathway or from the differential expression of a small amount of cuticle biosynthesis related genes? Does CD2 regulate the expression of other transcription factors known to affect cuticle formation? Does CD2 regulate additional pathways? Can novel cuticle biosynthesis related genes be identified? To answer these questions, the transcriptome of the *cd2* mutant and its WT were compared, focusing on the epidermis, since this study primarily focuses on the cuticle. The outer epidermis of *cd2* and M82 was harvested in triplicates using Laser Capture Microdissection (LCM), which should increase the relative concentration of cuticle-related transcripts, followed by RNA-amplification and Illumina sequencing. Two stages of the fruit development were selected to determine if CD2 function changes during fruit ontogeny. An early stage of fruit development (15 dpa) was targeted as this corresponds to a period of rapid expansion that is associated with a high rate of cuticle biosynthesis and restructuring. Furthermore, a late stage of development (Turning) was also targeted as ripening is a stage of profound metabolomic changes and also because a link between MADS-box ripening regulators and cuticle deposition has previously been reported (Hen-Avivi *et al.*, 2014).

- Differentially expressed genes at 15 dpa

Transcripts corresponding to 53 and 7 loci were identified as expressed at lower or higher levels, respectively, in the mutant fruit epidermis compared to that of the WT (Fig. 3.18). Of these, differential expression was confirmed by semi-quantitative PCR (semi-qPCR) and/or quantitative PCR (qPCR) for 46 loci (Fig. 3.18). Only two genes were found to be more expressed in *cd2* at 15 dpa: Solyc06g035940, a HD-Zip IV family member, and Solyc09g091550, a methyltransferase. Solyc06g035940 is one of the closest homologs of CD2 (Fig. 3.2) and qPCR analysis confirmed that its expression is substantially higher in the *cd2* mutant throughout fruit ontogeny (Fig. 3.19). Unlike CD2, Solyc06g035940 expression is not enriched in the outer epidermis (Figs. 3.16B and 3.19).

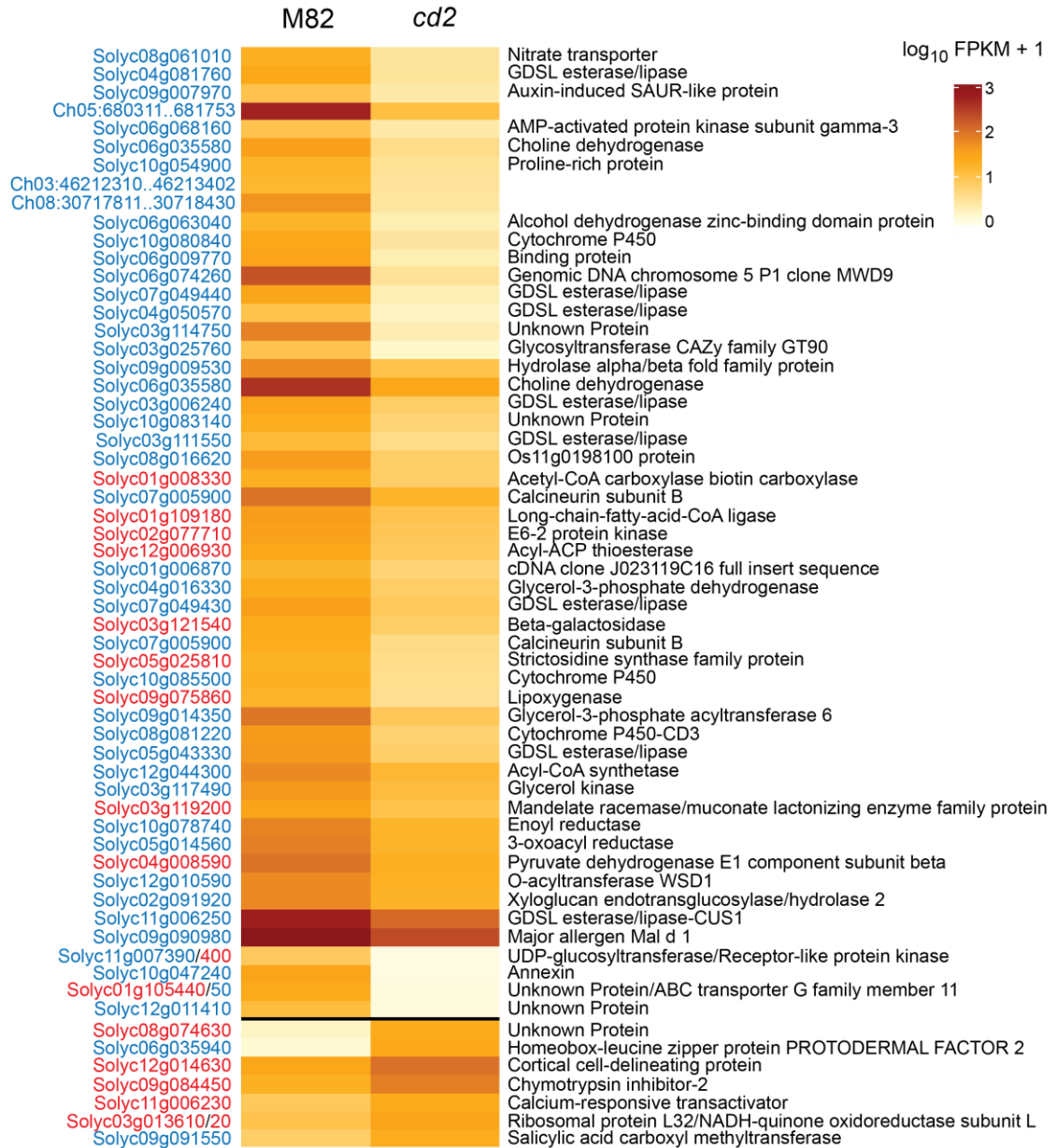


Figure 3.18. Heatmap representation of genes that are differentially expressed in epidermal cells of 15 dpa fruits of the *cd2* mutant and the wild type M82, based on LCM/RNA-seq data. The genomic region of the 2.40 version of the sequenced *S. lycopersicum* genome is given if no gene was identified in the differentially expressed sequence. If more than one gene may correspond to the differentially expressed sequence, based on alignment ambiguity, all candidate genes are given, separated by a / indicator. Color coding of the genes: blue, differential expression confirmed by semi-qPCR; red, differential expression infirmed by semi-qPCR. Gene annotation is consistent with the SGN database (<http://solgenomics.net/>).

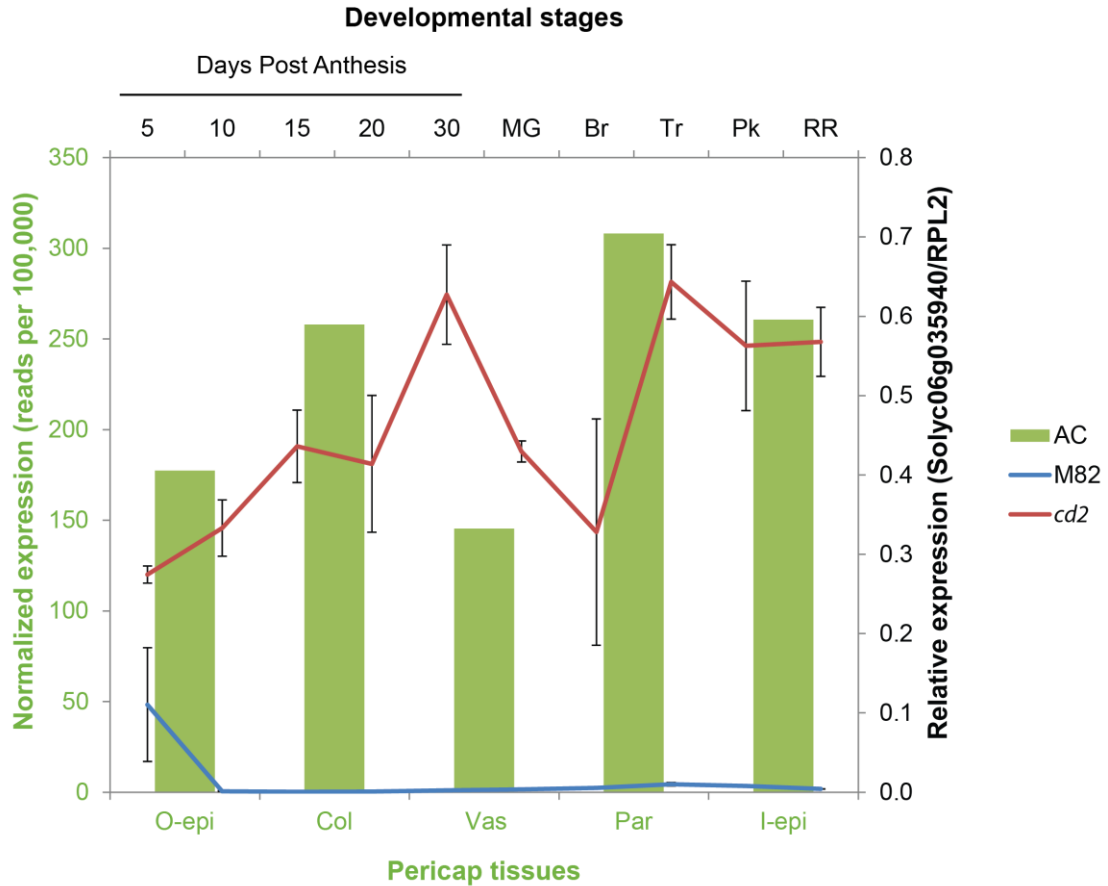


Figure 3.19. Expression pattern of Solyc06g035940, a member of the HD-Zip IV subfamily of transcription factors. Solyc06g035940 transcript levels throughout fruit ontogeny in *cd2* compared to M82 are represented with lines plotted on the right and top axes. Transcript levels in 5 tissues of 10 dpa pericarp of AC fruits are indicated in green columns plotted on the left and bottom axes. MG, Mature Green; Br, Breaker; Tr, Turning; Pk, Pink; RR, Red Ripe; O-epi, Outer epidermis; Col, Collenchyma; Vas, Vascular tissue; Par, Parenchyma; I-epi, Inner epidermis. The tissue-specific data were derived from Illumina re-sequencing of the amplified RNAs published in Matas *et al.* (2011).

The expression patterns of the differentially expressed genes at the 15 dpa stage of development across five tissues of the pericarp are shown in Fig. 3.20. Most of the differentially expressed genes were highly expressed in the outer epidermis, from which it can be inferred that the transcriptome of the outer-epidermis was successfully targeted, and that CD2 regulates epidermal-specific genes. Furthermore, many differentially expressed genes were also highly expressed in the inner epidermis, a tissue that likely has many similar functions to those of the outer epidermis, and with which it has a related ontogeny. Solyc10g047240, an annexin, stands out as having strong spatial variation in expression, with ~90% of its transcripts being detected in the vascular tissue. It is possible that if the RNA-seq experiment was done on the pericarp, more DE genes with enriched expression in the vascular tissue would have been detected. This scenario is plausible since the GUS-expression experiment showed a strong staining of this tissue.

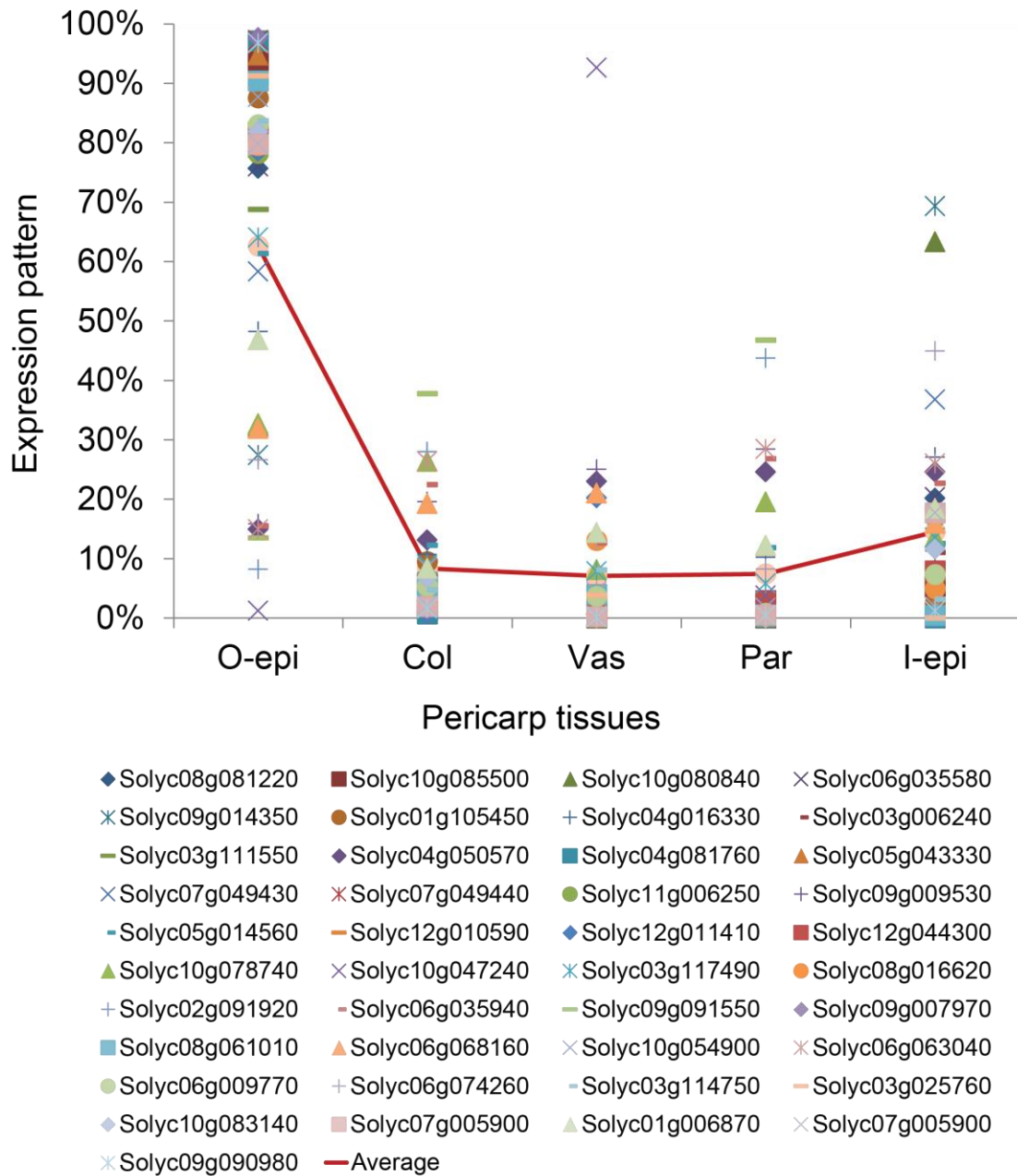


Figure 3.20. Tissue-specific expression pattern of the differential expressed genes identified at 15 dpa by RNA-seq and confirmed by qPCR. Red line represents the average of expression percentage in each tissue. O-epi, Outer epidermis; Col, Collenchyma; Vas, Vascular tissue; Par, Parenchyma; I-epi, Inner epidermis. The data were derived from Illumina re-sequencing of the amplified RNAs published in Matas *et al.* (2011).

- *Cuticle - related genes*

Gene Ontology analysis revealed that 62% of the target gene candidates confirmed by qPCR are annotated as participating in lipid metabolic processes and 19% are annotated as being involved in cuticle development (Fig. 3.18). Two of these genes have previously been shown to catalyze specific chemical steps in cutin polymer biosynthesis: Solyc11g006250 (CUS1) is a GDSL lipase/esterase responsible for the polymerization of cutin (Yeats *et al.*, 2012; Yeats *et al.*, 2014), as described in Chapter 2, and Solyc08g081220 (CD3) catalyzes cutin precursor hydroxylation (Shi *et al.*, 2013). Furthermore, the closest Arabidopsis homologs of Solyc09g014350 and Solyc01g105450 (At2g38110 and At1g17840, respectively), are involved in cuticle biosynthesis and transport. At2g38110 is glycerol-3-phosphate *sn*-2-acyltransferase 6 (GPAT6), required for the incorporation of C16 monomers into flower cutin (Li-Beisson *et al.*, 2009) and At1g17840 encodes WBC11/ABCG11, a plasma membrane localized transporter required for cutin and wax transport to the extracellular matrix (Bird *et al.*, 2007; Panikashvili *et al.*, 2007). qPCR analysis of *CD1*, *CD3*, *SIGPAT6* and *SIABCG11* confirmed that their transcripts are expressed in immature green fruit, when expansion is coupled with cuticle biosynthesis. Throughout fruit ontogeny, their transcripts were expressed at lower levels in the *cd2* mutant than in M82 (Fig. 3.21) and accumulated preferentially in the outer and/or inner epidermis, in accordance with their role in cuticle biosynthesis (Fig. 3.21).

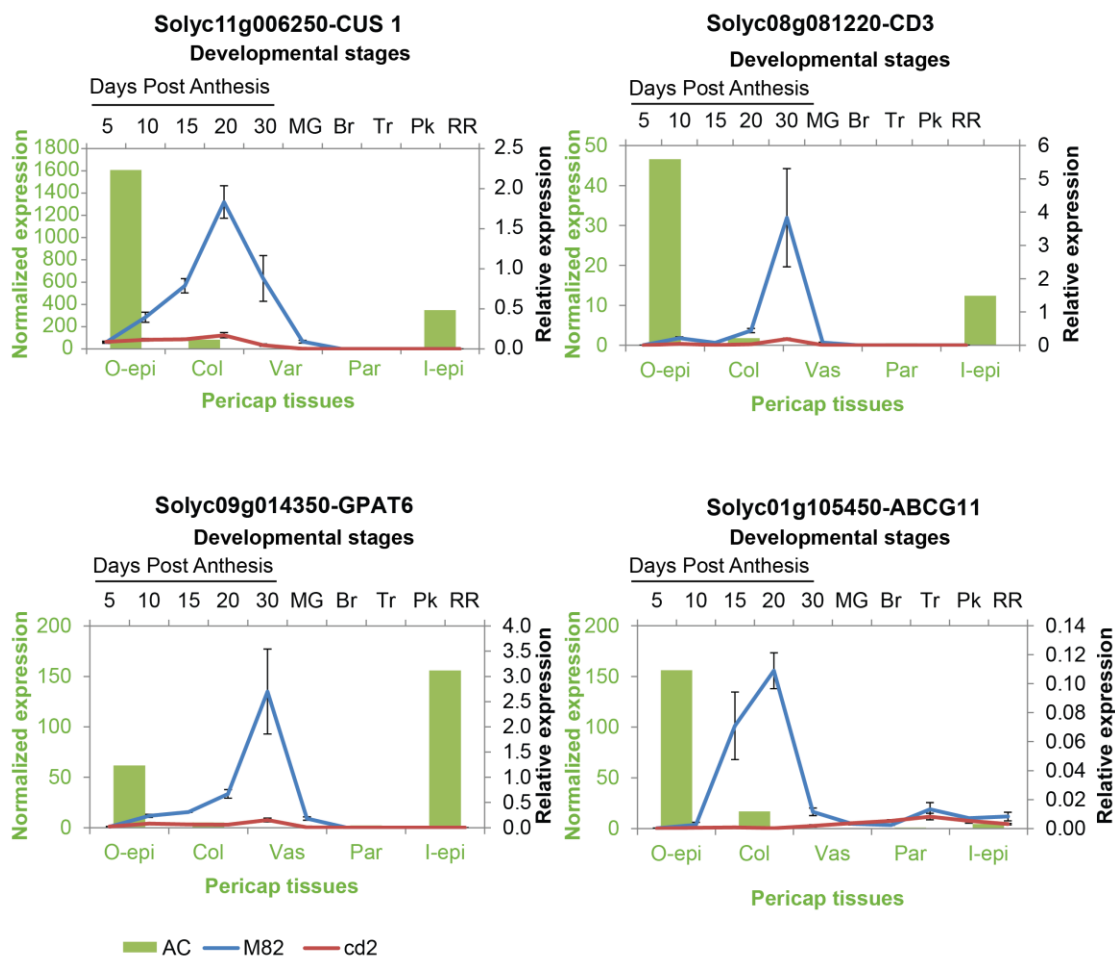


Figure 3.21. Expression pattern of cuticle-related genes identified in the RNA-seq analysis of 15 dpa fruit. Transcript levels throughout fruit ontogeny in *cd2* compared to those in M82 are represented with lines plotted on the right and top axes. The normalized gene expression (reads per 100,000) in 5 tissues of the 10 dpa pericarp of AC fruits are indicated in green columns plotted on the left and bottom. MG, Mature Green; Br, Breaker; Tr, Turning; Pk, Pink; RR, Red Ripe; O-epi, Outer epidermis; Col, Collenchyma; Vas, Vascular tissue; Par, Parenchyma; I-epi, Inner epidermis. The black secondary y axis represent qPCR analysis of the gene of interest.

The identification of four cuticle-related genes, with lower expression in *cd2* than in M82, and the severe cutin deficient phenotype of the *cd2* mutant clearly indicate that CD2 regulates cutin biosynthesis and transport. To determine whether other cuticle-related genes are regulated by CD2, which were not identified by the RNA-seq experiment, the expression of tomato homologs of known cuticle-related Arabidopsis genes was tested by qPCR, using the pericarp of 15 dpa *cd2* and M82 fruits. Of these, *CER6* (Solyc02g085870), a fatty acid β -ketoacyl-CoA synthase which catalyzes the initial condensation reaction believed to be rate limiting in the cuticular wax elongation process (Millar *et al.*, 1999), *GPAT4* (Solyc01g094700), an acyltransferase essential for cutin synthesis in leaf and stem in Arabidopsis (Li *et al.*, 2007) and *ABCG12/WBC12* (Solyc11g065350), a transporter that heterodimerizes with ABCG11 to transport cuticular waxes into the extracellular matrix (McFarlane *et al.*, 2010), were found to be also less expressed in the *cd2* mutant (Fig. 3.22). No clear difference of expression (data not shown) was identified for *FDH* (Solyc03g005320), *HTH* (Solyc03g121600), *CER3* (Solyc03g117800), *CER7* (Solyc05g047420) and *LACS2* (Solyc01g079240).

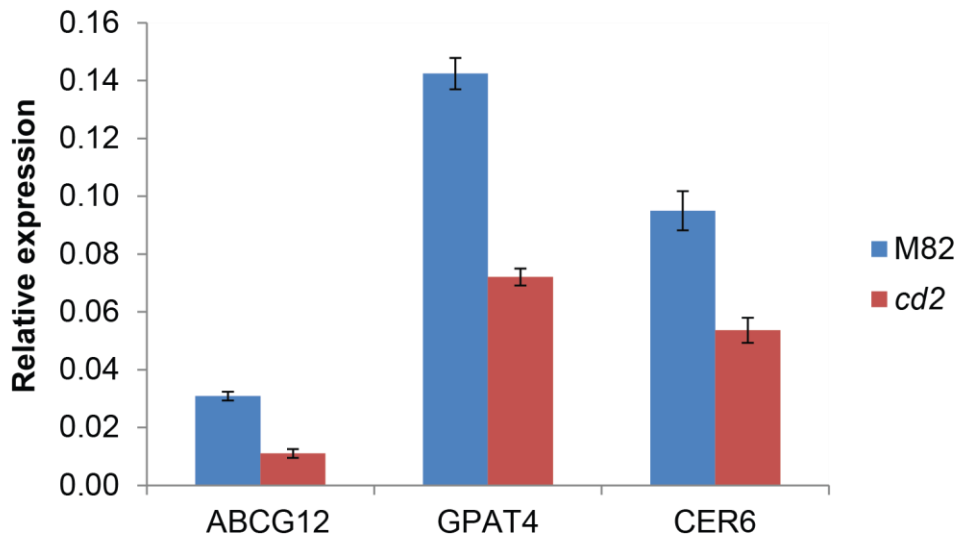


Figure 3.22. Identification of three additional cuticle-related genes regulated by *CD2*. The data were generated by qPCR using RNA extracted from 15 dpa pericarp tissue.

- *GDSLs*

The RNA-seq analysis identified a relatively high number of differentially expressed GDSLs. To determine how likely they are to share a similar function as CUS1, a phylogeny analysis was performed, assuming that a high degree of homology to CUS1 indicates a possible role as cutin synthase (Fig. 3.23). One of them, Solyc04g050570, clustered with CUS1 and has been tentatively renamed *CUS3* as it may also polymerize cutin (Yeats *et al.*, 2014). However, *CUS3* was not preferentially expressed in the epidermis, which would be expected for a cuticle-related gene (Fig. 3.24). The six additional identified GDSLs did not cluster in the same subclade as CUS1 (Fig. 3.23) but their transcripts accumulated preferentially in the outer, and sometimes in the inner, epidermis (Fig. 3.24). qPCR analysis of expression during

fruit ontology confirmed that the expression of all the identified GDSL was lower in *cd2* than in M82 and, except for Solyc07g049440 and Solyc03g111550, their expression peaked during fruit expansion (Fig. 3.24).

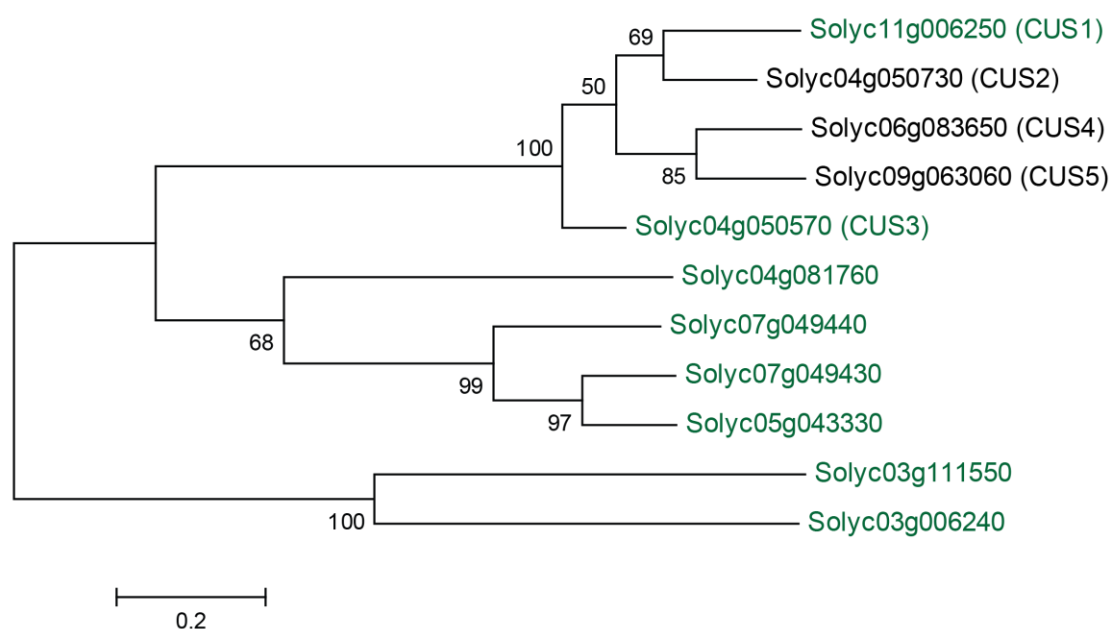


Figure 3.23. Phylogenetic analysis of the closest homologs of CUS1 and of the GDSLs identified in the RNA-seq analysis. The tree was constructed from amino acid sequences extracted from SGN (<http://solgenomics.net/>). The closest homologs of CUS1 are labeled CUS2-CUS5 and GDSLs identified in the RNA-seq analysis are labeled in green.

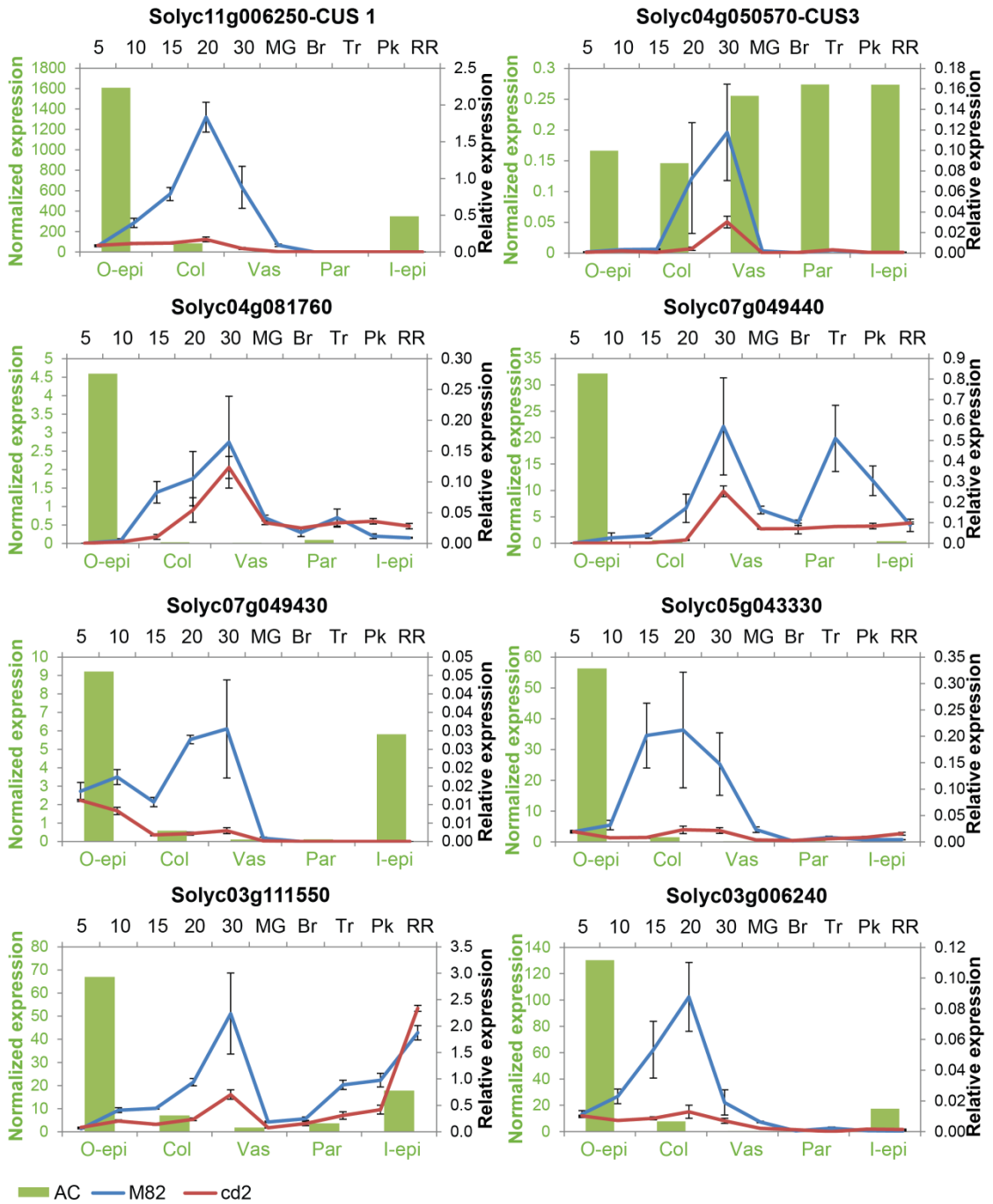


Figure 3.24. Differentially expressed GDSL expression patterns. Transcript levels throughout fruit ontogeny in *cd2* compared to M82 are represented with lines plotted on the right and top axes. The normalized gene expression (reads per 100,000) in 5 tissues of the 10 dpa pericarp of AC fruits are indicated in green columns plotted on the left and bottom axes. 5, 10, 15, 20 and 30 represent the number of days post anthesis. MG, Mature Green; Br, Breaker; Tr, Turning; Pk, Pink; RR, Red Ripe; O-

epi, Outer epidermis; Col, Collenchyma; Vas, Vascular tissue; Par, Parenchyma; I-epi, Inner epidermis.

- *Lipid-related genes*

The expression patterns of eight differentially expressed genes related to lipid metabolism are shown in Fig. 3.25. Both Solyc05g014560 (3-oxoacyl-reductase) and Solyc10g078740 (enoyl reductase) are predicted to be part of the fatty acid synthase complex, which is involved in *de novo* synthesis of fatty acids (http://lipidlibrary.aocs.org/plantbio/fa_biosynth/index.htm). Acyl-CoA synthetases form a diverse group of enzymes that activate many different types of carboxylic acids (Shockey *et al.*, 2003). Among these, LACS converts fatty acids into acyl-CoAs for a variety of processes, including wax and cutin formation and the synthesis of phospholipids and triacylglycerols synthesis, as well as β -oxidation (Shockey *et al.*, 2003; Fulda *et al.*, 2004; Lü *et al.*, 2009). Despite pertaining to the same group, Solyc12g044300 is not closely related to LACS1 and LACS2, enzymes activating fatty acids for cutin and wax synthesis (Lü *et al.*, 2009), but some of its closest Arabidopsis homologs were found to activate methyl and phenyl-fatty acids (Kienow *et al.*, 2008). Solyc12g010590 belongs to the wax ester synthase/diacylglycerol acyltransferase gene family. One member of this family, WSD1 (At5g37300) is responsible for cuticular wax ester formation (Li *et al.*, 2008). Glycerol is necessary for glycerolipid biosynthesis and is also a component of cutin (Wei *et al.*, 2001; Graça *et al.*, 2002). Two differentially expressed genes encoding for enzymes involved in glycerol metabolism, a glycerol-3-phosphate dehydrogenase (Solyc04g016330), which catalyzes the reduction of dihydroxyacetone phosphate (DHAP) to glycerol-3-

phosphate (G-3-P), an essential precursor for the synthesis of glycerolipids, and a glycerol kinase (Soly03g117490) were identified. Genes involved in lipid signaling were also identified as differentially expressed. One on those is Soly08g016620, which closest Arabidopsis homolog (At5g46220) is an unknown protein involved in ceramide metabolism. Ceramides and their sphingolipid derivatives are lipids with signaling and regulatory roles (Dunn *et al.*, 2004; Hannun *et al.*, 2008). Finally, Soly10g047240 is an annexin. Annexins are known to bind a wide range of phospholipids (Mortimer *et al.*, 2008). The expression of Soly10g047240 in the vascular tissue was unlike that of the other differentially expressed genes, which were preferentially expressed in the outer epidermis, but consistent with annexins expression in Arabidopsis which were detected in the vascular tissue, but also in the epidermis (Clark *et al.*, 2001).

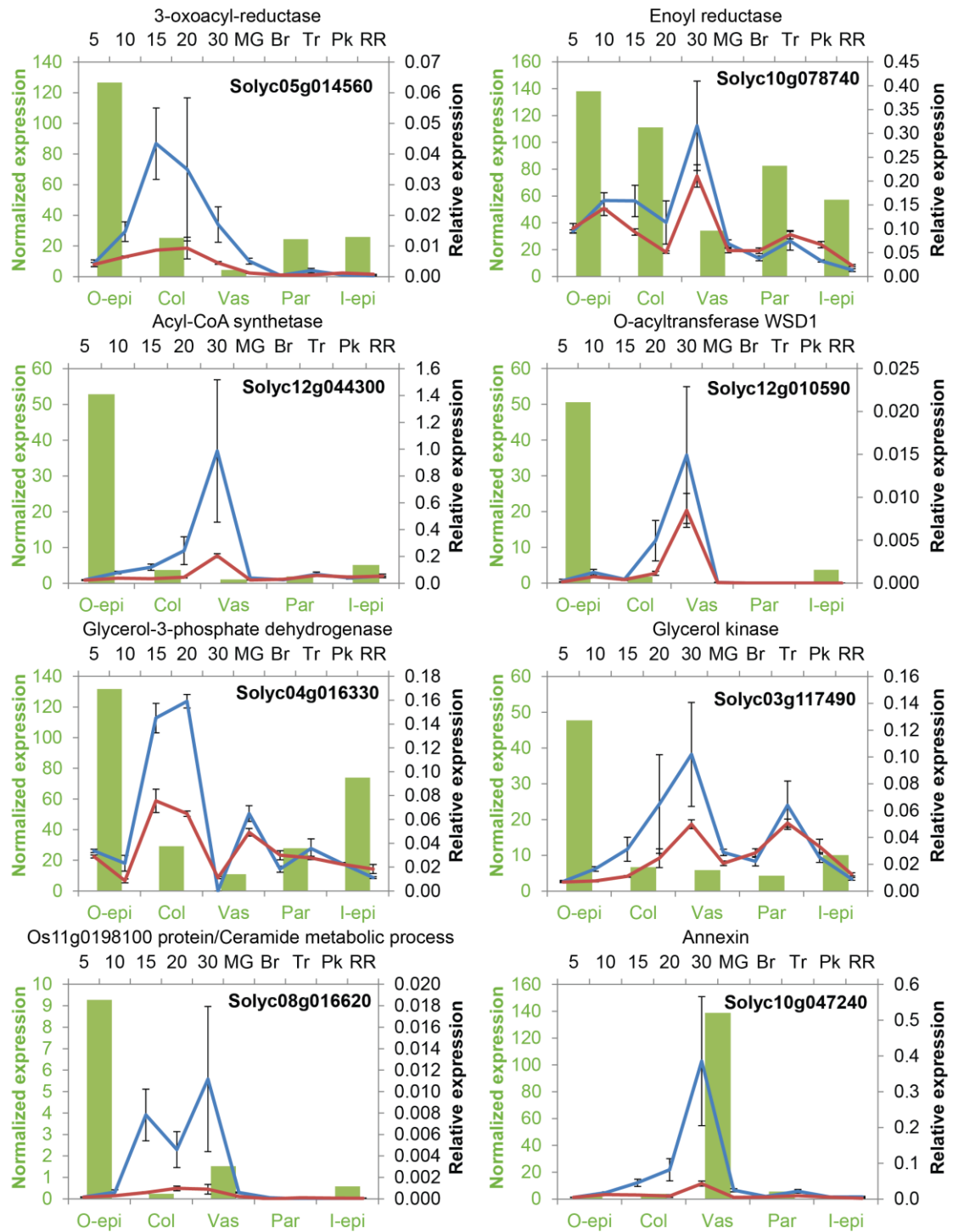


Figure 3.25. Lipid-related genes differentially expressed in the epidermis of 15 dpa *cd2* and M82 fruits. Transcript levels throughout fruit ontogeny in *cd2* compared to M82 are represented with lines plotted on the right and top axes. The normalized gene expression (reads per 100,000) in 5 tissues of the 10 dpa pericarp of AC fruits are indicated in green columns plotted on the left and bottom axes. 5, 10, 15, 20 and 30

represent the number of days post anthesis. MG, Mature Green; Br, Breaker; Tr, Turning; Pk, Pink; RR, Red Ripe; O-epi, Outer epidermis; Col, Collenchyma; Vas, Vascular tissue; Par, Parenchyma; I-epi, Inner epidermis.

- *Additional differentially expressed genes*

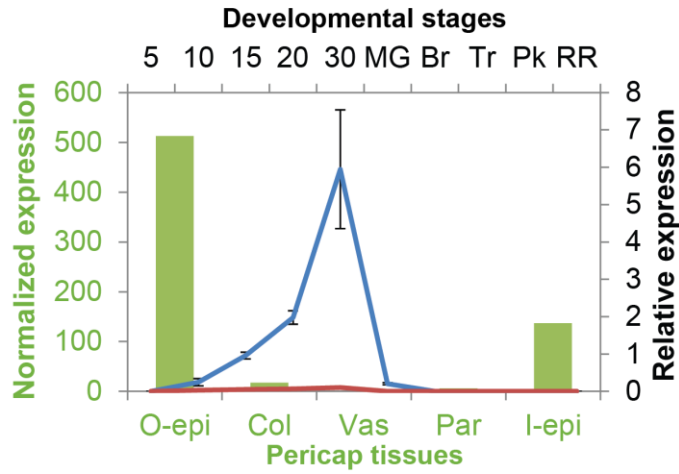
Analysis of epidermal gene expression of validated differentially expressed genes throughout fruit development identified three that were particularly differentially expressed between *cd2* and M82. Solyc06035580 was preferentially expressed in the outer and inner epidermis, and its expression in fruit pericarp rose from 5dpa until 30 dpa in the WT to drop thereafter (Fig. 3.26). However, its expression levels were extremely low in the *cd2* mutant. Solyc06035580 is annotated as a choline dehydrogenase and since choline is a component of phosphatidylcholine, a role of Solyc06035580 in lipid metabolism is possible.

Solyc09g007970, another outer-epidermis specific gene, was also specifically expressed during fruit expansion in WT (Fig. 3.26). This gene encodes a Small Auxin-Up RNA (SAUR)-Like protein, family which is known to be rapidly induced in response to auxin (McClure *et al.*, 1987).

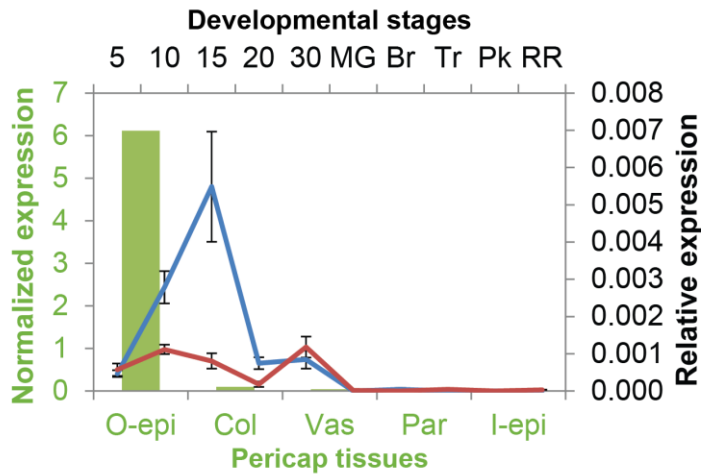
Finally, Solyc11g007390 had two peaks of expression: one at 30 dpa and another one at the Tr stage (Fig. 3.26). Surprisingly, no expression was detected in any of the 5 tissues of the pericarp (Fig. 3.26). Solyc11g007390 encodes a predicted UDP-glucosyltransferase. Several related enzymes have been shown to catalyze the last step of anthocyanin biosynthesis in litchi (*Litchi chinensis* Sonn.; Zhao *et al.*, 2012), gentian

(*Gentiana triflora*; Fukuchi-Mizutani *et al.*, 2003) and soybean (*Glycine max* (L.)
Merr.; Kovinich *et al.*, 2010).

Solyc06g035580 Choline dehydrogenase



Solyc09g007970 Auxin-induced SAUR-like protein



Solyc11g007390 UDP-glucosyltransferase (Anthocyanin biosynthesis)

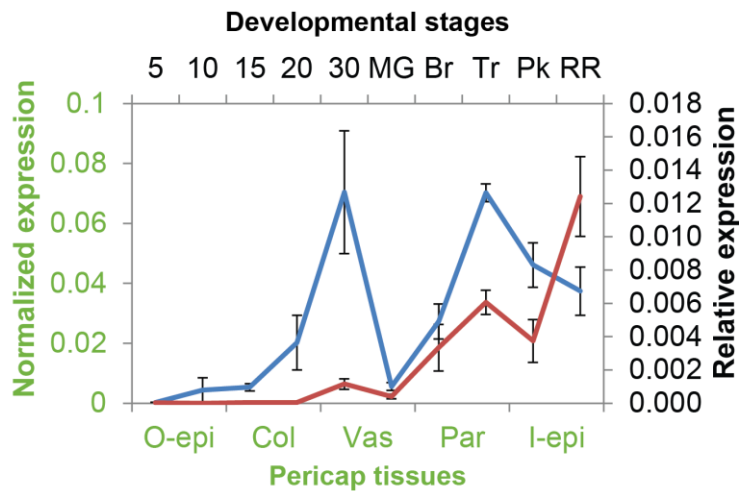


Figure 3.26. Tissue-specific and ontogeny expression pattern of 15 dpa RNA-seq candidates confirmed by qPCR. Transcript levels throughout fruit ontogeny in *cd2* compared to M82 are represented with lines plotted on the right and top axes. The normalized gene expression (reads per 100,000) in 5 tissues of the 10 dpa pericarp of AC fruits are indicated in green columns plotted on the left and bottom axes. 5, 10, 15, 20 and 30, number of days post anthesis. MG, Mature Green; Br, Breaker; Tr, Turning; Pk, Pink; RR, Red Ripe; O-epi, Outer epidermis; Col, Collenchyma; Vas, Vascular tissue; Par, Parenchyma; I-epi, Inner epidermis.

- Differentially expressed genes at Turning stage

Since CD2 transcripts and proteins were detected in ripening fruits, as well as in expanding fruits (Figs. 3.3B, 3.5 and 3.15), the LCM-RNA-seq profiling analysis was repeated for the Turning (Tr) stage, in order to determine whether the same or different sets of genes are regulated by CD2 at different developmental stages. The experimental design was the same as for the 15 dpa experiment (Illumina sequencing of LCM-isolated epidermal cells), but a larger number of differentially expressed genes was identified at the Tr stage than in the early developing fruit: transcripts corresponding to 40 and 61 loci were less or more abundant, respectively, in the *cd2* mutant than the WT fruit (Figs. 3.27 and 3.28). However, qPCR analysis confirmed the differential expression for only 18 and 38 genes, less or more expressed in *cd2* than in M82 respectively (Figs. 3.27 and 3.28).

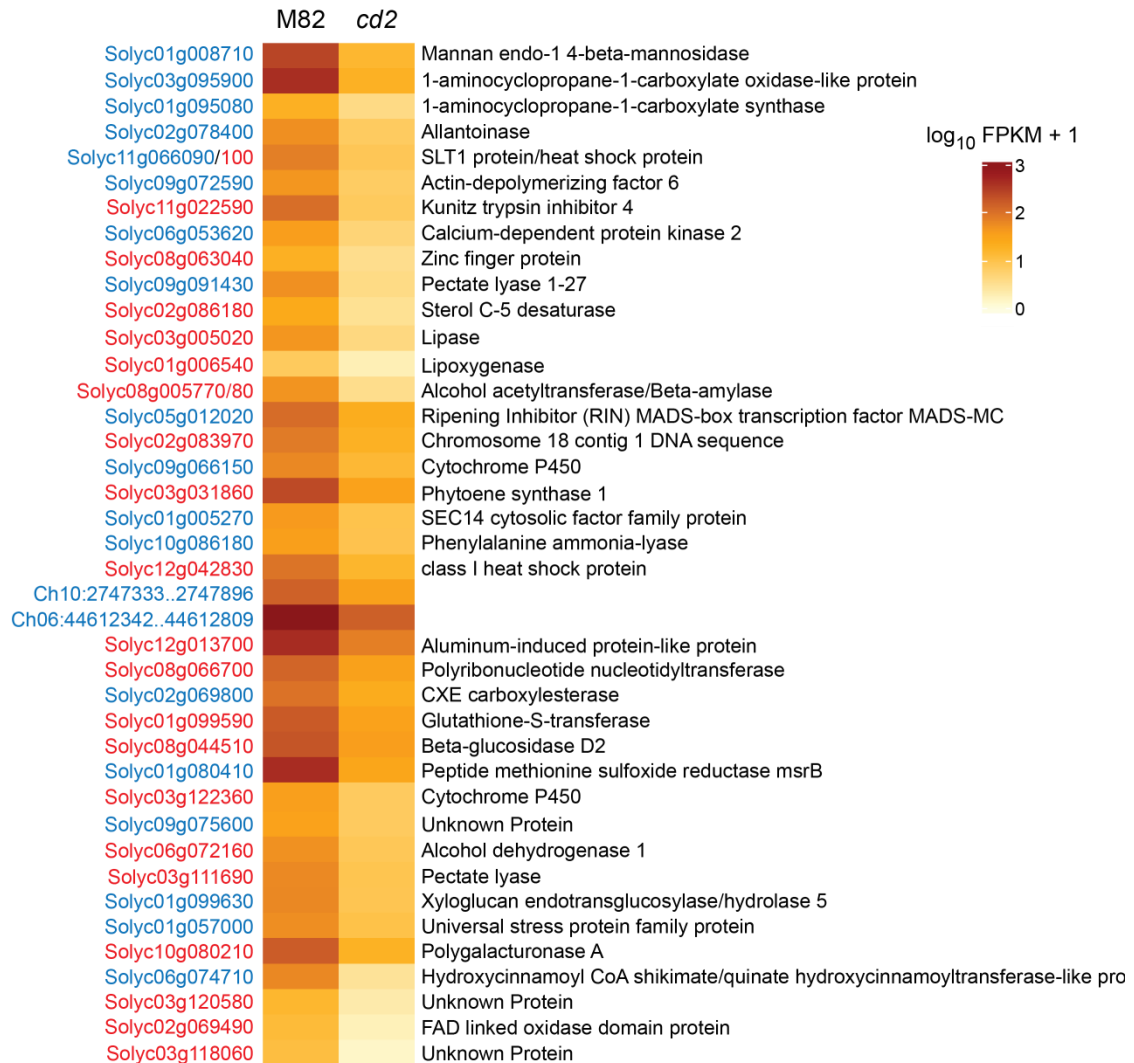


Figure 3.27. Heatmap representation of genes with lower expression in epidermal cells of Tr stage fruit of the *cd2* mutant and the wild type M82, based on LCM/RNA-seq data. The genomic region of the 2.40 version of the sequenced *S. lycopersicum* genome is given if no gene was identified in the differentially expressed sequence. If more than one gene may correspond to the differentially expressed sequence, based on alignment ambiguity, all candidate genes are given, separated by a / indicator. Color coding of the genes: blue, differential expression confirmed by semi-qPCR; red, differential expression inquired by semi-qPCR. Gene annotation is consistent with the SGN database (<http://solgenomics.net/>).

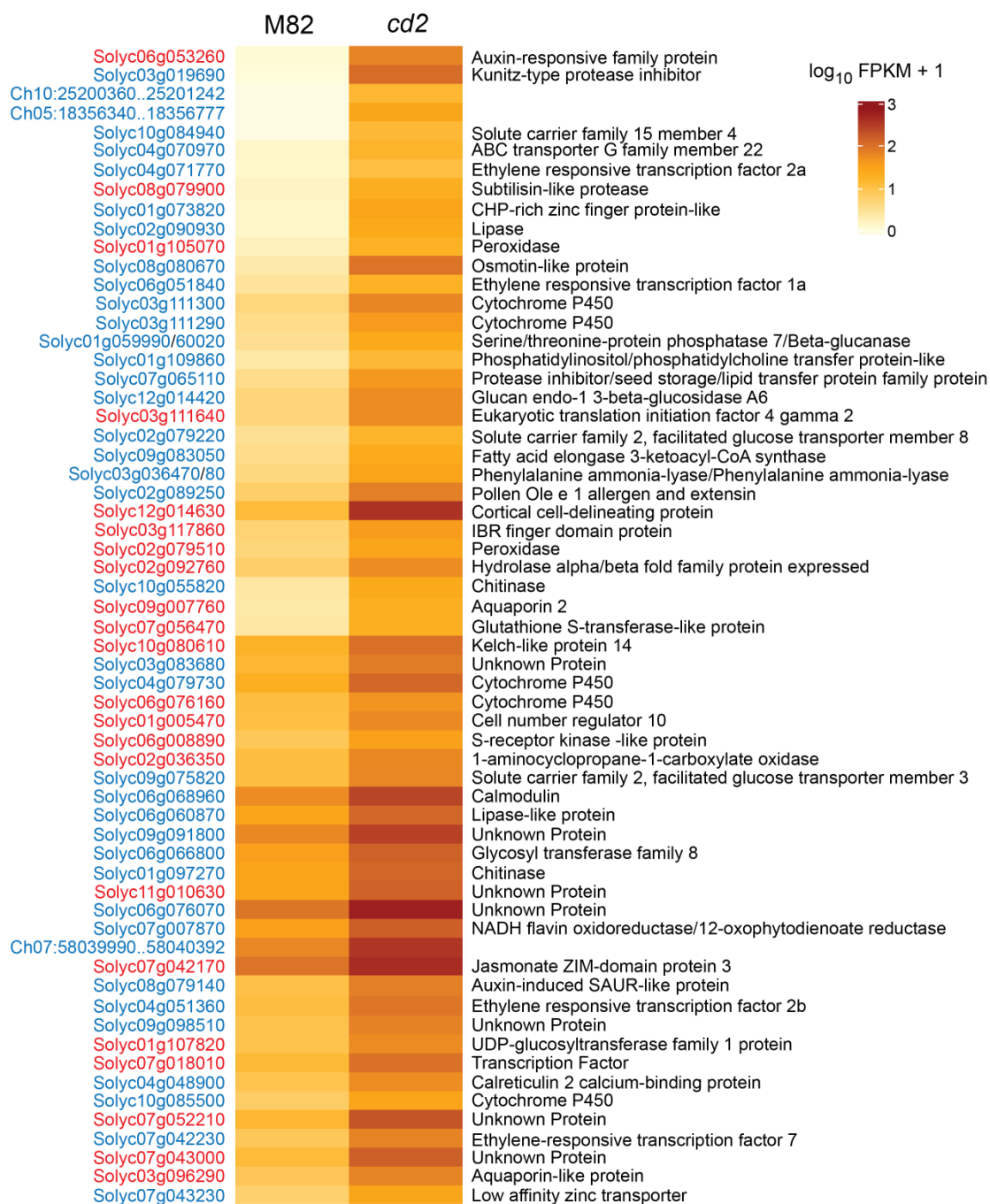


Figure 3.28. Heatmap representation of genes with higher expression in epidermal cells of Tr stage fruit of the *cd2* mutant and the wild type M82, based on LCM/RNA-seq data. The genomic region of the 2.40 version of the sequenced *S. lycopersicum* genome is given if no gene was identified in the differentially expressed sequence. If more than one gene may correspond to the differentially expressed sequence, based on alignment ambiguity, all candidate genes are given, separated by a / indicator. Color coding of the genes: blue, differential expression confirmed by semi-

qPCR; red, differential expression in confirmed by semi-qPCR. Gene annotation is consistent with the SGN database (<http://solgenomics.net/>).

- *Lipid-related genes*

As seen with the equivalent analysis of 15 dpa fruit, numerous lipid-related genes were identified as differentially expressed (Fig. 3.29). For example At1g14820, the closest Arabidopsis homolog of Solyc01g005270, is annotated as a Sec14p-like phosphatidylinositol transfer family protein, which family participates in various plant signal transduction processes (Gosh *et al.*, 2011) and Solyc01g109860 is also predicted to be a phosphatidylinositol transfer protein-like. Solyc07g065110 may also have a function in lipid metabolism as one of its annotations is “lipid transfer protein”. However, expression analysis throughout fruit development indicated expression in immature fruits and not the expected expression in ripening stages. Fatty acid biosynthesis is potentially disrupted at Tr stage, as well as at 15 dpa, since a 3-ketoacyl-CoA synthase, Solyc09g083050 showed higher expression in *cd2* than in M82. Finally, transcript levels of a lipase (Solyc02g090930) and a lipase-like protein (Solyc06g060870) were higher in *cd2* at various stages of fruit development.

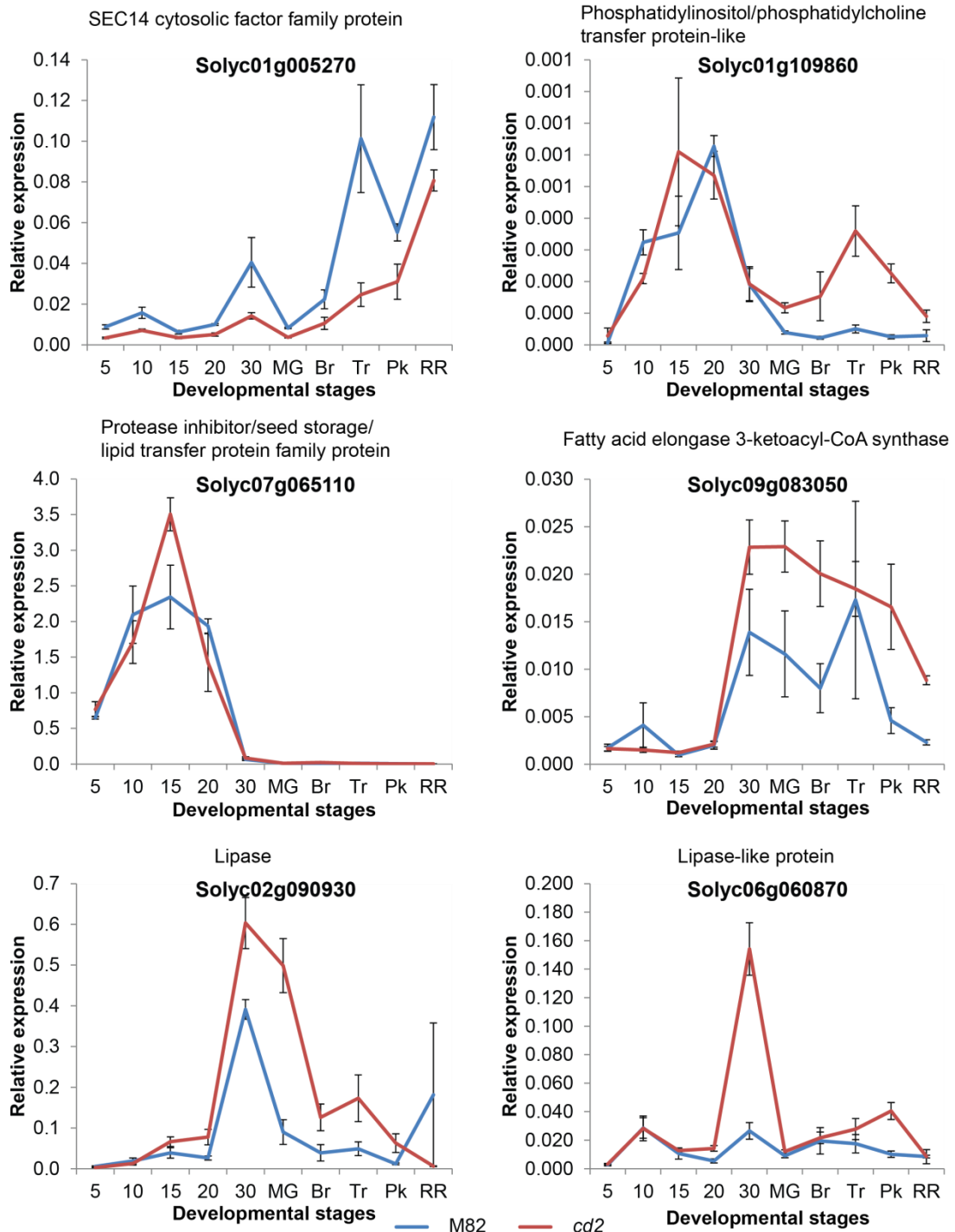


Figure 3.29. Lipid-related genes differentially expressed at Tr stage between *cd2* and M82 fruit epidermis. Transcript levels throughout fruit ontogeny in *cd2* compared to M82 were obtained by qPCR analysis. 5, 10, 15, 20 and 30, number of

days post anthesis. MG, Mature Green; Br, Breaker; Tr, Turning; Pk, Pink; RR, Red Ripe.

- *Phenylpropanoid biosynthesis related genes*

Four genes involved in the phenylpropanoid pathway were differentially expressed in tomato fruit (Fig. 3.30). Interestingly, evidence of a reduction of anthocyanin levels in the Arabidopsis mutant *anl2* and the tomato mutant *pe* were reported (Kubo *et al.*, 1999; Nadakuduti *et al.*, 2012). A total of 4 phenylalanine ammonia lyase (PAL) genes are present in the Arabidopsis genome of which 3 were identified as being differentially expressed between *cd2* and M82 Tr stage fruit (Fig. 3.30). PAL catalyzes the first committed step in the phenylpropanoid pathway (MacDonald *et al.*, 2007). The phenylpropanoid pathway is further affected with the lower accumulation of a hydroxycinnamoyl-coenzyme A shikimate:quinic acid hydroxycinnamoyl-transferase (HCT): Solyc06g074710 (Fig. 3.30). HCT catalyzes the formation of *p*-coumaroyl shikimate and of caffeoyl CoA, two biosynthetic steps of the phenylpropanoid pathway (Fraser and Chapple, 2011).

An additional phenylpropanoid-related gene, Solyc12g042600, was identified as differentially expressed, although qPCR analysis did not confirm the differential expression. Solyc12g042600 may catalyze the transfer of glucose from UDP-glucose to a flavanol, one of the last steps in anthocyanin pigment biosynthesis. Another UDP-glucosyltransferase, Solyc11g007390, was identified among the differentially expressed genes at 15 dpa indicating that the anthocyanin deficiency affecting the

sticky peel mutant (Nadakuduti *et al.*, 2012) may result from the reduction of the levels of UDP-glucosyltransferases.

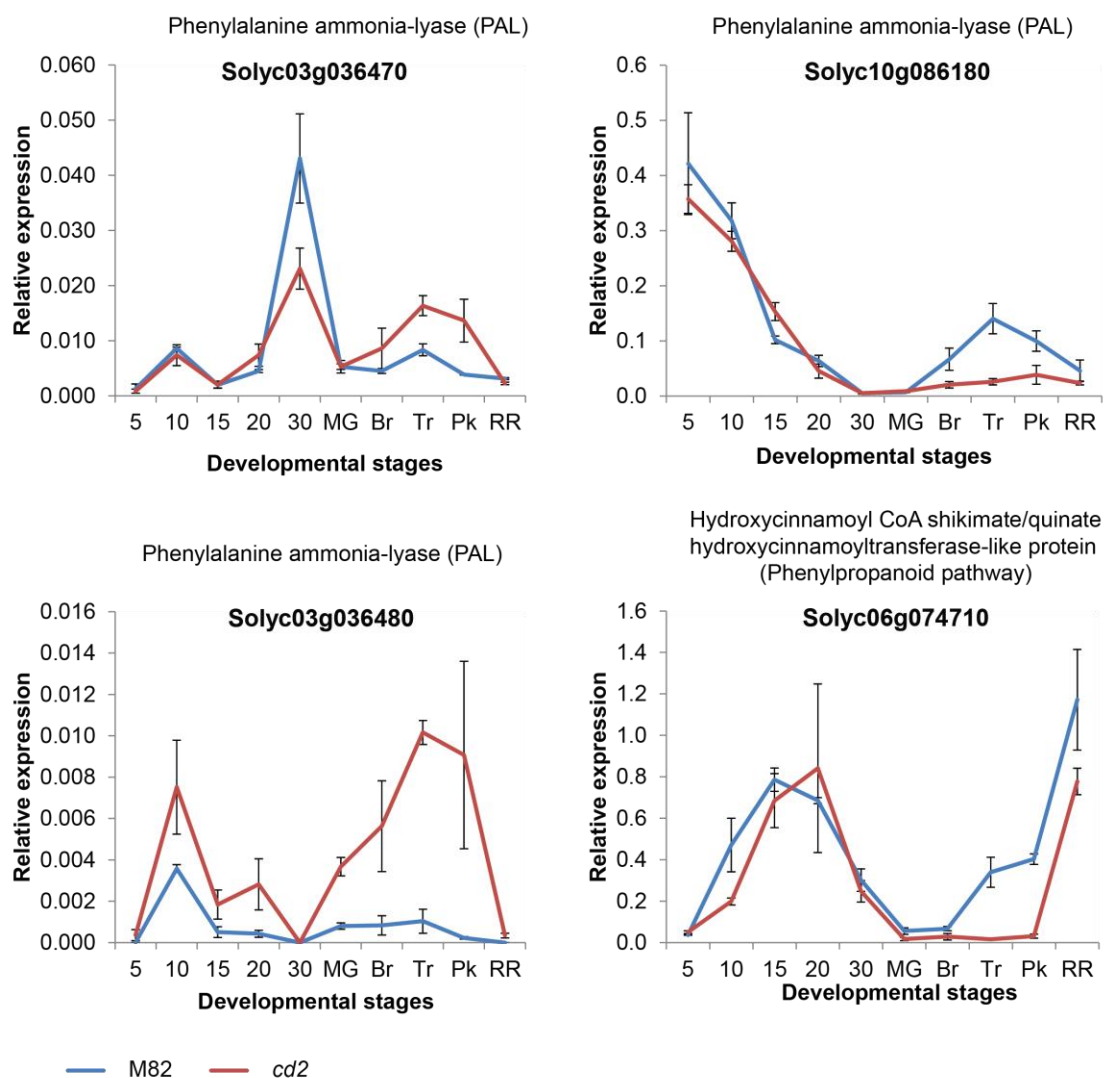
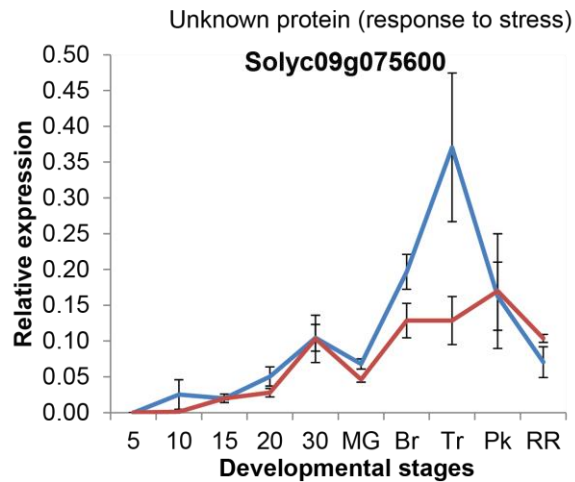
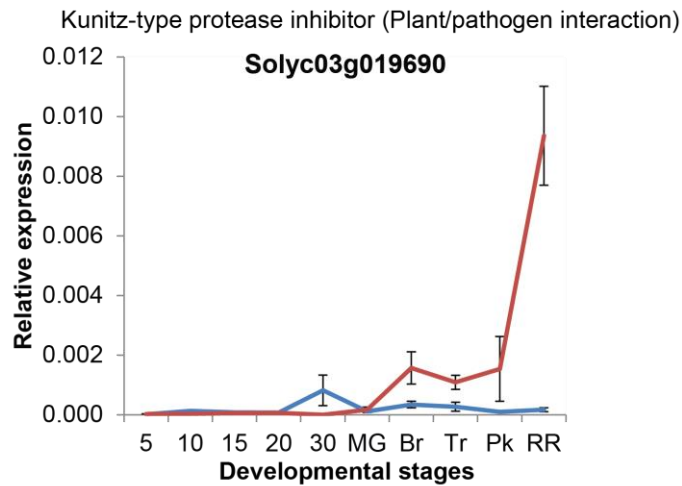
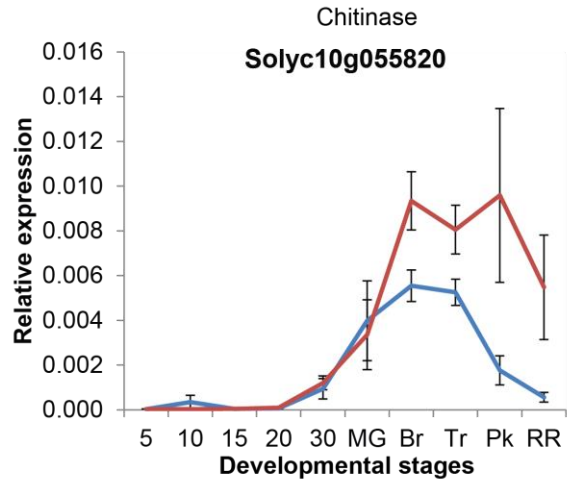


Figure 3.30. Phenylpropanoid-related genes differentially expressed at Tr stage between *cd2* and M82 fruit epidermis. Transcript levels throughout fruit ontogeny were obtained by qPCR analysis. 5, 10, 15, 20 and 30, number of days post anthesis. MG, Mature Green; Br, Breaker; Tr, Turning; Pk, Pink; RR, Red Ripe.

- *Stress related genes*

Gene Ontology analysis determined that many differentially expressed genes are involved in biotic or abiotic stress responses, but more so for the set of genes found to be more expressed in the *cd2* mutant compared to the WT. The expression of three differentially expressed genes that are known to be stress responsive is shown in Fig. 3.31. Overall, they were more expressed during fruit maturation and they were differentially expressed between *cd2* and M82 during the ripening stages, but not during the expansion stages (Fig. 3.31).



— M82 — *cd2*

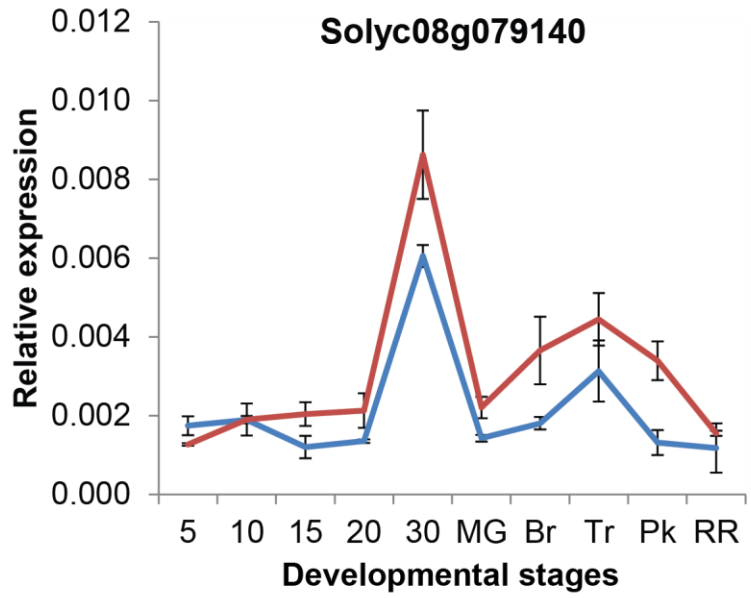
Figure 3.31. Stress-related genes differentially expressed at Tr stage between *cd2* and M82 fruit epidermis. Transcript levels throughout fruit ontogeny were obtained

by qPCR analysis. 5, 10, 15, 20 and 30, number of days post anthesis. MG, Mature Green; Br, Breaker; Tr, Turning; Pk, Pink; RR, Red Ripe.

- *Hormone and ripening related genes*

The large number of differentially expressed genes annotated as being involved in stress responses may be associated with abnormal levels of hormones, such as salicylic and jasmonic acids which are key in the plant-pathogen interactions (Robert-Seilaniantz *et al.*, 2011). Supporting this idea, the expression levels of Solyc08g079140, which belongs to the SAUR-like auxin responsive protein family, and Solyc07g007870, a NADH flavin oxidoreductase/12-oxophytodienoate reductase that catalyzes a step in jasmonate biosynthesis (Delker *et al.*, 2008), were higher in *cd2* fruits from 30 dpa to Pink (Pk) stage than in M82 fruits (Fig. 3.32). Solyc08g079140 may be involved in systemic acquired resistance and salicylic acid mediated signaling pathway, as the annotation of its closest Arabidopsis homolog, At3g60690, suggests (<http://www.arabidopsis.org/>).

SAUR-like auxin-responsive protein family



NADH flavin oxidoreductase/12-oxophytodienoate reductase
(Jasmonate biosynthesis)

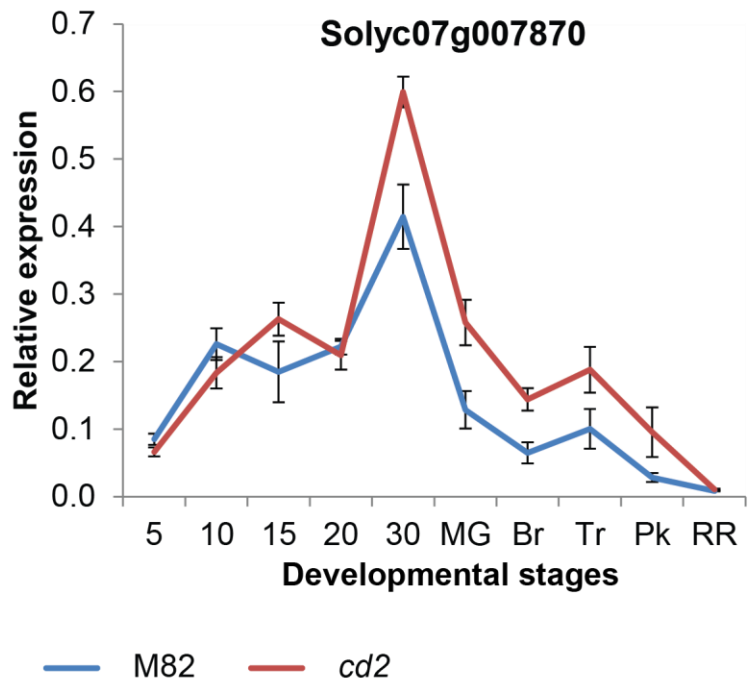


Figure 3.32. Hormone-related genes differentially expressed at Tr stage between *cd2* and M82 fruit epidermis. Transcript levels throughout fruit ontogeny were

obtained by qPCR analysis. 5, 10, 15, 20 and 30, number of days post anthesis. MG, Mature Green; Br, Breaker; Tr, Turning; Pk, Pink; RR, Red Ripe.

Four ethylene responsive transcription factors were identified as being expressed at higher levels in *cd2* than M82 Tr stage fruit (Fig. 3.33) and qPCR analysis showed that of these, Solyc04g051360 and Solyc07g042230 were preferentially, and substantially more expressed in the mutant during fruit ripening (Fig. 3.33). These two genes belong to the very large AP2/EREBP family of transcription factors (e.g. 147 members in Arabidopsis) that are divided into four major subfamilies: AP2, RAV, ERF and DREB. AP2/EREBP. These transcription factors have a major role in integrating environmental signals in the modulation of plant growth (Dietz and Vogel, 2010) and the DREB and ERF subfamilies are documented as being involved in abiotic stress response (Mizoi *et al.*, 2012).

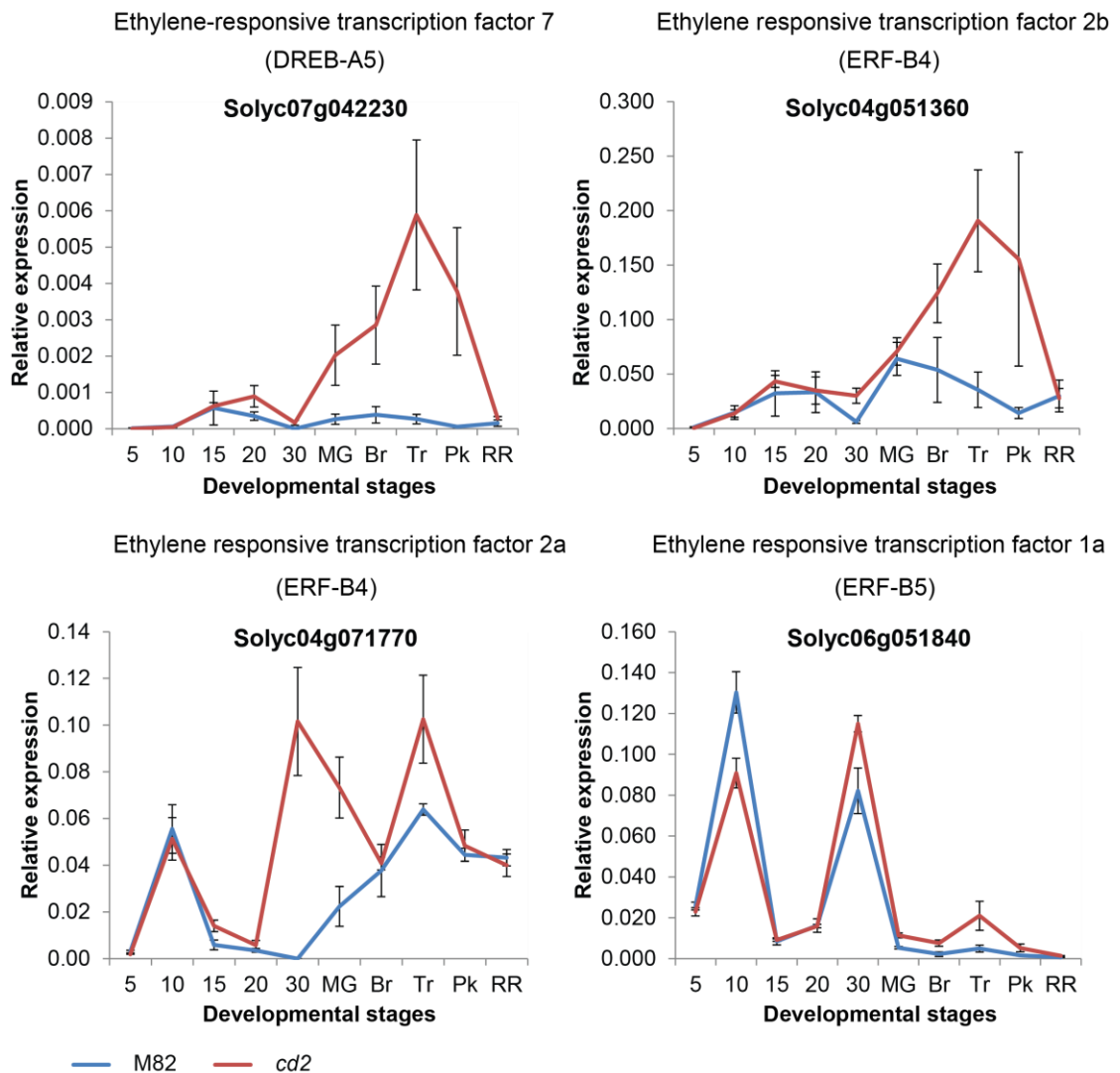
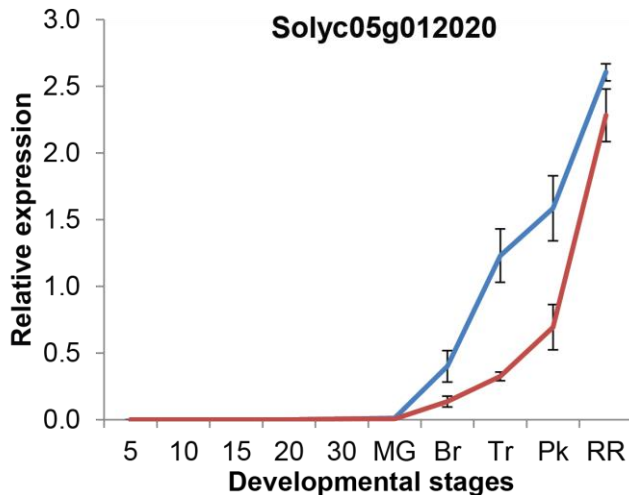


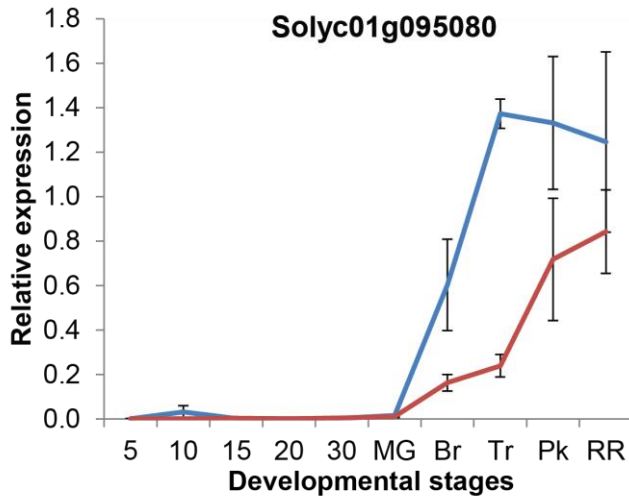
Figure 3.33. Ethylene responsive TF genes differentially expressed at Tr stage between *cd2* and M82 fruit epidermis. The AP2/EREBP subfamily of the Arabidopsis closest homologs is given between parentheses. Transcript levels throughout fruit ontogeny were obtained by qPCR analysis. 5, 10, 15, 20 and 30, number of days post anthesis. MG, Mature Green; Br, Breaker; Tr, Turning; Pk, Pink; RR, Red Ripe.

Ethylene is a hormone regulating the ripening process of climacteric fruits, so the ethylene responsive transcription factors identified in this experiment could indicate that ripening is impaired in *cd2*. Supporting this idea, some well-known ripening-related genes have been identified as differentially expressed. One of them is the MADS-box transcription factor Ripening Inhibitor (RIN) which is an essential regulator of fruit ripening by controlling all ripening pathways including the biosynthesis and perception of ethylene (Giovannoni, 2007; Seymour *et al.*, 2013). RIN has been shown to directly interact with the promoter of Solyc01g095080 (ACS2; X59139.1; Fujisawa *et al.*, 2011), a 1-aminocyclopropane-1-carboxylate synthase gene that largely contributes to the increase in ethylene levels in ripening fruit (Barry *et al.*, 2007). Furthermore, RIN has also been shown to bind to the promoter of Solyc01g008710 (AY046588), an endo-(1,4)- β -mannanase 4 (MAN4) that is involved in cell-wall modifications during ripening (Fujisawa *et al.*, 2011). The transcription pattern of these three genes was very similar with minimal expression until the MG stage and a major increase in expression starting at the Breaker (Br) stage (Fig. 3.34). Furthermore, the expression of these three genes was lower in *cd2* compared to M82, consistent with the idea that RIN regulates the expression of ACS2 and MAN4 (Fig. 3.34).

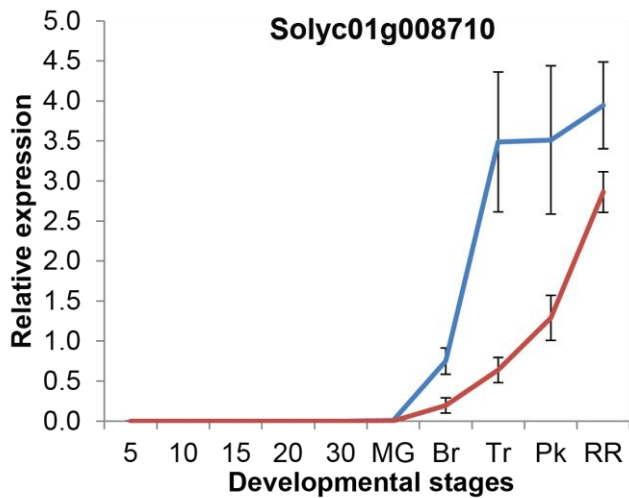
Ripening Inhibitor (RIN)
MADS-box transcription factor MADS-MC



1-aminocyclopropane-1-carboxylate (ACC) synthase



Mannan endo-1 4-beta-mannosidase



— M82 — cd2

Figure 3.34. Ripening-related genes differentially expressed at Tr stage between *cd2* and M82 fruit epidermis. Transcript levels throughout fruit ontogeny were obtained by qPCR analysis. 5, 10, 15, 20 and 30, number of days post anthesis. MG, Mature Green; Br, Breaker; Tr, Turning; Pk, Pink; RR, Red Ripe.

ABA accumulation is impaired during ripening of *cd2* mutant fruits

The role of ethylene in fruit ripening is very well established (Giovannoni, 2007), and recent studies indicate that an increase of the amount of the hormone abscisic acid (ABA) at the onset of ripening triggers ethylene biosynthesis (Zhang *et al.*, 2009; Jia *et al.*, 2011; Zaharah *et al.*, 2013). In addition to its role in fruit ripening, several studies showed that ABA regulates the expression of transcription factors regulating cuticle biosynthesis (Cominelli *et al.*, 2008; Kosma *et al.*, 2009; Seo *et al.*, 2011). ABA has also a fundamental role in biotic and abiotic stress response (Mauch-Mani and Mauch, 2005; Tuteja, 2007). Since differentially expressed genes having a role in all the aforementioned pathways have been detected in the RNA-seq experiment, the measurement of ABA levels in M82 and *cd2* was undertaken to investigate if ABA levels are affected in *cd2*. While the levels of ABA were no different between WT and *cd2* in leaves, seeds and expanding and mature green tomatoes, the ABA peak which happened during M82 fruit ripening was substantially reduced in the *cd2* mutant (Fig. 4.35a,b). The expression of genes related to ABA biosynthesis and signaling were evaluated in Pk stage fruits, stage with the highest amount of ABA, to determine whether their expression patterns explain the decrease in ABA levels in ripening *cd2* fruit (Fig. 4.36A). However, no significant change in expression of 10 genes involved in ABA biosynthesis and signaling was apparent. To

further test the hypothesis, the expression of the four genes, with the lowest expression in *cd2* compared to M82, was assessed at several stages spanning fruit development. The peak of NCED07 and NCED08 expression was shifted towards turning in *cd2* and ABA2 and ABI-03 expression is slightly lower in *cd2* during fruit ripening (Fig. 4.36B).

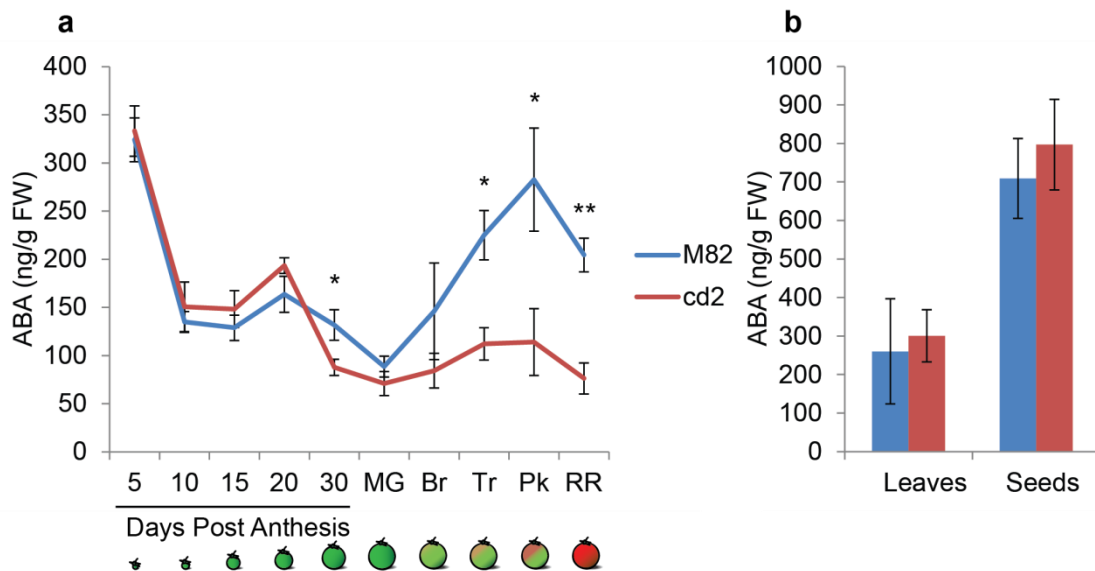


Figure 4.35. ABA levels in the *cd2* mutant. (a) ABA levels throughout fruit ontogeny of the cutin mutant *cd2* and its WT (M82). (b) ABA levels in developing leaves of fully mature plants (leaf size < 2 cm) and in mature seeds. n = 4 for all tissues. *, $\alpha = 0.5$ and **, $\alpha = 0.01$.

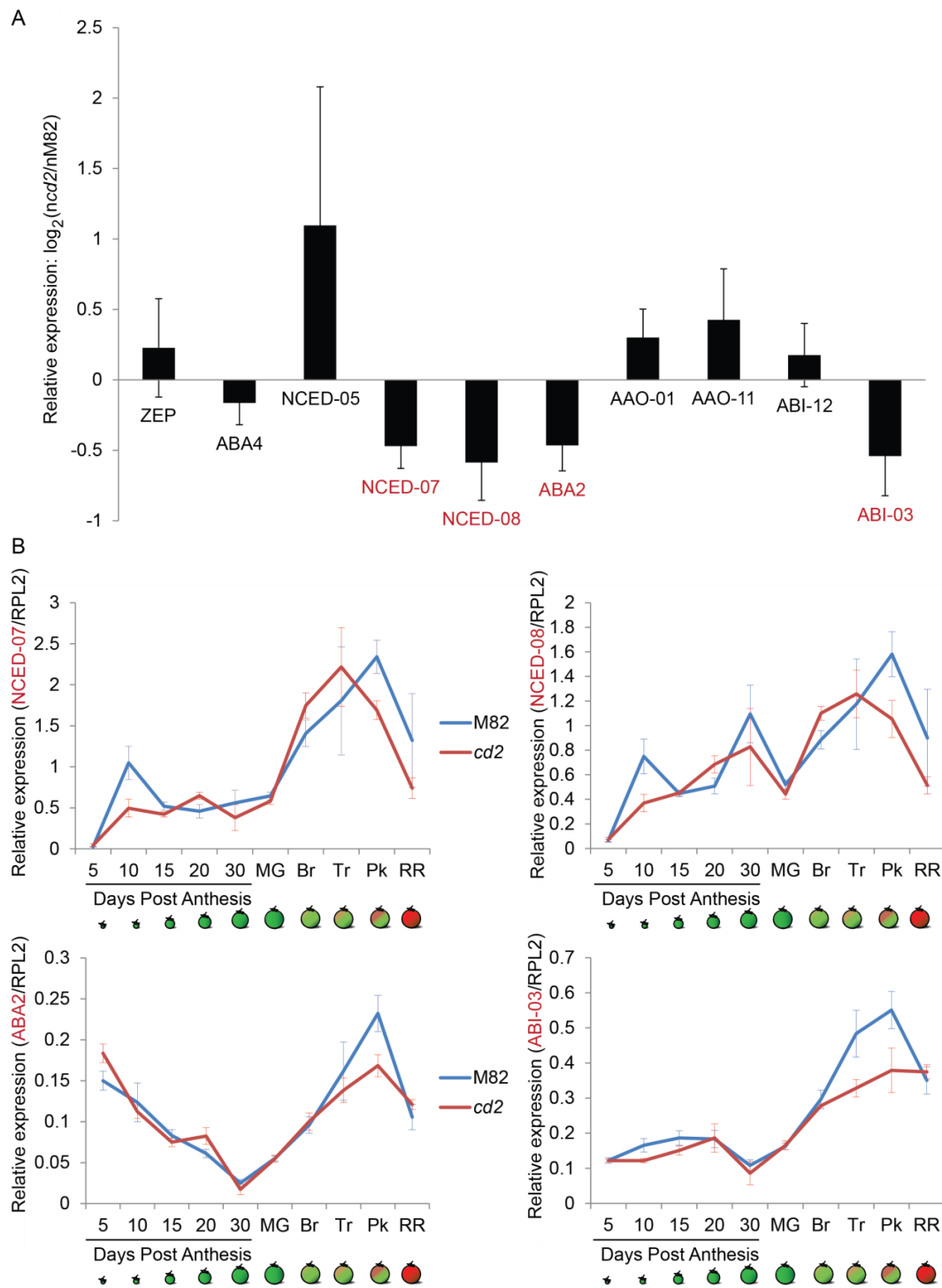


Figure 4.36. ABA biosynthesis and signaling gene expression in the *cd2* mutant. (A) Gene expression in Pink stage fruit pericarp. (B) Gene expression of a subset of previously tested genes during fruit ontogeny. n = 3.

Cuticle or lipid-related candidate genes

16 and 20% of differentially expressed epidermal genes identified in the 15 dpa and Tr stage RNA-seq experiments, respectively, have an unknown function and/or the pathways in which they function have yet to be determined. These genes are therefore candidates for being involved in processes and pathways that are already associated with *CD2*: cuticle and lipid metabolism, anthocyanin biosynthesis, ripening and stress responses. For example, two and one ABC transporters have been identified as targets of *CD2* in the 15 dpa and Tr stage RNA-seq experiments respectively. One of them, ABCG11, is a transporter of cutin monomers (Bird *et al.*, 2007; Panikashvili *et al.*, 2007; Fig. 3.21), while the substrates of the other two (Solyc12g011410, ABCG26, and Solyc04g070970, ABCG22) are unknown. The ABC family is very large (129 members in *Arabidopsis*; Sánchez-Fernández *et al.*, 2001) and is composed of 8 major subfamilies (Verrier *et al.*, 2008), but all identified ABC transporter belong to the same subfamily: G. Solyc12g011410 (ABCG26) was mostly expressed in expanding fruits, in the two tissues of the pericarp where *CD2* transcripts were also the most abundant: the outer epidermis and the vascular tissue (Fig. 4.37). The expression of the other ABCG transporter, Solyc04g070970 (ABCG22) was clearly higher in the *cd2* mutant starting at 30 dpa and subsequently through ripening (Fig. 4.37).

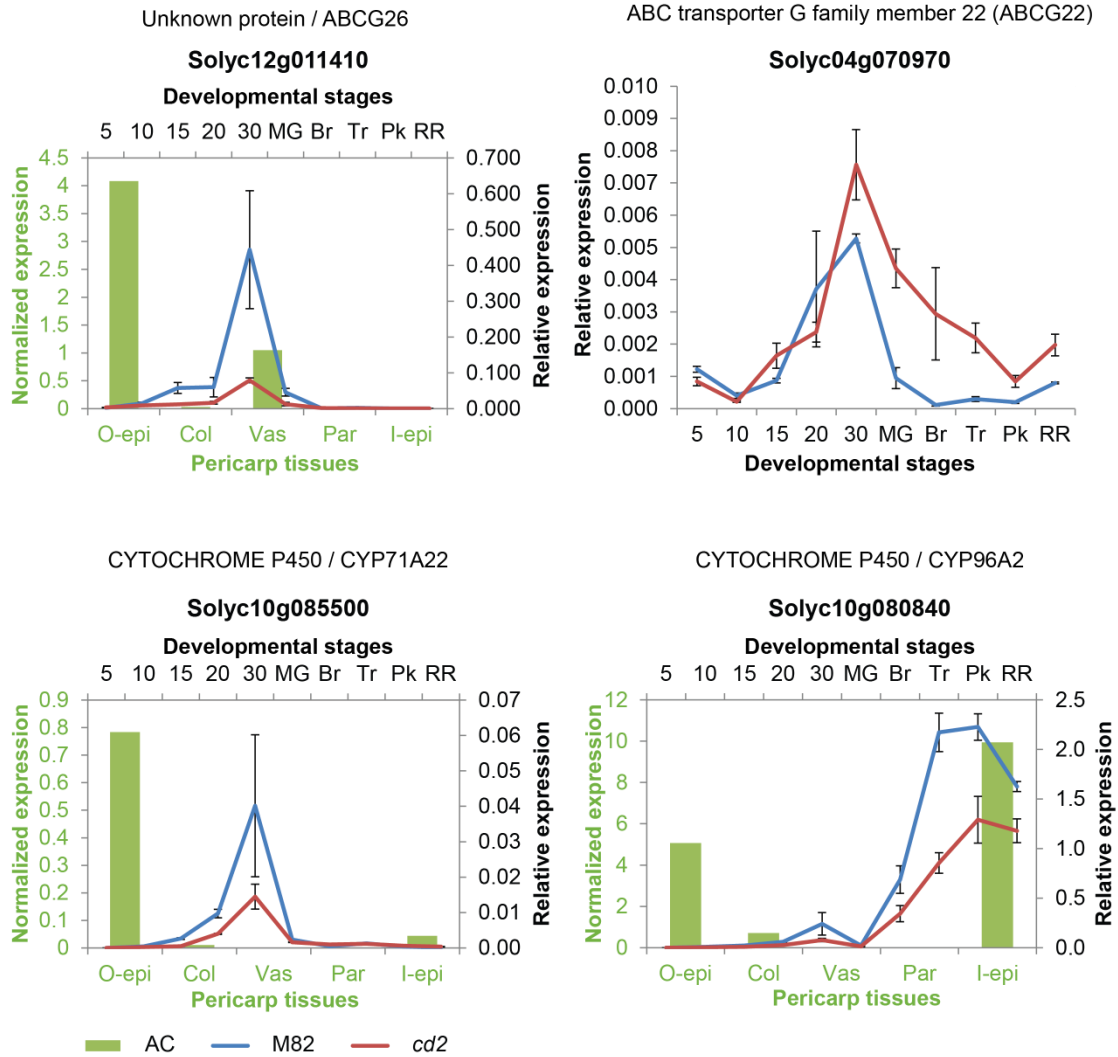


Figure 4.37. ABCG transporter and CYT P450 genes differentially expressed in *cd2* versus M82. Transcript levels throughout fruit ontogeny in *cd2* compared to M82 are represented with lines plotted on the right and top axes. The normalized gene expression (reads per 100,000) in 5 tissues of the 10 dpa pericarp of AC fruits are indicated in green columns plotted on the left and bottom axes. 5, 10, 15, 20 and 30, number of days post anthesis. MG, Mature Green; Br, Breaker; Tr, Turning; Pk, Pink; RR, Red Ripe.

Cytochromes P450 (CYP450) proteins comprise the largest family of plant proteins and members catalyze diverse reactions (Morant *et al.*, 2003). Three CYP450 were identified by the 15 dpa RNA-seq experiment, one of which, Solyc08g081220 (CD3), is involved in cutin biosynthesis (Isaacson *et al.* 2009, Shi *et al.*, 2013). The expression pattern of Solyc10g085500 (CYP71A22), which was expressed principally in the outer epidermis of expanding fruits, suggests that it also could be involved in cutin biosynthesis. Although identified as differentially expressed in the 15 dpa RNA-seq experiment, Solyc10g080840 (CYP96A2) was expressed mainly during fruit ripening, and was specific to the outer and inner epidermis (Fig. 4.37).

Discussion

CD2 expression patterns

In this study, complementary approaches were undertaken to evaluate the spatial and temporal pattern of *CD2* expression and to identify the genes that it regulates. The proposed role of *CD2* in regulating cuticle biosynthesis would suggest that its expression would take place in aerial organs. Indeed, *CD2* transcripts were detected in tomato leaves, flowers, fruits and stems; however, *CD2* transcripts and proteins were also detected in roots, which do not have a cuticle. Expression in roots is not unique to *CD2* as nine of the 16 members of the Arabidopsis HD-ZIP IV family are expressed in roots, including the two closest homologs of *CD2*, *ANL2* and *HDG1* (Nakamura *et al.*, 2006). Additionally, *OCL1* and *AmHDG1*, two close homologs of *CD2* from maize and *Ammopiptanthus mongolicus*, respectively, are also expressed in roots (Javelle *et al.*, 2010; Wei *et al.*, 2012). GUS staining indicates that *CD2* is

strongly expressed in the phloem of the root. However, *HDG1* is only expressed at the periphery of emergent lateral roots (Nakamura *et al.*, 2006) and *ANL2* is expressed in the epidermal and lateral root cap cells of the primary root, and in the lateral root initial (Kubo *et al.*, 2008). *ANL2* has been shown to be required for the maintenance of root epidermal cell identity (Kubo *et al.*, 2011). Since neither *ANL2* nor *HDG1* appear to be expressed in the root vascular tissue, *CD2* may have a different role in root formation from its close Arabidopsis homologs. Considering the cutin phenotype of the *cd2* mutant, it is tempting to hypothesize that *CD2* may regulate root suberin biosynthesis. Indeed, suberin structure and composition are closely related to those of cutin: similar to cutin, suberin is a polyester of fatty acids but these polymers differ in terms of phenolic content, carbon chain length and degree of unsaturation (Kosma *et al.*, 2014). Furthermore, cutin and suberin probably share similar biosynthetic routes as certain cuticle-related genes, or close homologs, have been shown to also act in suberin formation (Cominelli *et al.*, 2008; Kosma *et al.*, 2014; Landgraf *et al.*, 2014). However, root suberin composition is not significantly altered in the *pe* mutant making this unlikely (Nadakuduti *et al.*, 2012). Another possible explanation is that *CD2* transcripts or proteins may play a role in transmitting signals from roots to aerial organs through the phloem. Indeed, the plant use a long-distance communication network, involving RNA and protein phloem translocation, to transmit environmental inputs, sensed by mature organs, to developing regions (Lough and Lucas, 2006).

The proposed role of *CD2* in regulating cutin biosynthesis implies that its expression would coincide with the rate of cuticle formation and, thus, aerial organ expansion, assuming constant cuticle thickness. Expression analysis using qPCR did

not suggest that CD2 is more abundantly expressed in expanding organs, although this result is contradicted by the GUS staining experiment, which showed a decrease of expression in ripening fruits. However, CD2 transcripts were detected in maturing fruits of *S. pimpinellifolium* and of the Heinz tomato cultivar by independent RNA-seq experiments, corroborating the qPCR results. Various possible explanations could account for CD2 expression in mature and immature plant organs. First, even though the rate of cuticle biosynthesis is the highest in expanding organs, cuticle deposition still occurs in mature organs. For example, the deposition of cuticular waxes increases significantly during ripening of apple fruits (Ju and Bramlage, 2001) and some species are able to regenerate their epicuticular waxes if they are removed from mature leaves (Neinhuis *et al.*, 2001). Second, CD2 may participate in other metabolic processes and therefore it may regulate a different set of genes in immature and mature organs. This hypothesis is supported by the RNA-seq results presented in this manuscript. Lastly, CD2 may necessitate the presence of other protein(s) to form a transcriptional complex and the presence or absence of these hypothetical partners may determine if CD2 actively regulates gene expression.

In accordance with its regulatory role in cutin biosynthesis, CD2 transcript levels are high in the outer epidermis of the fruit. GUS expression revealed that the inner epidermis, which is responsible for the formation of a thin inner cuticle separating the pericarp from the locular cavity, also strongly expresses *CD2*. However, most tissues showed a moderate expression of the GUS reporter gene, indicating that CD2 transcripts are enriched in, but are not specific to, the epidermal layers. Epidermal expression was also detected in leaf, in the fruit petiole and in the trichomes

of leaves and petioles. Such an epidermal localization is expected, as in Arabidopsis, *HDG1* is specifically expressed in trichomes while *ANL2* is expressed in both epidermal cells and trichomes (Nakamura *et al.*, 2006; Kubo *et al.*, 2008) and the number of glandular trichomes was reported to be reduced in the tomato *pe* mutant (Nadakuduti *et al.*, 2012). However, GUS expression revealed a strong expression of *CD2* in the phloem of various organs (Fig. 3.6 to 3.14), which could result from artifactual contamination as suggested by tissue-specific RNA-seq analysis of the fruit pericarp (Fig. 3.16B). However, another RNA-seq analysis showed that *CD2* is highly expressed in the funiculus, which is mainly composed of vascular tissue, corroborating the GUS expression pattern (Fig. 3.16A). The function of *CD2* in the phloem is unclear. However, it has been suggested that the vascular tissue is the main site of ABA biosynthesis in unstressed plants (Nambara E and Marion-Poll, 2005), and since ABA levels are lower in *cd2* ripening fruits (Fig 3.35), it may be that *CD2* regulates ABA biosynthesis. This represents an interesting area of future research.

Processes regulated by CD2

Two different mutations affecting *CD2* gene expression lead to a severe reduction in the fruit and leaf cutin layers (Isaacson *et al.*, 2009; Nadakuduti *et al.*, 2012). This is associated with a reduction in the expression of several cutin-related genes. Indeed, differential expression analysis identified four genes with a clear role in cutin biosynthesis and transport (*CUS1*, *CD3*, *GPAT6* and *ABCG11*) and additional qPCR analysis identified three additional cuticle biosynthesis and transport related genes, *GPAT4*, *CER6* and *ABCG12*, with a decreased expression in *cd2* mutant. By

regulating the expression of this set of genes, *CD2* regulates the formation of cutin precursors at many stages, from fatty acyl CoA formation, monomer export through the plasma membrane and their polymerization in the apoplast. Such a role in cuticle biosynthesis and export appears to be conserved across species, as close homologs of *CD2* have been reported to regulate similar sets of genes. For examples, in Arabidopsis, HDG1 was found to directly regulate the expression of *BODYGUARD* and *FIDDLEHEAD* (Wu *et al.*, 2011), and *OCLI*, a close homolog of *CD2* from maize, was found to trigger the expression of three proteins annotated as ABCG11, and the regulation of at least one of these is likely to be direct (Javelle *et al.*, 2010).

With respect to other cuticle components, the altered cuticular wax composition observed in the *pe* and *cd2* mutants (Isaacson *et al.*, 2009; Nadakuduti *et al.*, 2012) may be explained by the reduction of expression of *CER6*, *ABCG12* and *ABCG11*, which was observed in *cd2*. The *cer6* mutation in tomato results in a decrease in levels of long chain alkanes, iso-alkanes and anteiso-alkanes in the fruit cuticular waxes (Leide *et al.*, 2007; Smirnova *et al.*, 2013). No clear trend of altered long chain alkanes was observed in *pe* and *cd2* fruit, but such a phenotype was observed in *pe* leaves (Isaacson *et al.*, 2009; Nadakuduti *et al.*, 2012). It would be interesting to test whether the leaf phenotype results from a severe reduction of *CER6* expression.

In Arabidopsis, a role for *ANL2* in the regulation of anthocyanin biosynthesis has been proposed, as the *anl2* mutant fails to accumulate anthocyanin to WT levels (Kubo *et al.*, 1999). Patterns of anthocyanin accumulation and *ANL2* expression show

a close correlation in subepidermal cells but not in the epidermis, suggesting that *ANL2* may affect anthocyanin accumulation in a tissue-specific manner (Kubo *et al.*, 2008). In WT tomato stems, anthocyanins were found not only in the epidermal and subepidermal cells but also around the vasculature (Nadakuduti *et al.*, 2012). This pattern of anthocyanin accumulation is strikingly similar to the GUS expression pattern obtained in this study, indicating that the *cd2* mutation affects anthocyanin accumulation. Accordingly, various anthocyanin-related genes were found to be differentially expressed at both 15 dpa and Tr stage of *cd2* and WT tomato fruit.

An apparent relationship between cuticle formation and anthocyanin biosynthesis is not unique to *pe* and *anl2*, as an increase of cuticular waxes levels and anthocyanin abundance was observed in transgenic *Eucalyptus* lines over-expressing two C-repeat binding factors (EguCBF1a/b; Navarro *et al.*, 2011) and in the activation-tagging line of the Arabidopsis MYB96 transcription factor (Seo *et al.*, 2010). However, these three factors are mainly involved in the plant stress response: the CBF pathway has a prominent role in freezing tolerance and MYB96 regulates multiple traits related to drought tolerance (Seo *et al.*, 2011). *CD2* may also broadly regulate stress responses as a strikingly high number of up-regulated genes at the Tr stages (67%) have the GO annotation “response to stress”. Furthermore, the number of glandular type IV trichomes, which contain volatile terpenes that are believed to be important as a deterrent against pests, is lower in the *pe* mutant in the WT (Nadakuduti *et al.*, 2012). However, it is not known whether *CD2* regulates stress-related genes or if their increased expression is an indirect consequence of the plant responding to the effects of the mutation on other processes. Indeed, the fact that stress-related genes are

not particularly differentially expressed at 15 dpa, and that they are expressed at higher, rather than lower levels in the *cd2* mutant at the Tr stage, suggests indirect regulation. In support of this idea, numerous stress-related genes were found to be differentially expressed in a mutant of ACC1, an acetyl-Coenzyme A carboxylase that generates malonyl-CoA precursors for cuticular wax synthesis (Lü *et al.*, 2011). However, the authors point out that malonyl-CoA, or subsequent lipid-based molecules, may serve as a signal in stress responses. This idea is particularly interesting in the context of this study since numerous lipid-related genes are differentially expressed in *cd2* compared to M82 and many of them appear to act in lipid-signaling pathways.

The results of this study suggest that *CD2* serves as a regulator of lipid metabolism not only for constitutive lipids but also for lipids involved in signaling. Processes that were identified as potentially abnormal in *cd2* include numerous aspects of lipid metabolism, including fatty acid and glycerolipid biosynthesis, fatty acid activation, as well as sphingolipid and phospholipid based signaling. Lipid signaling has potentially a central role in epidermal cell formation (Ohashi *et al.*, 2003; Javelle *et al.*, 2011). Indeed, an HD-ZIP IV transcription factor, *GLABRA2*, regulates root-hair pattern formation through the modulation of phospholipid signaling (Ohashi *et al.*, 2003). Therefore, the reduction of the number of glandular trichome and stomata observed in the *pe* mutant may result from a similar mechanism (Nadakuduti *et al.*, 2012). Apart from their structural role, Very-Long-Chain Fatty Acids (VLCFAs) have also been reported to have additional functions. For example, it is known that the VLCFA C24:0 can activate ethylene biosynthesis by inducing ACO transcript

accumulation (Qin *et al.*, 2007). This is intriguing since the expression of the ethylene biosynthetic gene ACC and ethylene responsive factors was affected by the *CD2* mutation (Fig. 3.33 and 3.34). Furthermore, SAUR-like auxin-responsive proteins were also found to be differentially expressed between *cd2* and M82, suggesting that the auxin pathway may also be disrupted. An increasing amount of evidence shows that auxin and ethylene interact in regulating many biological processes, such as root elongation and fruit ripening (Růžička *et al.*, 2007; Tarinotti *et al.*, 2007). Understanding the nature of the interactions between lipids and hormones resulting in *cd2* mutant phenotype warrants further investigation.

In addition to ACC, the *RIN* MADS-box transcription factor showed a decrease of expression in the *cd2* mutant. *RIN* is a key regulator of ethylene dependent and independent fruit ripening (Giovannoni *et al.*, 2007), so its reduced expression in *cd2* suggest that this process is impaired in the mutant. Another modulator of fruit ripening is ABA (Koyama *et al.*, 2010; Jia *et al.*, 2011; Sun *et al.*, 2012; Wang *et al.*, 2012; Soto *et al.*, 2013; Wang *et al.*, 2013; Zaharah *et al.*, 2013). Indeed, an increase of ABA levels at the onset of ripening triggers ethylene biosynthesis, which in turn enhances ripening (Zaharah *et al.*, 2013). The ABA levels of ripening *cd2* fruits are substantially lower than those of the WT, indicating that the ripening process may be altered in the mutant. In fact, *cd2* fruits take several more days than the WT fruits to fully ripen. However, the mechanism by which the *CD2* mutation triggered changes in levels of hormones and transcription factor regulating fruit ripening remains to be investigated.

Conclusion

The evidence presented in this study indicates that CD2 is a major regulator of lipid metabolism, including cuticle biosynthesis and transport. RNA-seq analysis showed that pleiotropic processes are affected by *CD2* mutation and further studies investigating the direct targets of CD2 will provide insights into the hierarchical regulatory networks of these seemingly unrelated processes. Furthermore, no known cuticle associated transcription factors have been identified as target of CD2 which may suggest that CD2 acts downstream of the regulatory pathway.

Materials and Methods

Plant Materials

Seeds of the *pe* mutant were kindly provided by Dr. Cornelius Barry (Michigan State University). The *cd2* and *pe* tomato mutants and their corresponding WT cultivars, M82 and AC respectively, were grown in a greenhouse under 16 h of light and 8 h of dark using standard practices. Flowers were tagged at anthesis and the fruits were harvested 5, 10, 15, 20 and 30 days post anthesis. Ripening stages were determined as follows: Mature green- the fruit has fully expanded but is entirely green; Breaker, no more than 10% of the surface is either yellow, pink or red; Turning, the color change affects 10-30% of the fruit surface; Pink, 30- 60% of the fruit is colored; and Ripe Red, where the fruit is entirely red.

pCD2::GUS reporter gene construct and GUS staining

A region spanning 2,389 bp upstream of the *CD2* start codon was amplified from M82 genomic DNA introducing restriction sites for the enzymes SacI and NcoI with the forward, CCATTAGAGCTCGACATTGCATCAGAACGA, and reverse, CAAAATCCATGGAATAAAGCAAGAGAAACTCA, primers. The amplified segment was cloned into pCAMBIA1305.1 using SacI and NcoI and sequenced to identify any mutation introduced by PCR. The resulting construct was transformed into M82 calli, generated from seeds, via *Agrobacterium tumefaciens* infection at the Biotechnology Center of the Boyce Thompson Institute for Plant Research, Ithaca, NY (<http://bti.cornell.edu/research/research-resources/facilities-services/biotechnology-center>). Harvested tissues from T0, T1 and T2 plants were placed in cold acetone for 20 min, rinsed with water and enough fresh staining buffer (100mM $K_3Fe_2(CN)_6$, 100 mM $K_4Fe(CN)_6$, 0.5 M EDTA, 0.5 M Na_2HPO_4 pH 7, 10% Triton X-100, 2 mM X-Gluc) was added to cover the tissue. Vacuum was used to infiltrate the samples with the substrate for 15 min on ice. After overnight incubation at 37°C, the samples were placed in 70% ethanol and stored at 4°C overnight. The samples were sometimes further dissected to take pictures with a Zeiss SteREO Discovery.V12 stereomicroscope. The leaf pictures were taken with a Zeiss Axio Imager.A1 microscope after sectioning of GUS expressing samples embedded in OCT medium as described in Yeats *et al.* (2012).

Transient expression of pCaMV35S::CD2-RFP construct

The *CD2* coding sequence, without the stop codon, was amplified from immature tomato fruit cDNA introducing restriction sites for the enzymes BamHI and KpnI with the forward, TTGCTGGATCCCATGAATTTTGGGGGTTTTCTTGA, and reverse, TCAAAGGTACCCTTTCGCATTGAAGTGCAGCT, primers. The amplified segment was cloned into the customized “pMDC83_35S_GFP no gateway tdTom2 rev comp” plasmid using BamHI and KpnI, and sequenced to detect any potential mutation. The cloning was done so that CD2 sequence was in frame with the red fluorescent protein sequence (C-terminal RFP fusion) and driven by two CaMV35S promoters in tandem. Epidermal onion (*Allium cepa*) cells were bombarded with 1.1 µm tungsten beads coated with the plasmid using a helium-driven PDS-1000 particle delivery system (Bio-Rad, <http://www.bio-rad.com>) operating with a vacuum of 27.5 inch HG, a helium pressure of 1100 psi and a 6 cm target distance as described in Yamame *et al.* (2005). After over-night incubation in the dark, nuclei of peeled cell layers were stained with 1 µg.ml⁻¹ 4',6-diamidino-2-phenylindole (DAPI; Kapuscinski, 1995) in 1x Phosphate Buffer Saline (PBS; 1.15g/L Na₂HPO₄, 0.2g NaH₂PO₄, 9g NaCl, Ph 7.2) and pictures were taken with a Leica TCS SP5 confocal microscope using the excitation wavelength of 561 nm and an emission filter of 575LP (Leica Microsystems, Exton, PA, USA).

Light microscopy

Imaging of fruit cuticle was conducted as described in Yeats *et al.* (2012), but using Oil Red O as cuticular stain. Briefly, a saturated solution of Oil Red O in

isopropanol was diluted 3:2 with water, allowed to sit for 30 min, and filtered through a 0.8/0.2 µm Supor® membrane. 6 µm sections were incubated for 30 min with the filtered solution of Oil Red O under high humidity to avoid the stain to dry. The slides were washed with a sequential series of isopropanol dilution solutions in water (50%, 30%, 22%, 15% and 8%) and mounted with 8% isopropanol. The sections were viewed using an AxioImager A1 microscope with an Achroplan ×40/0.75 objective and AxioCam Mrc color video camera (Zeiss) using differential interference contrast optics.

Recombinant CD2 protein production in E.coli

The *CD2* coding region including the START codon but excluding the STOP codon was amplified by PCR using the forward primer GCGCGCCATATGAATTTTGGGGGTTTTCTTGATA and reverse primer TTAATTGCGGCCGCGCTTTCGCATTGAAGTGC, incorporating NdeI and NotI restriction sites at the 5' and 3' end of the product, respectively. After digestion of the PCR product and empty pET26b(+) with NdeI and NotI, the insert was ligated and transformed into *E. coli* (XL10-Gold) for propagation of the plasmid. The fidelity of the sequence was confirmed by sequencing and the *pet26b(+)::CD2* plasmid, encoding the *CD2* mature sequence and a C-terminal hexahistidine tag, was transformed into BL21(DE3) strain of *E. coli*.

A 50 mL overnight culture of non-inducing minimal medium (MDG medium; Studier, 2005) containing 30 µg/mL kanamycin was inoculated and used the next day to seed a 1.5 L culture in the same media, shaking at 37°C. At OD600, expression was

induced by the addition of 1 mM IPTG and cells were harvested by centrifugation after 6 hours of induction. Cells were lysed and inclusion bodies recovered according to the pET system manual (Merck). The inclusion bodies were solubilized in 20 mM sodium phosphate buffer (pH 7.4) with 8 M urea, 0.5 M NaCl and 30 mM imidazole and the recombinant CD2 protein was purified using a HisPur™ Ni-NTA resin with denaturing conditions according to the product manual (Thermo scientific). The purified CD2 protein was concentrated using a Vivaspin 20 (3000 MWCO) centrifugal ultrafiltration unit (Sartorius Stedim).

CD2 antibody production and purification:

A polyclonal antibody was generated in rabbits by Pacific Immunology Corporation from purified recombinant CD2 protein. To purify the final bleed, 1 mg of recombinant CD2 was loaded on a 12% polyacrylamid gel and transferred onto a PVDF membrane by standard electrophoretic transfer. Poorly bound CD2 proteins were removed by a 5 min wash with 100 mM glycine/HCl pH 2.5. After two 2 min washes with TBST, the membrane was stained with Ponceau stain. The portion of the blot containing the antigen was cut, washed in water and TBST and cut in small strips (around 1 by 0.5 cm). The strips were blocked an hour in 5% fat-free milk in TBST. After wash, 2 mL of the final bleed and 6 mL of TBST were added to the strips and allowed to incubate for 2 to 3 hours at room temperature. The strips were then washed twice with TBST, covered with 0.1 M Glycine pH 2.5 and incubated for 5 minutes while shaking. The supernatant was transferred to a new tube containing 1/10 volume of 1 M Tris-HCl pH 8 to neutralize the solution. The extraction was repeated, the

supernatants pooled and sodium azide at a final concentration of 5 mM was added to the extract which was thereafter stored at -80°C for long-term storage.

Protein extraction and western blots:

Tissues were ground in liquid nitrogen and proteins were extracted by boiling for 5 min 100 µg of tissue in 300 µl of Laemmli buffer 1X. After 15 min centrifugation, the protein extracts were collected.

25 µg of proteins were ran in a BioRad precast gel (cat# 456-1044), wet-transferred for 1 hour at 100 V on PVDF membrane. After an hour blocking in 5% fat-free milk, the primary antibody was applied for an hour. After washes in TBST, the anti-rabbit antibody was applied for an hour and the membrane was washed again. The detection of horseradish peroxidase (HRP) enzyme activity was done using Thermo Scientific Pierce ECL Western Blotting Substrate.

Illumina sequencing

Pericarp samples of 15 dpa and Tr stage fruits were fixed, embedded in OCT medium (Sakura) and sectioned as described in Matas *et al.* (2011) with some modifications. Three biological replicates containing 5 fruits each were generated per sample, but the RNA amplification failed for one replicate of M82 15 dpa pericarp and so the DE analysis was done using only two biological replicates for this sample. Pericarp samples were dehydrated on microscope slides prior to microdissection by incubating the slides in 70%, 95% and 100% ethanol at -20°C for 1 min each. Approximately 12 mm² and 20 mm² of isolated outer epidermis from Tr and 15 dpa

fruits, respectively, were captured for each sample. Total RNA extraction and RNA amplification were also performed as in Matas *et al.* (2011). The library was prepared following the “TruSeq RNA Sample Prep v2 Low Throughput (LT) Protocol” provided by Illumina, starting at the step 11 of “Make RFP”, since the amplified RNA is already purified. Paired-end sequencing of bar coded samples was performed with the HiSeq Illumina instrument provided paired-end 2 x 100 bp reads. Between 19 and 32 million single reads were generated from the 15 dpa samples and between 18 and 48.5 million reads from the Tr samples, with a mean quality score of > 36 for all samples. The quality of the sequences was further checked with FastQC (<http://www.bioinformatics.babraham.ac.uk/projects/fastqc/>) and the reads were cleaned using the fastx tool (http://hannonlab.cshl.edu/fastx_toolkit/index.html): adaptor sequences and base-pairs with a quality lower than 20 were removed. Between 0.6 and 2.7 million reads were discarded per sample. DE genes were identified following the direction of the TUXEDO package (Trapnell *et al.*, 2012), using the *S. lycopersicum* genome, version 2.40 (<http://solgenomics.net/>).

Phylogenetic analysis

Amino acid sequences used in the phylogeny analyses were downloaded from SGN (<http://solgenomics.net/>) or TAIR (<http://www.arabidopsis.org/>) and aligned using ClustalW in MEGA5 (Fig.3.2; Tamura *et al.*, 2011) or MEGA6 (Fig.3.23; Tamura *et al.*, 2013). For Fig 3.2, the evolutionary history was inferred using the Maximum Parsimony method. The bootstrap consensus tree inferred from 1000 replicates was taken to represent the evolutionary history of the taxa analyzed

(Felsenstein J, 1985). Branches corresponding to partitions reproduced in less than 50% bootstrap replicates were collapsed. The percentage of replicate trees in which the associated taxa clustered together in the bootstrap test (1000 replicates) is shown next to the branches (Fig 3.2; Felsenstein J, 1985). The analysis involved 33 amino acid sequences. All positions containing gaps and missing data were eliminated. There were a total of 295 positions in the final dataset. Evolutionary analyses were conducted using MEGA5 (Tamura *et al.*, 2011)

For Fig. 3.23, the evolutionary history was inferred by using the Maximum Likelihood method based on the JTT matrix-based model (Jones *et al.*, 1992). The tree with the highest log likelihood (-3556.0444) is shown in Fig. 3.23. The percentage of trees in which the associated taxa clustered together is shown next to the branches. Initial tree(s) for the heuristic search were obtained by applying the Neighbor-Joining method to a matrix of pairwise distances estimated using a JTT model. The tree is drawn to scale, with branch lengths measured in the number of substitutions per site. All positions containing gaps and missing data were eliminated. There were a total of 201 positions in the final dataset. Evolutionary analyses were conducted in MEGA6 (Tamura *et al.*, 2013).

ABA measurements

Approximately 200-300 mg of finely ground plant material was vortexed in 500 µl of 1-propanol/H₂O/concentrated HCl (2:1:0.002). 80 ng of d₆-ABA was added as an internal standard. The samples were agitated at 4°C for 30 min, centrifuged 5 min at 13,000 rpm and 800 µl of dichloromethane was added to the supernatant. The

agitation and centrifugation steps were repeated and the lower phase was collected and dried at 35°C under a gentle stream of nitrogen gas. The extracts were resuspended in 100 µl of methanol and analyzed by a triple-quadrupole HPLC-MS/MS system (Quantum Access, Thermo Scientific) as described in Thaler *et al.*, (2010) at the Chemical Ecology Group Core Facility; with the selected reaction monitoring of compound-specific parent/product ion transitions: ABA 263 → 153; d₆-ABA 269 → 159.

Gene expression analysis by semiqPCR and qPCR

The differential expression of the DE genes identified by the Cuffdiff analysis (Trapnell *et al.*, 2012) was checked by using semi-quantitative PCR. Briefly, total RNA was extracted from fruit pericarp using the TRIzol® (Life Technology, catalog #15596-026) method, according to manufacturer's instructions. A total of 4 µg of RNA were used to generate cDNA using the Invitrogen™ Superscript II (SSII) reverse transcriptase. In detail, 1 µL of RQ1 DNase (Promega), 1 µL of RQ1 DNase 10x buffer (Promega) and 0.25 µL RNaseOut (Invitrogen) were added to 4 µg of total RNA and incubated at 37°C for 30 min to digest genomic DNA. 1 µL of RQ1 DNase stop solution (Promega) was added to the reactions which was incubated at 65°C for 10 min. 1 µL was saved to check for DNA contamination by PCR. 0.5 µL of oligo dT, 0.5 µL of hexamer and 1 µL of dNTP (10 mM) were added to the reactions and incubated at 65°C for 5 min, then put on ice for 1 min. 4 µL of the 5X first strand buffer provided with SSII, 2 µL MgCl₂, 2 µL DTT and 1 µL RNaseOUT were added to the reactions, and incubated at 42°C for 2 min. 1 µL Superscript II was added in the

reactions which were subsequently placed at 42°C for 50 min before being heated to 70°C for 15 min and stored at -20°C. Quality of the cDNA was checked using primers targeting the RPL2 transcript following conventional PCR conditions.

RPL2 (Solyc10g006580; forward primer: CAGCGGATGTCGTGCTATGAT; reverse primer: GGGATGCTCCACTGGATTCA) and/or Actin (Solyc05g054480; forward primer: AGATCCTCACCGAGCGTGGTTA; reverse primer: GAGCTGGTCTTTGAAGTCTCGA) were used in control reactions for semiqPCR or as reference gene for qPCR. 26 cycles were originally used for semiqPCR with an initial denaturation of the PCR reaction at 95°C for 4 min. The cycles started with a denaturation step at 95°C for 20 s, followed by an annealing step at 58°C for 30 s, an extension step at 72°C for 30 s and a final extension of 7 min at 72°C. The number of cycles was decreased or increased in a subsequent PCR if needed. The non-saturated bands were quantified densitometrically using the Alphamager 2200 v5.5 software. qPCR analysis was performed using the Affymetrix HotStart-IT SYBR Green qPCR Master Mix (catalog #75762) and a Life Technology/ABI Vii7 instrument with 3 biological replicates per sample following the standard run method provided by ViiA™ 7 Software v1.0. qPCR analysis: RPL2 was used as an endogenous control unless otherwise stated in the figures. The primers used are given in Tables 3.1 and 3.2.

Table 3.1. SGN IDs of the ABA synthesis and signaling related genes analyzed in this experiment and the qPCR primers used.

Gene Name	SGN ID	qPCR primers
ZEP	Solyc02g090890	F- TAGCAAACATCAGGCGTTGAG R- ACAATGTCCATGACATTCTCC
ABA4	Solyc02g086050	F- ATGACATTAGCATCTGCTTGG R- ATAGCAAGCAGAGAGACTG
NCED-05	Solyc05g053530	F- CTTTATGGCTATAGCTGAACC R- CATAAGGTACCCTTCATCTTC
NCED-07	Solyc07g056570	F- TGGTGACAACAAATATGGTGG R- CTCCAACCTCAAACCTCATTGC
NCED-08	Solyc08g016720	F- ATGCATGACACCACCAGACTC R- ACCGAGTTTGTCTTCTGTTTAC
ABA2	Solyc04g071940	F- TGGAATTGACGGTTGATGATG R- AGGGAGTGATTAACACACGAG
AAO-01	Solyc01g009230	F- CTAAACACTGGACATCACGAG R- AGCTGCTCTTGTTCACAATG
AAO-11	Solyc11g071600	F- TTCATGTGCTAAACAGTGGAC R- CTGCTTTAACAGCTTCTCTTG
ABI-12	Solyc12g096020	F- TGGAAAGAGGTGAAGGAATTG R- TCCACCACAATCACTGTTATG
ABI-03	Solyc03g121880	F- ATATCCGTGATTGTGGTGGAC R- CACACACCTTAAGCCCATAGG

Table 3.2. Primers used to confirm differential expression of genes identified in the RNA-seq experiment. In red are the genes which differential expression was infirmed by semi-qPCR

SGN ID	qPCR primers	Product size (bp)
15 dpa: differentially expressed genes less expressed in <i>cd2</i> than in M82		
Solyc01g006870	F-AATACCAGAGTGTGTGTTCTG R-TGTGGTATTGTCACCATCATG	218
Solyc01g008330	F-AACTCATCCTTGATATCGAGG R-GCACTCACTTCAAGTTCCAAT	241
Solyc01g105440	F-ATGTTGGTGGTTCACCTTGAT R-TCAGAACTACTACTGGAACG	234
Solyc01g105450	F-TGTTAGTCAAGGCTGGTGAAA R-TGCTATGTAAGGCTGATCCAA	233
Solyc01g109180	F-AATCACACTCAGATCTTCTCC	282

	R-TCTGATGGTAGTATCTCCAAG	
Solyc02g077710	F-AACTACCAGCAGCAACAGTTC R-TGGTTCATTGCAGCAAATTCC	407
Solyc02g091920	F-CATTGAAGGATGTGCAATGCC R-CGGAGCAAGCATTGATAAGAC	304
Solyc03g006240	F-AGGCAGCTTATCACCACATAG R-TACTCAGTATATCCCACAACC	123
Solyc03g025760	F-CTCAGCTGAAGGATTGACAAA R-CGTTTCGTGTGCTTCATTACAA	279
Solyc03g111550	F-TTCATTTCAGAAAGCAGTTCCC R-CTTATACATGGCTTCGGTAAG	209
Solyc03g114750	F-CCAAGAAGTTTAGCGTCATTG R-ATGGACAAGTAGAAGAAACGG	317
Solyc03g117490	F-TAGTTCAGTTGTAAGACCAGC R-TTGTGGCTACCAGTTAGTACA	345
Solyc03g119200	F-TGCAAGAAAGTCTTGCTGATG R-TCCTGAAGAGTGAACAAGCTC	344
Solyc03g121540	F-GTGCAGATATAAACGAATGGC R-ACAACCTCACCTCCATCAAAG	417
SL2.40ch03:46212310..46213402	F-CCGGCTATATACACAACCTATG R-TACCCAGAACTAGTCACAGA	275
Solyc04g008590	F-TCATGCAAGCTGCTAAGACAC R-CAATGGACCAATCATCTCACC	396
Solyc04g016330	F-TGAGATTGCACAAAGTCATGC R-GGCTTATGGAAAGAACAAAGC	242
Solyc04g050570	F-ATAGTGAAATAGGCACCCATG R-GGTGCATGTAATCAGTTGTTC	273
Solyc04g081760	F-CAGCTATACCTCTATCAACAC R-TGTATCATCTTCACATGTCCC	311
Solyc05g014560	F-ATCAGTAGTTGGCCTTGTGG R-CCATTCATTTGGCTGAAGAGG	376
Solyc05g025810	F-TTCTGGATTGCTCTAGTACAG R-AGTACAAGTATGCGAGTATGG	363
Solyc05g043330	F-TTTGAGACCATTTGTGCCTGC R-AGCAAGTTCAATTAGAAAGCC	340
SL2.40ch05:680311..681753	F-TCAAGTAACCGACAAACCATC R-TTGAATGGCATTAGGGACTC	246
Solyc06g009770	F-ATCAACACGAAGCTTGTGCAG R-TGCGCAATAATCATGGACTTG	357
Solyc06g035580	F-GTCACCATATGGCATTACCAT R-TTAGTTCCTTGCACCAACAAG	210
Solyc06g063040	F-CCTGATGGAATCGACATCTAC R-TTCCAATATTGCGACCAGAG	344
Solyc06g068160	F-ATTTTCAGCAACGGACTTGAG R-ACAACAACCTACACATCACTGC	318

Solyc06g074260	F-CAAACCTTCCTTCTACTCCAC R-CATACATGCTTAAGGTATCCC	317
Solyc07g005900	F-TGTCAACTGGATAGAAATGGC R-GAACTGCCAAGAATCTTCAGG	383
Solyc07g049430	F-TCATGTGCTCAATGTGATACC R-ATTTCTCATTGCATCCATCTC	368
Solyc07g049440	F-TTCATCCAACGGAGAGAAGT R-CACAACACCTTCCAGTTTACG	309
Solyc08g016620	F-CAGCTAGTTGTTGATCCATTC R-ATACTCAGCTGCCACTTGTTT	420
Solyc08g061010	F-AGAGACACCAAACACCTTACC R-ACACTCCTTATCTTTCCACAC	390
Solyc08g081220	F-TCTAGGCAAAGACTTGGCATA R-GCTCCTGGTTGATTAATACCA	258
SL2.40ch08:30717811..30718430	F-CGAGGATGATGCCTTGTTATT R-CATATCGAGTATACAGAGACC	276
Solyc09g007970	F-GGTTATACCTTCATCAGCGTG R-TCAGAAGCAGATTGAGATACG	310
Solyc09g009530	F-AGTTTGATCCGATGGAAGTAG R-GCGATGAATCGTTGTAGAATG	112
Solyc09g014350	F-AAGGTAAGTGGTGGTACATTG R-TTCTCCTTCTCCTTCTCCTTG	122
Solyc09g075860	F-GAGAACAGAATAGTGGAAAGG R-AGTCATGAAGTCCAAGCAGAA	285
Solyc09g090980	F-AACATTATGGGTGTAACACC R-GATACTCAGTTGTTGTCTTGC	370
Solyc10g047240	F-GATTATGCCTCTTCACTCACC R-AGACTCACACTGTTCTCTTG	254
Solyc10g054900	F-TCAACAACCTTATGCACCTCT R-TAAGAGAAGGTGGGAACAATG	247
Solyc10g078740	F-ATATGGAGGTGGTATGAGTTC R-CAGACCATTGTCAACATACAC	295
Solyc10g080840	F-CCATCAGTGTCTTTAGAGCAC R-CTTGCATGATGATGGAAGTAG	358
Solyc10g083140	F-GACGAATTCATGTGTATCATC R-CTCATAGATAACTTCAAGCAA	190
Solyc10g085500	F-GAGGTTCTTGGAGATACCAAG R-CCCATTCTATCTCGTGTATCC	446
Solyc11g006250	F-GTAGCATGTTGTGGACAAGGACCA R-TTTGCCCTCTCAGATGGATGGAAC	122
Solyc11g007390	F-TCCAGCAGTTAAGCTTCTAAC R-CCTGAGATAAATTCCAGGGAA	106
Solyc12g006930	F-GTCAAGTACATTGGCTGGATT R-TTTC AAGTCGAAGGACGTGTT	202
Solyc12g010590	F-CCGATCGATGATTCTTGTACC	393

	R-GGGAAGTGAAGGATTATCAGC	
Solyc12g011410	F-GATATTGCTCCTTCTAATACC R-TTAGGCTTGTGTTGTTAAAGC	159
Solyc12g044300	F-TTCTAGGACGTACAAATGCTG R-ACAGACGAGTTGGTATCTTGT	89
15 dpa: differentially expressed genes more expressed in <i>cd2</i> than in M82		
Solyc03g013610	F-AAAACGCACTTCGACCACAAA R-TTGAATTACCGGTAGAAAGAG	116
Solyc03g013620	F-AGACTTCGGATACTTGATCGA R-ATAGGAACACAGTCCAACCAA	228
Solyc06g035940	F-AATCCTGAGAGTAGTGTCTCTC R-TTTGCGTCTACGATTGACTTC	326
Solyc08g074630	F-TGGAGGATATTGGATTGGAAG R-AATCCTCAAGCTTGATCTCCA	108
Solyc09g084450	F-TTTCGATGTGATCGAGTTCGT R-CGTTAGATCTGCCTGAGTTAT	214
Solyc09g091550	F-AGTTCTTCACATGAATGGAGG R-GAGATCACTTATGGCTTGATC	115
Solyc11g006230	F-CAATCGTTATGGCTACAACA R-GTCCTTGATCAGACATAGAAC	274
Solyc12g014630	F-CAAGTAAGGTGTCCAAGAGAT R-TCCACAGTTGTTGAGAATGAG	228
Tr: differentially expressed genes less expressed in <i>cd2</i> than in M82		
Solyc01g005270	F-ATGCCACAATTCTTTGTCACC R-CCATAGCCCATCTAGTATATG	323
Solyc01g006540	F-CAAACCATTACCAGATGAAG R-CACACATGATGCATTGCATCA	333
Solyc01g008710	F-TGTACCCTAATCAATGGTTGC R-TTGCAAGACCACTTGATAACC	305
Solyc01g057000	F-TTGTGCTCATCATGTGCAATG R-TTTGTTCCATCGAGGTTGAAG	403
Solyc01g080410	F-TACCTCATCTGTTCTACTCTG R-AGGAGAAGTACCCAAAGAAGC	285
Solyc01g095080	F-TGATGGAACGGTTGATATTGC R-ACCAGTTGTCAATACATACGC	352
Solyc01g099590	F-GCCTGTTATTGTTTCATGATGG R-CAACATCAGGTGTAGGAAGAC	458
Solyc01g099630	F-ACAGTATAGGAGACTTCGTTG R-TAATATCCTCATGACTCCACC	276
Solyc02g069490	F-CTTGAGCTTTGGTTGATAGAG R-TTGAATTTGGAACAGGCAAGC	330
Solyc02g069800	F-AATCGGAGCTAGAACAGGAAC R-GATGAACTCTGCAATGGCTTC	365
Solyc02g078400	F-CTGGATGGAGATATTGACATG R-AGAGTCTTGATCCCATGTATG	355

Solyc02g083970	F-GAACACAACGATGCTCTCTAC R-AAATGCAGGACCAACAAATCG	409
Solyc02g086180	F-CTGGATGTTTGGAACTCTTCG R-ATAAGGAACATCCTTGAGTGC	88
Solyc03g005020	F-CACCACAATATTTGGTCTTGC R-AACGTCTTTGCTATCGGACAG	382
Solyc03g031860	F-AATCTCTTGTGCCTCCTACAA R-TGCAAAGCAGATAACTACGGA	251
Solyc03g095900	F-AGCTGTATGAACCAATCACTG R-CAGTAGTAGTTACTCACCAC	364
Solyc03g111690	F-TAGTTCTGGTGCCTCAACTG R-ACTTCTTAGCTTGCCTCTCTC	347
Solyc03g118060	F-CACTTGAACAGAAGGTGTTTCG R-AGTACTGCTAGTGCTAGCATG	339
Solyc03g120580	F-AGAGCATGTATTGTGATGTCG R-TAAGGGACAAGCTTAGTGCAG	320
Solyc03g122360	F-GGTCTTAAGGTGATTCAAGCT R-TGAGTGATGTTCACTTCCAAG	271
Solyc05g012020	F-ACTTGGAACAGCTTGAACGTC R-TACAACCTCCAGTAGCATCATG	344
Solyc06g053620	F-TTTAGCTGGGAGAACTACAG R-GAAGAATTGACTGCTCGAAGC	312
Solyc06g072160	F-TCTATTTGGAGGATGGAAACC R-GAGTGTACGCAAGACCTTATC	367
Solyc06g074710	F-TAAGTGGCTTCGAGACAACCTC R-AAGCATCAATGCTTCCATCTC	435
SL2.40ch06:44612342..44612809	F-GAATTAAGTGAACAGAAGACC R-TGTAATACTATCAGTTGAGGG	434
Solyc08g005770	F-GGGAGACCAGAGTTAACAAAA R-ATGGCCAATGGAGGTAAACTT	206
Solyc08g005780	F-TCAGGTTCCAGAACTGATGA R-CCGAGAAACATATTGCACTCT	245
Solyc08g044510	F-GAGGAATATATGACCTCATGC R-ACTTGTTGTACCAGTAAGCAG	336
Solyc08g063040	F-AATGTCAGGATCAGGATCAGG R-AGGTGGTGTAGTAGTACTGAG	346
Solyc08g066700	F-GTTCAATTGACTTGGATCAGC R-ATCTAACCAGCTTCTGTGACG	355
Solyc09g066150	F-GAGACGACGATTTTCGTTACAG R-TTTATCCAACCACCGTTCTGG	395
Solyc09g072590	F-TCTTTGTTTCATTGGTCTCCTG R-GCTGAAATAGGATAAGAGAGG	368
Solyc09g075600	F-ATGGAGATGGCTGATACGAGA R-TCACCAGTTTTCCACCACGAAG	240
Solyc09g091430	F-GGTTGGTGCCATTACTTCAAG	282

	R-GCTTTGAGATAGGAACTGATG	
Solyc10g080210	F-TTACTTGTGGTCCAGGTCATG R-TGGAAAGTTTGTGCTGCAATC	353
Solyc10g086180	F-CTCTACAAGTTTGTAGGGAG R-TTGTCCATTGCACATTGCTGT	111
SL2.40ch10:2747333..2747896	F-GAACTCGACAATGTAGATGTG R-GAATATGAGAGTCTGTAAGGG	319
Solyc11g022590	F-GTGGAGTTCTTTCCAGCATAAC R-CAGCCTTCTTGAAGTAAACAG	373
Solyc11g066090	F-GTTCATTGGTGGAACGATACT R-CAATTCAAGTACAGCTCCACT	228
Solyc11g066100	F-AAGCTAAGAACGGATTGGAGA R-GATACATCTTGGCAATGATCG	225
Solyc12g013700	F-TGATGGATCTGTGGTGATTTC R-TCAGACCAGTTAGCTTCACTG	255
Solyc12g042830	F-ATGGTTGAGGATGGAATTTTG R-CATCTTTCTTAGGTTTGTAC	217
Solyc12g042570	F-TATCTGCACTGTTGAGCTCTG R-CGTTAGATGTTGCTGTGCTTC	317
Solyc12g042580	F-TACACCATTTGGAGCAACAAC R-TATGATAGTCCAACGAACACC	368
Solyc12g042590	F-AGATCTGACCATACTCTC R-GCCATTTGGTCTATCAACAAC	302
Solyc12g042600	F-TATCTCATCTTCGATAGGAG R-AATGTGAGATGAACCTCCTTC	350
Tr: differentially expressed genes more expressed in <i>cd2</i> than in M82		
Solyc01g005470	F-GGTTGGCAAGGAAATATGGAT R-CCACTAGCCAATGTCACATAA	240
Solyc01g059990	F-GTTAACCAAAGCAGGAACTTG R-CAACTTGCCATCACATTCTGA	313
Solyc01g060020	F-TGCATTTGGTGCACACATGA R-TCACTAGTGAGTGAAGAAGCA	261
Solyc01g073820	F-ACTTCGGTTCTCCTTACGAAG R-CAGGTGGTCTCAATATAAGAC	424
Solyc01g097270	F-CACAAGTTCGAGCAACGTATC R-TCTGTCAACAACAGATAGCAG	392
Solyc01g105070	F-GACACCTCGTATTTCTCTAAC R-CAGGAGCAACAATAAGTTCAG	355
Solyc01g109860	F-GTTCGAATGATCTCTCACGTA R-TGTGCTGGTGAATAGCACAAC	91
Solyc01g107820	F-ACACTGGAAGGAATATCAGCA R-CCATCCATTGTAAGATGATCC	288
Solyc02g036350	F-CCTGATGGAAACAGAATGTCC R-CACACTACCAGACAAGAGTAC	412
Solyc02g079220	F-TACTTCTTCTTGCCTGAGACG	436

	R-TCCAGTGCACAGCTTATGAAC	
Solyc02g079510	F-AGCTATTGCTGCTCGTGATTC R-GCAGTTGTAGTATTCCCAGTC	423
Solyc02g089250	F-TCAATCCAATAGGAGGACTTC R-TGACAGGTGTTTGTGTAAGT	395
Solyc02g090930	F-ATGCATGAGAGTGATTGGCTT R-TGATCAGATGATCCAAGCCTG	93
Solyc02g092760	F-GCCATATCATAACAGAGCTCAA R-CTAGAAGAAGCATCAGCAGTA	199
Solyc03g019690	F-TTACAACCTCCGATGTAGGACG R-GGCTGATCTTTCCTAGACAC	375
Solyc03g036470	F-TTGGATGGAAGCTCTTATGTG R-ATGTTCCGGAGAGCATAACGAT	94
Solyc03g036480	F-ATCTAATCTGACAGCAGGAAG R-GCAATATTTGTGTACGGAACC	87
Solyc03g083680	F-TGAAGAGCGTTATGAAGGTTG R-ACAAAGTCATCGCCATGGAAG	285
Solyc03g096290	F-CAATGAACAAGCATGGAAGGA R-GCATGTTGTGTAATGGACTTG	262
Solyc03g111290	F-GCTTTATCCACCAGTAGCATG R-AGCACGGTGATGGATTCTTAC	403
Solyc03g111300	F-GTGCTTGAATGAATCCATGAG R-AACCACCAACCATATGTGCAG	398
Solyc03g111640	F-TGCCAATGCATACGAGATATG R-AGGAAAGAGAACACTGAAAGG	430
Solyc03g117860	F-AAGGCATTGGAATTGCCAGAC R-AACAACCAACGAGTGACTGC	277
Solyc04g048900	F-ATGATCCTGATCTCTACGTGC R-AATGTATGTGCGTCCATGCTG	385
Solyc04g051360	F-TTATTGGACATACCTCTACGG R-ATCCAGATGAAGAAGAAGGGT	240
Solyc04g070970	F-ATGGCTCTGTTGATGACTCTA R-CTTAGGAGGAAGTAGGCTAAC	91
Solyc04g071770	F-TAGATTTCCATGGAGGACAAC R-TAGCTAGAAGAAGGTGGATAG	292
Solyc04g079730	F-GTTGAAATGGATAGGCAGAGC R-GTTCGACCAGCAACAATCTTG	464
SL2.40ch05:18356340..18356777	F-GTGTTTTTTGACCCATTTCCAC R-GTGTGTCAATGCATCTATTTG	383
Solyc06g008890	F-AAGATCATGGAAGTCGTGGAC R-ACTATCTTGTCCACGCTCTAC	441
Solyc06g051840	F-ATCTTTCTTCTCCTACCTCTG R-CCATTAGTACATCAACACTGG	426
Solyc06g053260	F-TGGGGTAGTGGAGATCACAAAC R-GCATGAGTTTCTTTGTGCGATC	346

Solyc06g060870	F-CAGATGATTTAAGCACGTGTG R-AGTAGCCTCACAAGACTTCTC	430
Solyc06g066800	F-AATTGAGGGATATGGTGGATG R-TTCTTATACTCCTCGAGTTCC	412
Solyc06g068960	F-CTTCAAGACATGGAAGAAGTG R-GATCATTCTGGTACAATCCTG	360
Solyc06g076070	F-ATGCACAATGGGTTGGTTGAT R-AGATGAAGAACGTTATGAAGG	199
Solyc06g076160	F-TAGAATGGACCATGGCAGAAC R-CAATTGCTAGCTCAACAAGTG	435
Solyc07g007870	F-TTGCAGTGGTGGATACTAG R-CTGAAATTCACCAGCAAGTGC	440
Solyc07g018010	F-AGATCACCACCATCTTCTTCC R-ATCGGGATCGTTTAGAGAAGC	282
Solyc07g042170	F-TTTACCTATTGCGAGAAGAGC R-GCCTATTTAGTCTTTGGTCTC	416
Solyc07g042230	F-CCGTGACAGAATATGGTTAGG R-TCATCATGCAACACTACTTCC	360
Solyc07g043000	F-AACCACCACCAGCAATAATAC R-TGCCTTCAACTATGACAATGC	364
Solyc07g043230	F-ATTATTCTCGCTCACAACCTCC R-AACCAATAGCCAAGAGTAGAC	338
Solyc07g052210	F-TAAGTGTTCAAACTCTGAG R-CTCTTCAAGCTTATCATCACC	184
Solyc07g056470	F-AATCCACGTGACTTGTGAGTC R-TTCCTCAAATCCTCGTCTCTG	312
SL2.40ch07:58039990..58040392	F-CGATGATTTAAAGAAGCAGAG R-TTGGTATCGGAGTAGGTGTTG	348
Solyc07g065110	F-ATGCTGCAGAAACACCAGAAG R-TTAACATCCATCGGGAACCTT	242
Solyc08g079140	F-TCAGCAGAGCGATTTCAAACC R-ACGTTCTCAAATTCGGATACC	322
Solyc08g079900	F-CTACACAAATCCACAGGTAGG R-TAGCCAATGCCAACACAACCTG	386
Solyc08g080670	F-CAAACACCTTAGCTGAATACG R-CTGTAGTCCAACCTCTGACAAG	357
Solyc09g007760	F-TTCACTTGGCTACAATTCCTG R-CATCCAAGCTTTGTTATGTC	96
Solyc09g075820	F-GTCAAAGTGTAACAGTGTGTG R-ATCATATCCGTTAGCATGTCC	284
Solyc09g083050	F-AAGTGTAATAGTGCTGTGTGG R-CATCAATCTCATCCATCCAAG	82
Solyc09g091800	F-TAAGAGTTGGGAGTCGTATAG R-CAATGAAGGCCACCACCAATG	431
Solyc09g098510	F-ACTACTACAAATCACCACCAC	409

	R-ACGTGAAGACACACAGAGAAC	
Solyc10g055820	F-TACTGCTTCCTTAGAGAACAG R-TCCTGAACCCTGTTATCATT	392
Solyc10g080610	F-GGAGATGGAATCAGTGTATGG R-AAGGTCCGATAACCAAGATCC	448
Solyc10g084940	F-TCCTTATCCTTGGAATAGCAG R-CGAATAATTCCTCGCAACAAC	299
Solyc10g085500	F-TACACCCTCCAATTCCATTTC R-CCCATTCCTATCTCGTGTATCC	358
SL2.40ch10:25200360..25201242	F-GAAACTACACACAGCTGAAAG R-ACATGGATCACTTCTTAGAGG	346
Solyc11g010630	F-GATTCAGTAGCCATCAAGCTG R-TCTTGCCTATCCAGATACATG	402
Solyc12g014420	F-AAAGCCAGGTGGTGAAGATTC R-GTGTATCAGGATTATGACACG	228
Solyc12g014630	F-GACAAGTAAGGTGTCCAAGAG R-TCCACAGTTGTTGAGAATGAG	230

Acknowledgements and Relative Contribution

I would like to acknowledge Dr. Xueyong Yang who purified the CD2 antiserum, Dr. Yueping Liu who performed the CD2 expression qPCR analyses.

REFERENCES

- Ariel F, Manavella P, Dezar C, Chan R. (2007). The true story of the HD-Zip family. *TRENDS in Plant Science* 12(9), 419-426.
- Barry CS, Giovannoni JJ. (2007). Ethylene and fruit ripening. *Journal of Plant Growth Regulation* 26, 143-159.
- Bird S, Gray J. (2003). Signals from the cuticle affect epidermal cell differentiation. *New Phytologist* 157, 9-23.
- Bird D, Beisson F, Brigham A, Shin J, Greer S, *et al.* (2007). Characterization of Arabidopsis ABCG11/WBC11, an ATP binding cassette (ABC) transporter that is required for cuticular lipid secretion. *The Plant Journal* 52(3), 485-498.
- Chen X, Goodwin M, Boroff VL, Liu X, Jenks MA. (2003). Cloning and Characterization of the WAX2 Gene of Arabidopsis Involved in Cuticle Membrane and Wax Production. *The Plant Cell*, 15, 1170-1185.
- Chew W, Hrmova M, Lopato S. (2013). Role of homeodomain leucine zipper (HD-Zip) IV transcription factors in plant development and plant protection from deleterious environmental factors. *International Journal of Molecular Sciences* 14, 8122-8147.
- Clark GB, Sessions A, Eastburn DJ, Roux SJ. (2001). Differential expression of members of the annexin multigene family in Arabidopsis. *Plant Physiology* 126(3), 1072-1084.
- Cominelli E, Sala T, Calvi D, Gusmaroli G, Tonelli C. (2008). Over-expression of the Arabidopsis *AtMYB41* gene alters cell expansion and leaf surface permeability. *The Plant Journal* 53, 53-64.
- Delker C, Stenzel I, Hause B, Miersch O, Feussner I, Wasternack C. (2008). Jasmonate biosynthesis in *Arabidopsis thaliana* – enzymes, products, regulation. *Plant Biology* 8(3), 297-306.
- Di Cristina M, Sessa G, Dolan L, Linstead P, Baima S, *et al.* (1996). The Arabidopsis *Athb-10* (GLABRA2) is an HD-Zip protein required for regulation of root hair development. *The Plant Journal* 10(3), 393-402.
- Dietz K-J, Vogel MO. (2010). AP2/EREBP transcription factors are part of gene regulatory networks and integrate metabolic, hormonal and environmental signals in stress acclimation and retrograde signaling. *Protoplasma* 245, 3-14.

- Dunn TM, Lynch DV, Michaelson LV, Napier JA. (2004). A post-genomic approach to understanding sphingolipid metabolism in *Arabidopsis thaliana*. *Annals of Botany* 93, 483-497.
- Felsenstein J. (1985). Confidence limits on phylogenies: An approach using the bootstrap. *Evolution* 39, 783-791.
- Fraser CM, Chapple C. (2011). The phenylpropanoid pathway in Arabidopsis. The Arabidopsis Book 9:e0152.
- Fu R, Liu W, Li Q, Li J, Wang L, Ren Z. (2013). Comprehensive analysis of the homeodomain-leucine zipper IV transcription factor family in *Cucumis sativus*. *Genome* 56, 395-405.
- Fujisawa M, Nakano T, Ito Y. (2011). Identification of potential target genes for the tomato fruit-ripening regulator RIN by chromatin immunoprecipitation. *BMC Plant Biology* 11(26), doi:10.1186/1471-2229-11-26
- Fukuchi-Mizutani M, Okuhara H, Fukui Y, Nakao M, Katsumoto Y, *et al.* (2003). Biochemical and Molecular Characterization of a Novel UDP-Glucose:Anthocyanin 3'-O-Glucosyltransferase, a Key Enzyme for Blue Anthocyanin Biosynthesis, from Gentian. *Plant Physiology* 132(3), 1652-1663.
- Fulda M, Schnurr J, Abbadi A, Heinz E, Browse J. (2004). Peroxisomal acyl-coA synthetase activity is essential for seedling development in *Arabidopsis thaliana*. *The Plant Cell* 16(2), 394-405.
- Ghosh R, Bankaitis VA. (2011). Phosphatidylinositol transfer proteins: Negotiating the regulatory interface between lipid metabolism and lipid signaling in diverse cellular processes. *BioFactors* 37(4), 290-308.
- Giovannoni JJ. (2007). Fruit ripening mutants yield insights into ripening control. *Current Opinion in Plant Biology* 10, 283-289.
- Graça J, Schreiber L, Rodrigues J, Pereira H. (2002). Glycerol and glyceryl esters of ω -hydroxyacids in cutins. *Phytochemistry* 61, 205-215.
- Ho LC, Grange RI, Picken AJ. (1987). An analysis of the accumulation of water and dry matter in tomato fruit. *Plant, Cell and Environment* 10, 157-162.
- Hannun YA, Obeid LM. (2008). Principles of bioactive lipid signalling: lessons from sphingolipids. *Nature Reviews Molecular Cell Biology* 9, 139-150.
- Hen-Avivi S, Lashbrooke J, Costa F, Aharoni A. (2014). Scratching the surface: genetic regulation of cuticle assembly in fleshy fruit. *Journal of Experimental Botany* 65(16), 4653-4664.

- Hunt G, Baker E. (1980). Phenolic constituents of tomato fruit cuticles. *Phytochemistry* 19, 1415-1419.
- Isaacson T, Kosma DK, Matas AJ, Buda GJ, He Y, *et al.* (2009). Cutin deficiency in the tomato fruit cuticle consistently affects resistance to microbial infection and biomechanical properties, but not transpirational water loss. *The Plant Journal* 60, 363–377.
- Javelle M, Vernoud V, Depège-Fargeix N, Arnould C, Oursel D, *et al.* (2010). Overexpression of the epidermis-specific homeodomain-leucine zipper IV transcription factor OUTER CELL LAYER1 in maize identifies target genes involved in lipid metabolism and cuticle biosynthesis. *Plant Physiology* 154, 273-286.
- Javelle M, Vernoud V, Rogowsky P, Ingram G. (2011). Epidermis: the formation and functions of a fundamental plant tissue. *New Phytologist* 189, 17-39.
- Jetter R, Kunst L, Samuels A. (2006). Composition of plant cuticular waxes. In: *Biology of the plant cuticle*. Oxford, UK: Blackwell, 145-181.
- Jia H-F, Chai Y-M, Li C-L, Lu D, Luo J-J, *et al.* (2011). Abscisic acid plays an important role in the regulation of strawberry fruit ripening. *Plant Physiology* 157, 188-199.
- Jones DT, Taylor WR, Thornton JM. (1992). The rapid generation of mutation data matrices from protein sequences. *Computer Applications in the Biosciences* 8, 275-282.
- Ju Z, Bramlage WJ. (2001). Developmental changes of cuticular constituents and their association with ethylene during fruit ripening in ‘Delicious’ apples. *Postharvest Biology and Technology* 21, 257–263.
- Kamata N, Okada H, Komeda Y, Takahashi T. (2013). Mutations in epidermis-specific HD-ZIP IV genes affect floral organ identity in *Arabidopsis thaliana*. *The Plant Journal* 75, 430-440.
- Kannangara R, Branigan C, Liu Y, Penfield T, Rao V, *et al.* (2007). The transcription factor WIN1/SHN1 regulates cutin biosynthesis in *Arabidopsis thaliana*. *The Plant Cell* 19, 1278-1294.
- Kapuscinski J. (1995). DAPI: a DNA-specific fluorescent probe. *Biotechnic & Histochemistry* 70(5), 220-233.
- Kienow L, Schneider K, Bartsch M, Stuible H-P, Weng H, *et al.* (2008). Jasmonates meet fatty acids: functional analysis of a new acyl-coenzyme A synthetase family from *Arabidopsis thaliana*. *Journal of Experimental Botany* 59(2), 403-419.

- Kosma DK, Bourdenx B, Bernard A, Parsons EP, Lü S, Joubès J, Jenks MA. (2009). The impact of water deficiency on leaf cuticle lipids of arabidopsis. *Plant Physiology* 151, 1918-1929.
- Kosma DK, Murmu J, Razeq FM, Santos P, Bourgault R, *et al.* (2014). AtMYB41 activates ectopic suberin synthesis and assembly in multiple plant species and cell types. *The Plant Journal* 80(2), 216-229.
- Kovinich N, Saleem A, Arnason JT, Miki B. (2010). Functional characterization of a UDP-glucose:flavonoid 3-*O*-glucosyltransferase from the seed coat of black soybean (*Glycine max*(L.) Merr.). *Phytochemistry* 71, 1253-1263.
- Koyama K, Sadamatsu K, Goto-Yamamoto N. (2010). Abscisic acid stimulated ripening and gene expression in berry skins of the Cabernet Sauvignon grape. *Functional & Integrative Genomics* 10, 367-381.
- Kubo H, Peeters AJM, Aarts MGM, Pereira A, Koornneef M. (1999). ANTHOCYANINLESS2, a homeobox gene affecting anthocyanin distribution and root development in Arabidopsis. *The Plant Cell* 11, 1217-1226.
- Kubo H, Kishi M, Goto K. (2008). Expression analysis of ANTHOCYANINLESS2 gene in Arabidopsis. *Plant Science* 175, 853-857.
- Kubo H, Hayashi K. (2011). Characterization of root cells of *anl2* mutant in *Arabidopsis thaliana*. *Plant Science* 180, 679-685.
- Kunst L, Samuels, A. (2003). Biosynthesis and secretion of plant cuticular wax. *Progress in lipid research* 42(1), 51-80.
- Kurata T, Kawabata-Awai C, Sakuradani E, Shimizu S, Okada K, Wada T. (2003). The YORE-YORE gene regulates multiple aspects of epidermal cell differentiation in Arabidopsis. *The Plant Journal* 36(1), 55-66.
- Landgraf R, Smolka U, Altmann S, Eschen-Lippold L, Senning M, *et al.* (2014). The ABC transporter ABCG1 is required for suberin formation in potato tuber periderm. *The Plant Cell* 26(8), 3403-3415.
- Lee DR. (1988). Vasculature of the abscission zone of tomato fruit: implications for transport. *Canadian Journal of Botany* 67, 1898-1902.
- Leide J, Hildebrandt U, Reussing K, Riederer M, Vogg G. (2007). The developmental pattern of tomato fruit wax accumulation and its impact on cuticular transpiration barrier properties: effects of a deficiency in a β -ketoacyl-coenzyme A synthase (LeCER6).
- Li Y, Beisson F, Koo AJK, Molina I, Pollard M, *et al.* (2007). Identification of acyltransferases required for cutin biosynthesis and production of cutin with

- suberin-like monomers. *Proceedings of the National Academy of Sciences USA* 104(46), 18339-18344. *Plant Physiology* 144, 1667-1679.
- Li F, Wu X, Lam P, Bird D, Zheng H, *et al.* (2008). Identification of the wax ester synthase/acyl-coenzyme A: diacylglycerol acyltransferase WSD1 required for stem wax ester biosynthesis in *Arabidopsis*. *Plant Physiology* 148(1), 97-107.
- Li-Beisson Y, Pollard M, Sauveplane V, Pinot F, Ohlrogge JB, Beisson F. (2009) Nanoridges that characterize the surface morphology of flowers require the synthesis of cutin polyester. *Proceedings of the National Academy of Sciences USA* 106: 22008–2201
- Lolle S, Cheung, A. (1993). Fiddlehead: An *Arabidopsis* mutant constitutively expressing an organ fusion program that involves interactions between epidermal cells. *Developmental Biology* 155(1), 250-258.
- Lough TJ, Lucas WJ. (2006). Integrative plant biology: role of phloem long-distance macromolecular trafficking. *Annual Review of Plant Biology* 57, 203-232.
- Lü S, Song T, Kosma DK, Parsons EP, Rowland O, Jenks MA. (2009). *Arabidopsis CER8* encodes LONG-CHAIN ACYL-COA SYNTHETASE 1 (LACS1) that has overlapping functions with LACS2 in plant wax and cutin synthesis. *The Plant Journal* 59(4), 553-564.
- Lü S, Zhao H, Parsons EP, Xu C, Kosma DK, *et al.* (2011). The glossyhead1 allele of ACC1 reveals a principal role for multidomain acetyl-coenzyme A carboxylase in the biosynthesis of cuticular waxes by *Arabidopsis*. *Plant Physiology* 157, 1079-1092.
- Masucci J, Rerie WG, Foreman DR, Zhang M, Galway ME, *et al.* (1996). The homeobox gene *GLABRA 2* is required for position-dependent cell differentiation in the root epidermis of *Arabidopsis thaliana*. *Development* 122, 1253-1260.
- Matas AJ, Yeats TH, Buda GJ, Zheng Y, Chatterjee S, *et al.* (2011). Tissue- and cell-type specific transcriptome profiling of expanding tomato fruit provides insights into metabolic and regulatory specialization and cuticle formation. *The Plant Cell* 23, 3893–3910.
- Markakis MN, Boron AK, Van Loock B, Saini K, Cirera S, *et al.* (2013) Characterization of a Small Auxin-Up RNA (SAUR)-like gene involved in *Arabidopsis thaliana* development. *PLoS ONE* 8(11): e82596. doi:10.1371/journal.pone.0082596
- MacDonald MJ, D’Cunha GB. (2007). A modern view of phenylalanine ammonia lyase. *Biochemistry and Cell Biology* 85(3), 273-282.

- Mauch-Mani B and Mauch F. (2005). The role of abscisic acid in plant-pathogen interactions. *Current Opinion in Plant Biology* 8, 409-414.
- McClure BA, Guilfoyle T. (1987). Characterization of a class of small auxin-inducible soybean polyadenylated RNAs. *Plant Molecular Biology* 9, 611-623.
- McFarlane HE, Shin JJH, Bird DA, Samuels AL. (2010). *Arabidopsis* ABCG transporters, which are required for export of diverse cuticular lipids, dimerize in different combinations. *The Plant Cell* 22, 3066-3075.
- Millar AA, Clemens S, Zachgo S, Giblin EM, Taylor DC, Kunst L. (1999). *CUT1*, an *Arabidopsis* gene required for cuticular wax biosynthesis and pollen fertility, encodes a very-long-chain fatty acid condensing enzyme. *The Plant Cell* 11, 825-838.
- Mizoi J, Shinozaki K, Yamaguchi-Shinozaki K. (2012). AP2/ERF family transcription factors in plant abiotic stress responses. *Biochimica et Biophysica Acta – Gene Regulatory Mechanisms* 1819(2), 86-96.
- Morant M, Bak S, Møller BL, Werck-Reichhart D. (2003). Plant cytochromes P450: tools for pharmacology, plant protection and phytomediation. *Current Opinion in Biotechnology* 14(2), 151–162.
- Mortimer JC, Laohavisit A, Macpherson N, Webb A, Brownlee C, *et al.* (2008). Annexins: multifunctional components of growth and adaptation. *Journal of Experimental Botany* 59(3), 533-544.
- Muir S, Collins GJ, Robinson S, Hughes S, Bovy A, *et al.* (2001). Overexpression of petunia chalcone isomerase in tomato results in fruit containing increased levels of flavonols. *Nature Biotechnology* 19, 470-474.
- Mukherjee K, Brocchieri L, Brüglin T. (2009). A comprehensive classification and evolutionary analysis of plant homeobox genes. *Molecular Biology and Evolution* 26(12), 2775-2794.
- Nadakuduti SS, Pollard M, Kosma DK, Allen Jr. C, Ohlrogge JB, Barry CS. (2012). Pleiotropic phenotypes of the sticky peel mutant provide new insight into the role of CUTIN DEFICIENT2 in epidermal cell function in tomato. *Plant Physiology* 159, 945–960.
- Nakamura M, Katsumata H, Abe M, Yabe N, Komeda Y, *et al.* (2006). Characterization of the class IV homeodomain-leucine zipper gene family in *Arabidopsis*. *Plant Physiology* 141, 1363–1375.
- Nambara E, Marion-Poll A. (2005). Abscisic acid biosynthesis and catabolism. *Annual Review of Plant Biology* 56, 165-185.

- Navarro M, Ayax C, Martinez Y, Laur J, El Kayal W, *et al.* (2011). Two EguCBF1 genes overexpressed in *Eucalyptus* display a different impact on stress tolerance and plant development. *Plant Biotechnology Journal* 9, 50-63.
- Neinhuis C, Koch K, Barthlott W. (2001). Movement and regeneration of epicuticular waxes through plant cuticles. *Planta* 213, 427-434.
- Ohashi Y, Oka A, Rodrigues-Pousada R, Possenti M, Ruberti I, *et al.* (2003). Modulation of phospholipid signaling by GLABRA2 in root-hair pattern formation. *Science* 300, 1427-1430.
- Panikashvili D, Savaldi-Goldstein S, Mandel T, Yifhar T, Franke RB, *et al.* (2007). The Arabidopsis DESPERADO/AtWBC11 transporter is required for cutin and wax secretion. *Plant Physiology* 145(4), 1345-1360.
- Peterson K, Shyu C, Burr CA, Horst RJ, Kanaoka MM, *et al.* (2013). Arabidopsis homeodomain-leucine zipper IV proteins promote stomatal development and ectopically induce stomata beyond the epidermis. *Development* 140, 1924-1935.
- Qin Y-M, Hu C-Y, Pang Y, Kastaniotis AJ, Hiltunen JK, Zhu Y-X. (2007). Saturated very-long-chain fatty acids promote cotton fiber and *Arabidopsis* cell elongation by activating ethylene biosynthesis. *The Plant Cell* 19, 3692-3704.
- Rerie W, Feldmann K, Marks M. (1994). The GLABRA2 gene encodes a homeo domain protein required for normal trichome development in Arabidopsis. *Genes & Development* 8, 1388-1399.
- Robert-Seilaniantz A, Grant M, Jones JDG. (2011). Hormone crosstalk in plant disease and defense: More than just JASMONATE-SALICYLATE antagonism. *Annual Review of Phytopathology* 49, 317-343.
- Růžička K, Ljung K, Vanneste S, Podhorská R, Beeckman T, *et al.* (2007). Ethylene regulates root growth through effects on auxin biosynthesis and transport-dependent auxin distribution. *The Plant Cell* 19, 2197-2212.
- Sánchez-Fernández R, Davies TGE, Coleman JOD, Rea PA. (2001). The *Arabidopsis thaliana* ABC protein superfamily, a complete inventory. *The Journal of Biological Chemistry* 276(32), 30231–30244.
- Schrack K, Nguyen D, Karlowski W, Mayer K. (2004). START lipid/sterol-binding domains are amplified in plants and are predominantly associated with homeodomain transcription factors. *Genome Biology*, 5(6).
- Sessa G, Morelli G, Ruberti I. (1993). The Athb-1 and -2 HD-Zip domains homodimerize forming complexes of different DNA binding specificities. *The EMBO Journal* 12(9), 3507-0517.

- Seo PJ, Park C-M. (2010). MYB96-mediated abscisic acid signals induce pathogen resistance response by promoting salicylic acid biosynthesis in *Arabidopsis*. *New Phytologist* 186, 471-483.
- Seo PJ, Park C-M. (2011). Cuticular wax biosynthesis as a way of inducing drought resistance. *Plant Signaling & Behavior* 6(7), 1043-1045.
- Seymour GB, Ostergaard L, Chapman NH, Knapp S, Martin C. (2013). Fruit development and ripening. *Annual Review of Plant Biology* 64, 219-241.
- Shi JX, Adato A, Alkan N, He Y, Lashbrooke J, *et al.* (2013). The tomato SISHINE3 transcription factor regulates fruit cuticle formation and epidermal patterning. *New Phytologist* 197(2), 468-480.
- Shockey JM, Fulda MS, Browse J. (2003). Arabidopsis contains a large superfamily of acyl-activating enzymes. Phylogenetic and biochemical analysis reveals a new class of acyl-coenzyme A synthetases. *Plant Physiology* 132, 1065-1076.
- Smirnova A, Leide J, Riederer M. (2013). Deficiency in a very-long-chain fatty acid β -ketoacyl-coenzyme A synthase of tomato impairs microgametogenesis and causes floral organ fusion. *Plant Physiology* 161, 196-209.
- Stark R, Tian S. (2006). The cutin biopolymer matrix. In: *Biology of the plant cuticle*. Oxford, UK: Blackwell, 126-144.
- Soto A, Ruiz KB, Ravaglia D, Costa G, Torrigiani P. (2013). ABA may promote or delay peach fruit ripening through modulation of ripening- and hormone-related gene expression depending on the developmental stage. *Plant Physiology and Biochemistry* 64 11-24.
- Studier FW. (2005). Protein production by auto-induction in high-density shaking cultures. *Protein Expression & Purification* 41, 207-234.
- Sun L, Sun Y, Zhang M, Wang L, Ren J, *et al.* (2012). Suppression of 9-cis-epoxycarotenoid dioxygenase, which encodes a key enzyme in abscisic acid biosynthesis, alters fruit texture in transgenic tomato. *Plant Physiology* 158, 283-298.
- Takada S, Takada N, Yoshida A. (2013). ATML1 promotes epidermal cell differentiation in Arabidopsis shoots. *Development* 140, 1919-1923.
- Tamura K, Stecher G, Peterson D, Filipinski A, Kumar S. (2013). MEGA6: Molecular Evolutionary Genetics Analysis version 6.0. *Molecular Biology and Evolution* 30, 2725-2729.
- Tamura K, Peterson D, Peterson N, Stecher G, Nei M, Kumar S. (2011). MEGA5: Molecular Evolutionary Genetics Analysis using Maximum Likelihood,

Evolutionary Distance, and Maximum Parsimony Methods. *Molecular Biology and Evolution* 28, 2731-2739.

- Thaler JS, Agrawal AA, Halitschke R. (2010). Salicylate-mediated interactions between pathogens and herbivores. *Ecology* 91(4), 7075-1082.
- Trainotti L, Tadiello A, Casadoro G. (2007). The involvement of auxin in the ripening of climacteric fruits comes of age: the hormone plays a role of its own and has an intense interplay with ethylene in ripening peaches. *Journal of Experimental Botany* 58(12), 3299-3308.
- Trapnell C, Roberts A, Goff L, Pertea G, Kim D, Kelley DR, *et al.* (2012). Differential gene and transcript expression analysis of RNA-seq experiments with TopHat and Cufflinks. *Nature Protocols* 1(7), 562-578.
- Tsuji J, Coe L. (2013). The *glabra1* mutation affects the stomatal patterning of *Arabidopsis thaliana* rosette leaves. *BioOne* 84(2), 92-97.
- Tuteja N. (2007). Abscisic acid and abiotic stress signaling. *Plant Signaling & Behavior* 2(3), 135-138.
- Verrier PJ, Bird D, Burla B, Dassa E, Forestier C, *et al.* (2008). Plant ABC proteins – a unified nomenclature and updated inventory. *Trends in Plant Science* 13(4), 151-159.
- Wang Y, Wu Y, Duan C, Chen P, Li Q, *et al.* (2012). The expression profiling of the *CsPYL*, *CsPP2C* and *CsSnRK2* gene families during fruit development and drought stress in cucumber. *Journal of Plant Physiology* 169, 1874-1882.
- Wang Y, Wang Y, Ji K, Dai S, Hu Y, *et al.* (2013). The role of abscisic acid in regulating cucumber fruit development and ripening and its transcriptional regulation. *Plant Physiology and Biochemistry* 64, 70-79.
- Wei Y, Periappuram C, Datla R, Selvaraj G, Zou J. (2001). Molecular and biochemical characterizations of a plastidic glycerol-3-phosphate dehydrogenase from *Arabidopsis*. *Plant Physiology and Biochemistry* 39, 841-848.
- Wei Q, Kuai B, Hu P, Ding Y. (2012). Ectopic-overexpression of an HD-Zip IV transcription factor from *Ammopiptanthus mongolicus* (Leguminosae) promoted upward leaf curvature and non-dehiscent anthers in *Arabidopsis thaliana*. *Plant Cell, Tissue and Organ Culture* 110, 299-306.
- Wu R, Li S, He S, Waßmann F, Yu C, *et al.* (2011). CFL1, a WW domain protein, regulates cuticle development by modulating the function of HDG1, a class IV homeodomain transcription factor, in rice and *Arabidopsis*. *The Plant Cell* 23, 3392-3411.

- Xia Y, Yu K, Navarre D, Seebold K, Kachroo A, Kachroo P. (2010). The glabral mutation affects cuticle formation and plant responses to microbes. *Plant Physiology* 154, 833-846.
- Yamane H, Lee S-J, Kim B-D, Tao R, Rose JKC. (2005). A coupled yeast signal sequence trap and transient plant expression strategy to identify genes encoding secreted proteins from peach pistils. *Journal of Experimental Botany* 56, 2229–2238.
- Yeats TH, Martin LBB, Viart H M-F, Isaacson T, He Y, *et al.* (2012). The identification of cutin synthase: formation of the plant polyester cutin. *Nature Chemical Biology* 8, 609-611.
- Yeats TH, Rose JKC. (2013). The formation and function of plant cuticles. *Plant Physiology* 163, 5-20.
- Yeats TH, Huang W, Chatterjee S, Viart HM-F, Clausen MH, Stark RE, Rose JKC. (2014). Tomato Cutin Deficient 1 (CD1) and putative orthologs comprise an ancient family of cutin synthase-like (CUS) proteins that are conserved among land plants. *The Plant Journal* 77, 667–675.
- Zaharah SS, Singh Z, Symons GM, Reid JB. (2013). Mode of action of abscisic acid in triggering ethylene biosynthesis and softening during ripening in mango fruit. *Postharvest Biology and Technology* 75, 37-44.
- Zhang M, Yuan B, Leng P. (2009a). The role of ABA in triggering ethylene biosynthesis and ripening of tomato fruit. *Journal of Experimental Botany* 60(6), 1579-1588.
- Zhao Y, Zhou Y, Jiang H, Li X, Gan D, *et al.* (2011). Systematic analysis of sequences and expression patterns of drought-responsive members of the HD-Zip gene family in maize. *Plos One*, 6(12), e28488. doi:10.1371/journal.pone.0028488.
- Zhao ZC, Hu GB, Hu FC, Wang HC, Yang ZY, Lai B. (2012). The UDP glucose: flavonoid-3-*O*-glucosyltransferase (*UFGT*) gene regulates anthocyanin biosynthesis in litchi (*Litchi chinensis* Sonn.) during fruit coloration. *Molecular Biology Reports* 39(6), 6409-6415.

CHAPTER 4

Absciscic Acid is Required for Cuticle Formation

Abstract

The structure and composition of fruit and leaf cuticles from tomato (*Solanum lycopersicum*) mutants (*sitiens*, *flacca* and *notabilis*) that are deficient in abscisic acid (ABA) biosynthesis were assessed to test the hypothesis that ABA regulates cuticle development. Initial studies revealed that both leaves and fruits from the ABA deficient lines were more resistant to the necrotrophic fungus *Botrytis cinerea* than those of the corresponding wild type genotypes. Moreover, the mutant fruits also showed less transpirational water loss during storage, following harvesting at the ripe stage, than wild type fruits. These two phenotypes are consistent with the ABA mutants having abnormal cuticles, but more definitive evidence was provided by transmission electron microscopic (TEM) studies, which revealed cuticle structural abnormalities and a thinner leaf cuticle than that of the wild type, although no structural differences in the fruit cuticle were noted. Chemical analysis of the leaf cuticles further showed that the levels of coumaric acid isomers and the cutin monomer 10(9),16-dihydroxyhexadecanoic acid were significantly lower in the mutant genotypes. The ABA mutant leaf waxes showed a more complex pattern of differences compared with the wild type: alkanes shorter than C₃₁ and isoalkanes accumulated to higher levels in the mutant genotypes, but alkanes \geq C₃₁, the anteisoalkane C₃₂, amyrins and taraxasterol were less abundant. This trend suggests that ABA plays a role in the compositional regulation of cuticular waxes, thereby influencing cuticular permeability. Additionally, transcript expression analyses of genes involved in cutin and wax biosynthesis, transport and regulation, suggested a general down-regulation of this pathway in the ABA mutants. The only gene that was found to be expressed at a higher level was *CER4*, which encodes an enzyme that catalyzes the formation of primary alcohols and wax esters. Taken together, these data suggest a role for ABA in cuticle development independent of the effects of osmotic stress.

Introduction

The plant cuticle is an extracellular waxy layer, composed of a cutin matrix of ω -hydroxylated fatty acids covalently linked by ester bonds, which is covered by and interspersed with a structurally diverse range of hydrophobic waxes. The cuticle covers the epidermis of aerial organs and is a key barrier to desiccation and pathogen entry, and so it is required from the onset of organ formation through ontogeny. Being a fundamental part of organ development, its formation is genetically encoded to provide for a uniform protective cover throughout organ development (Yeats and Rose, 2013).

In addition to being an intrinsic part of developmental programs, cuticle formation is dynamic, and its composition and coverage change in response to environmental cues, such as light/dark, U.V. radiation and drought (Hooker *et al.*, 2002; Cameron *et al.*, 2006; Shepherd and Griffiths, 2006; Kosma *et al.*, 2009; Go *et al.*, 2014; Martin *et al.*, 2014). Thus, water deficit triggers an increase in the accumulation of both cutin monomers and waxes, resulting in a thicker, less permeable cuticle in *Arabidopsis* (Kosma *et al.*, 2009). A key factor of drought response is the phytohormone abscisic acid (ABA; Liu *et al.*, 2005) so the consequences of ABA treatment on cuticle composition and gene expression have been investigated (Kosma *et al.*, 2009). While the levels of waxes, and in particular alkanes, increase following ABA treatment, few changes in the amount or composition of cutin monomers are generally observed, suggesting that additional factors trigger changes in the cuticle under water stress (Kosma *et al.*, 2009). Furthermore, the expression levels of numerous wax biosynthesis related genes are known to respond to

ABA treatment (Kosma *et al.*, 2009; Seo *et al.*, 2009; Seo *et al.*, 2011; Wang *et al.*, 2012a). For example, the expression of *ECERIFERUM 1 (CER1)*, which encodes an enzyme that is responsible for producing alkanes from very-long-chain acyl-CoA (Bernard *et al.*, 2012), is induced by ABA treatment (Kosma *et al.*, 2009). Furthermore, the presence of *cis*-ABA-responsive elements in the promoters of some wax-related genes, such as *ECERIFERUM 6 (CER6)*; Hooker *et al.*, 2002), suggest that there is a direct action of ABA on wax regulation under drought conditions. Additionally, some Arabidopsis transcription factors that are associated with cuticle biosynthesis, such as *MYB96*, are regulated by ABA (Cominelli *et al.*, 2008; Seo *et al.*, 2009).

Several recent reports indicate that the relationship between ABA and cutin is complex. Indeed, ABA biosynthesis and signaling has been found to be impaired in mutants with disrupted cutin biosynthesis, suggesting that cutin components may be involved in mediating osmotic stress signaling (Wang *et al.*, 2011). In addition, the transcription factor NF-X LIKE2 (NFLX2) suppresses ABA accumulation and ABA responses, possibly to avoid osmotic stress response under normal conditions (Lisso *et al.*, 2011). NFLX2 has further been shown to bind to the promoter of *SHINE 1 (SHN1)* transcription factor, which directly regulates cutin formation (Kannangara *et al.*, 2007; Lisso *et al.*, 2012), and *BODYGUARD (BDG)*, an α/β -hydrolase fold protein that is required for cuticle integrity (Kurdyukov *et al.*, 2006). Therefore, NFLX2 is a negative regulator of both ABA and cutin biosynthesis.

Collectively, these studies show that ABA regulates cuticle formation. However, it is not clear if ABA is only an environmental regulator of cuticle formation, or if it is also required for genetically encoded cuticle biosynthesis, or both. Indeed, in addition to its role in plant response to water stress, ABA also regulates many aspects of plant ontogeny, including the maintenance of shoot growth in well-watered plants (Sharp *et al.*, 2000), the promotion of seed dormancy and the synthesis of seed storage proteins and lipids (Finkelstein *et al.*, 2002). Consequently, this study aims to test if ABA is required for cuticle formation independently of water stress induced cuticle biosynthesis.

To address this hypothesis, tomato (*Solanum lycopersicum*) ABA deficient lines (*notabilis*, *flacca* and *sitiens*) were used in this study. *notabilis* (*not*) has a mutation in 9-cis-epoxycarotenoid dioxygenase (NCED) which is believed to be a key regulatory enzyme of the ABA biosynthesis pathway (Burbidge *et al.*, 1999; Thompson *et al.*, 2000). The mutation in *sitiens* (*sit*) affects an aldehyde oxidase (AO) which catalyzes the last step of the pathway (Harrison *et al.*, 2011), while *flacca* (*flc*) has a mutation in a molybdenum cofactor (MoCo) sulfurase required for the activation by sulfuration of the MoCo of AO (Sagi *et al.*, 2002). The severity of these mutant phenotypes correlates with their shoot ABA concentration (from 5 week old plants), with *not* having the mildest phenotype, and the highest level of ABA, and *sit* having the most severe phenotype (Tal and Nevo, 1973; Taylor and Tarr, 1984).

In this study, the role of ABA in cuticle formation was investigated by assessing cuticle structure, by transmission electron microscopic (TEM) and light

imaging, and composition, by chemical analysis of fruits and leaves of ABA deficient mutants. Additionally, the expression of genes involved in cuticle biosynthesis, transport and regulation was evaluated to determine the incidence of ABA deficiency on the cuticle pathway. Finally, pathogen sensitivity and fruit cuticular permeability were tested to determine if the functions of the ABA deficient line cuticle are impaired.

Results

ABA deficiency leads to a reduction of the plant and organ size

Most of the published analyses of ABA levels in the ABA-deficient *not*, *sit* and *flc* tomato mutants have focused on the leaves. So, in this study, ripening fruits and mature seeds were tested to determine if the decrease of ABA in these mutants is reproducible in other organs. The results show that ABA levels were consistently reduced in the mutants (Fig. 4.1). The reduction in ABA levels was greatest in Pink (Pk) stage fruits, with an 88% and 99% decrease in *flc* in the Ailsa Craig (*flc(AC)*) and Rheinlands Ruhm (*flc(RR)*) backgrounds, respectively. A substantial reduction was also evident in leaves and seeds, ranging from 41% in *not(AC)* leaves to 83% in *not(AC)* seeds. Furthermore, the mutants were statistically different from each other in leaf for the RR background and in seed for both backgrounds. ABA levels were lower in *sit(RR)* than in *flc(RR)* in both leaves and seeds, as was previously reported, but the trend was opposite for *not(AC)* and *flc(AC)* seeds (Tal and Nevo, 1973; Taylor and Tarr, 1984).

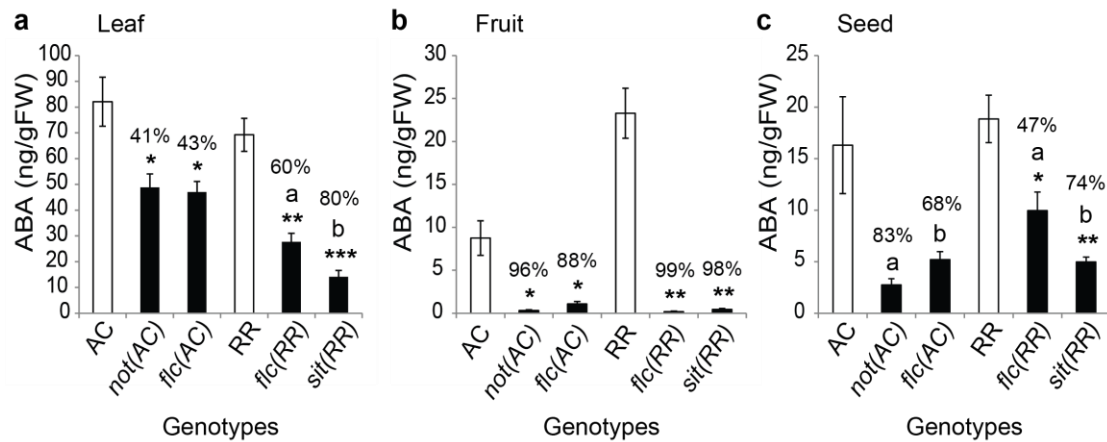


Figure 4.1. ABA levels in three organs of four ABA deficient lines. (a) Developing leaves of fully mature plants (leaf size < 2 cm, n = 4 with one missing value for *sit*). (b) Pink stage fruit pericarp (n = 4). (c) Mature seeds (n = 4). Differences between the mutants and their corresponding WT genotypes were assessed using a 2 tailed T-test with: * $\alpha = 0.05$; ** $\alpha = 0.01$; ***p-value < 0.001. If two mutants in the same genetic background were statistically different from one another at $\alpha = 0.05$, the letters ‘a’ and ‘b’ were used. Percentages of decreased amounts of ABA in the mutants compared to their WT are indicated above the mutant bar. AC, Ailsa Craig; *not(AC)*, *notabilis* in AC background (AC); *flc(AC)*, *flacca* in (AC); RR, Rheinlands Ruhm; *flc(RR)*, *flacca* in (RR); *sit(RR)*, *sitiens* in (RR).

Plant growth was generally impaired in ABA deficient plants, resulting in smaller plants (Fig. 4.2), with smaller curly leaves (Fig. 4.3) and smaller fruits (Fig. 4.4). Reduction of organ size, including for roots, has previously been reported (Rančić *et al.*, 2010; Sharp *et al.*, 2000; Nitsch *et al.*, 2012). ABA deficient plants were wilted if not well-watered and were much more sensitive than their Wild Types (WT) to pruning and hot temperatures, both of which often resulting in leaves and/or stems death.

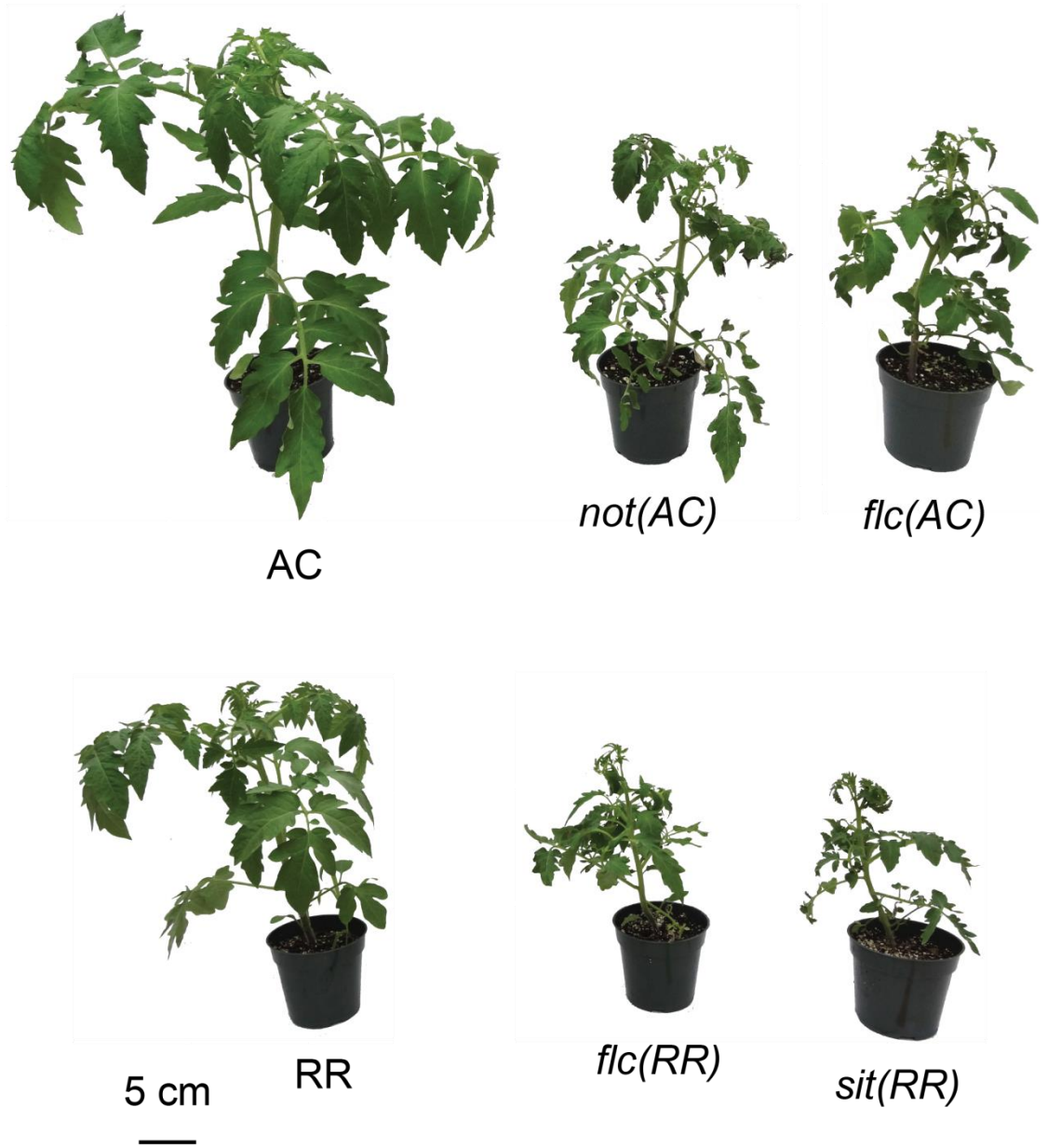


Figure 4.2. Abscisic acid (ABA) deficient mutant whole plant phenotypes. Pictures of representative 5-week old seedlings are shown.

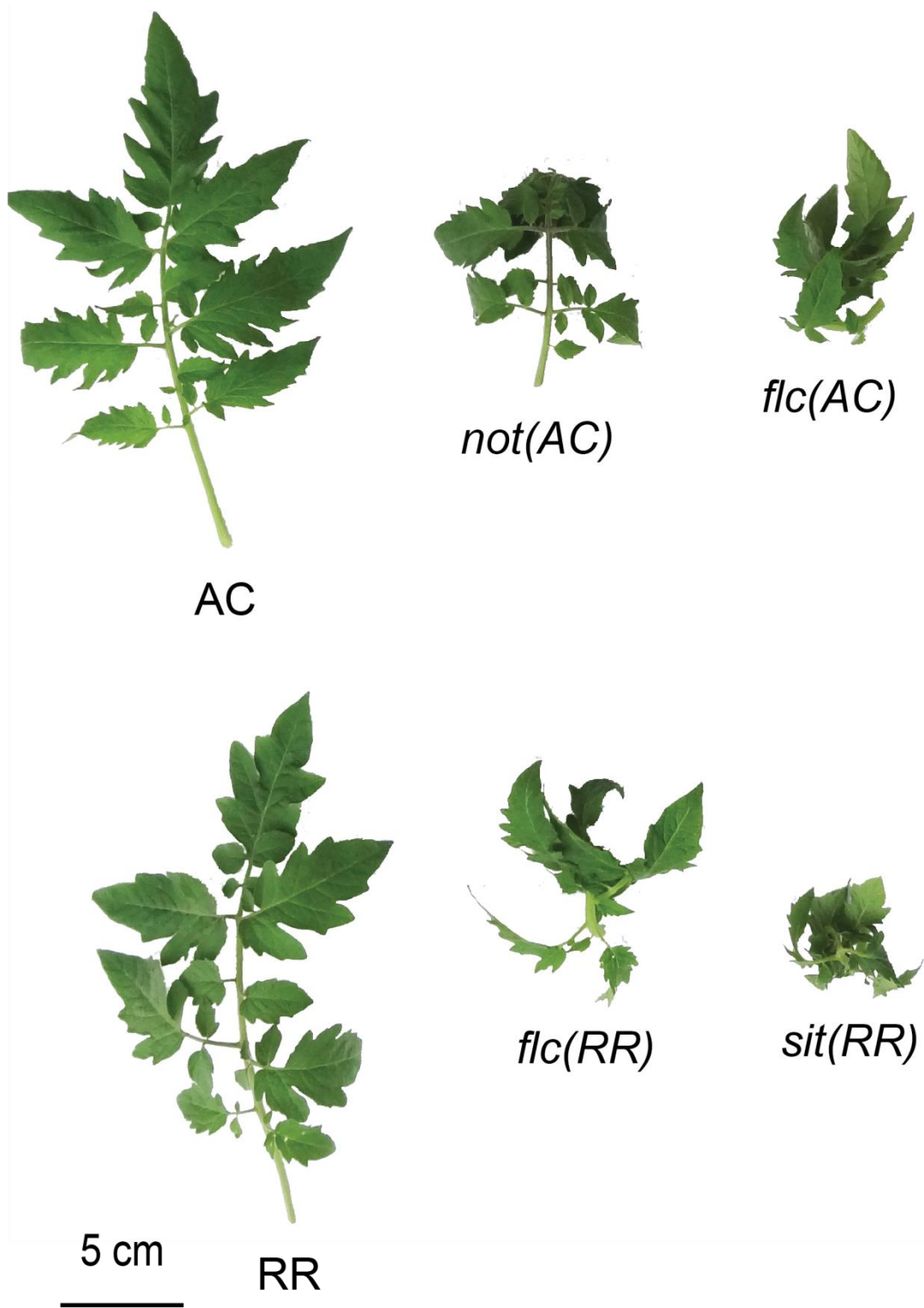


Figure 4.3. ABA deficient mutant leaf phenotypes. Photographs of the youngest mature leaf of 5-week old seedlings are represented.

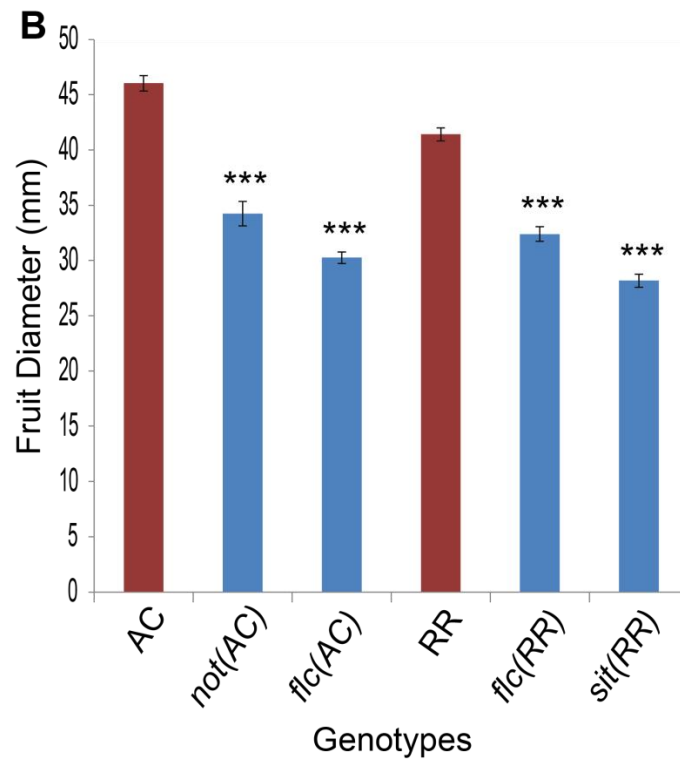
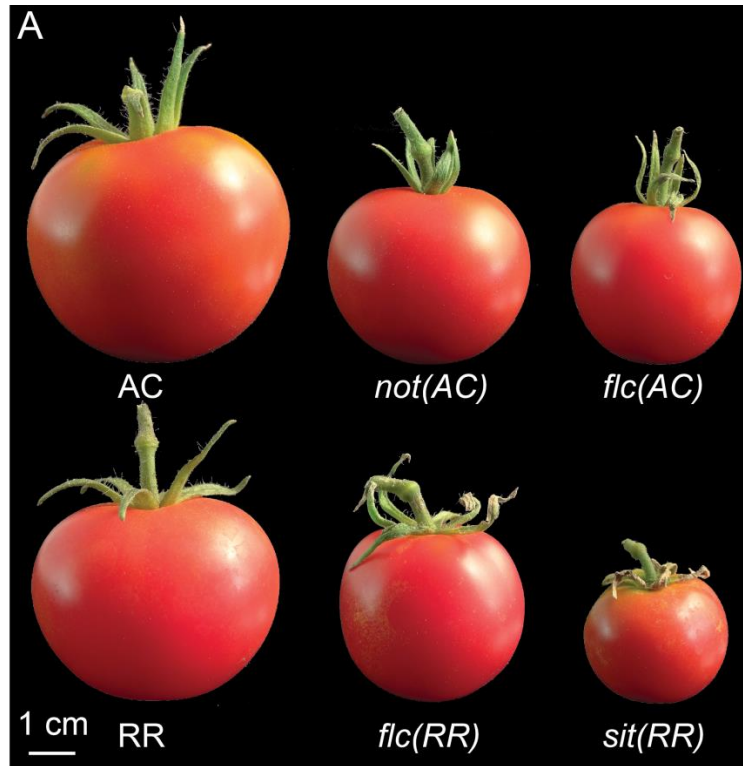


Figure 4.4. ABA deficient mutant fruit phenotypes. (A) Pictures of representative Red Ripe stage fruits. Scale bar, 1 cm. (B) Diameters of Red Ripe stage fruits, $20 \leq n \leq 62$. *** p-value < 0.001.

Effect of ABA deficiency on leaf and fruit cuticle ultrastructure

The ultrastructure of the leaf and fruit cuticles of *flc* and *sit*, and their respective WT genotypes, was assessed using TEM. The cuticles of small expanding mutants fruits of similar diameters (~13.5 mm) was thicker than the respective WTs (Figs. 4.5 and 4.7), while the cuticle of the adaxial and abaxial leaf surfaces was on average thinner (Figs. 4.7, 4.8, 4.9 and 4.10). The cuticle morphologies of the WT and the mutant fruit cuticles were indistinguishable (Figs. 4.5 and 4.6), but various abnormalities were observed in the mutant leaf cuticles. For example, while the cuticle of the WTs was reticulate between the polysaccharide cell wall and the amorphous cuticle proper, the cuticle of the mutants had sporadic electron-translucent globules (Figs. 4.7c, 4.8c, d and 4.10c). The thickness of the polysaccharide cell wall and cuticle of the mutants was often more variable than was seen in the WTs giving a wavy appearance of the cuticle (Figs. 4.7d and 4.9c, d). Occasional disruption of the cuticle was also observed (Fig. 4.8d). Irregularities in appearance of the cuticle and the polysaccharide cell wall have previously been reported for *sit* in Moneymaker background (Curvers *et al.*, 2010), but the mutant leaf cuticle was reported to be thicker than that of WT, contradicting the results of this study. This apparent contradiction may be explained by a lack of contrast in the TEM micrograph represented in Fig 2 of Curvers *et al.* (2010) between the cuticle and cell wall of the WT, making it difficult to distinguish the cuticle. Indeed, it appears that the thin region that the authors (Curvers *et al.*, 2010) define as the cuticle was mislabeled and a re-examination of the images published in the article indicates that the WT cuticle was not thinner than that of the mutants. Lastly, an unexpected phenotype observed in this

current study was the presence of chloroplasts in the epidermis of *sit* leaves (Fig. 4.8c).

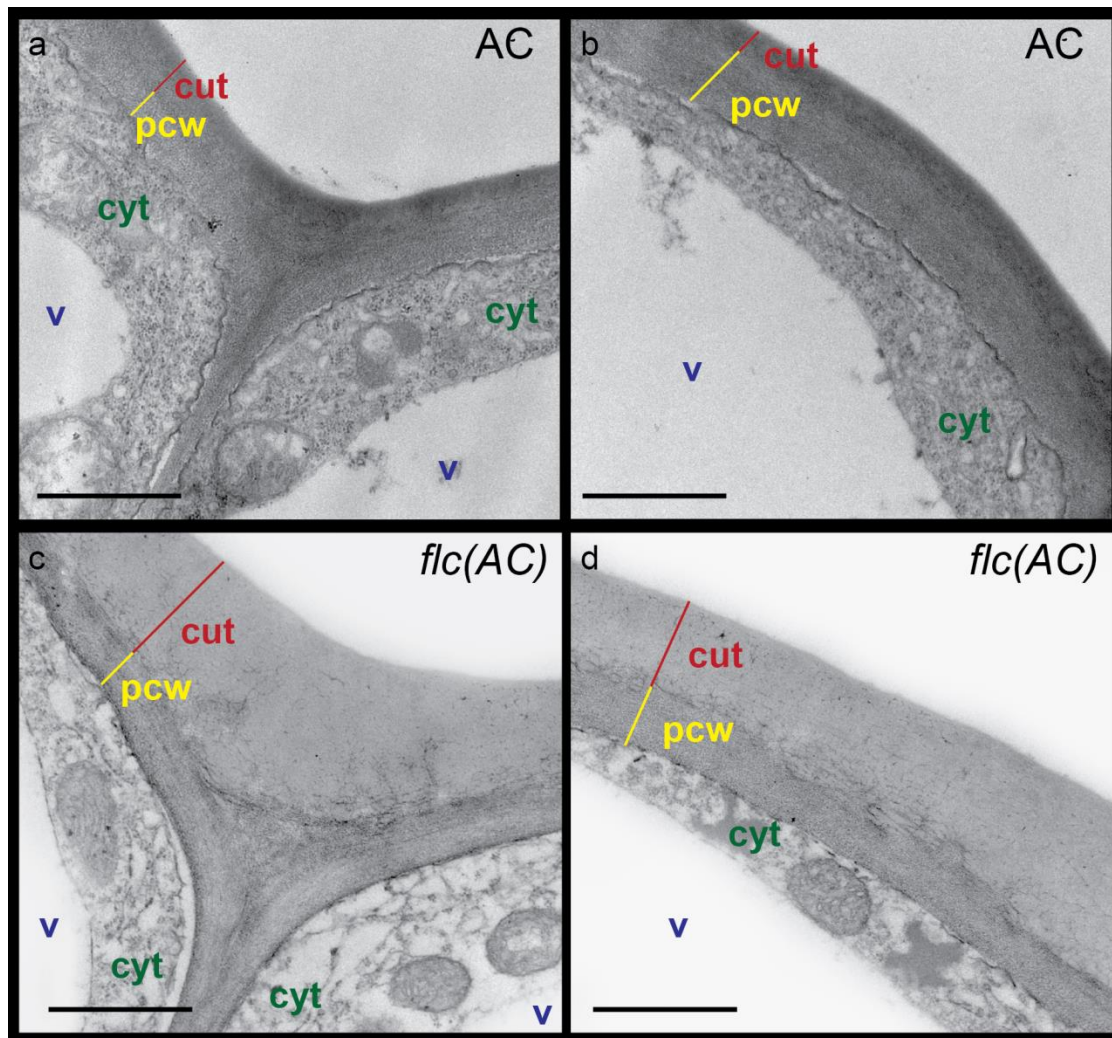


Figure 4.5. Transmission electron microscopy (TEM) micrographs of the cuticle of small expanding fruit outer epidermis. (a, c) Outer epidermal cell junction. (b, d) Outer periclinal wall of an epidermal cell. Mean diameters: AC, 13.46 mm; *flc(AC)*, 13.50 mm. Scale bars, 1 μ m. Cut, cuticle; pcw, polysaccharide cell wall; cyt, cytoplasm; v, vacuole.

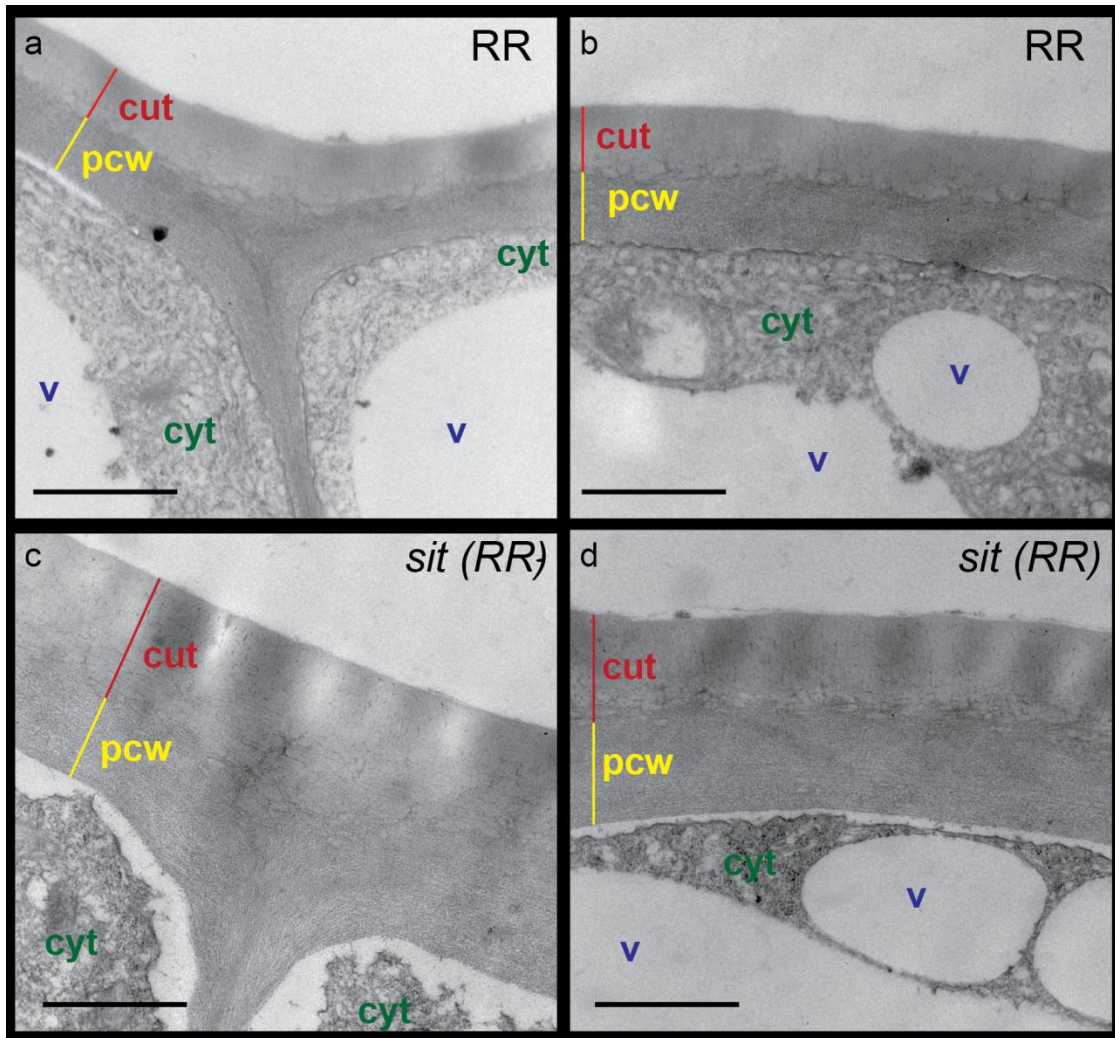


Figure 4.6. TEM micrographs of the outer cuticle of small expanding fruit. (a, c) Outer epidermal cell junction. **(b, d)** Outer periclinal wall of an epidermal cell. Mean diameters: RR, 13.66 mm; *sit(RR)*, 13.63 mm. Scale bars, 1 μ m. Cut, cuticle; pcw, polysaccharide cell wall; cyt, cytoplasm; v, vacuole.

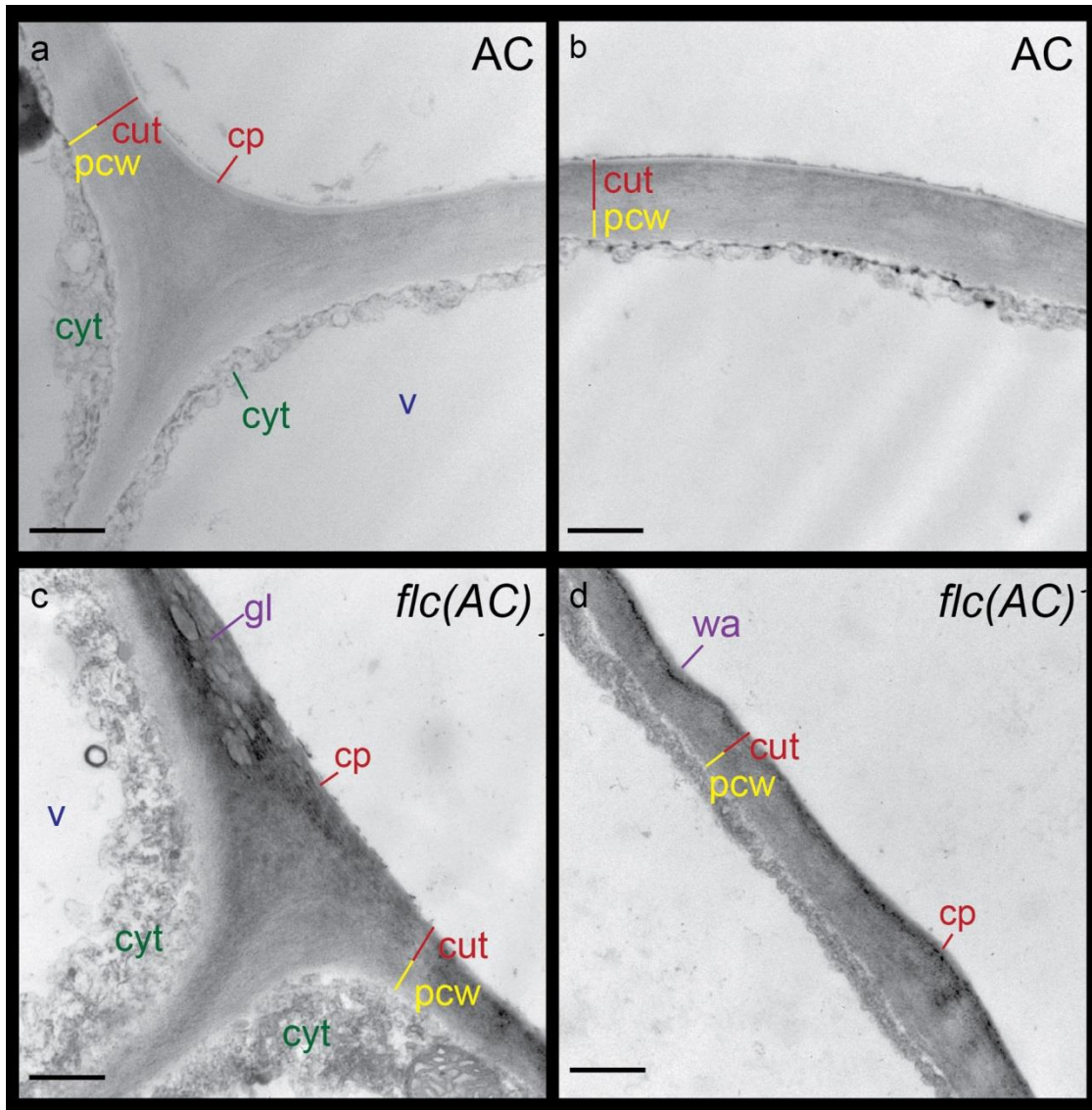


Figure 4.7. TEM micrographs of the cuticle of the adaxial epidermis of fully expanded leaflets. (a, c) Outer epidermal cell junction. (b, d) Outer periclinal wall of an epidermal cell. Scale bars, 500 nm. Cp, cuticle proper, cut, cuticular membrane; cyt, cytoplasm; gl, cuticular globules; pcw, polysaccharide cell wall; v, vacuole, wa, wavy cuticle.

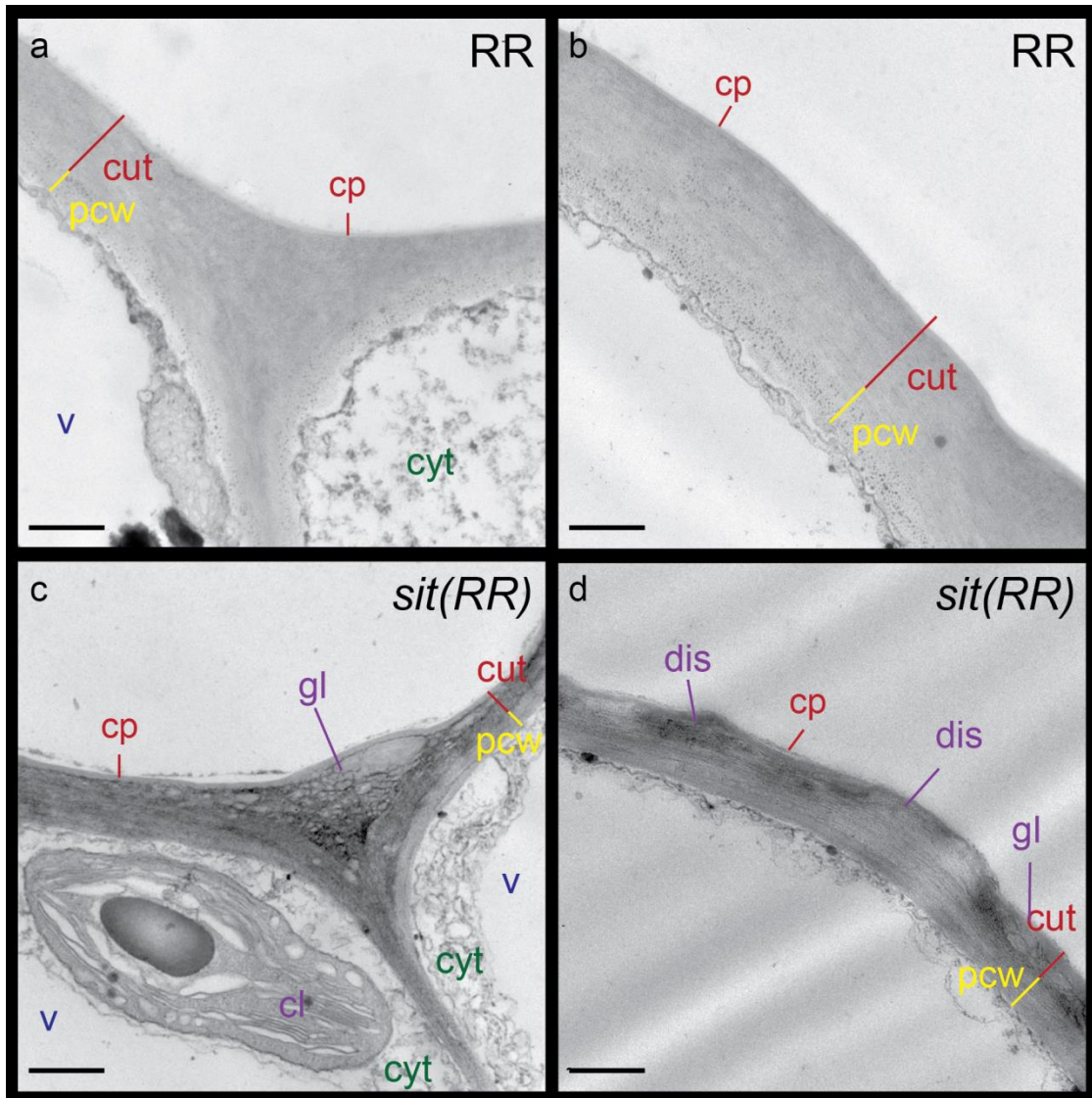


Figure 4.8. TEM micrographs of the cuticle of the adaxial epidermis of fully expanded leaflets. (a, c) Outer epidermal cell junction. (b, d) Outer periclinal wall of an epidermal cell. Scale bars, 500 nm. Cl, chloroplast; Cp, cuticle proper, cut, cuticular membrane; cyt, cytoplasm; dis, disrupted cuticle; gl, cuticular globules; pcw, polysaccharide cell wall; v, vacuole.

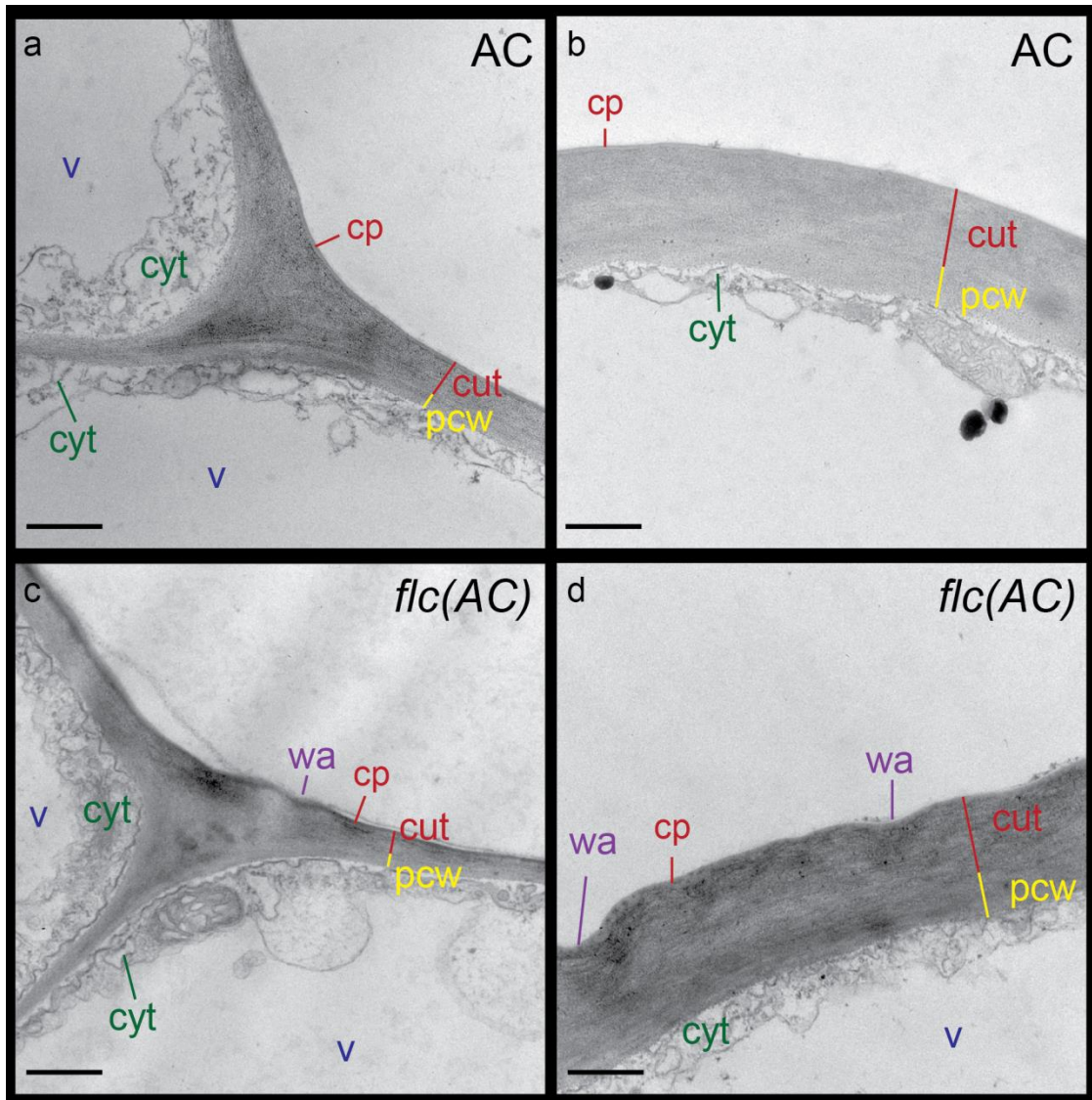


Figure 4.9. TEM micrographs of the cuticle of the abaxial epidermis of fully expanded leaflets. (a, c) Outer epidermal cell junction. (b, d) Outer periclinal wall of an epidermal cell. Scale bars, 500 nm. Cp, cuticle proper, cut, cuticular membrane; cyt, cytoplasm; pcw, polysaccharide cell wall; v, vacuole; wa, wavy cuticle.

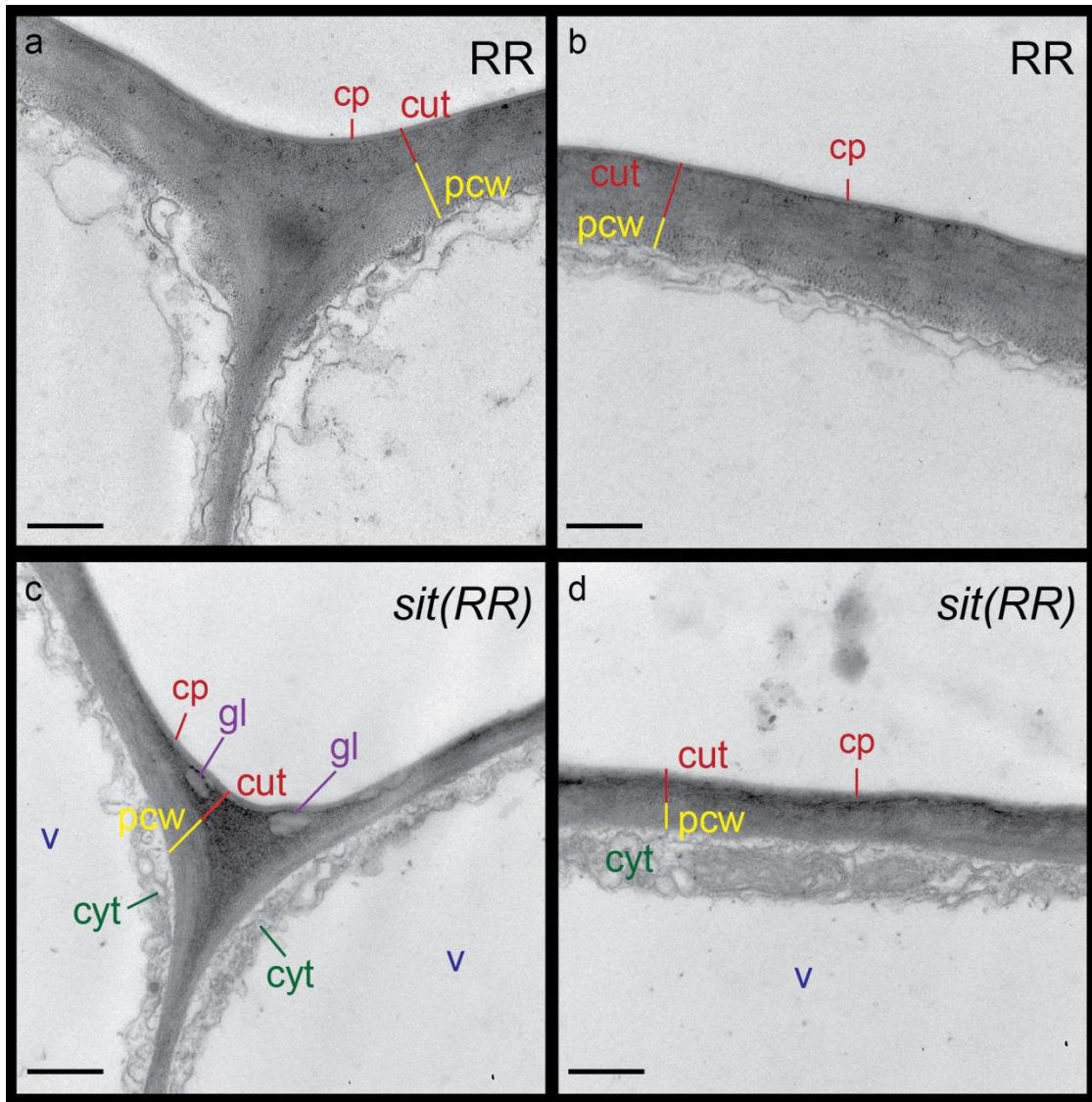


Figure 4.10. TEM micrographs of the cuticle of the abaxial epidermis of fully expanded leaflets. (a, c) Outer epidermal cell junction. (b, d) Outer periclinal wall of an epidermal cell. Scale bars, 500 nm. Cp, cuticle proper, cut, cuticular membrane; cyt, cytoplasm; gl, cuticular globule; pcw, polysaccharide cell wall; v, vacuole.

Light microscopy of the fruit cuticle of the ABA deficient lines

Light microscopy analyses of fruits of the same diameter (~26 mm), regardless of developmental age, further confirmed that the ABA-deficient fruit cuticles are thicker than those of the WT (Fig. 4.11). However, the WT fruits were substantially larger at maturity than those of the mutants, from which it may be concluded that WT fruits are at an earlier developmental stage than the mutant fruits when harvested at the same size for analysis. It may therefore be reasoned that the mutant fruits had more time to accumulate a cuticle, which might account for the thicker cuticle phenotype. The cuticles of Mature Green (MG) stage fruits were therefore analyzed to account for this issue, and it was observed that those of the mutants, from fruits at the same developmental stage, were penetrating further into subepidermal layers (Fig. 4.12).

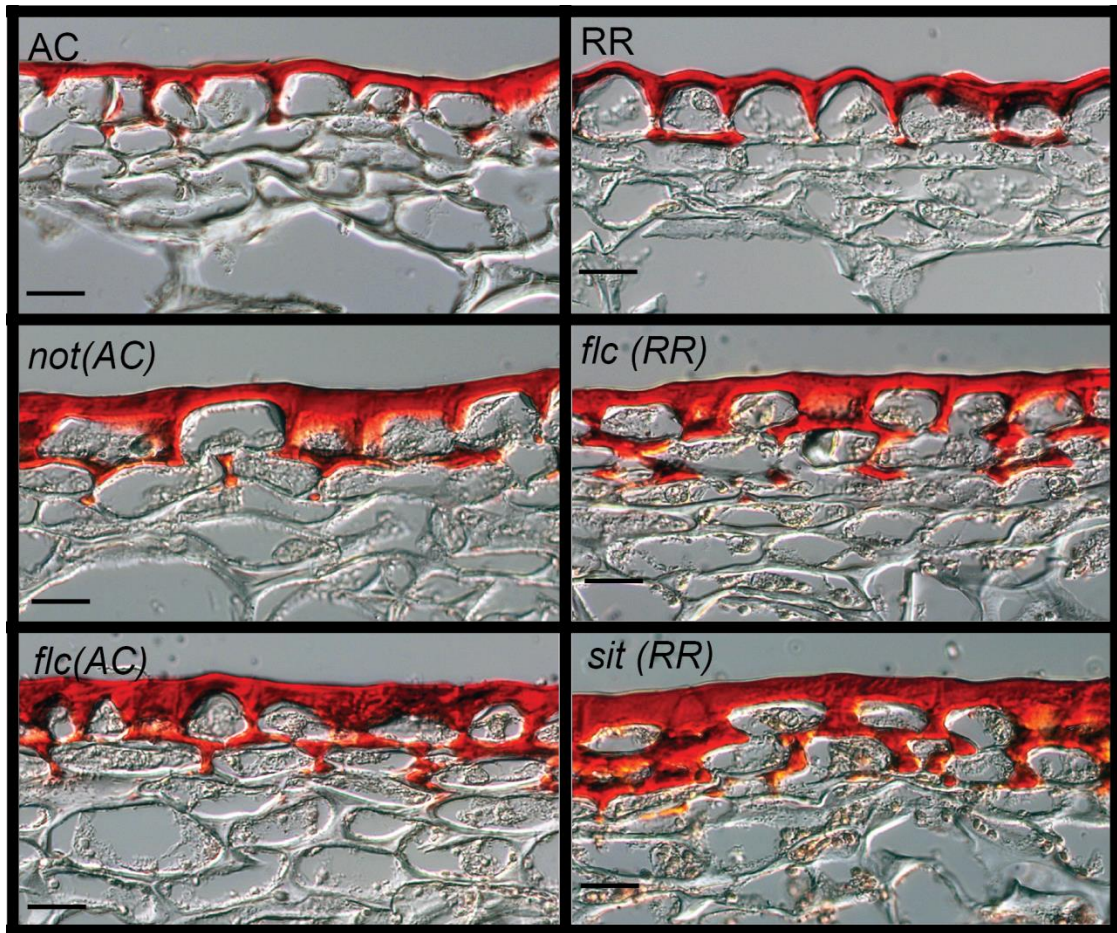


Figure 4.11. Micrographs of fruit cuticle. Light microscopy images of sections of similar size fruits. Mean diameters: AC, 26.26 mm; *not(AC)*, 26.21 mm; *flc(AC)*, 26.44 mm; RR, 25.85 mm; *flc(RR)*, 26.21 mm; *sit(RR)*, 26.50 mm. The cuticle is stained red with the Oil red O dye.

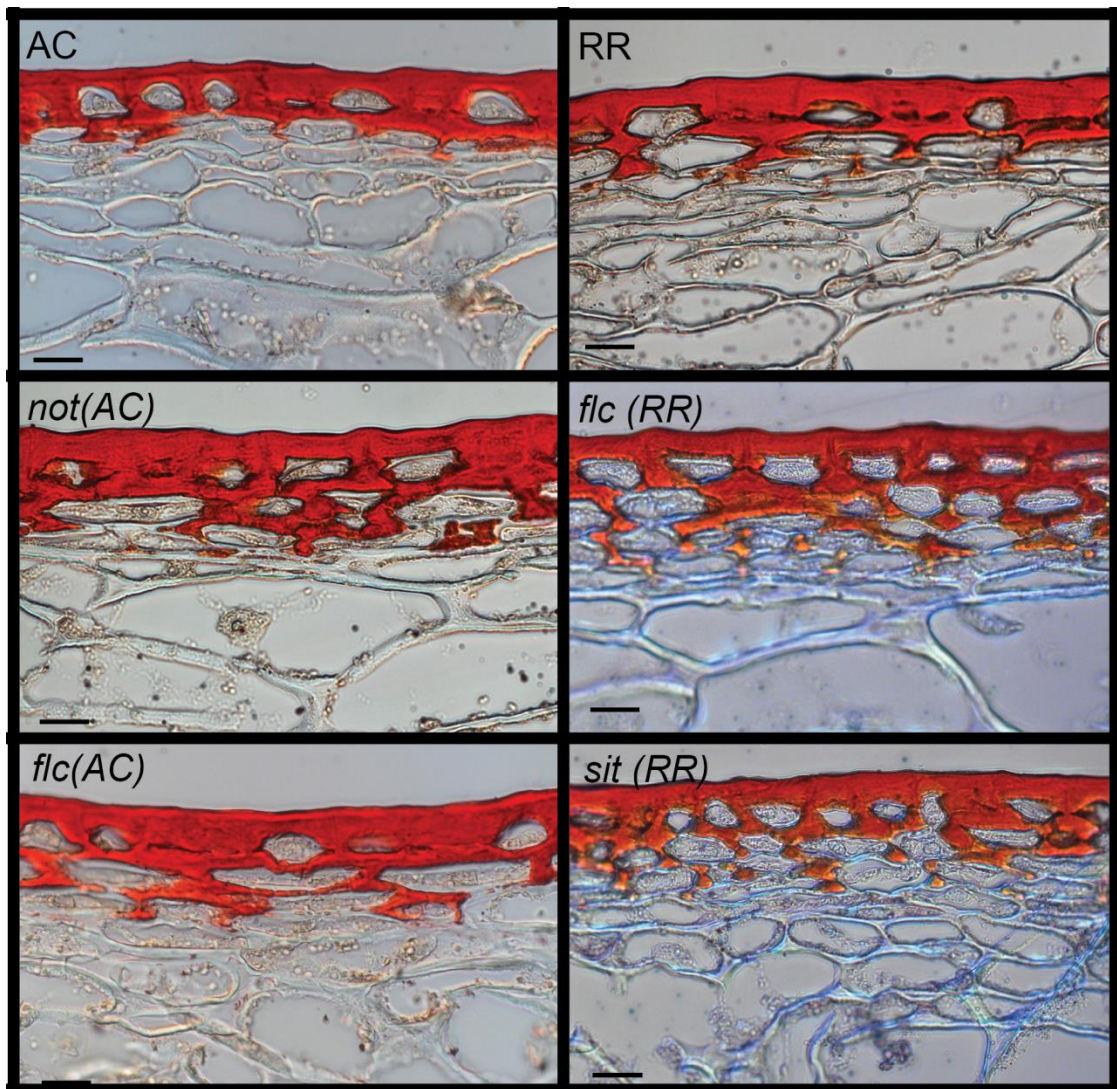


Figure 4.12. Micrographs of fruit cuticle. Light microscopy images of 6 μm thick sections of Mature Green stage fruits. Scale bars, 20 μm. The cuticle is stained red with the Oil red O dye.

Chemical analysis of cutin and wax coverage

A plausible explanation for the increased thickness of the MG fruit cuticles of the mutants compared to their WT is that it reflects an indirect effect of fruit size: the same amount of cuticle is synthesized and deposited in both mutants and WT fruits, but since the mutant fruit surface area is smaller, the resulting cuticular coverage is thicker. To test this hypothesis, a biochemical quantification of cutin coverage in MG fruits comparing cutin levels per μg^2 and per fruit was undertaken.

Unexpectedly, the increased cuticular thickness of the mutant fruits observed in micrographs was not confirmed by biochemical analysis (Fig. 4.11, 4.12 and 4.13AB). Indeed, the amounts of total identified cutin monomers per square cm of MG fruits were significantly higher for *not(AC)* and *flc(RR)* but not for the other mutants (Fig. 4.13B) and the expected increase of cutin coverage for the mutants compared to their WT was not seen for similar size fruits either (Fig. 4.13A). This discrepancy between microscopy imaging and chemical analysis may be explained by cuticular structure. Three-dimensional imaging of tomato fruit cuticle revealed the existence of subepidermal globules of cuticle detached from the main cuticle covering the epidermis (Buda *et al.*, 2009). Since the cuticle of the mutants penetrated further into subepidermal cells than those of the WTs, the amount of subepidermal globules could be substantially higher for the mutant genotypes. Therefore, it is possible that the lack of consistency seen between micrographs and chemical analysis results from the loss of detached subepidermal globules during cuticle isolation, although this idea has yet to be addressed experimentally.

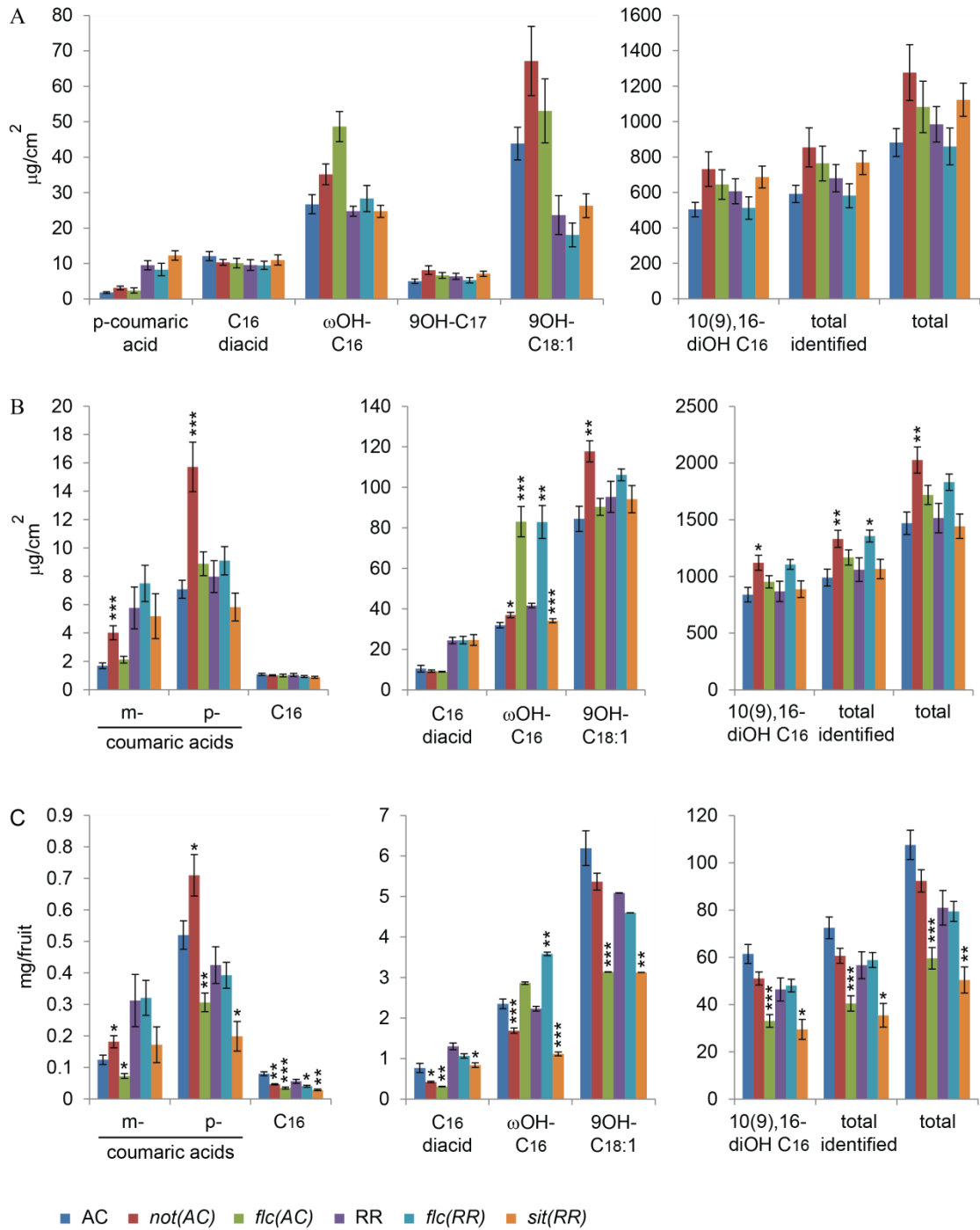


Figure 4.13. Analysis of ABA deficient mutant fruit cutin. (A) Cutin analysis of fruits of ~26 mm of diameter ($5 \leq n \leq 8$). (B) Amount of cutin monomers per cm^2 of MG fruits ($n = 7$). (C) Amount of cutin monomers per fruit of the same MG fruits as in (A) (average of 7 fruits). Significant differences between the mutants and their WT are given by a 2 tailed Student's t test with: * $\alpha = 0.05$; ** $\alpha = 0.01$; ***p-value < 0.001.

Despite this unexpected result, cutin coverage per fruit was assessed (Fig. 4.13C). The cutin coverage in WT, *not(AC)* and *flc(RR)* MG fruits was similar, but levels were significantly lower for *flc(AC)* and *sit(RR)* fruits (Fig. 4.13C). The fact that *flc(AC)* and *sit(RR)* were also the genotypes with the greatest fruit size difference compared with WT (Fig. 4.4) suggests that fruit size influences total amount of cutin per fruit. This relationship was further demonstrated in Fig. 4.14 which shows that there was no correlation between fruit size and cutin coverage per square centimeter (the P-value for this correlation is 0.2839; Fig. 4.14A), but that there was a clear correlation between fruit size and cutin coverage per fruit (the P-value for this correlation is 1.885e-09; Fig. 4.14B). This result suggests that cutin biosynthesis is co-regulated with epidermal cell expansion (the smaller size of the ABA-deficient mutant fruits is due to reduced cell expansion rather than a decrease of cell division (Rančić *et al.*, 2010; Nitsch *et al.*, 2012)), rather than each epidermal cell synthesizing a pre-determined amount of cutin.

Collectively, these results show no evidence for a cutin phenotype in ABA-deficient fruits.

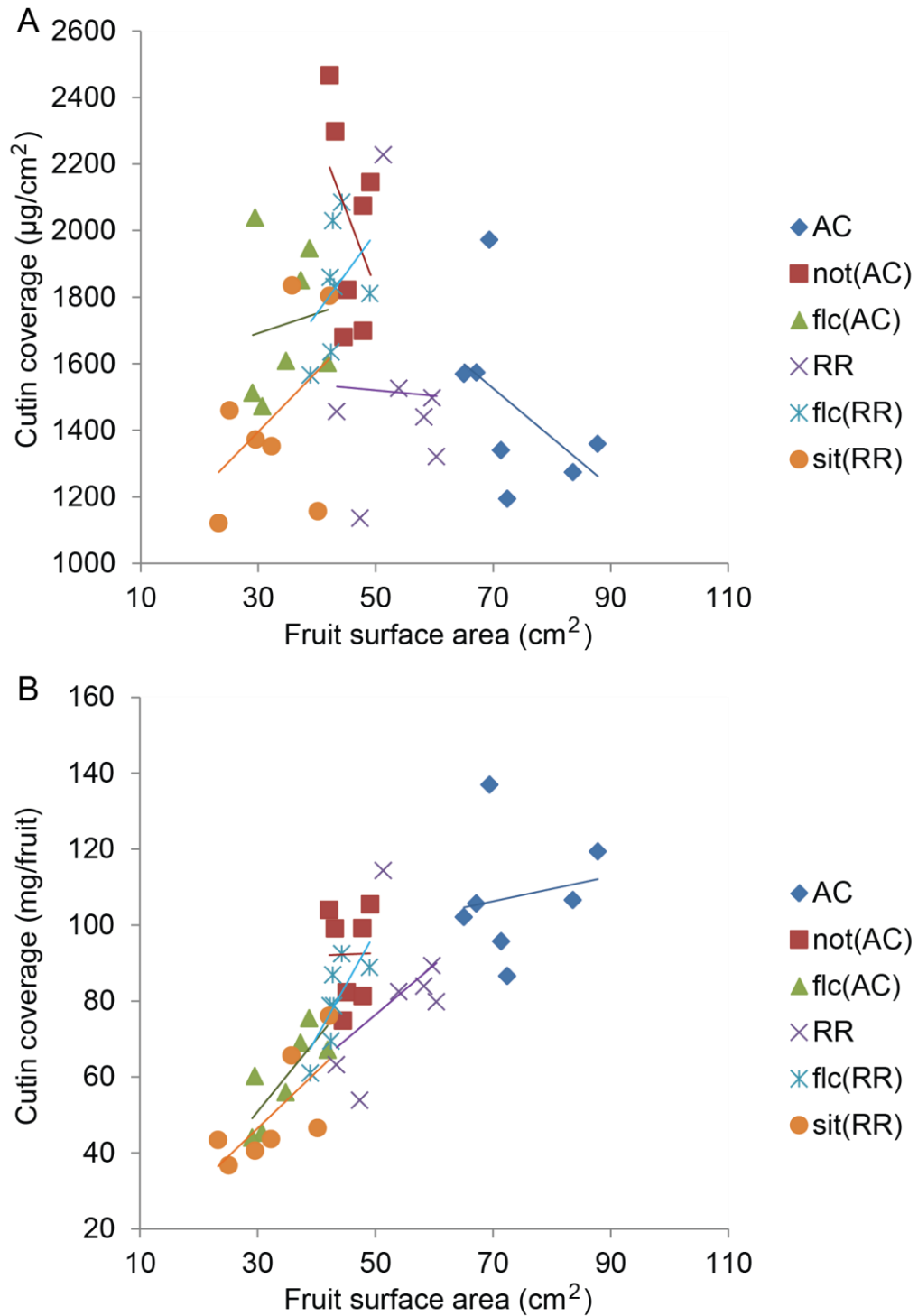


Figure 4.14. Relationship between MG fruit size and cutin coverage. (A) Total cutin coverage of MG fruits per square centimeter. **(B)** Total cutin coverage of MG fruits per fruit. Lines of correlations were drawn for each genotype.

Similarly, the total amounts of cuticular waxes of ~26 mm diameter fruits were greater for *not(AC)* only, with no clear trend when considering the wax species individually: no compound showed consistent and significantly different levels in the WT fruits compared with those of the four ABA mutants (Fig. 4.15A). Nevertheless, the variations of each compound are relatively well conserved between the ~26 mm diameter fruits and the MG fruits (Fig. 4.15AB). At the MG stage, the total amount of cuticular waxes per square cm was significantly different between the mutants and their respective WT genotypes, but again, this difference was not consistent among the mutants since this amount was higher for *not(AC)* and *flc(RR)* while lower for *flc(AC)* and *sit(RR)* (Fig. 4.15B). However, the levels of waxes per fruit were substantially reduced for most compounds in each of the mutants, consistent with the fact that the mutant fruits are smaller (Fig. 4.15C). Interestingly, the trends of the total accumulation of cuticular waxes mirror very well those for cutin suggesting a close relationship between cutin and wax biosynthesis regulation (Figs. 4.13ABC, 4.15ABC).

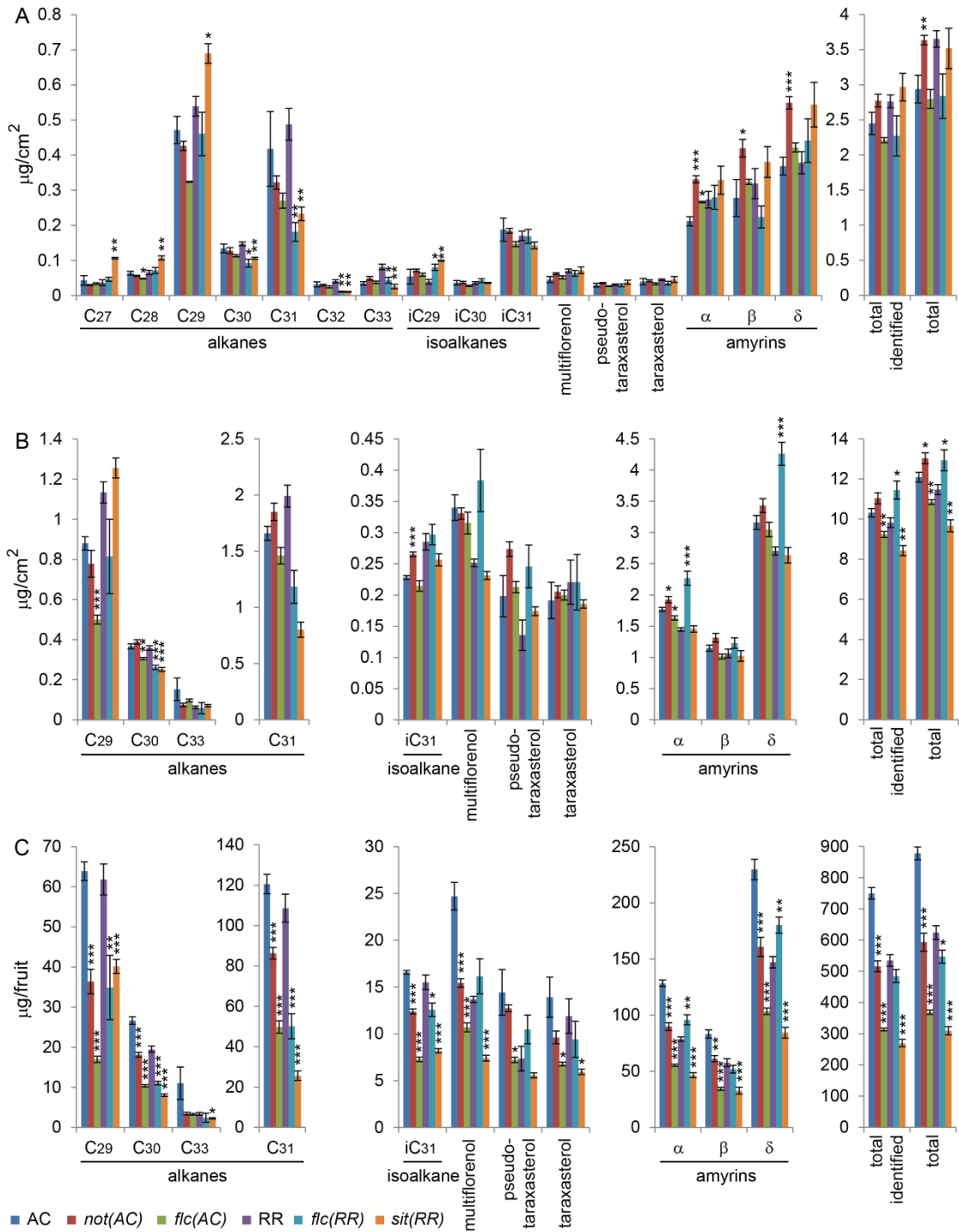


Figure 4.15. Analysis of fruit cuticular waxes in ABA deficient mutants. (A) Wax analysis of ~26 mm diameter fruits (2 fruits per pool, $3 \leq n \leq 5$). **(B)** Amount of cuticular wax of MG fruits per cm^2 (4 fruits per pool, $n = 5$). **(C)** Amount of cuticular wax of MG fruits per fruit (average of 4 fruits, $n = 5$). Differences between the

mutants and their WT were assessed using a 2 tailed Student's *t* test with: * $\alpha = 0.05$; ** $\alpha = 0.01$; *** p -value < 0.001.

Leaf cutin analysis revealed consistently lower levels of coumaric acids isomers, caffeic acid and 10(9),16-dihydroxyhexadecanoic acid in the mutants, but cutin coverage was reduced for *flc(AC)* and *sit(RR)* only (Fig. 4.16). Phenolic compounds (i.e. ferulate, caffeate, coumarate) have previously been detected in cutin of leaf, but high levels, as it is the case in this experiment could reflect some aspect of the growth condition such as biotic or abiotic stresses (Fig. 4.16; Richmond and Martin, 1959).

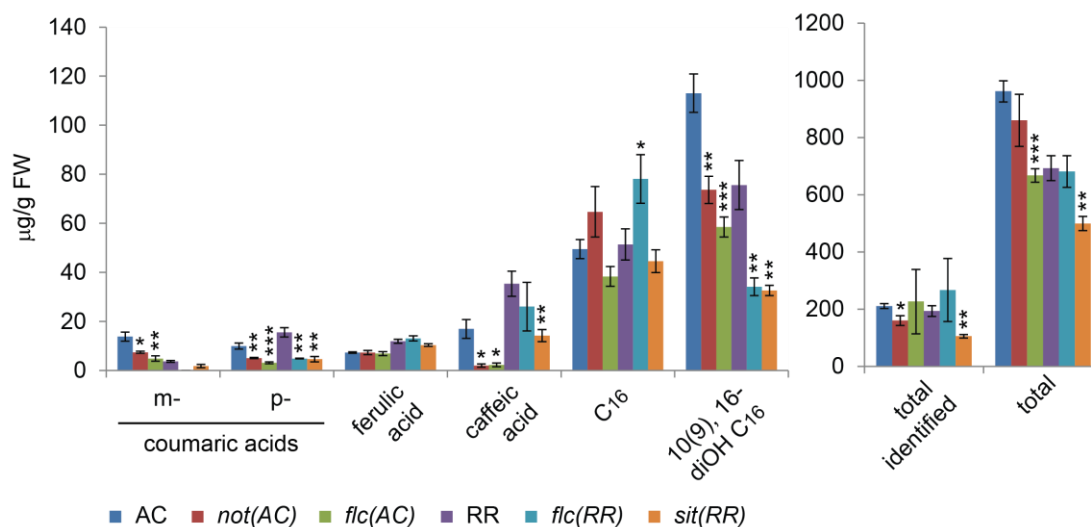


Figure 4.16. Leaf cutin analysis of ABA deficient lines. $n = 6$. Significant differences between the mutants and their WT are given by a 2 tailed Student's *t* test with: * $\alpha = 0.05$; ** $\alpha = 0.01$; *** p -value < 0.001.

The levels of most wax species were consistently higher in the mutants (alkanes of chain length from C_{27} to C_{30} , and isoalkanes from C_{29} to C_{31}) but levels of

the predominant compound, hentriacontane (C_{31}), are lower, resulting in an overall decrease of wax coverage for *flc(AC)* and *sit(RR)* (Fig. 4.17). The decrease of hentriacontane occurs in fruit waxes as well but the increase of the other waxes does not clearly happen in fruit. It has previously been reported that the composition of cutin and wax may vary between organs (Martin *et al.*, 2014) and so, the differences of cuticular composition between fruits and leaves could result from regulatory variations.

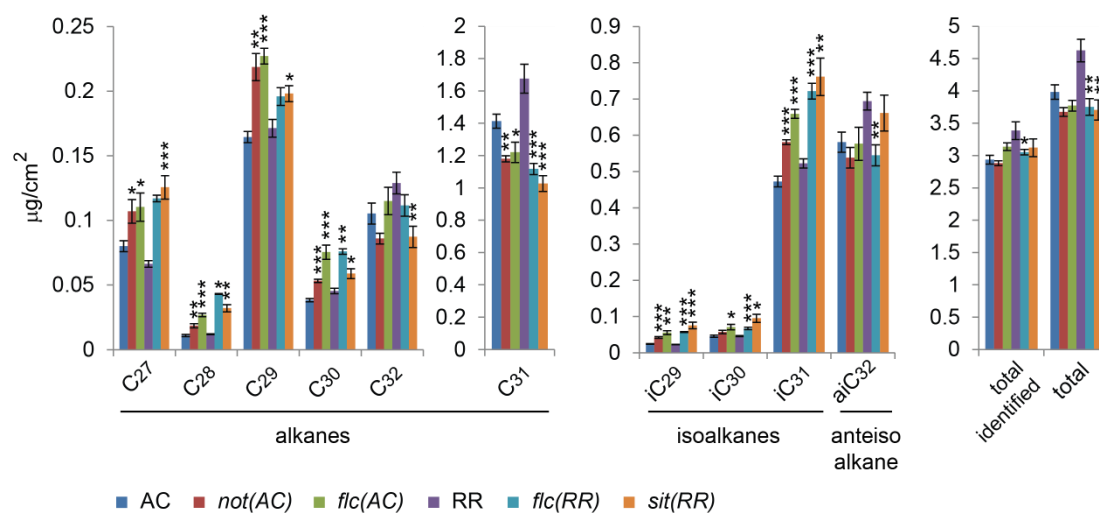


Figure 4.17. Analysis of leaf cuticular waxes from ABA deficient mutants. $n = 5$. Significant differences between the mutants and their WT are given by a 2 tailed Student's t test with: * $\alpha = 0.05$; ** $\alpha = 0.01$; *** p -value < 0.001 .

Effect of ABA application on ABA deficient leaves

Application of ABA to WT leaves resulted in an increase in cutin coverage in those of AC but not the RR genotype (Fig. 4.18). The coumaric acid isomers were nevertheless increased for both sprayed WT, with a higher effect in AC. The coumaric, caffeic and 10(9),16 dihydroxyhexadecanoic acids are lower in the mutants, consistent with the results of Fig. 4.16. Spraying ABA on the mutants provoked an increase of most of the compounds affected by ABA deficiency, arguing for a partial rescue of the phenotype (Fig. 4.18).

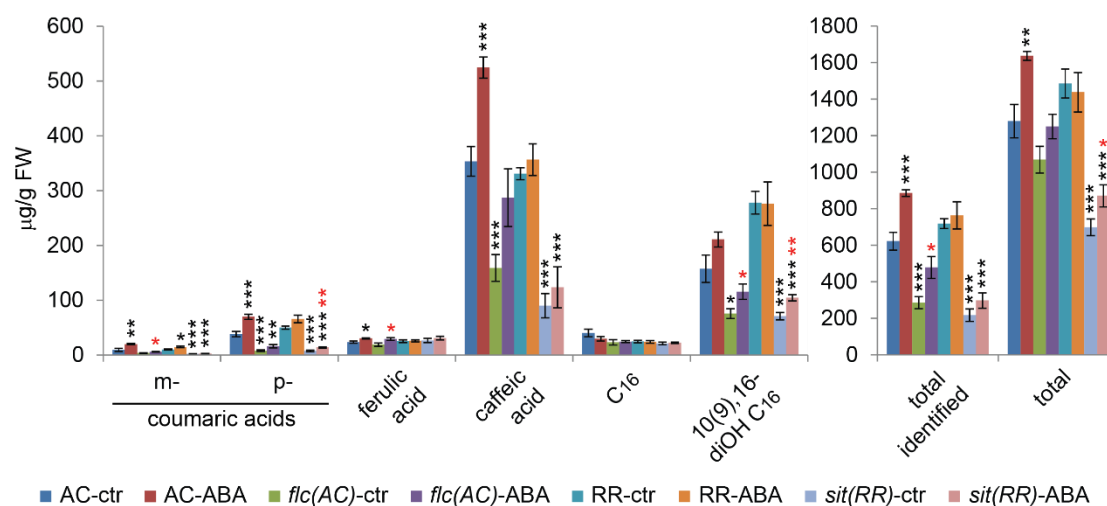


Figure 4.18. Leaf cutin phenotype is partially rescued by ABA application. Black and red stars represent statistical differences with WT-ctr and with mutant-ctr respectively. -ctr, plants were sprayed with H₂O + 0.1% ethanol; -ABA, plants were sprayed with 100 µM ABA. * $\alpha = 0.05$; ** $\alpha = 0.01$; *** p -value < 0.001. n = 6.

The increase of the alkane C_{27} , and the isoalkanes iC_{29} , iC_{30} and iC_{31} in the mutants, along with the decrease of hentriacontane, is verified in this experiment but the higher concentration of the samples permitted additional compounds to be identified: while the isoalkane iC_{33} is more abundant in the mutants, they are depleted in numerous other compounds: the alkane C_{33} , the anteisoalkane aiC_{32} , amyriols and taraxasterol, showing a clear but contradictory effect of ABA deficiency (Fig. 4.19). The effect of spraying ABA on the WTs was nearly non-existent which was not expected as the alkanes have been shown to be responsive (Kosma *et al.*, 2009). The ABA-deficient line phenotype being partially rescued only, it is possible that the amount of ABA penetrating the leaves was not enough to induce the expected increase of alkanes. The application of ABA did not fully restore the normal amount of waxes but partially rescued the increased (for the alkane C_{27} and the isoalkanes of chain length from C_{29} to C_{31}) and the decreased (for the alkanes of chain length from C_{31} to C_{33} , the anteisoalkane aiC_{32} , amyriols and taraxasterol) waxes in at least one of the mutants. Furthermore, the total amount of waxes, which is lower in the mutants, is significantly higher for the sprayed mutants (Fig. 4.19).

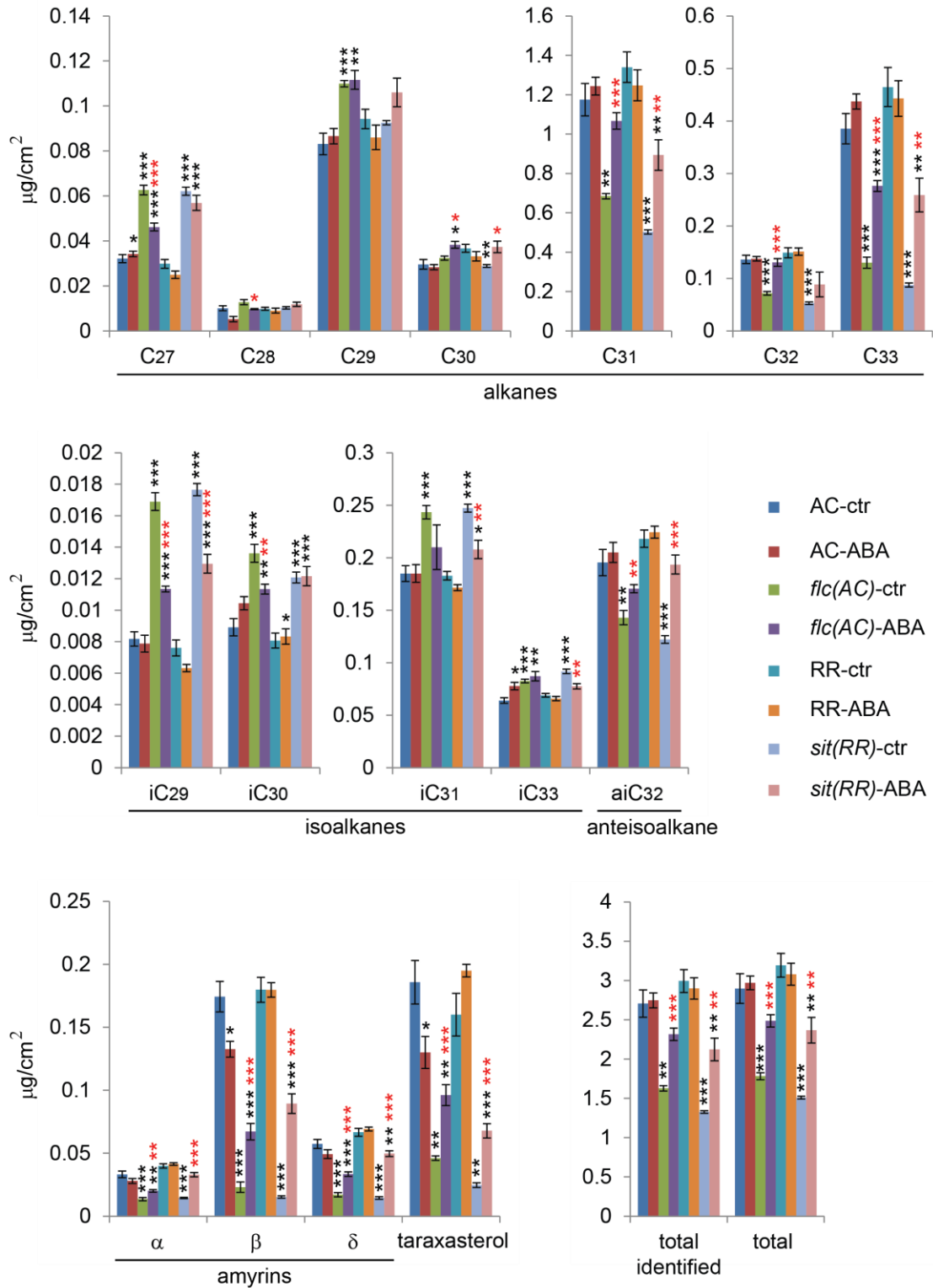


Figure 4.19. Leaf wax phenotype is partially rescued by ABA application. Black and red stars represent statistical differences with WT-ctr and with mutant-ctr

respectively. –ctr, plants were sprayed with H₂O + 0.1% ethanol; -ABA, plants were sprayed with 100 µm ABA. * α = 0.05; ** α = 0.01; ***p-value < 0.001. n = 5.

The cuticular pathway is down-regulated in the ABA deficient lines

ABA deficiency results in complex variations of cuticular wax composition and in a decrease of the levels of various cutin monomers, at least in leaf. Cuticular gene expression was tested to determine if these variations result from a differential regulation of the cuticle pathway. Fig. 4.20A shows that the majority of the surveyed genes, involved in cutin and/or wax monomer biosynthesis and transport, are less expressed in the mutant backgrounds. In particular, the expression of *CUS1*, *CD3*, *GPAT4* and *GPAT6*, which are crucial for cutin monomers formation and polymerization into the cutin matrix (Isaacson *et al.*, 2009; Yang *et al.*, 2012), is substantially lower in the ABA deficient mutants compared to the WTs (Fig. 4.20A). Additionally, the expression of wax biosynthesis genes, such are *CER3* or *CER6*, and of the transporters of both cutin and wax monomers (*WBC11* and *WBC12*), is also substantially lower in the mutants compared to those of the WTs (Fig. 4.20A). The only gene with a significant increase of expression in the mutants is *CER4*, an alcohol-forming fatty acyl-coenzyme A reductase particularly important for primary alcohols and wax esters (Rowland *et al.*, 2006). Primary alcohols and wax esters are not massively accumulated in tomato so they were not identified in the samples and therefore, a possible phenotype was not identified. This overall decrease of expression of wax and cutin related genes in the ABA-deficient mutants correlates with the decrease of expression of three transcription factors known to regulate cuticle

formation: *MYB41*, *MYB30/96* and *MYB16/106* (the same tomato gene is the closest homolog of both *MYB30* and *MYB96*, the same holds true for *MYB16* and *MYB106*; Fig. 4.20B).

The cuticular gene expression in 15 days post anthesis (dpa) fruits follows a similar pattern than the one of leaf (Fig. 4.21A) although the reductions in expression are less significant as a whole and no difference was seen for the transcription factors (Fig. 4.21B). This could explain the lack of phenotype seen in the TEM pictures and the inconsistent differences of wax and cutin monomers accumulation between the mutants and their WT. However, the lack of clear gene expression differences could also be explained by the high abortion rate of the mutant flowers making it extremely difficult to obtain enough material for 3 biological replicates. Consequently, the material was harvested on plants grown months apart in different greenhouse rooms, by different people. Despite these limitations, *CER4* is still more expressed in the mutants and numerous other cuticular genes are less expressed as seen in leaf (*CUS1*, *CD3*, *CYP77A6*, *GPAT6*, *WBC12*, *CER3*).

This gene expression analysis suggests that ABA deficiency triggers a down-regulation of the cuticle pathway, at least in leaf, consistent with the idea that ABA regulates cuticle formation.

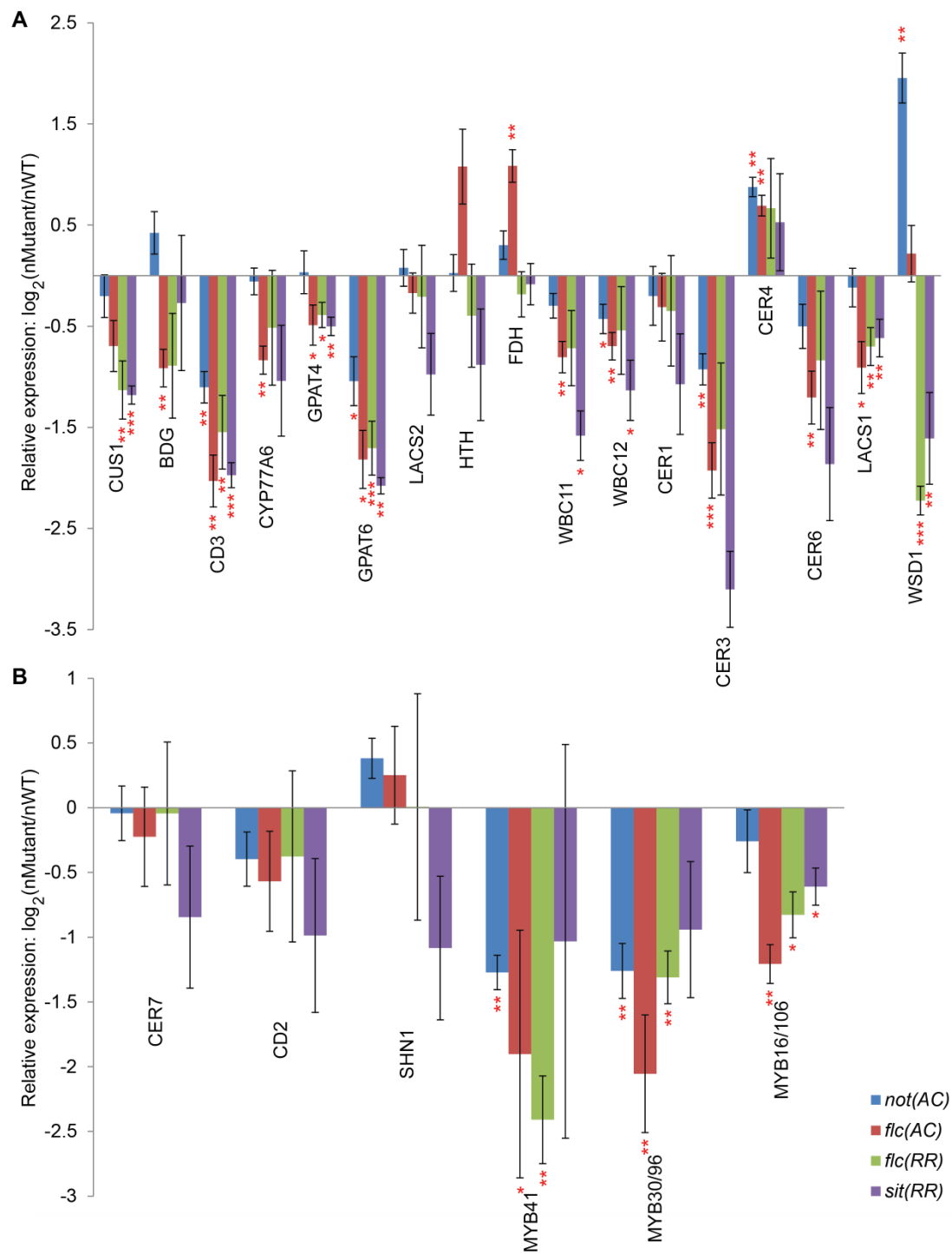


Figure 4.20. Cuticular gene expression in developing leaf of ABA deficient lines. (A) Expression of genes implicated in cutin and wax biosynthesis. (B) Expression of genes implicated in the regulation of cuticle biosynthesis. Leaf size < 2 cm. nMutant and nWT, gene expression normalized with RPL2.

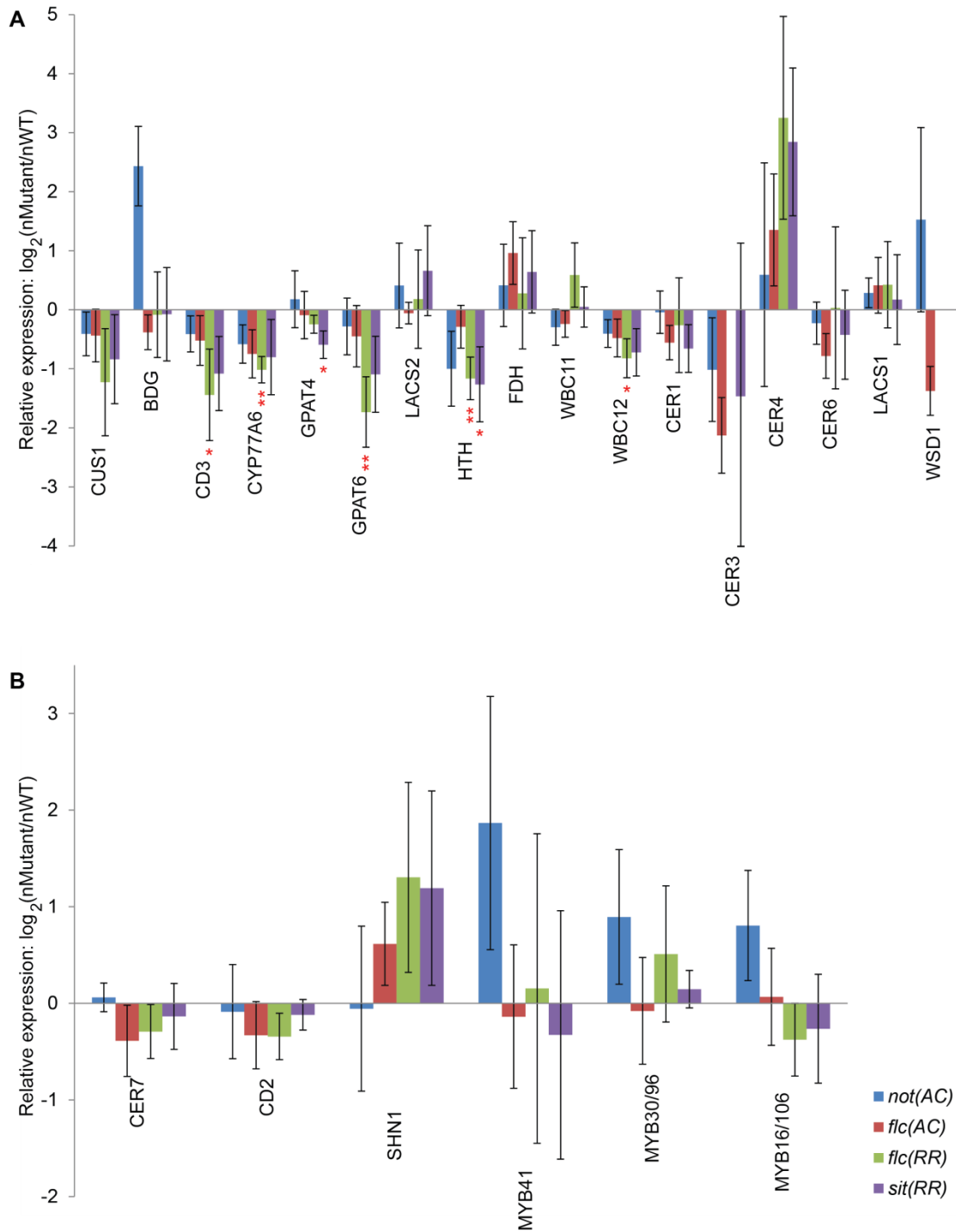


Figure 4.21. Cuticular gene expression in 15 dpa fruit of ABA deficient lines. (A) Expression of genes implicated in cutin and wax biosynthesis. **(B)** Expression of genes implicated in the regulation of cuticle biosynthesis. nMutant and nWT, gene expression normalized with RPL2. CER3-*flc(RR)*, WSD1-*flc(RR)* and *sit(RR)* were removed from plot due to error bar size.

ABA deficiency affects the water and pathogen barrier functions of the cuticle

Preventing pathogen attacks is one of the fundamental functions of the plant cuticle and changes in susceptibility to pathogens have been reported for numerous cuticular mutants (Bessire *et al.*, 2007; Chassot *et al.*, 2007; Tang *et al.*, 2007; Isaacson *et al.*, 2009; Voisin *et al.*, 2009). To assess the impact of the structural and compositional changes of the ABA-deficient mutant cuticles, susceptibility of leaf and fruit to the fungus *Botrytis cinerea* was assessed. The abaxial side of leaflets was inoculated with fungal spores and the level of susceptibility was measured 4 days later by counting lesions larger than the original inoculation site (Fig. 4.22A). Both WT's showed a high susceptibility to the fungus with 100% inoculated leaflets having a spreading lesion. The mutants showed a reduced susceptibility with *not* being intermediate (60% of spreading lesions) and *flc* and *sit* having the lowest infection rates (33% for *sit(RR)*, 30% for *flc(AC)*, and 0% for *flc(RR)*). This experiment was repeated on the adaxial side of the leaf to test if the presence of stomata influences the results (Fig. 4.22B). The percentage of infection was again much lower for the mutants, suggesting that the stomata do not influence the differential rate of infection. To further test this phenotype, Red fruits susceptibility was tested. To increase the chance of *Botrytis* to be able to penetrate the thick cuticle of the fruits, a higher percentage of glucose was added to the inoculation solution and an extremely high number of sporangia was used to infect the fruits. The ABA-deficient lines were, as a whole, significantly less susceptible to *Botrytis* than their respective wild-type with

not being intermediate (60% of infection at 3 weeks post inoculation (wpi)) and *sit* being the most resistant with no fruit infected at 3 wpi (Fig. 4.22B).

The wilted phenotype of the ABA deficient mutants is attributed to their inability to prevent water loss by stomatal closure (Tal, 1966). Nevertheless, water loss through leaf cuticle has been found to be slightly higher in the three mutants (Tal, 1966) and a clear increase of *sit* leaf cuticle permeability has been reported before (Curvers *et al.*, 2010). To further investigate if cuticular permeability is higher in the ABA-deficient lines, the water loss of Red fruits, which lack stomata, was monitored under controlled conditions. The results mimic the pathogen susceptibility results with the mutants being more resistant to water loss than their respective WT, *not* having an intermediate phenotype and *flc* and *sit* significantly losing less water. Such a phenotype is opposite of what would be expected based on the leaf permeability experiments, but could be explained by the apparent increased thickness of the mutants' cuticle.

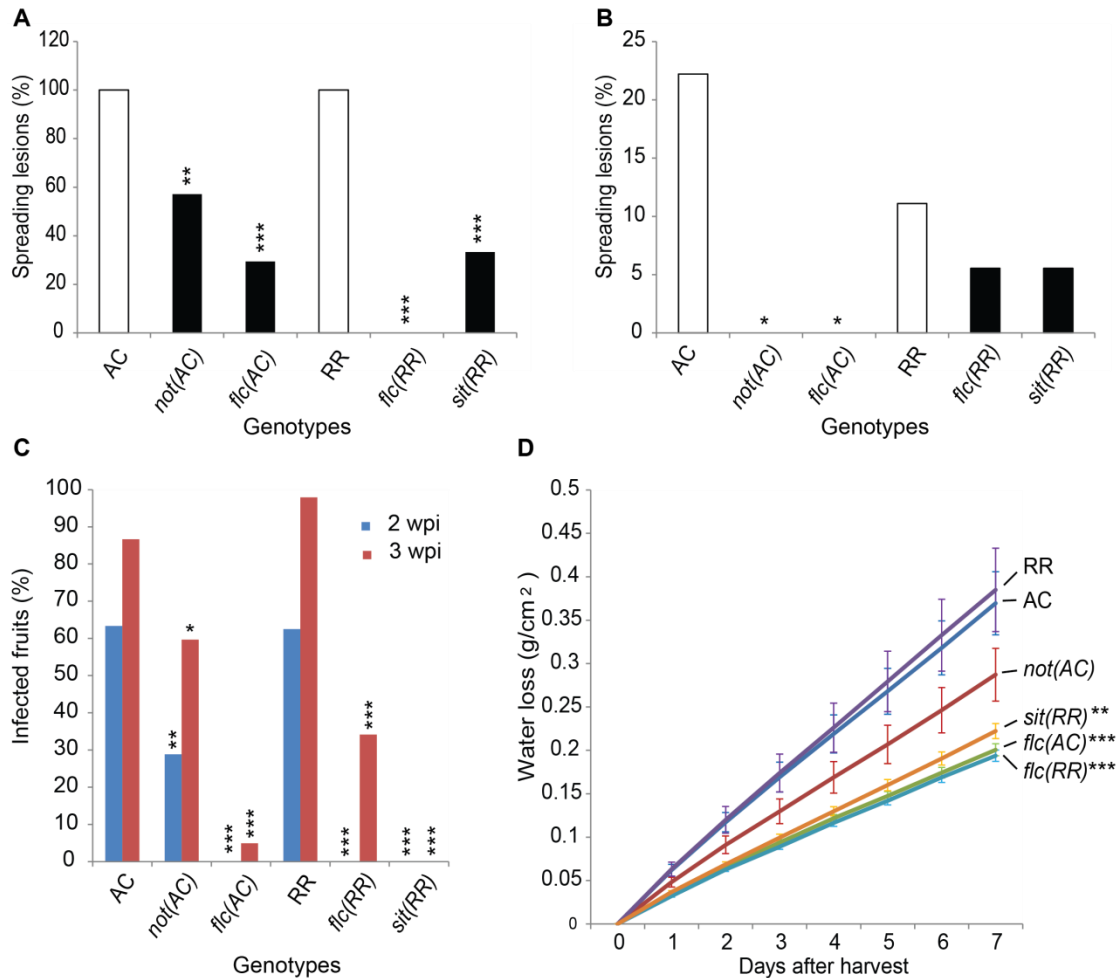


Figure 4.22. ABA deficient line sensitivity to the fungus *Botrytis cinerea* and fruit cuticular permeability. (a) Percentage of infected leaflets 4 days after inoculation of the abaxial side with *Botrytis cinerea* spores ($12 \leq n \leq 18$). (b) Percentage of infected leaflets 7 days after inoculation of the adaxial side with *Botrytis cinerea* spores. (c) Percentage of infected Red fruits 2 and 3 weeks after deposition of *Botrytis cinerea* spores. (d) Analysis of cuticular transpirational water loss of Red fruits ($75 \leq n \leq 86$). * $\alpha = 0.05$; ** $\alpha = 0.01$; *** $p < 0.001$. wpi, weeks after inoculation.

Cutin deficiency does not affect ABA accumulation in leaf.

Down-regulation of ABA biosynthesis and signaling has been reported for some cutin deficient mutants in *Arabidopsis* (Wang *et al.*, 2011). To test if a similar

phenotype is observed in tomato, three different cutin deficient (*cd*) mutants were used: *cd1* has a mutation in *CUS1*, which encodes for a cutin synthase required for cutin polymerization (Yeats *et al.*, 2012), *cd3* has a mutation in *CYP86A69* which is a fatty acid hydroxylase important for cutin monomer biosynthesis (Shi *et al.*, 2013) and *cd2* and *pe* have a mutation in a HD-ZIP IV transcription factor (Isaacson *et al.*, 2009; Nadakuduti *et al.*, 2012). The cutin layer of these mutants is reduced by ~95% in fruit and it has been verified that *pe* has a reduced cutin layer in leaf as well (Isaacson *et al.*, 2009; Nadakuduti *et al.*, 2012). Only *pe* had a statistically different amount of ABA but ABA levels were higher instead of being lower as expected (Fig. 4.23). These specific mutations did not trigger a down-regulation of the ABA pathway.

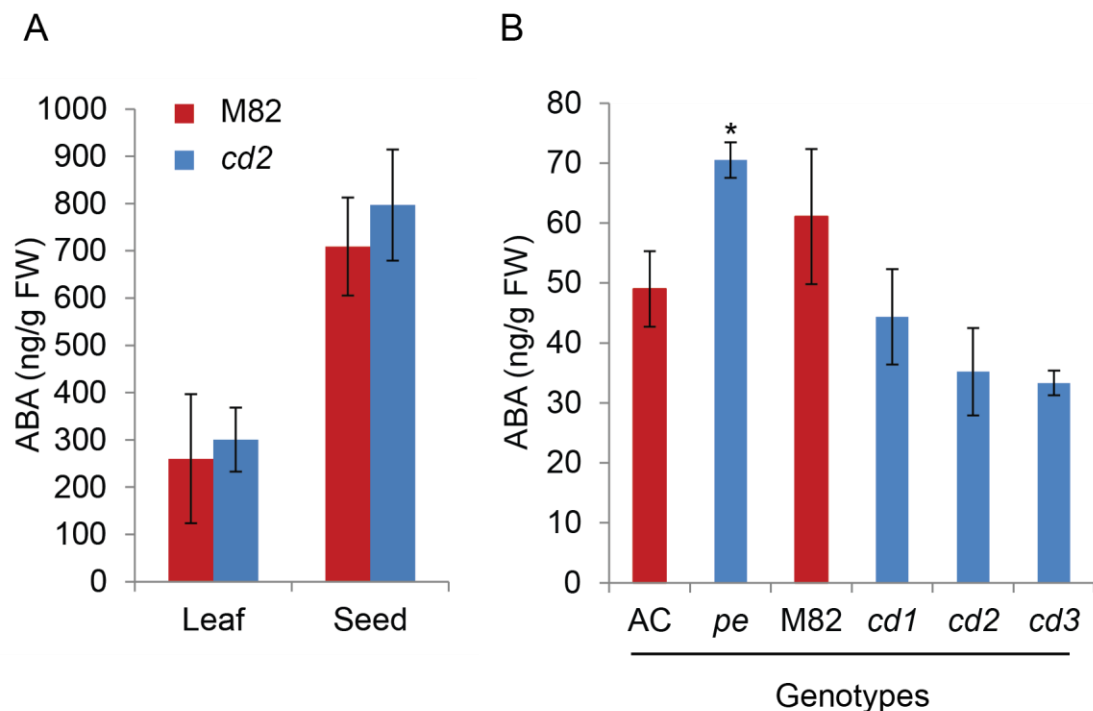


Figure 4.23. ABA content in some tomato cutin deficient mutants. (A) ABA content in emerging leaf and mature seed of *cd2* mutant. (B) ABA content in emerging leaf. *pe*, *sticky peel*; *cd*, *cutin deficient*. The discrepancy between the scales of A and B

could result from a change of sensitivity of the GC-MS/MS over-time. This difference did not affect the relative abundance of the samples.

Discussion

ABA deficiency affects plant development

The results presented in this study show that ABA deficient plants are smaller than WT. The reduction in size of the organs of ABA deficient plants is a consequence of reduced levels of ABA, independent of the effects on the plant water balance, and is at least partially attributable to higher ethylene levels (Tal *et al.* 1979; Sharp *et al.*, 2000; Nitsch *et al.*, 2012). It has been hypothesized that ABA has a negative effect on ethylene production, resulting in increased cell expansion during tomato fruit ontogeny (Nitsch *et al.*, 2012) and enhanced root elongation (Spollen *et al.*, 2000). In addition, other phenotypes of the ABA-deficient plants, such as leaf epinasty (Fig. 4.3) and adventitious rooting on stems have been attributed to an excess of ethylene (Sharp *et al.*, 2000). However, the leaf epinasty phenotype seen in the ABA-deficient mutants can be compared to the leaf deformation often associated with impaired cuticle, as is the case with the *Arabidopsis* *bdg*, *fiddlehead (fdh)* and *lcr* mutants (Voisin *et al.*, 2009). It is therefore possible that cuticular defects result in an ABA/ethylene imbalance, in turn affecting leaf shape. In fact, ABA biosynthesis and signaling are repressed in a number of cutin mutants, including *bdg* and *lcr* (Wang *et al.*, 2011).

The presence of chloroplasts was detected in the fruit epidermis of *sit*, which is unusual. However, an increase of size and number of plastids has previously been

reported for *flc* and *sit*, as well as *high pigment 3 (hp3)*, another tomato ABA deficient mutant: The number of plastids was doubled in MG fruits of *hp3* and they were 30% larger (Galpaz *et al.*, 2008). The number of plastids of *flc(RR)* and *sit(RR)* was also found to be increased (by 36% and 59% respectively, Galpaz *et al.*, 2008), perhaps as an attempt from the plant to increase ABA production.

ABA is a key regulator of cuticle biosynthesis

The results presented in this study suggest that ABA enhances cutin formation during leaf development regardless of environmental cues. Indeed, several cutin components accumulated less in the leaves of ABA deficient mutants than in those of the WTs. Furthermore, ABA application successfully increased the levels of the main tomato cutin monomer, 10-16,dihydroxyhexadecanoic acid, for the two tested mutants (*flc(AC)* and *sit(RR)*) and failed to significantly increase the WT levels of this monomer. Consequently, ABA is required for the formation of WT levels of cutin but increased amounts of ABA, as seen in response to water stress, do not result in increased cutin levels. Application of exogenous ABA on Arabidopsis plants have previously been shown not have an effect on WT cutin levels (Kosma *et al.*, 2009), supporting the hypothesis that ABA does not act as an environmental regulator of cutin synthesis.

Similarly, no difference of wax composition was consistently seen for the two sprayed WTs. This result was less expected since ABA treatment led to an increase of alkanes in Arabidopsis (Kosma *et al.*, 2009). It is possible that the amount of ABA penetrating the leaf was not sufficient to trigger such response. However, this

treatment partially rescued the wax phenotype of the ABA-deficient lines indicating that the ABA deficiency is responsible for it and that ABA is required for cuticular wax deposition during leaf ontogeny. Despite a general decrease of wax-related gene expression (at the exception of *CER4*), ABA deficiency results in an increase of the alkanes from C₂₇ to C₃₀ and of the isoalkanes from C₂₉ to C₃₁. On the contrary, longer chain alkanes (C₃₁ and C₃₃), but also the anteisoalkane C₃₂, amyryns and taraxasterol are less abundant in the mutants. Longer chain alkanes are believed to be particularly important to survive water stress as their levels are highly increased by drought (Bondada *et al.*, 1996; Kosma *et al.*, 2009) and plants living in hot and dry environments tend to have a higher proportion of the longer alkanes (Wilkinson and Mayeux, 1990; Stevens *et al.*, 1994; Dodd and Rafii, 2000; reviewed in Shepherd and Griffiths, 2006 and Kosma and Jenks, 2007). The longer chain alkanes may correlate with a denser, more highly packed hydrophobic layer making the cuticle less permeable. Since ABA is implicated in osmotic stress response, this hormone may be particularly important for the endogenous regulation of the longer-chain alkanes.

The gene expression analysis of a subset of genes involved in the synthesis, transport, polymerization and regulation of cuticle is a first step to attempt to unravel the molecular link between cuticle coverage and composition and ABA deficiency. The expression of three transcription factors involved in cuticle formation (*MYB41*, *MYB30/96* and *MYB16/106*) is impaired in the ABA-deficient mutants but the expression of other transcriptional regulators such as *CER7*, *CD2* and *SHN1* is unaffected in the mutants. This suggests that ABA partly regulates cuticle formation through the modulation of the expression of some transcription factors but that it does

not affects the entirety of the regulatory pathway of cuticle formation. This is not surprising as the defects of the ABA-deficient mutant cuticles are not severe.

The decrease of expression in the ABA mutants, compared to their WT, of a number of genes involved in cutin formation, such as *CUS1*, *CD3*, *GPAT4*, *GPAT6*, and *WBC11*, correlates well with the decrease of expression of the MYB transcription factors and with the decrease of cutin coverage seen in leaves. The phenotype of the cuticular waxes of the leaves of the ABA deficient plants is more complex, but it can be partially explained by the expression analysis. For example, *CER1* and *CER3* are known to interact together to synthesize alkanes both shorter and longer than C_{31} (Bourdenx *et al.*, 2011; Bernard *et al.*, 2012) and overexpression of *CER1* substantially increased the levels of iso-alkanes (Bourdenx *et al.*, 2011). The down-regulation of *CER3* transcripts seen in ABA deficient leaves could be partly responsible for the reduction of C_{31} and C_{33} alkanes, while the increase of C_{27} to C_{30} alkanes and iC_{29} , iC_{30} , iC_{31} and iC_{33} isoalkanes could be attributed to an increased activity of homologs of *CER1/3*.

However, the decrease of expression of *CER6* can also explain the decrease in long chain and the increase in shorter chains alkanes seen in ABA mutant leaves as it suggests a reduction in very-long-chain fatty acid elongation. Indeed, *CER6*, a component of the Fatty Acid Elongase complex that has previously been shown to be involved in the production of alkanes longer than C_{30} in the leaves (Vogg *et al.*, 2004), is down-regulated in the mutant leaves. Similarly, the isoalkanes also show a shift towards shorter chain lengths, due to a much higher relative increase in the isoalkane

iC₂₉ than the isoalkanes iC₃₁ and iC₃₃. That all the isoalkanes increase to some degree though suggests an overall increase in the production of iso fatty acids. In summary, the decrease of the cutin-related gene expression in leaves of ABA mutants correlates nicely with the lower cutin coverage but a broader survey is needed to explain the compositional variations of the waxes.

The fruit cuticle is not as affected by ABA deficiency as the leaf cuticle: no ultrastructure abnormalities were detected; cutin and wax amounts and composition were not meaningfully different and the cuticle-related gene expression was not substantially different. It is possible that the cuticle of fruit does not need to be as closely regulated than the one of leaf. In fact, the surface/volume ratio is much higher for leaf than for fruit so water loss is facilitated in leaf. Furthermore, many fruits are also devoid of stomata, the major source of leaf water loss. Finally, the fruit cuticle is in general thicker than the one of leaf, but is often more permeable as well (Becker *et al.*, 1986; Araus *et al.*, 1991; Schreiber and Riederer, 1996), suggesting that water loss is not a major concern for the fruit. Indeed, it may even be necessary for fruit growth (Martin and Rose, 2014).

A permeable/disrupted cuticle may confer resistance to *B. cinerea* through a decrease of ABA levels

Inoculation of leaf and fruit of ABA-deficient lines with *Botrytis cinerea* spores shows that ABA deficiency leads to decreased pathogen susceptibility. These results are in agreement with earlier observations in which the leaves of *sit* were found to be more resistant to *Botrytis cinerea* (Audenaert *et al.*, 2002; Asselbergh *et al.*,

2008) and *Oidium neolycopersici* (Achuo *et al.*, 2006). The Arabidopsis ABA mutants *aba2* and *aba3* are also more resistant to *B. cinerea* (L'Haridon *et al.*, 2011). The mechanisms leading to such resistance are still being investigated but *sit* appears to have its defense baseline always activated and to react stronger and faster to infection by accumulating hydrogen peroxide among other mechanisms (Asselbergh *et al.*, 2007; Asselbergh *et al.*, 2008). Furthermore, strong evidences show that ABA interferes with the plant ability to successfully block pathogen infection. In fact, a single application of ABA, not expecting to change *sit* phenotype, increased its susceptibility to *B. cinerea* (Achuo *et al.*, 2006). Increased susceptibility was also reported for the WT in Audenaert *et al.* (2002); although this result could not be repeated in a subsequent study (Achuo *et al.* 2006). Furthermore, it has been proposed that ABA negatively modulates the salicylic acid-dependent defense pathway which could partly explain *sit* resistance to *B. cinerea* (Audenaert *et al.*, 2002). In addition, effectors of *Pseudomonas syringae* were found to induce ABA biosynthesis and signaling genes, which antagonizes SA-mediated defenses, in turn resulting in plant susceptibility to the pathogen (de Torres-Zabala *et al.*, 2007; de Torres-Zabala *et al.*, 2009). Finally, ABA production not only correlates with tomato ripe fruit susceptibility to *B. cinerea* but also, several genes implicated in ABA biosynthesis and signaling are up-regulated in susceptible red fruits infected with *B. cinerea* while the opposite trend is seen in resistant MG fruits (Blanco-Ulate *et al.*, 2013). Collectively, these results indicate that ABA increases pathogen susceptibility by negatively regulating plant defense pathways.

A permeable cuticle is likely to be central to pathogen resistance. In fact, several *Arabidopsis* cuticle mutants, or over-expressing lines, are resistant to *B. cinerea* infections and also have a more permeable cuticle (Bessire *et al.*, 2007; Chassot *et al.*, 2007; Tang *et al.*, 2007; Buxdorf *et al.*, 2014). The resistance to *B. cinerea* is lost if the permeability phenotype is rescued (Voisin *et al.*, 2009). Furthermore, hydrogen peroxide accumulation by itself does not confers resistance to *Botrytis*: SHN3 over-expressing lines are more resistant to *B. cinerea* and have a more permeable cuticle but the SHN3-RNAi lines, which cuticle is not more permeable than the WT, have increased susceptibility to *Botrytis* despite an elevated accumulation of hydrogen peroxide (Buxdorf *et al.*, 2014). It is suggested that the plant senses the abnormal cuticle, in particular the cutin monomers, and reacts by turning its defense on (Schweizer *et al.*, 1996; Fauth *et al.*, 1998; Bessire *et al.*, 2007; Chassot *et al.*, 2007, Serrano *et al.*, 2014). Permeability of the cuticle may be necessary for either mimicking pathogen attack or to allow signals movements. Cuticular permeability is associated with a disrupted cuticle at least for the cuticle mutants *bodyguard* and *lacerata*, and for over-expressing cutinase lines (Sieber *et al.*, 2000; Kurdyukov *et al.*, 2006; Chassot *et al.*, 2007; Voisin *et al.*, 2009).

It is possible that the resistance to *B. cinerea* observed in some cutin mutant results from a lower accumulation of ABA. Indeed, Wang *et al.* (2011) observed an unexpected down-regulation of ABA biosynthesis and signaling in various cutin mutants. To gain further insight into this process, the ABA levels of the *cd1*, *cd2*, *cd3* and *pe* tomato mutants were assessed. No difference of ABA levels was observed in leaf at the exception of *pe* which seemed to have a higher accumulation of ABA. The

fruits of the *cd* mutants have also been reported to be more susceptible to *B. cinerea* than M82 (Isaacson *et al.*, 2009). Pathogen susceptibility of leaf and leaf cuticle permeability remain to be tested but the fruits were reported to be severely susceptible to *Botrytis* infection while cuticular permeability was substantial for *cd1* only (Isaacson *et al.*, 2009). Further investigations are required but it is tempting to hypothesize that the down-regulation of the ABA pathway seen in cutin mutants is part of a defense mechanism that the cell turns on after sensing cutin monomers released in permeable cuticle.

Conclusion

The results presented here indicate that ABA modulates the regulation of both cutin and waxes and that this phytohormone is necessary for development of the cuticle regardless of water stress. A regulatory model of cuticle formation is emerging in the literature based on the characterization of several transcription factors and RNAi mechanism, but it is likely that more regulators are yet to be discovered. Based on the broad response of the cuticle pathway to ABA deficiency, it is probable that ABA is upstream of a regulatory cascade. The tomato ABA-deficient lines would be a good resource to identify additional cuticular regulators affected by ABA deficiency. Additionally, ABA levels have previously been shown to be correlated to *Botrytis cinerea* susceptibility while ABA pathway is down-regulated in a set of cutin mutants. It is possible that a permeable cuticle triggers plant defense responses, one of which being the down-regulation of the ABA pathway.

Material and Methods

Plant materials

The tomato (*Solanum lycopersicum*) wild-types Ailsa Craig and Rheinlands Ruhm and their mutants, *not*, *flc* and *sit*, were obtained from the UC Davis/C.M. Rick Tomato Genetics Resource Center, University of California, Davis, USA. Plants were grown in a greenhouse under 16 h of light and 8 h of dark using standard practices. Ripening stages were determined as followed: Mature green- the fruit has reached its full size but is entirely green. Breaker- there is a “break” in color, either yellow, pink or red on no more than 10% of the surface. Turning- the color change affects between 10 to 30% of the fruit surface. Pink- between 30 to 60% of the fruit is pink or red. Red- more than 90% of the surface is red. Ripe Red- the fruit is entirely red.

ABA measurements

The plant material was ground into fine powder and ~200-300 mg was mixed into 500 µl of 1-propanol/H₂O/concentrated HCl (2:1:0.002). 80 ng of D6-ABA was added as an internal standard. The samples were agitated at 4°C for 30 min, centrifuged and 800 µl of dichloromethane was added to the supernatant. Another 30 min agitation step followed after which the samples were centrifuged, the lower phase was collected and dried at 35°C under a gentle stream of nitrogen gas. The extracts were resuspended in 100 µl of methanol and analyzed by HPLC-MS/MS at the Chemical Ecology Group Core Facility.

ABA complementation

100 μ M (\pm)-ABA (Sigma) in 0.1% ethanol was sprayed on 3 week old seedlings every 5 days for 2 weeks as described in Achuo *et al.* (2006) and Curvers *et al.* (2010). Controls were sprayed with 0.1% ethanol. Cutin and wax were isolated from the youngest fully expanded leaf of 5 week old plants, using the two leaflets closest to the distal leaflet.

Water loss measurements

Red fruits were harvested, their pedicel scar was covered with high vacuum grease (silicone lubricant, Dow Corning) and they were placed in an incubation chamber at ~35% humidity and ~22°C in the dark. Fruit surface area was determined by taking 3 distinct measurements of the fruit diameter. The fruits were weighed every day to determine the amount of water loss.

Botrytis cinerea treatments

Leaf material was harvested from the youngest fully expanded leaf of 6 week old plants, using the two leaflets closest to the distal leaflet. Each leaflet was placed on the lid of a petri dish containing 1.5% agar to maintain humidity levels. A 10 μ l drop of 0.01 M glucose, 6.7 Mm $\text{K}_2\text{H}_2\text{PO}_4$, pH 5 containing ~4000 sporangia was deposited on the leaflets. The concentration of glucose was determined based on Audenaert *et al.* (2002).

Red fruits were harvested, placed in a humidity chamber and four 10 µl drops were deposited around the pistil scar. Each drop contained around 2 million sporangia in 0.1 M glucose, 67 Mm K_2HPO_4 , pH 5.

Light microscopy

Tissue fixation and embedding were performed as in Buda *et al.* (2009). Saturated solution of Oil Red O (Alfa Aesar, <http://www.alfa.com>) in isopropyl alcohol was diluted 3:2 with distilled water, mixed well, allowed to sit for 30 min at room temperature, and filtered to remove precipitates. The solution was then applied on 6 µm sections for 30 min in a humidity chamber. The slides were gently taken through a series of 50%, 30%, 22%, 15% and 8% isopropyl alcohol and mounted in the last dilution. The stained slides were viewed on an AxioImager A1 microscope (Zeiss) using differential interference contrast optics (DIC) technique. Photoshop CS5 software (Adobe) was used to adjust levels and color balance.

Transmission electron microscopy (TEM)

The leaf tissue was selected as described in the “*Botrytis cinerea* treatments” section. Leaflets were cut in pieces of approximately 5 by 5 mm while ~3 by 3 mm cubes of tomato pericarp were excised. The harvested tissue was placed in a fixative consisting of 1% glutaraldehyde in 0.1 M sodium cacodylate buffer (pH 7.2) for 60 min on ice. The samples were washed 3 times in wash buffer (0.1 M sodium cacodylate buffer, pH 7.2) for ~5 min each and subsequently post-fixed in 0.5% OsO_4 in 0.1 M sodium cacodylate buffer (pH 7.2) for 60 min on ice. The washing step was

then repeated. Samples were dehydrated with a series of acetone dilution (10%, 30%, 50%, 70%, 90% and 100%) for 20 min each, with the 100% solution being replaced by fresh acetone after 10 min. Infiltration of the samples was done by immersing them in 75% acetone - 25% Spurr's Low Viscosity Resin (EMS; Ft. Washington, PA) overnight, followed by 2 hr immersions in 50% resin/50% acetone and 75% resin/75%. The samples were then infiltrated with 100% resin overnight. Polymerization of resin was performed at 60°C for 10 hours.

60 nm sections were cut with a diamond knife on a Reichert Jung Ultracut E ultramicrotome and collected on Formvar-coated nickel grids. The grids were stained in conventional uranyl acetate/lead citrate, washed with DH_2O and dried. The sections were viewed with a Zeiss Libra 120 transmission electron microscope at 120kv.

Cutin monomer and wax analysis

Cutin and wax were isolated from the youngest fully expanded leaf of 6 week old plants, using the two leaflets closest to the distal leaflet. Cuticular wax extraction was done by dipping the leaflets in chloroform, containing 50 or 100 μg of tetracosane, for 30 seconds. Cutin isolation was done as described in Li-Beisson *et al.* (2013).

Fruit cuticle was enzymatically isolated by collecting the exocarp with a razor blade and incubating it at 42°C with 0.2% (v/v) pectinase (Sigma, P2611) and 1% (v/v) cellulase (Sigma, C2605) in 6.558 g/L citric acid, 5.526 g/L sodium citrate, pH 4 with 0.2 g/L sodium azide to prevent microbial growth. Isolated cuticles were washed

in water, dried and rinsed 3 times with chloroform to remove cuticular waxes and contaminating lipid residues. Fruit cuticular waxes were extracted by dipping the fruits in two successive bath of chloroform for 1 min each. 50 or 100 µg of tetracosane were used as internal standard.

Depolymerization of leaf and fruit cutin was done following the base catalysis method described in Li-Beisson *et al.* (2013). Derivatization of cutin monomers and cuticular waxes were done following the silylation method (Li-Beisson *et al.*, 2013), once the wax extracts were filtered and dried with anhydrous sodium sulfate.

Both cutin and wax extracts were resuspended in 100 µl chloroform and ran into a gas chromatography (GC) Agilent 6850 instrument containing a DB-1 (30 m x 320 µm x 0.1 µm) column. The wax samples were injected in an oven at 50°C and the temperature was held constant for 2 min. The temperature was then increased by 40°C per min up to 200°C, and then by 4°C/min up to 235°C and held for 15 minutes. A final ramp of 10°C per min up to 315°C followed, and the last temperature was held for 15 min. The cutin monomer samples were injected in an oven at 50°C, which temperature was held for 2 min. A first temperature ramp followed with an increase of 40°C per min up to 120°C, which was held for 2 min. A last ramp of 10°C per min increased the temperature up to 320°C, held for 15 min.

Gene expression analysis

RNAs were extracted from emerging leaves (length < 2 cm) of mature plants and from the pericarp of fruits using TRIzol reagent (Life Technologies) and

following the company directions. cDNAs were generated using SuperScript II reverse transcriptase (Life Technologies) following the company instructions. qPCRs were performed on a Life Technologies/ABI Vii7 instrument at the Institute of Biotechnology Genomics Facility (Cornell, NY). A list of the primers used in this study is given in Table 4.1, along with the sol genomics network (SGN, <http://solgenomics.net/>) IDs of the targeted genes.

Table 4.1. SGN IDs of the tomato genes analyzed in this study and the qPCR primers used.

Gene Name	SGN ID	qPCR primers
CUS1	Solyc11g006250	F- GTAGCATGTTGTGGACAAGGACCA R- TTTGCCCTCTCAGATGGATGGAAC
BDG	Solyc08g008610	F- AGTCCTGTTACTGCTCGTCAG R- ATCGCGTGTACAATGTGTCTG
CD3	Solyc08g081220	F- AGATGCATTTCAGATTCGTGGC R- GCAACACTGCTGCTGCTATTG
CYP77A6	Solyc05g055400	F- ACATGTCATTGACCCATGCAG R- TCAAACCTTCTCGGGTTCCGGAC
GPAT4	Solyc01g094700	F- TGCCAGTAGCAGTGGATACAA R- TGTC AATTCATAAGTTGGCCT
GPAT6	Solyc09g014350	F- TGATAGGATTGTACCTGTGGC R- ACGTAATCTCATAAGTCGGTC
LACS2	Solyc01g079240	F- TTGCAGACTGGTTCTGCATTA R- TATCAAACCTGTGAGCACTGCA
HTH	Solyc06g062600	F- AATAGTGGGAGGAGGCACAG R- AGTGTCAGCCAAAGAGATGTG
FDH	Solyc03g005320	F- GCCATTAGTTCTTCCTATGTC R- AGAAATGCTCGAATGCCAGCT
WBC11	Solyc03g019760	F- GGTC ACTATCTGCATTGGAAC R- GACGAAAGAAGGGAATCCTCC
WBC12	Solyc11g065350	F- ACACTATGGCGTTGCAGCTTT R- CACATAACGGAAGAATCTAGC
CER1	Solyc03g065250	F- GTGGGACGTAGCATTGAGTC R- TTCGATTATCACCCCTTTCAGT
CER3	Solyc03g117800	F- GAGCATGGAGGATATTTGGTG R- CTCATAAGACACCCTTCGC
CER4	Solyc06g074390	F- TGTTGTTGTTAACCTAGCTGC R- GTTGAGAACGTTTATAGCTCC

CER6	Solyc02g085870	F- CTTTCATGGAACATTCGCGTC R- CACCAAGACCTGACCTTTCAAG
LACS1	Solyc01g079240	F- TTGAGTTTGACAAGGAGTTGG R- GTTTAGCTGCTGCATTAAGCC
WSD1	Solyc01g011430	F- CATTGAGTCCATCATCAAGGC R- CTTGCTCAGTGTTGATTCTTG
CER7	Solyc05g047420	F- AAGTACATGGCGAATGACAGT R- TCTGCCGAACCTGATAGTGAG
CD2	Solyc01g091630	F- ACGTGGTGATGAACGGTGGA R- AAGGCTACCGTCAAGAGTGA
SHN1	Solyc03g116610	F- GCAACGCCATTGGGGTTCT R- ATCATACGCTCGGGCAGCTT
MYB41	Solyc10g005460	F- TGTGGAGGAGCAATCATCATC R- CCGAAATCGTACTAGAGTTCG
MYB30/96	Solyc03g116100	F- TTGTTTCAAGCGGAGAGCAAG R- TGCTGGTGCATTAATAGCATC
MYB16/106	Solyc02g088190	F-GCAAATGACTAGTGTGGTGTG R- GAAGACAATCAACATGAGGTC

Acknowledgments and Relative Contribution

The TEM photographs were taken in the Skidmore College microscopy facility by, or with the help of, Dr. David Domozych. Cutin monomers and wax compounds were identified by Eric Fich using GC/MS spectra.

REFERENCES

- Achuo EA, Prinsen E, Höfte M. (2006). Influence of drought, salt stress and abscisic acid on the resistance of tomato to *Botrytis cinerea* and *Oidium neolycopersici*. *Plant Pathology*. 55, 178-186.
- Audenaert K, De Meyer GB, Höfte MM. (2002). Abscisic acid determines basal susceptibility of tomato to *Botrytis cinerea* and suppresses salicylic acid-dependent signaling mechanisms. *Plant Physiology* 128, 491-501.
- Araus JL, Febrero A, Vendrell P. 1991. Epidermal conductance in different parts of durum wheat grown under Mediterranean conditions: the role of epicuticular waxes and stomata. *Plant, Cell and Environment* 14, 545-558.
- Asselbergh B, Curvers K, França S, Audenaert K, Vuylsteke M, *et al.* (2007). *Plant Physiology* 144, 1863-1877.
- Asselbergh B, Achuo AE, Höfte M, Van Gijsegem F. (2008). Abscisic acid deficiency leads to rapid activation of tomato defence responses upon infection with *Erwinia chrysanthemi*. *Molecular Plant Pathology* 9(1), 11-24.
- Becker M, Kerstiens G, Schönherr J. (1986). Water permeability of plant cuticles: permeance, diffusion and partition coefficients. *Trees* 1, 54-60.
- Bernard A, Domergue F, Pascal S, Jetter R, Renne C, *et al.* (2012). Reconstitution of plant alkane biosynthesis in yeast demonstrates that Arabidopsis ECERIFERUM1 and ECERIFERUM3 are core components of a very-long-chain alkane synthesis complex. *The Plant Cell* 24, 3106-3118.
- Bessire M, Chassot C, Jacquat AC, Humphry M, Borel S, Petetot JMC, *et al.* (2007). A permeable cuticle in *Arabidopsis* leads to a strong resistance to *Botrytis cinerea*. *EMBO J.* 26, 2158–2168.
- Blanco-Ulate B, Vincenti E, Powell ALT, Cantu D. (2013). Tomato transcriptome and mutant analyses suggest a role for plant stress hormones in the interaction between fruit and *Botrytis cinerea*. *Frontiers in Plant Science* 4(142).
- Bondada BR, Oosterhuis DM, Murphy JB, Kim KS. (1996). Effect of water stress on the epicuticular wax composition and ultrastructure of cotton (*Gossypium hirsutum* L.) leaf, bract, and boll. *Environmental and Experimental Botany* 36(1), 61-69.
- Bourdenx B, Bernard A, Domergue F, Pascal S, Léger A, *et al.* (2011). Overexpression of Arabidopsis ECERIFERUM1 promotes wax very-long-

chain alkane biosynthesis and influences plant response to biotic and abiotic stresses. *Plant Physiology* 156, 29-45.

- Buda GJ, Isaacson T, Matas AJ, Paolillo DJ, Rose JKC. (2009). Three-dimensional imaging of plant cuticle architecture using confocal scanning laser microscopy. *The Plant Journal* 60, 378-385.
- Burbidge A, Grieve TM, Jackson A, Thompson A, McCarty DR, Taylor IB. (1999). Characterization of the ABA-deficient tomato mutant *notabilis* and its relationship with maize *Vp14*. *The Plant Journal* 17, 427-431.
- Buxdorf K, Rubinsky G, Barda O, Burdman S, Aharoni A, Levy M. (2014). The transcription factor *SISHINE3* modulates defense responses in tomato plants. *Plant Mol. Biol.* 84, 37-47.
- Cameron KD, Teece MA, Smart LB. (2006). Increased Accumulation of Cuticular Wax and Expression of Lipid Transfer Protein in Response to Periodic Drying Events in Leaves of Tree Tobacco. *Plant Physiology* 140, 176-183.
- Chassot C, Nawrath C, Métraux JP. (2007). Cuticular defects lead to full immunity to a major plant pathogen. *The Plant Journal* 49: 972-980.
- Cominelli E, Sala T, Calvi D, Gusmaroli G, Tonelli C. (2008). Over-expression of the Arabidopsis *AtMYB41* gene alters cell expansion and leaf surface permeability. *The Plant Journal* 53, 53-64.
- Curvers K, Seifi H, Mouille G, de Rycke R, Asselbergh B, *et al.* (2010). Abscisic acid deficiency causes changes in cuticle permeability and pectin composition that influence tomato resistance to *Botrytis cinerea*. *Plant Physiology* 154, 847-860.
- de Torres-Zabala M, Truman W, Bennett MH, Lafforgue G, Mansfield JW, *et al.* (2007). *Pseudomonas syringae* pv. *tomato* hijacks the Arabidopsis abscisic acid signaling pathway to cause disease. *The EMBO journal* 26, 1434-1443.
- de Torres-Zabala M, Bennett MH, Truman W, Grant MR. (2009). Antagonism between salicylic and abscisic acid reflects early host-pathogen conflict and moulds plant defence responses. *The Plant Journal* 59, 375-386.
- Dodd RS, Rafii ZA. (2000). Habitat-related adaptive properties of plant cuticular lipids. *Evolution* 54, 1438-1444.
- Duan HD, Schuler MA. (2005). Differential expression and evolution of the Arabidopsis CYP86A subfamily. *Plant Physiology* 137, 1067-1081.
- Fauth M, Schweizer P, Buchala A, Markstädter C, Riederer M, *et al.* (1998). Cutin monomers and surface wax constituents elicit H₂O₂ in conditioned cucumber

- hypocotyl segments and enhance the activity of other H₂O₂ elicitors. *Plant Physiology* 117, 1373-1380.
- Finkelstein RR, Gampala SSL, Rock CD. (2002). Abscisic acid signaling in seeds and seedlings. *The Plant Cell* 14(S1), S15-S45.
- Galpaz N, Wang Q, Menda N, Zamir D, Hirschberg J. (2008). Abscisic acid deficiency in the tomato mutant *high-pigment 3* leading to increased plastid number and higher fruit lycopene content. *The Plant Journal* 53, 717-730.
- Go YS, Kim H, Kim HJ, Suh MC. (2014). *Arabidopsis* cuticular wax biosynthesis is negatively regulated by the *DEWAX* gene encoding an AP2/ERF-type transcription factor. *The Plant Cell* 26(4) 1666-1680.
- Harrison E, Burbidge A, Okyere JP, Thompson AJ, Taylor IB. (2011). Identification of the tomato ABA-deficient mutant *sitiens* as a member of the ABA-aldehyde oxidase gene family using genetic and genomic analysis. *Plant Growth Regulation* 64(3), 301-309.
- Hooker TS, Millar AA, Kunst L. (2002). Significance of the expression of the CER6 condensing enzyme for cuticular wax production in *Arabidopsis*. *Plant Physiology* 129, 1568-1580.
- Isaacson T, Kosma DK, Matas AJ, Buda GJ, He Y, Yu B, Pravitasari A, Batteas JD, Stark RE, Jenks MA, Rose JKC. (2009). Cutin deficiency in the tomato fruit cuticle consistently affects resistance to microbial infection and biomechanical properties, but not transpirational water loss. *The Plant Journal* 60, 363–377.
- Jia H-F, Chai Y-M, Li C-L, Lu D, Luo J-J, *et al.* (2011). Abscisic acid plays an important role in the regulation of strawberry fruit ripening. *Plant Physiology* 157, 188-199.
- Kannangara R, Branigan C, Liu Y, Penfield T, Rao V, *et al.* (2007). The transcription factor WIN1/SHN1 regulates cutin biosynthesis in *Arabidopsis thaliana*. *The Plant Cell* 19(4), 1278-1294.
- Kosma DK, Jenks MA. (2007). Eco-physiological and molecular-genetic determinants of plant cuticle function in drought and salt stress tolerance. In: *Advances in Molecular Breeding toward Drought and Salt Tolerant Crops* (M.A. Jenks, P.M. Hasegawa and S.M. Jain, eds.) Dordrecht, The Netherlands: Springer, pp. 91-120.
- Kosma DK, Bourdenx B, Bernard A, Parsons EP, Lü S, Joubès J, Jenks MA. (2009). The impact of water deficiency on leaf cuticle lipids of *Arabidopsis*. *Plant Physiology* 151, 1918-1929.

- Koyama K, Sadamatsu K, Goto-Yamamoto N. (2010). Abscisic acid stimulated ripening and gene expression in berry skins of the Cabernet Sauvignon grape. *Funct. Integr. Genomics* 10, 367-381.
- Kurdyukov S, Faust A, Nawrath C, Bär S, Voisin D, *et al.*, (2006). The epidermis-specific extracellular BODYGUARD controls cuticle development and morphogenesis in *Arabidopsis*. *The Plant Cell* 18, 321-339.
- L'Haridon F, Besson-Bard A, Binda M, Serrano M, Abou-Mansour E, *et al.* (2011). A permeable cuticle is associated with the release of reactive oxygen species and induction of innate immunity. *PLOS Pathogens* 7(7), e1002148.
- Li-Beisson Y, Shorrosh B, Beisson F, Andersson MX, Arondel V, *et al.* (2013). Acyl-Lipid Metabolism. The American Society of Plant Biologists. *The Arabidopsis Book* 11:e0161.
- Lisso J, Schröder F, Fisahn J, Müssig C. (2011). NFX1-LIKE2 (NFXL2) Suppresses Abscisic Acid Accumulation and Stomatal Closure in *Arabidopsis thaliana*. *PLoS ONE* 6(11), e26982.
- Lisso J, Schröder F, Schippers JHM, Müssig C. (2012). NFL2 modifies cuticle properties in *Arabidopsis*. *Plant Signaling & Behavior* 7(5), 551-555.
- Liu F, Jensen CR, Andersen MN. (2005). A review of drought adaptation in crop plants: changes in vegetative and reproductive physiology induced by ABA-based signals. *Australian Journal of Agricultural Research* 56, 1245-1252.
- Martin LBB, Rose JKC. (2014). There's more than one way to skin a fruit: formation and functions of fruit cuticles. *Journal of Experimental Botany* 65(16), 4639-4651.
- Nadakuduti SS, Pollard M, Kosma DK, Allen Jr. C, Ohlrogge JB, Barry CS. (2012). Pleiotropic phenotypes of the *sticky peel* mutant provide new insight into the role of *CUTIN DEFICIENT2* in epidermal cell function in tomato. *Plant Physiology* 159, 945-960.
- Nitsch L, Kohlen W, Oplaat C, Charnikhova T, Cristescu S, *et al.* (2012). ABA-deficiency results in reduced plant and fruit size in tomato. *Journal of Plant Physiology* 169, 878– 883.
- Raffaele S, Vaillau F, Léger A, Joubès J, Miersch O, *et al.* (2008). A MYB transcription factor regulates very-long-chain fatty acid biosynthesis for activation of the hypersensitive cell death response in *Arabidopsis*. *The Plant Cell* 20, 752-767.

- Rančić D, Pekić Quarrie S, Pećinar I. (2010). Anatomy of tomato fruit and fruit pedicel during fruit development. *Microscopy: Science, Technology, Applications and Education*. A. Méndez-Vilas and J. Díaz (Eds.).
- Richmond DV and Martin JT. (1959). Studies of plant cuticle III. The composition of the cuticle of apple leaves and fruits. *Annals of Applied Biology* 47(3), 583-592.
- Rowland O, Zheng H, Hepworth SR, Lam P, Jetter R, Kunst L. (2006). CER4 encodes an alcohol-forming fatty acyl-coenzyme A reductase involved in cuticular wax production in *Arabidopsis*. *Plant Physiology* 142(3), 866-877.
- Sagi M, Scazzocchio C, Fluhr R. (2002). The absence of molybdenum cofactor sulfuration is the primary cause of the *flacca* phenotype in tomato plants. *The Plant Journal* 31, 305–317.
- Schreiber L, Riederer M. 1996. Ecophysiology of cuticular transpiration: comparative investigation of cuticular water permeability of plant species from different habitats. *Oecologia* 107, 426-432.
- Schweizer P, Felix G, Buchala A, Müller C, Métraux J-P. (1996). Perception of free cutin monomers by plant cells. *The Plant Journal* 10(2), 331-341.
- Seo PJ, Xiang F, Qiao M, Park J-Y, Lee YN, *et al.* (2009). The MYB96 Transcription Factor Mediates Abscisic Acid Signaling during Drought Stress Response in *Arabidopsis*. *Plant Physiology* 151, 275-289.
- Seo PJ, Lee SB, Suh MC, Park M-J, Go YS, Park C-M. (2011a). The MYB96 transcription factor regulates cuticular wax biosynthesis under drought conditions in *Arabidopsis*. *The Plant Cell* 23, 1138-1152.
- Seo PJ, Park C-M. (2011b). Cuticular wax biosynthesis as a way of inducing drought resistance. *Plant Signaling & Behavior* 6(7), 1043-1045.
- Serrano M, Coluccia F, Torres M, L'Haridon F, Métraux J-P. (2014). The cuticle and plant defense to pathogens. *Frontiers in Plant Science* 5(274).
- Sharp RE, LeNoble ME, Else MA, Thorne ET, Gherardi F. (2000). Endogenous ABA maintains shoot growth in tomato independently of effects on plant water balance: evidence for an interaction with ethylene. *Journal of Experimental Botany* 51:350, 1575-1584.
- Shepherd T, Griffiths, DW. (2006). The effects of stress on plant cuticular waxes. *New Phytologist* 171,469-499.
- Shi JX, Adato A, Alkan N, He Y, Lashbrooke J, *et al.* (2013). The tomato SISHINE3 transcription factor regulates fruit cuticle formation and epidermal patterning. *New Phytologist* 197(2), 468-480.

- Sieber P, Schorderet M, Ryser U, Buchala A, Kolattukudy P, *et al.* (2000). Transgenic arabidopsis plants expressing a fungal cutinase show alterations in the structure and properties of the cuticle and postgenital organ fusions. *The Plant Cell* 12, 721-737.
- Soto A, Ruiz KB, Ravaglia D, Costa G, Torrigiani P. (2013). ABA may promote or delay peach fruit ripening through modulation of ripening- and hormone-related gene expression depending on the developmental stage. *Plant Physiology and Biochemistry* 64 11-24.
- Spollen WG, LeNoble ME, Samuels TD, Bernstein N, Sharp RE. (2000). Abscisic acid accumulation maintains maize primary root elongation at low water potentials by restricting ethylene production. *Plant Physiology* 122, 967-676.
- Stevens JF, Hart H, Bolck A, Swaving JH, Malingre TM. (1994). Epicuticular wax composition of some European *Sedum* species. *Phytochemistry* 35, 389-399.
- Sun L, Sun Y, Zhang M, Wang L, Ren J, *et al.* (2012). Suppression of 9-cis-epoxycarotenoid dioxygenase, which encodes a key enzyme in abscisic acid biosynthesis, alters fruit texture in transgenic tomato. *Plant Physiology* 158, 283-298.
- Tal M. (1966). Abnormal stomatal behavior in wilted mutants of tomato. *Plant Physiology* 41, 1387-1391.
- Tal M, Nevo Y. (1973). Abnormal stomatal behavior and root resistance, and hormonal imbalance in three wilted mutants of tomato. *Biochemical Genetics* 8(3), 291-300.
- Tal M, Imber D, Erez A, Epstein E. (1979). Abnormal stomatal behavior and hormonal imbalance in *flacca*, a wilted mutant of tomato. V. Effect of abscisic acid on indoleacetic acid metabolism and ethylene evolution. *Plant Physiology* 63, 1044-1048.
- Taylor IB and Tarr AR. (1984). Phenotypic interactions between abscisic acid deficient tomato mutants. *Theor. Appl. Genet.* 68, 115-119.
- Tang D, Simonich MT, Innes RW. (2007). Mutations in LACS2, a long-chain acyl-coenzyme a synthetase, enhance susceptibility to avirulent *Pseudomonas syringae* but confer resistance to *Botrytis cinerea* in *Arabidopsis*. *Plant Physiology*. 144, 1093–1103.
- Thompson AJ, Jackson AC, Symonds RC, Mulholland BJ, Dadswell AR, *et al.* (2000). Ectopic expression of a tomato 9-cis-epoxycarotenoid dioxygenase gene causes over-production of abscisic acid. *The Plant Journal* 23(3), 363-374.

- Vogg G, Fisher S, Leide J, Emmanuel E, Jetter R, *et al.* (2004). Tomato fruit cuticular waxes and their effects on transpiration barrier properties: functional characterization of a mutant deficient in a very-long-chain fatty acid β -ketoacyl-CoA synthase. *Journal of Experimental Botany* 55(401), 1401-1410.
- Voisin D, Nawrath C, Kurdyukov S, Franke RB, Reina-Pinto JJ, *et al.* (2009). Dissection of the complex phenotype in cuticular mutants of Arabidopsis reveals a role of SERRATE as a mediator. *PLoS Genetics* 5(10), e1000703.
- Wang Z-Y, Xiong L, Li W, Zhu J-K, Zhu J. (2011). The plant cuticle is required for osmotic stress regulation of abscisic acid biosynthesis and osmotic stress tolerance in Arabidopsis. *The Plant Cell* 23, 1971-1984.
- Wang Y, Wan L, Zhang L, Zhang Z, Zhang H, *et al.* (2012a). An ethylene response factor OsWR1 responsive to drought stress transcriptionally activates wax synthesis related genes and increases wax production in rice. *Plant Mol Biol.* 78, 275-288.
- Wang Y, Wu Y, Duan C, Chen P, Li Q, *et al.* (2012b). The expression profiling of the *CsPYL*, *CsPP2C* and *CsSnRK2* gene families during fruit development and drought stress in cucumber. *Journal of Plant Physiology* 169, 1874-1882.
- Wang Y, Wang Y, Ji K, Dai S, Hu Y, *et al.* (2013). The role of abscisic acid in regulating cucumber fruit development and ripening and its transcriptional regulation. *Plant Physiology and Biochemistry* 64, 70-79.
- Wilkinson R, Mayeux HS Jr. (1990). Composition of epicuticular wax on *Opuntia engelmannii*. *Botanical Gazette* 151, 342-347.
- Yang W, Simpson JP, Li-Beisson Y, Beisson F, Pollard M, Ohlrogge JB, (2012). A land-plant-specific glycerol-3-phosphate acyltransferase family in Arabidopsis: substrate specificity, *sn-2* preference, and evolution. *Plant Physiology* 160, 638-652.
- Yeats TH, Martin LBB, Viart H M-F, Isaacson T, He Y, *et al.* (2012). The identification of cutin synthase: formation of the plant polyester cutin. *Nature Chemical Biology* 8, 609-611.
- Yeats TH, Rose JKC. (2013). The formation and function of plant cuticles. *Plant Physiology* 163, 5-20.
- Zaharah SS, Singh Z, Symons GM, Reid JB. (2013). Mode of action of abscisic acid in triggering ethylene biosynthesis and softening during ripening in mango fruit. *Postharvest Biology and Technology* 75, 37-44.

- Zhang M, Yuan B, Leng P. (2009a). The role of ABA in triggering ethylene biosynthesis and ripening of tomato fruit. *Journal of Experimental Botany* 60(6), 1579-1588.
- Zhang M, Yuan B, Leng P. (2009). Cloning of 9-*cis*-epoxycarotenoid dioxygenase (NCED) gene and the role of ABA on fruit ripening. *Plant Signaling & Behavior* 4(5), 460-463.

CHAPTER 5

Conclusions and Future Directions

This dissertation describes research aimed at advancing understanding of the mechanisms and regulation of plant cuticle formation, both by characterizing genes (*CUTIN DEFICIENT 1; CD1*) and (*CUTIN DEFICIENT 2; CD2*) that are required for tomato fruit cutin polymer accumulation, and by investigating a potential role of the hormone abscisic acid (ABA) in the regulation of cuticle biosynthesis.

Chapter 2 focuses on the characterization of CD1, a GDSL-motif lipase/hydrolase family protein that is required for cutin biosynthesis. The extracellular localization of this acyltransferase, which is preferentially expressed in young expanding organs with a high rate of cuticle production, together with its ability to polymerize the cutin monomer 2-mono(10,16-dihydroxyhexadecanoylglycerol) (2-MHG) *in vitro*, and the accumulation of 2-MHG in the cutin polymer deficient mutant *cd1* mutant, resulted in the conclusion that CD1 is a cutin synthase. More recent studies of putative orthologs from *Arabidopsis thaliana* and the moss *Physcomitrella patens* have revealed that the enzymatic activity of CD1 is conserved among land plants, suggesting that this mechanism of cutin polymerization appeared early in embryophyte evolution (Yeats *et al.*, 2014). This class of proteins was therefore renamed cutin synthase like (CUS) proteins (Yeats *et al.*, 2014). Plant GDSL lipase/hydrolase families are relatively large (over 100 members in *Arabidopsis* and *Oryza sativa*; Ling, 2008; Chepyshko *et al.*, 2012), but only a small number of genes clusters in the same CUS-encoding subclade as CD1 (Yeats *et al.*, 2014). In tomato (*Solanum lycopersicum*), CD1 has four close homologs and it may be that at least one of them is responsible for the residual cutin observed in the *cd1* mutant. Additionally, they may catalyze cutin polymerization through secondary branching, as *in vitro*

biochemical analysis showed that CD1 catalyzes the formation of primarily linear cutin oligomeric products and cutin is known to be a branched polymer (Yeats *et al.*, 2014). Lastly, CD1 close homologs may be responsible for suberin polymerization. Suberin structure and composition are closely related to those of cutin: similar to cutin, suberin is a polyester of fatty acids but these polymers differ in terms of phenolic content, carbon chain length and degree of unsaturation (Kosma *et al.*, 2014). Cutin and suberin probably share similar biosynthetic routes as certain cuticle-related genes, or close homologs, have been shown to also act in suberin formation (Cominelli *et al.*, 2008; Kosma *et al.*, 2014; Landgraf *et al.*, 2014). For example, overexpression of the *A. thaliana* transcription factor AtMYB41 results in transgenic lines with a defective cuticle and ectopic suberin accumulation (Cominelli *et al.*, 2008; Kosma *et al.*, 2014). Additionally, a new study indicated that a potato (*Solanum tuberosum*) ABCG transporter, ABCG1, is required for suberin formation in the tuber periderm, suggesting that it transports suberin components across the plasma membrane (Landgraf *et al.*, 2014), while two ABCG transporters are known to be required for both cutin precursors and cuticular wax transport (Bird *et al.*, 2007; Panikashvili *et al.*, 2007; McFarlane *et al.*, 2010). In conclusion, GDSL lipase/hydrolase proteins have potentially more than one function in cuticle formation as many independent studies have identified members encoding proteins that have been identified in extracellular matrix, or as genes that are regulated by cuticle-related transcription factors (Cominelli *et al.*, 2008; Yeats *et al.*, 2010; Shi *et al.*, 2011; Girard *et al.*, 2012; Chapter 3 of this thesis).

Chapter 3 describes the expression and regulatory pathways of *CD2*, a putative HD-ZIP IV transcription factor. *CD2* appears to be widely expressed, as all tested organs showed expression regardless of the age of development. Furthermore, even though *CD2* transcripts strongly accumulate in the fruit outer and inner epidermis, layers that both form cuticles (Matas *et al.*, 2011), GUS promoter fusion studies revealed that *CD2* is expressed in the majority of the tomato fruit tissues, especially the phloem. The potential role of *CD2* in the phloem, or in an organ such as the root that does not have a cuticle, is not clear. However, *CD2* transcripts or proteins may play a role in transmitting signals from roots to aerial organs through the phloem as the plant use a long-distance communication network, involving RNA and protein phloem translocation, to transmit environmental inputs, sensed by mature organs, to developing regions (Lough and Lucas, 2006). Nonetheless, the involvement of *CD2* in cutin synthesis was confirmed by RNA-seq analysis as several genes with a well-established role in cutin biosynthesis, transport or polymerization were identified as differentially expressed between the *cd2* mutant and its WT genotype. This analysis also revealed that *CD2* broadly affects the expression of numerous lipid-related genes, which collectively modulate lipid metabolism from biosynthesis to signaling. Additionally, a set of genes associated with anthocyanin biosynthesis was identified as being differentially expressed between the WT and the mutant, which is congruent with the previously observed anthocyanin deficiency in the *pe* and *anl2* mutants (Kubo *et al.*, 1999; Kubo and Hayashi, 2011; Nadakuduti *et al.*, 2012). Furthermore, the identification of stress- and ripening-related genes as potential targets of *CD2* suggests that the regulation of cuticle formation is integral to many plant developmental

processes. However, another explanation may be that the differential expression of genes involved in these pathways resulted from the disrupted cuticle, rather than direct regulation by CD2. To test this idea, a valuable next step would be to identify the direct targets of CD2, possibly by using the CD2 antiserum in a chromatin immunoprecipitation-sequencing (ChIP-seq) experiment. Such an approach would have the potentiality to both identify the promoters to which CD2 binds, and also reveal the DNA-motifs that it recognizes. Furthermore, the antiserum may also be used to identify potential CD2 binding partners through protein co-immunoprecipitation (Co-IP) protein pull down experiments.

Much of what is known about the regulation of cuticle formation has resulted from the study of transcription factors (Hen-Avivi *et al.*, 2014). However, plant hormones must inevitably also influence cuticle formation, given their fundamental functions in regulating organ growth (Santner *et al.*, 2009). ABA has received some attention in the context of its key role in modulating water stress responses, including environmentally driven cuticle changes in order to reduce water loss (Kosma *et al.*, 2009; Chater *et al.*, 2014). However, to date, it is has not been demonstrated that ABA also modulates cuticle formation during organ ontogeny. This question is addressed in Chapter 4, by comparing the leaf and fruit cuticles of ABA-deficient tomato plants with those of the corresponding WT plants. This study provided evidence that ABA regulates cuticle formation independent of water stress. This was particularly apparent for the leaf cuticle of ABA-deficient mutants, which had a thinner cuticle and an altered wax composition compared to WT leaves. It was also observed that the ABA-deficient mutants are more resistant to the fungus *Botrytis cinerea*. A similar

phenotype has been observed for various cuticle deficient mutants so the relationship between ABA, impaired cuticle formation and pathogen resistance should be investigated. The resistance of the ABA-deficient mutant *sitiens* to *B. cinerea* may result from the release of the negative modulation of ABA on the plant defense response, and therefore the cuticle may not be responsible for the pathogen resistance (Audenaert *et al.*, 2002). However, Wang *et al.* (2011) observed an unexpected down-regulation of ABA biosynthesis and signaling in various cutin mutants. Consequently, it is possible that the pathogen resistance observed in some cuticle mutants is due to a down-regulation of the ABA pathway triggered by the sensing of cuticle disruption or increased permeability. To start investigating this idea, the phenotype of some cutin mutants is summarized in Table 5.1. This summary shows that resistance to *B. cinerea* is always paired with a disrupted and very permeable cuticle and with a down-regulation of the ABA pathway, thus supporting this hypothesis.

Table 5.1. Correlation between cuticle permeability, resistance to *B. cinerea* and down-regulation of the ABA pathway.

Cutin mutant	Cuticle permeability	Cuticle disruption	<i>B. cinerea</i> susceptibility	ABA pathway down-regulation	Reference
<i>bdg</i>	~37% extracted chlorophyll vs ~10% for WT after 1h	yes	Resistant	strong	Kurdyukov <i>et al.</i> , 2006 Voisin <i>et al.</i> , 2009 Wang <i>et al.</i> , 2011
<i>att1-2</i>	~2 fold higher water loss in dark	no?	N/A	Yes	Xiao <i>et al.</i> , 2004 Wang <i>et al.</i> ,

					2011
<i>lacs2</i>	Strong toluidine blue staining	yes	Resistant	Moderate	Bessire <i>et al.</i> , 2007 Tang <i>et al.</i> , 2007 Wang <i>et al.</i> , 2011
<i>gpat4gpat8</i>	Extreme staining with toluidine blue	no? Thinner cuticle	N/A	Strong	Li <i>et al.</i> , 2007 Wang <i>et al.</i> , 2011
<i>lcr</i>	30-35% extracted chlorophyll vs ~15% for WT after 1h	yes	Resistant	Extreme	Voisin <i>et al.</i> , 2009 Wang <i>et al.</i> , 2011
<i>sitiens</i>	Strong toluidine blue staining	yes	Resistant	Strong reduction of ABA	Curvers <i>et al.</i> , 2010
<i>cd2/pe</i>	~8% extracted chlorophyll vs ~6% for WT after 1h for leaf Slight increase of water loss in fruit	N/A for leaf thinner but not disrupted cuticle for fruit	Increased fruit susceptibility	No	Isaacson <i>et al.</i> , 2009 Nadakuduti <i>et al.</i> , 2012
<i>cd1</i>	Significant increase of water loss in fruit	N/A for leaf thinner but not disrupted cuticle for fruit	Increased fruit susceptibility	No	Isaacson <i>et al.</i> , 2009
<i>cd3</i>	Slight increase of water loss in fruit	N/A for leaf thinner but not disrupted cuticle for fruit	Increased fruit susceptibility	No	Isaacson <i>et al.</i> , 2009

REFERENCES

- Audenaert K, De Meyer GB, Höfte MM. (2002). Abscisic acid determines basal susceptibility of tomato to *Botrytis cinerea* and suppresses salicylic acid-dependent signaling mechanisms. *Plant Physiology* 128, 491-501.
- Bessire M, Chassot C, Jacquat AC, Humphry M, Borel S, Petetot JMC, *et al.* (2007). A permeable cuticle in *Arabidopsis* leads to a strong resistance to *Botrytis cinerea*. *EMBO J.* 26, 2158–2168.
- Bird D, Beisson F, Brigham A, Shin J, Greer S, *et al.* (2007). Characterization of Arabidopsis ABCG11/WBC11, an ATP binding cassette (ABC) transporter that is required for cuticular lipid secretion. *The Plant Journal* 52(3), 485-498.
- Chater CCC, Oliver J, Casson S, Gray JE. (2014). Putting the brakes on: abscisic acid as a central environmental regulator of stomatal development. *New Phytologist* 202, 376-391.
- Chepyshko H, Lai C-P, Huang L-M, Liu J-H, Shaw J-F. (2012). Multifunctionality and diversity of GDSL esterase/lipase gene family in rice (*Oryza sativa* L. *japonica*) genome: new insights from bioinformatics analysis. *BMC Genomics* 13(309).
- Cominelli E, Sala T, Calvi D, Gusmaroli G, Tonelli C. (2008). Over-expression of the Arabidopsis *AtMYB41* gene alters cell expansion and leaf surface permeability. *The Plant Journal* 53, 53-64.
- Curvers K, Seifi H, Mouille G, de Rycke R, Asselbergh B, *et al.* (2010). Abscisic acid deficiency causes changes in cuticle permeability and pectin composition that influence tomato resistance to *Botrytis cinerea*. *Plant Physiology* 154, 847-860.
- Girard A-L, Mounet F, Lemaire-Chamley M, Gaillard C, Elmorjani K, Vivancos J, Runavot J-L, Quemener B, Petit J, Germain V, Rothan C, Marion D, Bakan B. (2012). Tomato GDSL1 is required for cutin deposition in the fruit cuticle. *The Plant Cell* 24, 3119–3134.
- Hen-Avivi S, Lashbrooke J, Costa F, Aharoni A. (2014). Scratching the surface: genetic regulation of cuticle assembly in fleshy fruit. *Journal of Experimental Botany* 65(16), 4653-4664.
- Isaacson T, Kosma DK, Matas AJ, Buda GJ, He Y, Yu B, Pravitasari A, Batteas JD, Stark RE, Jenks MA, Rose JKC. (2009). Cutin deficiency in the tomato fruit

- cuticle consistently affects resistance to microbial infection and biomechanical properties, but not transpirational water loss. *The Plant Journal* 60, 363–377.
- Kosma DK, Bourdenx B, Bernard A, Parsons EP, Lü S, Joubès J, Jenks MA. (2009). The impact of water deficiency on leaf cuticle lipids of *Arabidopsis*. *Plant Physiology* 151, 1918-1929.
- Kosma DK, Murmu J, Razeq FM, Santos P, Bourgault R, *et al.* (2014). AtMYB41 activates ectopic suberin synthesis and assembly in multiple plant species and cell types. *The Plant Journal* 80(2), 216-229.
- Kubo H, Peeters AJM, Aarts MGM, Pereira A, Koornneef M. (1999). ANTHOCYANINLESS2, a homeobox gene affecting anthocyanin distribution and root development in *Arabidopsis*. *The Plant Cell* 11, 1217-1226.
- Kubo H, Hayashi K. (2011). Characterization of root cells of *anl2* mutant in *Arabidopsis thaliana*. *Plant Science* 180, 679-685.
- Kurdyukov S, Faust A, Nawrath C, Bär S, Voisin D, *et al.*, (2006). The epidermis-specific extracellular BODYGUARD controls cuticle development and morphogenesis in *Arabidopsis*. *The Plant Cell* 18, 321-339.
- Landgraf R, Smolka U, Altmann S, Eschen-Lippold L, Senning M, *et al.* (2014). The ABC transporter ABCG1 is required for suberin formation in potato tuber periderm. *The Plant Cell* 26(8), 3403-3415.
- Li Y, Beisson F, Koo AJK, Molina I, Pollard M, Ohlrogge J. (2007). Identification of acyltransferases required for cutin biosynthesis and production of cutin with suberin-like monomers. *Proceedings of the National Academy of Sciences of the USA* 104(46), 18339-18344.
- Ling H. (2008). Sequence analysis of GDSL lipase gene family in *Arabidopsis thaliana*. *Pakistan Journal of Biological Sciences* 11(5), 763-767.
- Lough TJ, Lucas WJ. (2006). Integrative plant biology: role of phloem long-distance macromolecular trafficking. *Annual Review of Plant Biology* 57, 203-232.
- Matas AJ, Yeats TH, Buda GJ, Zheng Y, Chatterjee S, *et al.* (2011). Tissue- and cell-type specific transcriptome profiling of expanding tomato fruit provides insights into metabolic and regulatory specialization and cuticle formation. *The Plant Cell* 23, 3893–3910.
- McFarlane HE, Shin JJH, Bird DA, Samuels AL. (2010). *Arabidopsis* ABCG transporters, which are required for export of diverse cuticular lipids, dimerize in different combinations. *The Plant Cell* 22, 3066-3075.

- Nadakuduti SS, Pollard M, Kosma DK, Allen Jr. C, Ohlrogge JB, Barry CS. (2012). Pleiotropic phenotypes of the *sticky peel* mutant provide new insight into the role of *CUTIN DEFICIENT2* in epidermal cell function in tomato. *Plant Physiology* 159, 945-960.
- Nakamura M, Katsumata H, Abe M, Yabe N, Komeda Y, *et al.* (2006). Characterization of the class IV homeodomain-leucine zipper gene family in Arabidopsis. *Plant Physiology* 141, 1363–1375.
- Panikashvili D, Savaldi-Goldstein S, Mandel T, Yifhar T, Franke RB, *et al.* (2007). The Arabidopsis DESPERADO/AtWBC11 transporter is required for cutin and wax secretion. *Plant Physiology* 145(4), 1345-1360.
- Santner A, Calderon-Villalobos LIAC, Estelle M. (2009). Plant hormones are versatile chemical regulators of plant growth. *Nature Chemical Biology* 5(5), 301-307.
- Shi JX, Malitsky S, De Oliveira S, Branigan C, Franke RB, *et al.* (2011) SHINE Transcription Factors Act Redundantly to Pattern the Archetypal Surface of Arabidopsis Flower Organs. *PLoS Genetics* 7(5): e1001388.
- Tang D, Simonich MT, Innes RW. (2007). Mutations in LACS2, a long-chain acyl-coenzyme a synthetase, enhance susceptibility to avirulent *Pseudomonas syringae* but confer resistance to *Botrytis cinerea* in Arabidopsis. *Plant Physiology* 144, 1093–1103.
- Voisin D, Nawrath C, Kurdyukov S, Franke RB, Reina-Pinto JJ, *et al.* (2009). Dissection of the complex phenotype in cuticular mutants of Arabidopsis reveals a role of SERRATE as a mediator. *PLoS Genetics* 5(10), e1000703.
- Wang Z-Y, Xiong L, Li W, Zhu J-K, Zhu J. (2011). The plant cuticle is required for osmotic stress regulation of abscisic acid biosynthesis and osmotic stress tolerance in Arabidopsis. *The Plant Cell* 23, 1971-1984.
- Xiao F, Goodwin SM, Xiao Y, Sun Z, Baker D, *et al.* (2004). Arabidopsis CYP86A2 represses *Pseudomonas syringae* type III genes and is required for cuticle development. *EMBO Journal* 23, 2903-2913.
- Yeats TH, Howe, KJ, Matas AJ, Buda GJ, Thannhauser TW, Rose JKC. (2010). Mining the surface proteome of tomato (*Solanum lycopersicum*) fruit for proteins associated with cuticle biogenesis. *Journal of Experimental Botany* 13, 3759–3771.
- Yeats TH, Huang W, Chatterjee S, Viart HM-F, Clausen MH, *et al.* (2014). Tomato Cutin Deficient 1 (CD1) and putative orthologs comprise an ancient family of cutin synthase-like (CUS) proteins that are conserved among land plants. *The Plant Journal* 77, 667-675.

APPENDIX I

Catalyzing Plant Science Research with RNA-seq

* A version of this chapter has been published in:

Frontiers in Plant Science. (2013). 4(66). doi: 10.3389/fpls.2013.00066

Abstract

Next generation DNA sequencing technologies are driving increasingly rapid, affordable and high resolution analyses of plant transcriptomes through sequencing of their associated cDNA (complementary DNA) populations; an analytical platform commonly referred to as RNA-sequencing (RNA-seq). Since entering the arena of whole genome profiling technologies only a few years ago, RNA-seq has proven itself to be a powerful tool with a remarkably diverse range of applications, from detailed studies of biological processes at the cell type-specific level, to providing insights into fundamental questions in plant biology on an evolutionary time scale. Applications include generating genomic data for heretofore unsequenced species, thus expanding the boundaries of what had been considered “model organisms,” elucidating structural and regulatory gene networks, revealing how plants respond to developmental cues and their environment, allowing a better understanding of the relationships between genes and their products, and uniting the “omics” fields of transcriptomics, proteomics, and metabolomics into a now common systems biology paradigm. We provide an overview of the breadth of such studies and summarize the range of RNA-seq protocols that have been developed to address questions spanning cell type-specific-based transcriptomics, transcript secondary structure and gene mapping.

Keywords: RNA-seq, plant transcriptome, transcriptomics, systems biology, next generation sequencing

Introduction

Next generation sequencing (NGS) is underpinning an ongoing revolution in the life sciences and it is now difficult to identify areas of biology that are not already being profoundly affected by the massive amounts of high quality DNA sequence information that has been generated cost-effectively and efficiently, thanks to the rapid advancement of sequencing technologies. Plant biology is naturally no exception to this revolution; indeed the ease of genetic analyses in many plant species and the value of crop species have made plant science an especially fertile area for many of the “omics” technologies. Plant scientists are rapidly moving on from a decade where the first genome sequence of a plant, that of *Arabidopsis thaliana* (The Arabidopsis Genome Initiative, 2000), provided the major impetus for monumental forays into plant molecular investigations, to the present day where the growing number of sequenced plant genomes¹ is driving biological and evolutionary discovery across the plant taxonomic range.

In parallel with this explosion of genome sequence information, NGS has changed the scope and scale of transcriptome analysis and gene expression studies. RNA-sequencing (RNA-seq) technologies, which apply the principles of NGS to the complementary DNAs (cDNAs) derived from transcript populations, were first used to study plants only a few years ago (Weber *et al.*, 2007) and now provide ready access to high resolution transcriptome information to an extent that was once unimaginable.

¹ http://genomevolution.org/wiki/index.php/Sequenced_plant_genomes

This is exemplified by the 1KP project², which aims to sequence the transcriptomes of 1,000 plant species, and is just one of many current initiatives that are radically expanding the breadth and depth of our understanding of plant gene expression and evolution. Due to its accuracy and the ease of meaningful comparisons of samples not necessarily generated together, or even as part of the same experiment, RNA-seq is replacing other methods of quantifying transcript expression, including cDNA- and expressed sequenced tag (EST)-based microarray platforms (Alba *et al.*, 2004), as it overcomes many of their limitations (for an overview of RNA-seq technologies and comparisons with previous transcript detection technologies, see Wang *et al.*, 2009). For example, RNA-seq approaches have an open architecture, meaning that they are not restricted to detecting only those transcripts that are represented on microarrays, and also exhibit more extreme upper and lower limits of detection, which allows more accurate quantification of differential transcript expression, as well as the identification of low-abundance transcripts. Furthermore, no previous genome sequence knowledge is necessary, as RNA-seq data sets themselves can be used to create sequence assemblies for subsequent mapping of RNA-seq reads, along with the potential for detecting exon/exon boundaries, alternative splicing and novel transcribed regions in a single sequencing run. However, despite these advantages, RNA-seq profiling platforms come with their own practical challenges. Existing RNA-seq techniques generate large numbers of relatively short reads for a particular transcript and so the accurate assembly and annotation of the huge amounts of data

² <http://www.onekp.com>

generated by each run is still computationally difficult (Schliesky *et al.*, 2012). Moreover, various biases can be introduced during the RNA fragmentation step prior to library construction, and cDNA fragmentation enriches the reads mapping the 3' end of transcripts (Wang *et al.*, 2009).

Nonetheless, RNA-seq has emerged as a remarkable enabling technology that is increasingly being adopted by plant researchers from a broad range of disciplines and examples of some of the associated applications and fields of research are presented in this review.

Improving genome annotation with transcriptomic data

More than a decade after the publication of the first draft of the *A. thaliana* genome sequence (The Arabidopsis Genome Initiative, 2000) its annotation continues to be improved. Large amounts of Sanger sequencing-generated EST data provided the initial basis for gene identification and expression profiling (Zhu *et al.*, 2003), but such data are expensive and time consuming to generate, are inherently biased against low-abundance transcripts and are typically enriched in transcript termini (Filichkin *et al.*, 2010). RNA-seq circumvents these limitations and provides accurate resolution of splice junctions and alternative splicing events. For example, a survey of the Arabidopsis transcriptome using single-base resolution Illumina-generated reads identified thousands of novel alternatively spliced transcripts and indicated that at least 42% of intron-containing genes are alternatively spliced (Filichkin *et al.*, 2010). This percentage is considerably higher than previous estimations and is even greater (61%) when only the multiexonic genes are sampled (Marquez *et al.*, 2012). Similarly,

approximately 48% of rice (*Oryza sativa*) genes show alternative splicing patterns (Lu *et al.*, 2010), although more species need to be analyzed to determine whether this proportion is common. Mining RNA-seq data in search of transcription start site (TSS) variation is also improving gene structure annotation and alternative TSSs have been detected in ~10,000 loci through analyses of full-length Arabidopsis and rice cDNAs (Tanaka *et al.*, 2009). RNA-seq analysis also helps elucidate full-length transcript sequences, as has been demonstrated in a study where ~10% of the untranslated region (UTR) boundaries of rice genes could be extended (Lu *et al.*, 2010).

An ideal genome annotation would identify both genes that show invariant transcript sequences and those that exhibit alternative splicing, and additionally link these events to specific spatial, temporal, developmental, and/or environmental cues. Efforts in this direction are already underway and, as an example, it has been reported that abiotic stress in Arabidopsis can increase or decrease the proportions of apparently unproductive isoforms for some key regulatory genes, supporting the hypothesis that alternative splicing is an important mechanism in the regulation of gene function (Filichkin *et al.*, 2010).

For many heterozygous and out-crossing species, genome sequencing and annotation can only be considered complete once the breadth of intra-species polymorphism is also considered. The high quality reference genome of *A. thaliana* is based on the ecotype Columbia (Col-0). It has been reported that polymorphisms between different *A. thaliana* accessions is relatively high, with one single nucleotide polymorphism (SNP) every ~200 bp (Ossowski *et al.*, 2008). The complete re-

sequencing of the transcriptomes and annotation of different accessions may thus help interpret the functional consequences of polymorphism (Gan *et al.*, 2011). To this end, utilizing genomic and transcriptomic data for *in silico* gene prediction results in a more reliable annotated genome, with information on SNPs, insertion/deletions (indels), splice variants and expression variation. Furthermore, with its greater sensitivity, RNA-seq enables the detection of antisense transcripts and transcribed intergenic regions; topics that are discussed further in Section “Identifying and Characterizing Novel Non-Coding RNAs.”

Generating genomic and enabling proteomic resources for ‘non-model’ species

Despite the recent upsurge in published plant genome sequences, they still represent a very small fraction of plant taxonomic diversity and the availability of transcriptomic information based on Sanger sequence-derived ESTs is similarly sparse, rendering the study of “non-model” species challenging. The very large genomes often encountered in plants, frequently associated with high sequence repeat regions, makes *de novo* sequencing of the transcriptome an attractive alternative to generate genetic resources for species that are of considerable biological interest for reasons that relate to factors such as their evolutionary significance or economic importance. Examples of recent such initiatives include fern (Der *et al.*, 2011), eucalyptus (Mizrachi *et al.*, 2010), garlic (Sun *et al.*, 2012), pea (Franssen *et al.*, 2011), chestnut (Barakat *et al.*, 2009), chickpea (Garg *et al.*, 2011), olive (Alagna *et al.*, 2009), safflower (Lulin *et al.*, 2012), and Japanese knotweed (Hao *et al.*, 2011).

The annotation of genes identified by de novo sequencing typically relies on identifying homologs, and ideally orthologs, in species with an annotated genome if no appropriate EST databases are available. An example of such annotation, using a pre-existing EST database associated with the species of interest, was reported for melon (Dai *et al.*, 2011). Use of the annotated genome of a close-related species (e.g., Barrero *et al.*, 2011) is preferable, but if none is available, the *A. thaliana* genome sequence is still widely regarded as the “gold standard” and can be extremely valuable to this end (e.g., Bräutigam *et al.*, 2011). Further confirmation can then be sought by interrogating additional plant databases (e.g., Dassanayake *et al.*, 2009; Edwards *et al.*, 2012), although this depends on the standard of annotation and care should be taken that the database of interest is of high quality.

De novo RNA-seq to identify genetic polymorphisms also has great potential as a platform for molecular breeding, wherein multiple cultivars or close-related species with variations in traits of interest are sequenced and genetic variation is identified. This then allows the generation of molecular markers to facilitate progeny selection and molecular genetics research. As an example of this approach, the identification of 12,000 single sequence repeats (SSRs) in a single RNA-seq analysis of sesame (Zhang *et al.*, 2012) increased the number of known SSRs from 80 to several thousand with, on average, one genic-SSR per ~8 kb. Similarly, Haseneyer *et al.* (2011) sampled the transcriptomes of five winter rye inbred lines to identify 5,234 SNPs, which were then incorporated in a high-throughput SNP genotyping array, further demonstrating the value of RNA-seq as a tool for advanced molecular breeding.

Another striking example of the value of RNA-seq as an enabling technology is its application to advance the field of proteomics. High-throughput mass spectrometry-based protein identification relies on the availability of an extensive DNA sequence database in order to match experimentally determined peptide masses with the theoretical proteome generated by computationally translating transcripts. Indeed, the lack of extensive plant DNA sequence information and related resources is likely a contributing factor in the relatively slow progress in the arena of plant proteomics compared with proteome studies of other organisms for which high quality sequence has long been available. Lopez-Casado *et al.* (2012) recently demonstrated that RNA-seq-based transcriptome profiling can provide an effective data set for proteomic analysis of non-model organisms by de novo assembly of 454-based ESTs derived from the pollen of tomato (*Solanum lycopersicum*) and two wild relatives. Approximately the same number of proteins was identified when using either the RNA-seq-derived database, generated through a few 454 pyrosequencing runs, or a highly curated community database of tomato sequences generated over more than a decade. This suggests that RNA-seq will be invaluable in facilitating protein identification and that proteome studies need no longer be so taxonomically restricted.

Characterizing temporal, spatial, regulatory and evolutionary transcriptome landscapes

As with previous large-scale transcript profiling platforms, including microarrays, RNA-seq is increasingly being adopted to examine transcriptional dynamics during various aspects of plant growth and development. For example, an

analysis of the transcriptome of grape (*Vitis vinifera*) berries during three stages of development identified >6,500 genes that were expressed in a stage-specific manner (Zenoni *et al.*, 2010). Evidence of even greater transcriptomic complexity was provided by the detection of 210 and 97 genes that undergo alternative splicing in one or two stages, respectively. Similarly, Wang *et al.* (2012) analyzed the transcriptome of radish (*Raphanus sativum*) roots at two developmental stages and found >21,000 genes to be differentially expressed, including genes strongly linking root development with starch and sucrose metabolism and with phenylpropanoid biosynthesis. The radish genome has yet to be sequenced, but comparative sequence analysis of the radish RNA-seq data and the *Brassica rapa* genome sequence lead to the discovery of 14,641 SSRs.

Most RNA-seq analyses target whole organs, or sets of organs, which inherently prevents the identification of cell or tissue type transcripts, and thus spatially coordinated structural and regulatory gene networks. Furthermore, transcripts that are expressed at extremely low levels, or that are specific to an uncommon cell type in a complex organ or tissue, may be diluted below the limit of detection. Accordingly, RNA-seq analysis of discrete tissues or cell types has the potential to both yield an important level of spatial information and substantially increase the depth of sequence coverage. As an example, Chen *et al.* (2010) detected more than 1,000 genes that are specifically or preferentially expressed in *Arabidopsis* male meiocytes that had been isolated by mechanically disrupting anthers with forceps and collecting the released meiocytes with a capillary pipette. However, acquiring tissue or cell-specific samples with any degree of precision and minimal contamination is often

technically difficult, although several methods have been developed to facilitate this. For example, a cell type gene expression map of an Arabidopsis root was achieved by generating a set of transgenic Arabidopsis lines expressing green fluorescent protein (GFP) driven by various root cell type-specific promoters, digesting entire roots with cell wall degrading enzymes and fractionating the resulting protoplasts into distinct pools using an automated cell sorter (Birnbaum *et al.*, 2003). The constituent root cell type-related transcriptomes were then analyzed using a microarray, providing a high resolution profile of the spatial variation in the root transcriptome. An alternative approach, which requires no prior genetic transformation or cell wall digestion, is laser capture microdissection (LCM), where a laser is used to excise and isolate samples from tissue sections with micron-scale resolution. This technique has been effectively used by plant researchers in conjunction with microarray analysis (Nakazono *et al.*, 2003; Cai and Lashbrook, 2008; Agustí *et al.*, 2009; Brooks *et al.*, 2009; Matas *et al.*, 2010). More recently, Matas *et al.* (2011) used LCM in combination with RNA-seq (454 pyrosequencing) analysis to profile the transcriptomes of the five principal tissues of the developing tomato fruit pericarp. Approximately 21,000 unigenes were identified, of which more than half showed ubiquitous expression, while other subsets showed clear cell type-specific expression patterns, providing insights into numerous aspects of fruit biology. A similar number of genes was identified in an LCM-based study of the ontogeny of maize (*Zea mays*) shoot apical meristems using RNA-seq coupled with Illumina-based NGS (Takacs *et al.*, 2012). Interestingly, 59% of the transcripts were detected in all the samples, comprising the apical domains along a developmental gradient from maize embryos to seedlings; a value that is very similar

to the percentage of unigenes present in all tissues of the tomato fruit (57%) reported by Matas *et al.* (2011), and the proportion of ubiquitously detected transcripts in the root cell sorting analysis (Birnbaum *et al.*, 2003). RNA-seq profiling analyses of a number of mammalian tissues have also indicated a high proportion of ubiquitously expressed transcripts, which may indicate that this is a common feature of eukaryotes (Ramsköld *et al.*, 2009).

In addition to studies focusing on transcriptional changes during development, RNA-seq has already shown itself to be a highly effective strategy to study plant responses and adaptations to abiotic and biotic stresses. For example, by analyzing RNA-seq data derived from sorghum (*Sorghum bicolor*) plants treated with abscisic acid (ABA) or polyethylene glycol, in conjunction with published transcriptome analysis for *Arabidopsis*, maize, and rice, Dugas *et al.* (2011) discovered >50 previously unknown drought-responsive genes. Similarly, RNA-seq was used to reveal massive changes in metabolism and cellular physiology of the green alga *Chlamydomonas reinhardtii* when the cells become deprived of sulfur, and to suggest molecular mechanisms that are used to tolerate sulfur deprivation (González-Ballester *et al.*, 2010). Equivalent high resolution gene expression information has also resulted from studies of plant responses to pathogens and the complexities of the metabolic pathways associated with plant defense mechanisms. Published examples to date include a transcriptomic analysis of the infection of sorghum by the fungus *Bipolaris sorghicola* (Mizuno *et al.*, 2012) and an investigation into the defense mechanisms of soybean that provide resistance to *Xanthomonas axonopodis*, by comparing resistant and susceptible near-isogenic lines (Kim *et al.*, 2011).

As well as its applications to study spatial and temporal transcriptome dynamics, RNA-seq is also a potentially valuable tool to advance studies of plant evolution and polyploidy. As an illustration, a comparison of the leaf transcriptome of an allopolyploid relative of soybean with those of the two species that contributed to its homoelogenous genome, allowed the determination of the contribution of the different genomes to the transcriptome (Ilut *et al.*, 2012). Another study analyzed the transcriptome of nine distinct tissues of three species of the Poaceae family (Davidson *et al.*, 2012) to determine whether orthologous genes from these three species exhibit the same expression patterns. Knowledge of parental imprinting has also been substantially advanced by deep transcriptome surveys. Despite the discovery of genetic imprinting in maize 40 years ago, only seven maize imprinted genes were reported before large-scale transcriptomic sequencing was applied to maize endosperm, leading to the discovery of 179 imprinted genes and 38 imprinted long ncRNAs (lncRNAs; Zhang *et al.*, 2011). Studies of the embryo and endosperm of Arabidopsis and rice similarly increased the numbers of known imprinted genes and showed that imprinting is primarily endosperm-specific (Gehring *et al.*, 2011; Hsieh *et al.*, 2011; Luo *et al.*, 2011).

We note that the studies cited in this section highlight the tremendous diversity of RNA-seq applications and the breadth of research fields in which it is being adopted, and the purpose is to provide examples, rather than a comprehensive list.

Identifying and characterizing novel non-coding RNAs

Small RNAs (sRNAs) play important roles in gene post-transcriptional regulation (Baulcombe, 2004; Zamore and Haley, 2005) and there is great interest in developing techniques to comprehensively profile sRNA populations. In silico analysis provides a rapid way to identify putative sRNA genes (Chen *et al.*, 2003, 2011; Hirsch *et al.*, 2006) but RNA-seq technology represents an excellent means for sRNA discovery and validation. Indeed, deep sequencing of sRNAs has already been extensively used to find new sRNAs and especially microRNAs (miRNAs; Lu *et al.*, 2005; Moxon *et al.*, 2008; Szittyá *et al.*, 2008; Pantaleo *et al.*, 2010; Song *et al.*, 2010; Ferreira *et al.*, 2012, Xia *et al.*, 2012).

Characterization of miRNAs regulatory functions is likely to be facilitated by determining tissue-specific expression pattern, as shown by Breakfield *et al.* (2012) where RNA-seq was used to identify sRNAs from five Arabidopsis root tissues. Some sRNAs were expressed in all five tissues while others were tissue-specific, and some fluctuations in miRNA expression were also observed across developmental zones. In addition, growing numbers of RNA-seq studies are revealing the spatial and temporal differential expression of sRNAs in plant organs (Hirsch *et al.*, 2006; Moxon *et al.*, 2008; Pantaleo *et al.*, 2010; Calviño *et al.*, 2011). The availability of high-throughput RNA-seq data allowed Yang *et al.* (2012) to mine these databases and discover that ~12% of 354 high-confidence miRNA binding sites identified in Arabidopsis are affected by alternative splicing. The frequency of alternative splicing at miRNA binding sites is significantly higher than that at other regions, suggesting that alternative splicing is a significant regulatory mechanism. Small ncRNAs (sncRNAs)

are also implicated in abiotic stresses and many miRNAs and other sRNAs have been shown to be differentially expressed under phosphate starvation in *Arabidopsis* roots and shoots (Hsieh *et al.*, 2009), or under cold conditions (Zhang *et al.*, 2009). The large amounts of data easily generated by RNA-seq also enable comparisons of sRNA populations between species, as demonstrated by Moxon *et al.* (2008), who found two tomato miRNAs that were previously believed to be specific to *Arabidopsis* or moss. In contrast to the numerous studies of plant sRNAs, far less is known about lncRNAs (>200 nt), especially in plants, and few plant lncRNAs have been characterized to date (Au *et al.*, 2011; Kim and Sung, 2011; Zhu and Wang, 2012). Those that have been identified did not involve RNA-seq and so this represents an area with great potential for discovery.

Finally, sRNAs have been recently characterized in the context of association with epigenome modifications, including cytosine methylation of genomic DNA. While the majority of such work has involved animal systems, whole genome methylation analysis of epigenetic variation in *Arabidopsis* and rice embryo development, combined with sRNA analysis of the same tissues, confirmed a link between demethylation of certain gene promoters and associated miniature inverted repeats with changes in sRNA abundance (Cokus *et al.*, 2008; Lister *et al.*, 2008; Zemach *et al.*, 2010). Interestingly, while promoter demethylation of tomato ripening genes was also recently described, it did not occur in conjunction with notable changes in sRNAs (Zhong *et al.*, 2013). Genome-scale analyses of gene and sRNA expression via RNA-seq, combined with whole genome methylation analyses are now facilitating

the exploration of epigenomes in ways that could not have been considered prior to these high-throughput sequencing technologies.

From co-expression networks to integrative data analysis

Sequencing whole transcriptomes provides a high degree of detail, but deriving useful biological information from a long list of expressed genes is typically not trivial. One approach to using such information to develop and refine hypotheses is to construct networks of co-expressed genes and to use gene ontology (GO) information to help highlight important gene candidates as critical components of functional networks. Many such “guilt-by-association” gene co-expression networks have been constructed based on microarray data (Manfield *et al.*, 2006; Mao *et al.*, 2009; Childs *et al.*, 2011; Tohge and Fernie, 2012) and are now being more widely adopted to evaluate RNA-seq data (Dugas *et al.*, 2011; Iancu *et al.*, 2012; Li *et al.*, 2012). Indeed, the broad dynamic range of transcript level detection allowed by RNA-seq profiling, and particularly the detection of low-abundance transcripts, facilitates meaningful discrimination between different strengths of association in correlation analyses (Iancu *et al.*, 2012). The correlations between different genes forming the expression network are therefore more robust and the overall expression network quality is generally superior to that generated using microarrays.

Gene ontology enrichment analysis of RNA-seq data often illustrates the complexity of interacting pathways. For example, in a study of abiotic stress responses in maize, transcripts associated with numerous GO classifications were affected by drought treatment, including the categories “carbohydrate metabolic process,”

“response to oxidative stress,” and “cell division,” among others (Kakumanu *et al.*, 2012). The authors also showed that variations in GO term representation between organs can also provide valuable information and specifically, the drought-treated fertilized maize ovary exhibits a massive decrease of mRNAs involved in cell division and cell cycle, which could be the direct cause of the previously observed embryo abortion under drought conditions.

Functional networks can be made more robust by integrating multiple data types and various studies have coupled RNA-seq with proteomics and/or metabolomics, characterizing the apparent downstream consequences of transcript level variation. An example of such a “systems” study involved a comparative analysis of the transcriptome, proteome, and targeted metabolome of soybean seeds from transgenic lines with suppressed expression of the storage proteins glycinin and conglycinin (Schmidt *et al.*, 2011). This study showed no direct correlation between the levels of transcripts, proteins, and metabolites. Conversely, a significant correlation was found between the high expression of fatty acid synthesis genes and the high oil content in oil palm mesocarp (Bourgis *et al.*, 2011). These studies further demonstrate the value of characterizing biological processes from multiple “omics” perspectives, each of which can provide insights into different regulatory mechanisms. Surveying the metabolome and transcriptome in parallel can also help identify candidate genes involved in complex metabolic pathways. For example, Desgagné-Penix *et al.* (2012) took advantage of several opium poppy (*Papaver somniferum*) cultivars with known differential levels of benzylisoquinoline alkaloids (BIAs) and used a combination of RNA-seq and mass spectrometry to pinpoint key regulatory

steps of the almost completely defined morphine biosynthetic pathway, leading to the discovery of candidate genes implicated in BIA metabolism.

These examples show that the integration of transcriptomics, proteomics, and metabolomics can expose complex biological and biochemical interactions, paving the way to elucidate relationships between genotype and phenotype. Even greater resolution can be achieved by targeting tissues instead of whole organs (Rogers *et al.*, 2012).

A growing portfolio of RNA-seq analytical strategies

RNA-seq technologies can be adapted to answer specific biological questions. Four different adaptations or applications are described here.

Strand-specific RNA-seq

Standard RNA-seq methods do not discriminate between the DNA strands on which the RNAs are encoded. However, the ability to map a transcript to its specific coding strand is desirable as it improves transcript mapping accuracy by identifying non-coding antisense transcripts that may be involved in regulation at the messenger or at the chromatin levels (Ponting *et al.*, 2009; Liu *et al.*, 2010), helps determine the relative expression level of two genes on opposite DNA strands as well as their exact length, and allows the identification of the transcribed strand of ncRNAs. Levin *et al.* (2010) compared seven library construction methods to enable strand-specific RNA-seq analysis and overall, a dUTP method (Parkhomchuk *et al.*, 2009) was the most accurate and has the advantage of being compatible with paired-end sequencing. This

method has been successfully applied to plant RNA-seq with adaptations rendering it low-cost and high-throughput (Wang *et al.*, 2011; Zhong *et al.*, 2011). In short, the first cDNA strand is synthesized with dNTP while dUTP is incorporated in the second cDNA strand. After end repair, A-tailing and adaptor ligation, the dUTP-containing strand is digested and the remaining strand is PCR-amplified conferring strand specificity (Figure S1). As an example of the value of strand information, a study of tomato gene expression showed that while the majority of genes in the tissues analyzed had effectively the same expression profiles when analyzed by either double-stranded or strand-specific RNA-seq, approximately 5% of transcripts were associated with misleading results when assayed by double-stranded RNA-seq (dsRNA-seq) alone (Zhong *et al.*, 2011).

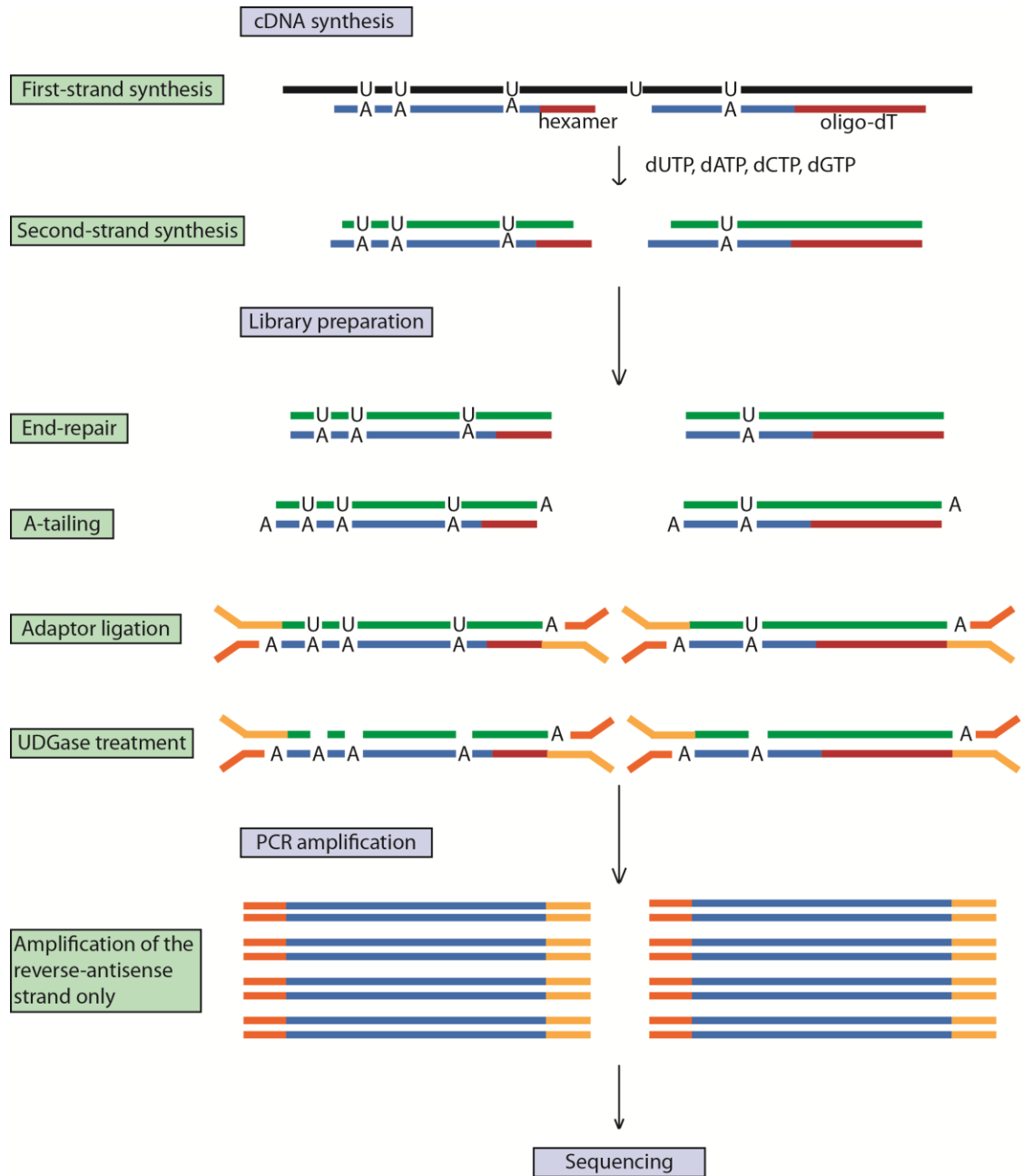


Figure S1. dUTP-based strand-specific RNA-seq. Strand-specificity is achieved by the second-strand cDNA incorporating dUTPs instead of dTTPs. Digestion of dUTPs by uracil-DNA glycosylase (UDGase) prevents this strand from being PCR amplified, conferring single-strand specificity.

Bulked segregant RNA-seq

Liu *et al.* (2012) demonstrated the application of RNA-seq for bulked segregant analysis (BSA) by mapping the maize mutant gene *gl3*. Transcriptome profiling is applied to a pool of two samples generated by mixing a bulk of mutant and wild-type (WT) plants (Figure S2). The mapping of the mutated gene is based on genetic linkage where linkage disequilibrium between markers and the causal gene is determined by quantifying the allelic frequencies between the two samples, giving the map position of the gene responsible for the mutant phenotype. Fine mapping of the mutated gene is facilitated by the RNA-seq data as its expression will often be down-regulated compared to the WT pool. Additionally, the SNPs linked to the mutated gene can be used for chromosome walking. Using RNA-seq for this purpose has therefore numerous advantages: (i) having a reference genome is not a prerequisite as *de novo* assembly of the transcriptome based on the RNA-seq data is sufficient; (ii) markers can be generated from the experimental data; and (iii) differential expression profiles between the mutant and the WT are generated at no extra cost. Furthermore, this approach can be modified to perform genome-wide association (GWAS) studies, accelerating breeding initiatives by providing markers targeting both genetic sequence (e.g., SNPs) and gene expression, using them to identify the genomic regions associated with the traits of interest (Harper *et al.*, 2012).

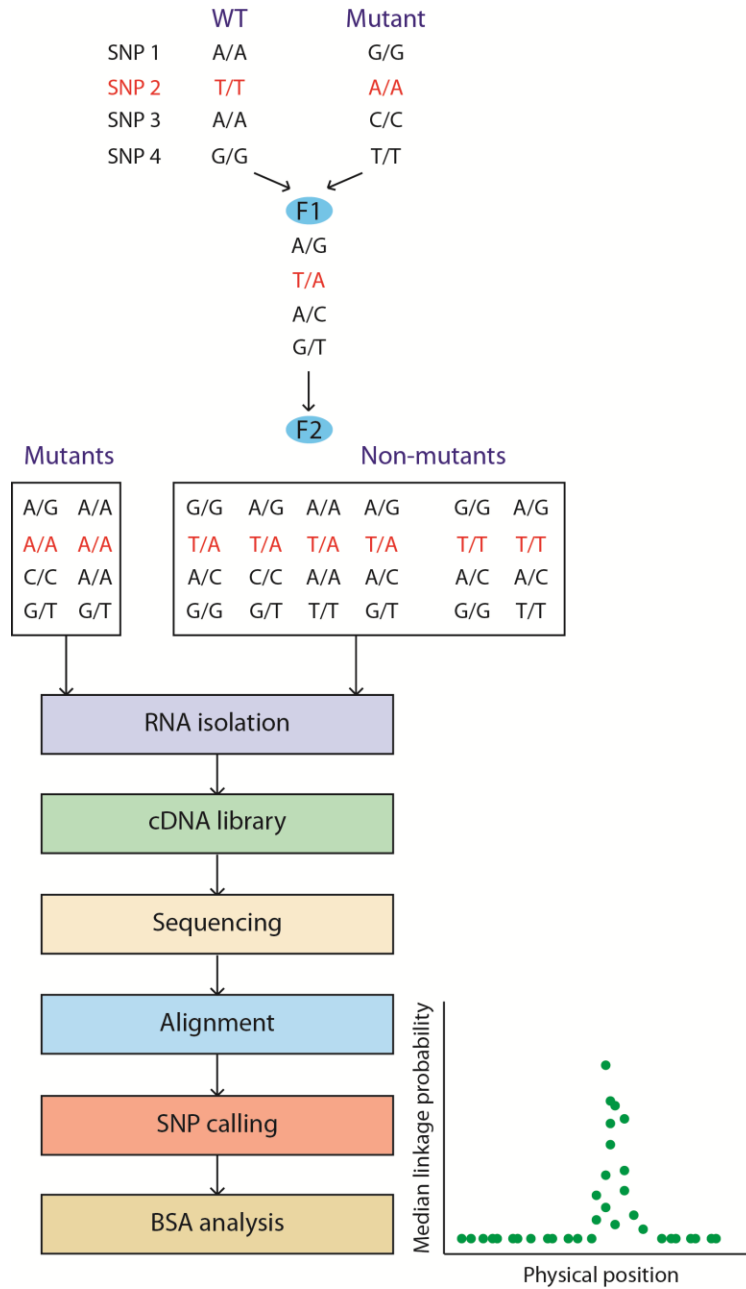


Figure S2. Bulked segregant analysis (BSA) using RNA-seq. Wild-type and mutant plants from different genetic backgrounds are crossed. In this example, four SNPs are listed with SNP 2 being closely related to the mutation to map. A plant from the F1 generation is selfed to generate the F2 segregating population. Mutant and non-mutant plants are processed independently and the BSA analysis allows visualization of the probability of each SNP marker being in complete linkage disequilibrium with the mutated gene.

Double-stranded RNA-seq

Secondary structures of RNAs are central to their function, maturation, and regulation; however, little is known about the double-stranded features of most RNAs. Zheng *et al.* (2010) reported an experimental strategy to survey RNA secondary structures in an analysis of the double-stranded species of RNAs from Arabidopsis flower buds. Specifically, the authors sequenced only the double-stranded RNAs (dsRNAs) and the double-stranded segments of RNAs by digesting the single-stranded RNAs with a ribonuclease treatment prior to library construction (Figure S3). As expected, highly structured RNA classes (e.g., rRNA, tRNA, and snRNA) were highly represented in the reads but, interestingly, other regions of various mRNAs, including introns, exons, and 5' and 3' UTRs were also present, indicating the presence of mRNA secondary structures. Moreover, the double-stranded regions of the introns, 3' and 5' UTRs appeared to be conserved, suggesting a common function. Notably, certain regions of the genome appear to be responsible for producing more dsRNAs than others, with transposable elements representing nearly 60% of these “hotspots.”

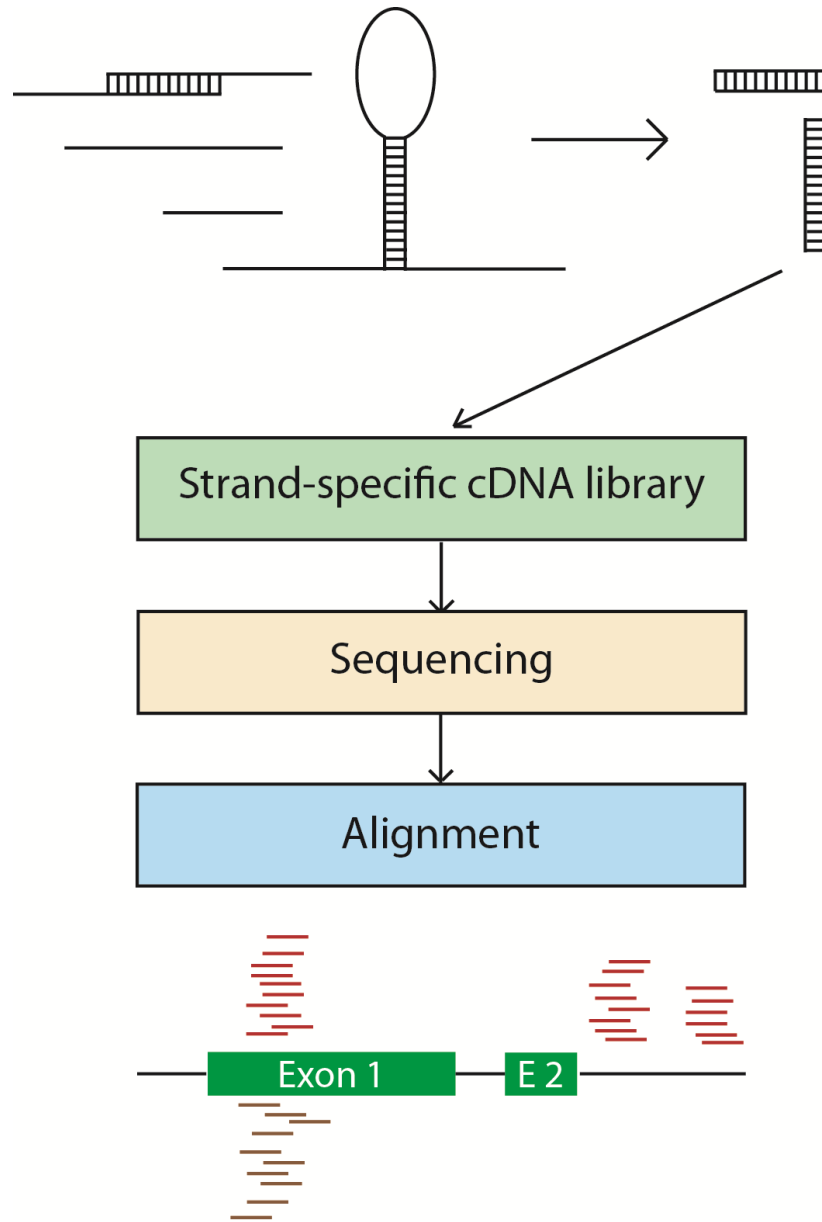


Figure S3. Double-stranded RNA-seq. A total RNA sample is isolated and single-stranded RNA is digested with a single-strand-specific ribonuclease. The reads generated from the strand-specific cDNA library are aligned to the genomic sequence and intra or inter-molecular pairing can be inferred based on the strand specificity of the mapped reads.

Differential RNA-seq

Differential RNA-seq (dRNA-seq) is based on a comparison of a terminator exonuclease treated RNA sample with its non-treated counterpart (Figure S4). The treatment removes the processed transcripts by degrading 5' monophosphate RNAs, which are characteristic of prokaryotic RNAs, and the primary unprocessed transcripts are not affected due to the presence of a 5' triphosphate. By comparing the maps of the reads derived from each sample, TSSs of operons are identified. dRNA-seq was first used to examine the transcriptome of the human pathogen *Helicobacter pylori* (Sharma *et al.*, 2010) and subsequently in studies of various prokaryotes, including the plant pathogen *Pseudomonas syringae* (Filiatrault *et al.*, 2011). This method was used to map TSSs of barley chloroplastic RNAs (Zhelyazkova *et al.*, 2012) and was possible as they have the same 5' monophosphate structure as prokaryotic RNAs, reflecting the endosymbiotic origin of chloroplasts. Four categories of TSSs were identified in this study: gTSSs (g: gene) located within 750 nucleotides upstream of annotated genes (the majority of TSSs); iTSSs (i: internal) located within annotated genes and giving rise to sense transcripts; aTSSs (a: antisense) giving rise to antisense transcripts; and oTSSs (o: orphan) located in intergenic regions. The analysis revealed that some individual transcriptional units of the chloroplastic operons can be transcribed individually as suggested by iTSSs and that ~35% of chloroplastic genes have aTSSs or oTSSs, providing evidence of extensive ncRNAs synthesis in chloroplasts.

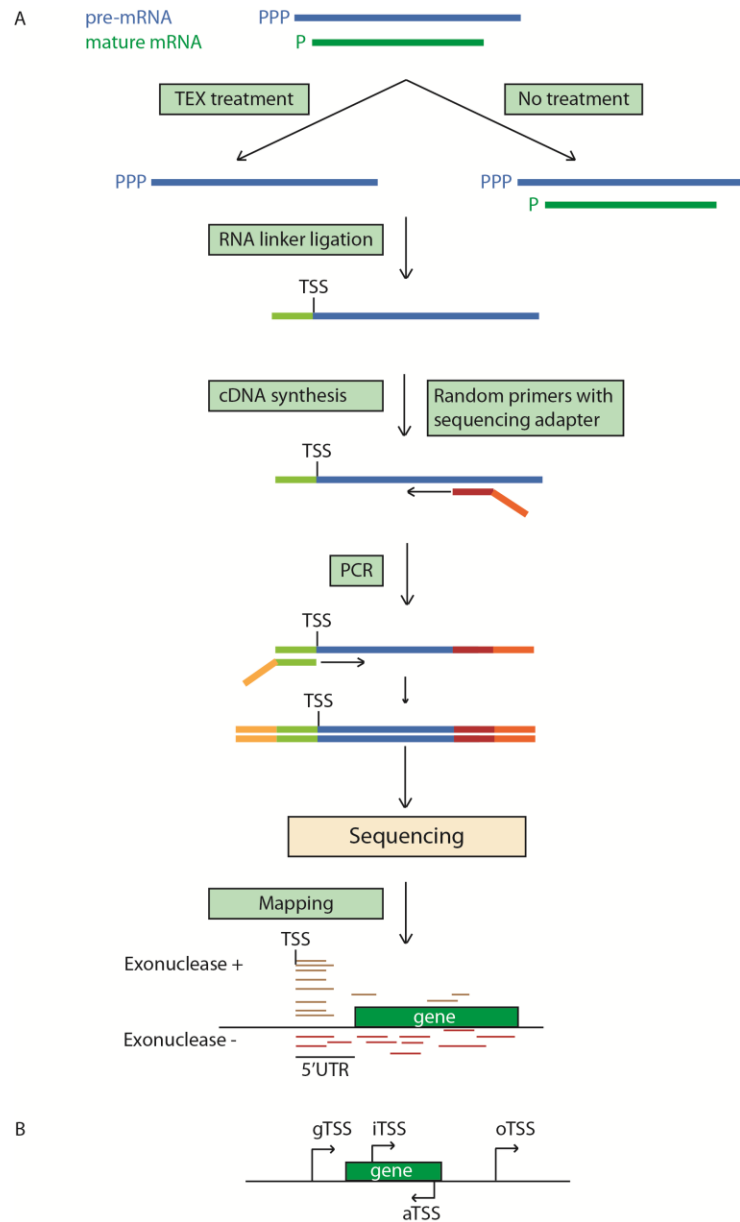


Figure S4. Differential RNA-seq. (A) 5' monophosphorylated chloroplastic mature transcripts are degraded with Terminator 5'-phosphate-dependent exonuclease (TEX) in the TEX treatment, enriching the sample with pre-mRNAs. The 5' ends of the pre-mRNAs are enriched in the treated sample because they are protected by the triphosphate and the TEX treatment removes degraded mRNAs (Sharma *et al.*, 2010). The enrichment can be enhanced by shearing the RNA before the TEX treatment. Sequencing reads starting exactly at the same nucleotide position in the exonuclease treatment denote the transcription start site. (B) Example of localization of different TSS. TSS, transcription start site; gTSS, gene TSS; iTSS, internal TSS; aTSS, antisense TSS; oTSS, orphan TSS.

Concluding Remarks

RNA-sequencing is now well-established as a versatile platform with applications in an ever growing number of fields of plant biology research. Ongoing developments in sequencing technologies, such as increased read lengths, greater numbers of reads per run, and advanced computational tools to facilitate sequence assembly, analysis, and integration with orthogonal data sets will further accelerate the breadth and frequency of its adoption by plant scientists. An important issue that still needs to be addressed is the inherent bias introduced by the different steps of library construction and so the tantalizing prospect of direct RNA-seq (Ozsolak and Milos, 2011) has great promise in this regard.

Acknowledgements and Relative contribution

Jocelyn K. C. Rose, James J. Giovannoni and Zhangjun Fei revised and contributed to the review on which this appendix is based. Funding to Jocelyn K. C. Rose and James J. Giovannoni for research in this area is provided by the NSF Plant Genome Research Program (DBI-0606595), and NSF EAGER award (Plant Genome Research Program) and the New York State Office of Science, Technology and Academic Research (NYSTAR).

REFERENCES

- Agustí J, Merelo P, Cercós M, Tadeo FR, Talón M. (2009). Comparative transcriptional survey between laser-microdissected cells from laminar abscission zone and petiolar cortical tissue during ethylene-promoted abscission in citrus leaves. *BMC Plant Biology* 9: 127.10.1186/1471-2229-9-
- Alagna F, D'Agostino N, Torchia L, Servili M, Rao R, Pietrella M, Giuliano G, Chiusano ML, Baldoni L, Perrotta G. (2009). Comparative 454 pyrosequencing of transcripts from two olive genotypes during fruit development. *BMC Genomics* 10: 399.10.1186/1471-2164-10-399
- Alba R, Fei Z, Payton P, Liu Y, Moore SL, Debbie P, Gordon J, Rose JKC, Martin G, Tanksley S, Bouzayen M, Jahn MJ, Giovannoni JJ. (2004). ESTs, cDNA microarrays, and gene expression profiling: tools for dissecting plant physiology and development. *The Plant Journal* 39 697–714.
- Au PCK, Zhu Q-H, Dennis ES, Wang M-B. (2011). Long non-coding RNA-mediated mechanisms independent of the RNAi pathway in animals and plants. *RNA Biology* 8 404–414.
- Barakat A, Diloreto DS, Zhang Y, Smith C, Baier K, Powell WA, Wheeler N, Sederoff R, Carlson JE. (2009). Comparison of the transcriptomes of American chestnut (*Castanea dentata*) and Chinese chestnut (*Castanea mollissima*) in response to the chestnut blight infection. *BMC Plant Biology* 9: 51.10.1186/1471-2229-9-51
- Barrero RA, Chapman B, Yang Y, Moolhuijzen P, Keeble-Gagnère G, Zhang N, Tang Q, Bellgard MI, Qiu D. (2011). De novo assembly of *Euphorbia fischeriana* root transcriptome identifies prostratin pathway related genes. *BMC Genomics* 12: 600.10.1186/1471-2164-12-600
- Baulcombe D. (2004). RNA silencing in plants. *Nature* 431 356–363.
- Birnbaum K, Shasha DE, Wang JY, Jung JW, Lambert GM, Galbraith DW, Benfey PN. (2003). A gene expression map of the *Arabidopsis* root. *Science* 302 1956–1960.
- Bourgis F, Kilaru A, Cao X, Ngando-Ebongue G-F, Drira N, Ohlrogge JB, Benfey PN. (2011). Comparative transcriptome and metabolite analysis of oil palm and date palm mesocarp that differ dramatically in carbon partitioning. *Proceedings of the National Academy of Sciences of the USA* 108 12527–12532.

- Bräutigam A, Kajala K, Wullenweber J, Sommer M, Gagneul D, Weber KL, Carr KM, Gowik U, Maß J, Lercher Mj, Westhoff P, Hibberd JM, Weber APM. (2011). An mRNA blueprint for C4 photosynthesis derived from comparative transcriptomics of closely related C3 and C4 species. *Plant Physiology* 155 142–156.
- Breakfield NW, Corcoran DL, Petricka JJ, Shen J, Sae-Seaw J, Rubio-Somoza I, Weigel D, Ohler U, Benfey PN. (2012). High-resolution experimental and computational profiling of tissue-specific known and novel miRNAs in *Arabidopsis*. *Genome Research* 22 163–176.
- Brooks L III, Strable J, Zhang X, Ohtsu K, Zhou R, Sarkar A, Hargreaves S, Elshire RJ, Eudy D, Pawlowska T, Ware D, Janick-Buckner D, Buckner B, Timmermans MCP, Schnable PS, Nettleton D, Scanlon MJ. (2009). Microdissection of shoot meristem functional domains. *PLoS Genetics* 5: e1000476.10.1371/journal.pgen.1000476
- Cai S, Lashbrook CC. (2008). Stamen abscission zone transcriptome profiling reveals new candidates for abscission control: enhanced retention of floral organs in transgenic plants overexpressing *Arabidopsis* ZINC FINGER PROTEIN2. *Plant Physiology* 146 1305–1321.
- Calviño M, Bruggmann R, Messing J. (2011). Characterization of the small RNA component of the transcriptome from grain and sweet sorghum stems. *BMC Genomics* 12: 356.10.1186/1471-2164-12-356
- Chen C, Farmer AD, Langley RJ, Mudge J, Crow JA, May GD, Huntley J, Smith AG, Retzel EF. (2010). Meiosis-specific gene discovery in plants: RNA-Seq applied to isolated *Arabidopsis* male meiocytes. *Plant Biology* 10 280.
- Chen C-J, Zhou H, Chen Y-Q, Qu L-H, Gautheret D. (2011). Plant noncoding RNA gene discovery by “single-genome comparative genomics”. *Bioinformatics* 17 390–400.
- Chen C-L, Liang D, Zhou H, Zhuo M, Chen Y-Q, Qu L-H. (2003). The high diversity of snoRNAs in plants: identification and comparative study of 120 snoRNA genes from *Oryza sativa*. *Nucleic Acids Research* 15 2601–2613.
- Childs KL, Davidson RM, Buell CR. (2011). Gene coexpression network analysis as a source of functional annotation for rice genes. *PLoS ONE* 6: e22196.10.1371/journal.pone.0022196
- Cokus SJ, Feng S, Zhang X, Chen Z, Merriman B, Haudenschild CD, Pradhan S, Nelson SF, Pellegrini SE, Jacobsen SE. (2008). Shotgun bisulphite sequencing of the *Arabidopsis* genome reveals DNA methylation patterning. *Nature* 452 215–219.

- Dai N, Cohen S, Portnoy V, Tzuri G, Harel-Beja R, Pompan-Lotan M, Carmi N, Zhang GF, Diber A, Pollock S, Karchi H, Yeselson Y, Petreikov M, Shen S, Sahar U, Hovav R, Lewinsohn E, Tadmor Y, Granot D, Ophir R, Sherman A, Fei ZJ, Giovannoni J, Burger Y, Katzir N, Schaffer AA. (2011). Metabolism of soluble sugars in developing melon fruit: a global transcriptional view of the metabolic transition to sucrose accumulation. *Plant Molecular Biology* 76 1–18.
- Dassanayake M, Haas JS, Bohnert HJ, Cheeseman JM. (2009). Shedding light on an extremophile lifestyle through transcriptomics. *New Phytologist* 183 764–775.
- Davidson RM, Gowda M, Moghe G, Lin H, Vaillancourt B, Shiu S-H, Jiang N, Buell CR. (2012). Comparative transcriptomics of three *Poaceae* species reveals patterns of gene expression evolution. *The Plant Journal* 71, 492–502.
- Der JP, Barker MS, Wickett NJ, Depamphilis CW, Wolf PG. (2011). De novo characterization of the gametophyte transcriptome in bracken fern, *Pteridium aquilinum*. *BMC Genomics* 12: 99.10.1186/1471-2164-12-99
- Desagné-Penix I, Farrow SC, Cram D, Nowak J, Facchini PJ. (2012). Integration of deep transcript and targeted metabolite profiles for eight cultivars of opium poppy. *Plant Molecular Biology* 79 295–313.
- Dugas DV, Monaco MK, Olsen A, Klein RR, Kumari S, Ware D, Klein, PE. (2011). Functional annotation of the transcriptome of *Sorghum bicolor* in response to osmotic stress and abscisic acid. *BMC Genomics* 12: 514.10.1186/1471-2164-12-514
- Edwards CE, Parchman TL, Weekley CW. (2012). Assembly, gene annotation and marker development using 454 floral transcriptome sequences in *Ziziphus celata* (Rhamnaceae), a highly endangered, florida endemic plant. *DNA Research*. 19 1–9.
- Ferreira TH, Gentile A, Vilela RD, Costa GGL, Dias LI, Endres L, Menossi M. (2012). microRNAs associated with drought response in the bioenergy crop sugarcane (*Saccharum spp.*). *PLoS ONE* 7: e46703. doi: 10.1371/journal.pone.0046703.
- Filiatrault MJ, Stodghill PV, Myers CR, Bronstein PA, Butcher BG, Lam H, Grills G, Schweitzer P, Wang W, Schneider DJ, Cartinhour SW. (2011). Genome-wide identification of transcriptional start sites in the plant pathogen *Pseudomonas syringae* pv. tomato str. DC3000. *PLoS ONE* 6: e29335.10.1371/journal.pone.0029335
- Filichkin SA, Priest HD, Givan SA, Shen R, Bryant DW, Fox SE, Wong W-K, Mockler TC. (2010). Genome-wide mapping of alternative splicing in *Arabidopsis thaliana*. *Genome Research* 20 45–58.

- Franssen SU, Shrestha RP, Brautigam A, Bornberg-Bauer E, Weber APM. (2011). Comprehensive transcriptome analysis of the highly complex *Pisum sativum* genome using next generation sequencing. *BMC Genomics* 12: 227.10.1186/1471-2164-12-227
- Gan X, Stegle O, Behr J, Steffen JG, Drewe P, Hildebrand KL, Lyngsoe R, Schultheiss SJ, Osborne EJ, Sreedharan VT, Kahles A, Bohnert R, Jean G, Derwent P, Kersey P, Belfield EJ, Harberd NP, Kemen E, Toomajian C, Kover PX, Clark RM, Ratsch G, Mott R. (2011). Multiple reference genomes and transcriptomes for *Arabidopsis thaliana*. *Nature* 477 419–423.
- Garg R, Patel RK, Jhanwar S, Priya P, Bhattacharjee A, Yadav G, Bhatia S, Chattopadhyay D, Tyagi AK, Jain M. (2011). Gene discovery and tissue-specific transcriptome analysis in chickpea with massively parallel pyrosequencing and web resource development. *Plant Physiology* 156 1661–1678.
- Gehring M, Missirlian V, Henikoff S. (2011). Genomic analysis of parent-of-origin allelic expression in *Arabidopsis thaliana* seeds. *PLoS ONE* 6: e23687.10.1371/journal.pone.0023687
- González-Ballester D, Casero D, Cokus S, Pellegrini M, Merchant SS, Grossman AR. (2010). RNA-seq analysis of sulfur-deprived *Chlamydomonas* cells reveals aspects of acclimation critical for cell survival. *Plant Cell* 22 2058–2084.
- Hao DC, Ge GB, Xiao PG, Zhang YY, Yang L. (2011). The first insight into the tissue specific taxus transcriptome via illumina second generation sequencing. *PLoS ONE* 6: e21220.10.1371/journal.pone.0021220
- Harper AL, Trick M, Higgins J, Fraser F, Clissold L, Wells R, Hattori C, Werner P, Bancroft I. (2012). Associative transcriptomics of traits in the polyploid crop species *Brassica napus*. *Nature Biotechnology* 30 798–802.
- Haseneyer G, Schmutzer T, Seidel M, Zhou R, Mascher M, Schön C-C, Taudien S, Scholz U, Stein N, Mayer KFX, Bauer E. (2011). From RNA-seq to large-scale genotyping: genomics resources for rye (*Secale cereale* L.). *BMC Plant Biology* 11: 131.10.1186/1471-2229-11-131
- Hirsch J, Lefort V, Vankersschaver M, Boualem A, Lucas A, Thermes C, d'Aubenton-Carafa Y, Crespi M. (2006). Characterization of 43 non-protein-coding mRNA genes in *Arabidopsis*, including the MIR162a-derived transcripts. *Plant Physiology* 140 1192–1204.
- Hsieh L-C, Lin S-I, Shih AC-C, Chen J-W, Lin W-Y, Tseng C-Y, Li W-H, Chiou T-J (2009). Uncovering small RNA-mediated responses to phosphate deficiency in *Arabidopsis* by deep sequencing. *Plant Physiology* 151 2120–2132.

- Hsieh T-F, Shin J, Uzawa R, Silva P, Cohen S, Bauer MJ, Hashimoto M, Kirkbride RC, Harada JJ, Zilberman D, Fischer RL. (2011). Regulation of imprinted gene expression in *Arabidopsis* endosperm. *Proceedings of the National Academy of Sciences of the USA*. 108 1755–1762.
- Iancu OD, Kawane S, Bottomly D, Searles R, Hitzemann R, McWeeney S. (2012). Utilizing RNA-seq data for de-novo coexpression network inference. *Bioinformatics* 28 1592–1597.
- Iltut DC, Coate JE, Luciano AK, Owens TG, May GD, Farmer A, Doyle JJ. (2012). A comparative transcriptomic study of an allotetraploid and its diploid progenitors illustrates the unique advantages and challenges of RNA-seq in plant species. *American Journal of Botany* 99 383–396.
- Kakumanu A, Ambavaram MMR, Klumas C, Krishnan A, Batlang U, Myers E, Grene R, Pereira A. (2012). Effects of drought on gene expression in maize reproductive and leaf meristem tissue revealed by RNA-seq. *Plant Physiology* 160 846–867.
- Kim E-D, Sung S. (2011). Long noncoding RNA: unveiling hidden layer of gene regulatory networks. *Trends in Plant Science*. 17 16–21.
- Kim KH, Kang YJ, Kim DH, Yoon MY, Moon JK, Kim MY, Van K, Lee S-H. (2011). RNA-seq analysis of a soybean near-isogenic line carrying bacterial leaf pustule-resistant and -susceptible alleles. *DNA Research* 18 483–497.
- Levin JZ, Yassour M, Adiconis X, Nusbaum C, Thompson DA, Friedman N, Gnirke A, Regev A. (2010). Comprehensive comparative analysis of strand-specific RNA sequencing methods. *Nature Methods* 7 709–715.
- Li W, Dai C, Liu C-C, Zhou XJ. (2012). Algorithm to identify frequent coupled modules from two-layered network series: application to study transcription and splicing coupling. *Journal of Computational Biology* 19 710–730.
- Lister R, O'Malley RC, Tonti-Filippini J, Gregory BD, Berry CC, Millar AH, Ecker JR. (2008). Highly integrated single-base resolution maps of the epigenome in *Arabidopsis*. *Cell* 133 523–536.
- Liu F, Marquardt S, Lister C, Swiezewski S, Dean C. (2010). Targeted 3' processing of antisense transcripts triggers *Arabidopsis* FLC chromatin silencing. *Science* 327 94–97.
- Liu S, Yeh C-T, Tang HM, Nettleton D, Schnable PS. (2012). Gene mapping via bulked segregant RNA-seq (BSR-Seq). *PLoS ONE* 7: e36406.10.1371/journal.pone.0036406

- Lopez-Casado G, Covey PA, Bedinger PA, Mueller LA, Thannhauser TW, Zhang S, Fei Z, Giovannoni JJ, Rose JKC. (2012). Enabling proteomic studies with RNA-seq: the proteome of tomato pollen as a test case. *Proteomics* 12 761–774.
- Lu C, Singh Tej S, Luo S, Haudenschild CD, Meyers BC, Green PJ. (2005). Elucidation of the small RNA component of the transcriptome. *Science* 309 1567–1569.
- Lu T, Lu G, Fan D, Zhu C, Li W, Zhao Q, Guo Y, Li W, Huang X, Han B. (2010). Function annotation of the rice transcriptome at single-nucleotide resolution by RNA-seq. *Genome Research* 20 1238–1249.
- Lulin H, Xiao Y, Pei S, Wen T, Shangqin H. (2012). The first illumina-based de novo transcriptome sequencing and analysis of safflower flowers. *PLoS ONE* 7: e38653.10.1371/journal.pone.0038653
- Luo M, Taylor JM, Spriggs A, Zhang H, Wu X, Russel S, Singh M, Koltunow A. (2011). A genome-wide survey of imprinted genes in rice seeds reveals imprinting primarily occurs in the endosperm. *PLoS Genetics* 7: e1002125.10.1371/journal.pgen.1002125
- Manfield IW, Jen C-H, Pinney JW, Michalopoulos I, Bradford JR, Gilmartin PM, Westhead DR. (2006). *Arabidopsis* co-expression tool (ACT): web server tools for microarray-based gene expression analysis. *Nucleic Acids Research* 34 504–509.
- Mao L, Van Hemert JL, Dash S, Dickerson JA. (2009). *Arabidopsis* gene co-expression network and its functional modules. *BMC Bioinformatics* 10: 346.10.1186/1471-2105-10-346
- Marquez Y, Brown JWS, Simpson C, Barta A, Kalyna M. (2012). Transcriptome survey reveals increased complexity of the alternative splicing landscape in *Arabidopsis*. *Genome Research* 22 1184–1195.
- Matas AJ, Agustí J, Tadeo FR, Talón M, Rose JKC. (2010). Tissue specific transcriptome profiling of the citrus fruit epidermis and subepidermis using laser capture microdissection. *Journal of Experimental Botany* 61 3321–3330.
- Matas AJ, Yeats TH, Buda GJ, Zheng Y, Chatterjee S, Tohge T, Ponnala L, Adato A, Aharoni A, Stark R, Fernie AR, Fei Z, Giovannoni JJ, Rose JKC. (2011). Tissue- and cell-type specific transcriptome profiling of expanding tomato fruit provides insights into metabolic and regulatory specialization and cuticle formation. *Plant Cell* 23 3893–3910.
- Mizrachi E, Hefer CA, Ranik M, Joubert F, Myburg AA. (2010). De novo assembled expressed gene catalog of a fast-growing eucalyptus tree produced by Illumina mRNA-Seq. *BMC Genomics* 11: 681.10.1186/1471-2164-11-681

- Mizuno H, Kawahigashi H, Kawahara Y, Kanamori H, Ogata J, Minami H, Itoh T, Matsumoto T. (2012). Global transcriptome analysis reveals distinct expression among duplicated genes during sorghum-*Bipolaris sorghicola* interaction. *BMC Plant Biology* 12: 121.10.1186/1471-2229-12-121
- Moxon S., Jing R., Szittyá G., Schwach F., Rusholme Pilcher R. L., Moulton V., Dalmay, T. (2008). Deep sequencing of tomato short RNAs identifies microRNAs targeting genes involved in fruit ripening. *Genome Research* 18 1602–1609.
- Nakazono M, Qiu F, Borsuk LA, Schnable PS. (2003). Laser-capture microdissection, a tool for the global analysis of gene expression in specific plant cell types: identification of genes expressed differentially in epidermal cells or vascular tissue of maize. *Plant Cell* 15 583–596.
- Ossowski S, Schneeberger K, Clark RM, Lanz C, Warthmann N, Weigel D. (2008). Sequencing of natural strains of *Arabidopsis thaliana* with short reads. *Genome Research* 18 2024–2033.
- Ozsolak F, Milos PM. (2011). RNA sequencing: advances, challenges and opportunities. *Nature Reviews Genetics* 12 87–98.
- Pantaleo V, Szittyá G, Moxon S, Miozzi L, Moulton V, Dalmay T, Burgyan J. (2010). Identification of grapevine microRNAs and their targets using high-throughput sequencing and degradome analysis. *The Plant Journal* 62 960–976.
- Parkhomchuk D, Borodina T, Amstislavskiy V, Banaru M, Hallen L, Krobitsch S, Lehrach H, Soldatov A. (2009). Transcriptome analysis by strand-specific sequencing of complementary DNA. *Nucleic Acids Research* 37 e123.
- Ponting CP, Oliver PL, Reik W. (2009). Evolution and functions of long noncoding RNAs. *Cell* 136 629–641.
- Ramsköld D, Wang ET, Burge CB, Sandberg R. (2009). An abundance of ubiquitously expressed genes revealed by tissue transcriptome sequence data. *PLoS Computational Biology* 5: e1000598.10.1371/journal.pcbi.1000598
- Rogers ED, Jackson T, Moussaieff A, Aharoni A, Benfey PN. (2012). Cell type-specific transcriptional profiling: implications for metabolite profiling. *The Plant Journal* 70 5–17.
- Schliesky S, Gowik U, Weber APM, Bräutigam A. (2012). RNA-seq assembly –are we there yet? *Front. Plant Science* 3: 220.10.3389/fpls.2012.00220
- Schmidt MA, Barbazuk WB, Sandford M, May G, Song Z, Zhou W, Nikolau BJ, Herman EM. (2011). Silencing of soybean seed storage proteins results in a rebalanced protein composition preserving seed protein content without major

- collateral changes in the metabolome and transcriptome. *Plant Physiology* 156 330–345.
- Sharma CM, Hoffmann S, Darfeuille F, Reignier J, Findeiß S, Sittka A, Chabas S, Reiche K, Hackermüller J, Reinhardt R, Stadler PF, Vogel J. (2010). The primary transcriptome of the major human pathogen *Helicobacter pylori*. *Nature* 464 250–255.
- Song C, Wang C, Zhang C, Korir NK, Yu H, Ma Z, Fang J. (2010). Deep sequencing discovery of novel and conserved microRNAs in trifoliolate orange (*Citrus trifoliata*). *BMC Genomics* 11: 431.10.1186/1471-2164-11-431
- Sun X, Zhou S, Meng F, Liu S. (2012). De novo assembly and characterization of the garlic (*Allium sativum*) bud transcriptome by Illumina sequencing. *Plant Cell* 31 1823–1828.
- Szittyá G, Moxon S, Santos DM, Jing R, Fevereiro MPS, Moulton V, Dalmay T. (2008). High-throughput sequencing of *Medicago truncatula* short RNAs identifies eight new miRNA families. *BMC Genomics* 9: 593.10.1186/1471-2164-9-593
- Takacs EM, Li J, Du C, Ponnala L, Janick-Buckner D, Yu J, Muehlbauer GJ, Schnable PS, Timmermans MCP, Sun Q, Nettleton D, Scanlon MJ. (2012). Ontogeny of the maize shoot apical meristem. *Plant Cell* 24 3219–3234.
- Tanaka T, Koyanagi KO, Itoh T. (2009). Highly diversified molecular evolution of downstream transcription start sites in rice and *Arabidopsis*. *Plant Physiology* 149 1316–1324.
- The *Arabidopsis* Genome Initiative. (2000). Analysis of the genome sequence of the flowering plant *Arabidopsis thaliana*. *Nature* 408 796–815.
- Tohge T, Fernie AR. (2012). Co-expression and co-responses: within and beyond transcription. *Frontiers in Plant Science* 3: 248.10.3389/fpls.2012.00248
- Wang L, Si Y, Dedow LK, Shao Y, Liu P, Brutnell TP. (2011). A low-cost library construction protocol and data analysis pipeline for Illumina-based strand-specific multiplex RNA-seq. *PLoS ONE* 6: e26426.10.1371/journal.pone.0026426
- Wang S, Wang X, He Q, Liu X, Xu W, Li L, Brutnell TP. (2012). Transcriptome analysis of the roots at early and late seedling stages using Illumina paired-end sequencing and development of EST-SSR markers in radish. *Plant Cell Reports* 31 1437–1447.
- Wang Z, Gerstein M, Snyder M. (2009). RNA-Seq: a revolutionary tool for transcriptomics. *Nature Reviews Genetics* 10 57–63.

- Weber APM, Weber KL, Carr K, Wilkerson C, Ohlrogge JB. (2007). Sampling the *Arabidopsis* transcriptome with massively parallel pyrosequencing. *Plant Physiology* 144 32–42.
- Xia R, Zhu H, An Y-q, Beers EP, Zongrang L. (2012). Apple miRNAs and tasiRNAs with novel regulatory networks. *Genome Biology* 13 R47.
- Yang X, Zhang H, Li L. (2012). Alternative mRNA processing increases the complexity of microRNA-based gene regulation in *Arabidopsis*. *The Plant Journal* 70 421–431.
- Zamore PD, Haley B. (2005). Ribo-gnome: the big world of small RNAs. *Science* 309 1519–1524.
- Zemach A, Kim MY, Silva P, Rodrigues JA, Dotson B, Brooks MD, Zilberman D. (2010). Local DNA hypomethylation activates genes in rice endosperm. *Proceedings of the National Academy of Sciences of the USA* 107 18729–18734.
- Zenoni S, Ferrarini A, Giacomelli E, Xumerle L, Fasoli M, Malerba G, Bellin D, Pezzotti M, Delledonne M. (2010). Characterization of transcriptional complexity during berry development in *Vitis vinifera* using RNA-Seq. *Plant Physiology* 152 1787–1795.
- Zhang H, Wei L, Miao H, Zhang T, Wang C. (2012). Development and validation of genic-SSR markers in sesame by RNA-seq. *BMC Genomics* 13: 316.10.1186/1471-2164-13-316
- Zhang J, Xu Y, Huan Q, Chong K. (2009). Deep sequencing of *Brachypodium* small RNAs at the global genome level identifies microRNAs involved in cold stress response. *BMC Genomics* 10: 449.10.1186/1471-2164-10-449
- Zhang M, Zhao H, Xie S, Chen J, Xu Y, Wang K, Zhao H, Guan H, Hu X, Jiao Y, Song W, Lai J. (2011). Extensive, clustered parental imprinting of protein-coding and noncoding RNAs in developing maize endosperm. *Proceedings of the National Academy of Sciences of the USA* 108 20042–20047.
- Zhelyazkova P, Sharma CM, Förstner KU, Liere K, Vogel J, Börner T. (2012). The primary transcriptome of barley chloroplasts: numerous noncoding RNAs and the dominating role of the plastid-encoded RNA polymerase. *Plant Cell* 24 123–136.
- Zheng Q, Ryvkin P, Li F, Dragomir I, Valladares O, Yang J, Cao K, Wang L-S, Gregory BD. (2010). Genome-wide double-stranded RNA sequencing reveals the functional significance of base-paired RNAs in *Arabidopsis*. *PLoS Genetics* 6: e1001141.10.1371/journal.pgen.1001141

- Zhong S, Fei Z, Chen Y-R, Zheng Y, Huang M, Vrebalov J, McQuinn R, Gapper N, Lui B, Xiang J, Shao Y, Giovannoni J. (2013). Single-base resolution methylomes of tomato fruit development reveal epigenome modifications associated with ripening. *Nature Biotechnology* 31 154–159.
- Zhong S, Joung J-G, Zheng Y, Chen Y-R, Liu B, Shao Y, Xiang JZ, Fei Z, Giovannoni JJ. (2011). High-throughput illumina strand-specific RNA sequencing library preparation. *Cold Spring Harbor Protocols*. 8 940–949.
- Zhu Q-H, Wang M-B. (2012). Molecular functions of long non-coding RNAs in plants. *Genes* 3 176–190.
- Zhu W, Schlueter SD, Brendel V. (2003). Refined annotation of the *Arabidopsis* genome by complete expressed sequence tag mapping. *Plant Physiology* 132 469–484.